NOTE

Due to the U.S. Geological Survey's maximum size limit for electronic National Earthquake Hazard Reduction Program Final Technical Report deliverables (10 MB), report figures, geologic maps, and trench logs included in this document are reduced resolution versions and may be difficult to read. For a full resolution document go to the Utah Geological Survey webpage at: http://geology.utah.gov/ghp/consultants/pubs/washington.htm

U.S. Geological Survey External Grant Award Number
G11AP20061

PALEOSEISMIC INVESTIGATION OF THE NORTHERN SECTION OF THE WASHINGTON FAULT ZONE, WASHINGTON COUNTY, UTAH, AND MOHAVE COUNTY, ARIZONA

Submitted by
William R. Lund[1]

With assistance from Tyler R. Knudsen[1], David B. Simon[2], Christopher B. DuRoss[3], Greg N. McDonald[3], John R. Hanson[4], Peter D. Rowley[5], and David K. Black[4]

[1]Utah Geological Survey, 88 E. Fiddler Canyon Road, Suite C
Cedar City, UT 84721
(435) 865-9034; (435) 865-9037 (fax)
billlund@utah.gov

[2]Simon Bymaster, Inc., 1025 E. 400 N.
Bountiful, UT 84010

[3] Utah Geological Survey, P.O. Box 146100
Salt Lake City, Utah 84114

[4] Rosenberg Associates, 352 East Riverside Drive, Suite A2
St. George, UT 84790

[5]Geologic Mapping, Inc.,
New Harmony, UT 84757

December 12, 2012

Research supported by the U.S. Geological Survey (USGS), Department of the Interior, under USGS award number G11AP20061. The views and conclusions contained in this document are those of the authors and should not be interpreted as necessarily representing the official policies, either expressed or implied, of the U.S. Government.

Although this product represents the work of professional scientists, the Utah Department of Natural Resources, Utah Geological Survey, makes no warranty, expressed or implied, regarding its suitability for a particular use. The Utah Department of Natural Resources, Utah Geological Survey, shall not be liable under any circumstances for any direct, indirect, special, incidental, or consequential damages with respect to claims by users of this product.

CONTENTS

INTRODUCTION TO THE WASHINGTON FAULT ZONE *by William R. Lund* 3

SURFICIAL GEOLOGY OF THE FORT PEARCE AND WASHINGTON HOLLOW SECTIONS OF THE WASHINGTON FAULT ZONE, WASHINGTON COUNTY, UTAH AND MOHAVE COUNTY, ARIZONA *by Tyler R. Knudsen* 16

UTAH GEOLOGICAL SURVEY DUTCHMAN DRAW SITE PALEOSEISMIC INVESTIGATION, FORT PEARCE SECTION, WASHINGTON FAULT ZONE, MOHAVE COUNTY, ARIZONA *by William R. Lund, Tyler R. Knudsen, Christopher B. DuRoss, and Greg N. McDonald*.....70

LONG-TERM VERTICAL SLIP-RATE ESTIMATES FROM DISPLACED MAFIC VOLCANIC FLOWS, FORT PEARCE AND SULLIVAN DRAW SECTIONS, WASHINGTON FAULT ZONE, MOHAVE COUNTY, ARIZONA *by William R. Lund and Tyler R. Knudsen*.....123

SURFACE-FAULT-RUPTURE-HAZARD INVESTIGATION FOR A TRANSPORTATION CORRIDOR, FORT PEARCE SECTION, WASHINGTON FAULT ZONE, WASHINGTON COUNTY, UTAH *by David B. Simon, John R. Hanson, Pete D. Rowley, and David K. Black*.....149

INTRODUCTION TO THE WASHINGTON FAULT ZONE

by
William R. Lund
Utah Geological Survey

CONTENTS

ABSTRACT 5
INTRODUCTION 5
Background 5
Purpose and Scope of Work 7
Setting 7
WASHINGTON FAULT ZONE 8
Overview 8
Evidence of Quaternary Surface Faulting 9
Previous Paleoseismic Investigations 9
REDUCING EARTHQUAKE LOSSES 10
REFERENCES 10

FIGURES

Figure 1. Location of the Washington fault zone and other large Quaternary faults in southwestern Utah 13
Figure 2. Washington fault zone study area showing fault sections as proposed by Pearthree (1988), UGS and UDOT trench locations, and the locations of earlier paleoseismic investigations 14
Figure 3. Intermountain Seismic Belt and significant Utah historical earthquakes 15

ABSTRACT

The Washington fault zone is a 97-km-long (straight line), down-to-the-west normal fault that extends from northern Arizona into southwestern Utah. The Washington fault zone is one of several large Quaternary normal faults that define a transitional boundary between the Colorado Plateau and Basin and Range physiographic provinces in northern Arizona and southwestern Utah. In Utah, the fault zone trends through the rapidly urbanizing St. George metropolitan area in Washington County. Scarps formed on unconsolidated basin-fill deposits and soft bedrock along the Washington fault zone in Utah and northernmost Arizona provide evidence of late Quaternary surface faulting. Therefore, the Washington fault zone is considered active and capable of producing future large earthquakes that represent a significant seismic hazard to the St. George metropolitan area.

Based on structural and geomorphic evidence, previous workers divided the Washington fault zone into three fault sections from south to north: Sullivan Draw, Mokaac, and Northern. New geologic mapping (Knudsen, this volume) identified the Washington Hollow fault, which is along strike with and north of the Washington fault zone, as a fourth section of the Washington fault zone distinct from the Northern section to the south. Because the previously defined Northern section is no longer the northernmost section of the Washington fault zone, to avoid future confusion Knudsen (this volume) has proposed renaming the Northern section the Fort Pearce section. Additionally, the new geologic mapping shows that the previously defined Mokaac section and the Dutchman Draw fault, previously mapped as independent structures, are strands of the larger Fort Pearce section, and Knudsen (this volume) redefined them as such.

The papers in this volume present the results of four investigations undertaken to acquire new geologic and paleoseismic data on the Washington fault zone in Utah and northernmost Arizona. (1) New surficial geologic mapping provides better information on the location and length of young surface ruptures and the relative ages of displaced surficial deposits along the Fort Pearce and Washington Hollow sections. (2) A paleoseismic trenching investigation of a scarp formed on a latest Quaternary alluvial fan near Dutchman Draw in Arizona provides new information on paleoearthquake timing, displacement, and recurrence necessary for evaluating the seismic hazard presented by the Fort Pearce section to the St. George metropolitan area. (3) Trace element and major oxide geochemical correlation and radiometric dating ($^{40}Ar/^{39}Ar$) of mafic volcanic flows displaced across the fault zone in Arizona provide long-term (early to middle Quaternary) vertical-slip-rate estimates for the Fort Pearce and Sullivan Draw sections. (4) A surface-fault-rupture-hazard investigation conducted by a geological consultant for the Utah Department of Transportation provides additional information on the number of earthquakes and displacement per earthquake on the Fort Pearce section.

INTRODUCTION

Background

The Washington fault zone is a 97-km-long (straight line), down-to-the-west normal fault that extends from northern Arizona into southwestern Utah. The Washington fault zone is

one of several large Quaternary normal faults that define a transitional boundary between the Colorado Plateau and Basin and Range physiographic provinces in northern Arizona and southwestern Utah (figure 1). In Utah, the fault zone trends through the rapidly urbanizing St. George metropolitan area in Washington County. Scarps formed on unconsolidated basin-fill deposits and soft bedrock along the Washington fault zone in Utah and northernmost Arizona provide evidence of late Quaternary surface faulting. Therefore, the Washington fault zone is considered active and capable of producing future large earthquakes that represent a significant seismic hazard to the St. George metropolitan area.

Based on structural and geomorphic evidence, previous workers divided the Washington fault zone into three fault sections from south to north: the Sullivan Draw, Mokaac, and Northern sections (Pearthree, 1988) (figure 2). New geologic mapping (Knudsen this volume) identified the Washington Hollow fault, which is along strike with and north of the Washington fault zone, as part of the Washington fault zone and distinct from the Northern section to the south. Because the previously defined Northern section is no longer the northernmost section of the Washington fault zone, to avoid future confusion Knudsen (this volume) has proposed renaming it the Fort Pearce section. Additionally, the new geologic mapping shows that the previously defined Mokaac section and the Dutchman Draw fault, previously mapped as independent structures, are strands of the larger Fort Pearce section, and Knudsen (this volume) redefines them as such.

In Utah, the Fort Pearce section trends through the St. George metropolitan area, which experienced a nearly 53% population increase between 2000 and 2010 (U.S. Census Bureau, 2011). Despite an economic downturn beginning in 2008, the area's rapid growth is expected to resume once the region's economy recovers. The 2010 U.S. Census placed the population of the St. George metropolitan area at 138,115 (U.S. Census Bureau, 2011), and estimates of future growth predict that the area's population will exceed 700,000 by 2050 (Utah Governor's Office of Planning and Budget, 2008). The communities of St. George (pop. 72,897), Santa Clara (pop. 6033), Ivins (pop. 6753), Hurricane (pop. 13,748), and La Verkin (pop. 4060) (U.S. Census Bureau, 2011) are all within 20 km of the Fort Pearce section (figure 2) and will experience strong ground shaking in the event of a large earthquake on that section of the Washington fault zone. Washington City (pop. 18,761) (U.S. Census Bureau, 2011) lies directly on the trace of the Fort Pearce section, and can expect surface-fault rupture in addition to strong ground shaking during a large Fort Pearce-section earthquake.

Recognizing the earthquake hazard presented by the Washington fault zone to the St. George metropolitan area, the Utah Quaternary Fault Parameters Working Group (UQFPWG), which is convened annually by the Utah Geological Survey (UGS) to help set Quaternary fault research priorities for Utah, identified the Fort Pearce (then Northern) section as one of its top five research priorities in 2008 (http://geology.utah.gov/ghp/workgroups/pdf/uqfpwg/UQFPWG-2008_Summary.pdf). In response to the UQFPWG priority ranking, the UGS undertook three investigations (geologic mapping, paleoseismic trenching, and correlation and dating of displaced lava flows) to better define the earthquake hazard presented by the Washington fault zone to the St. George metropolitan area. Results of those investigations are presented in the papers in this volume. This volume also includes the results of a surface-fault-rupture-hazard investigation conducted by Simon Bymaster, Inc. (SBI), for a Utah Department of Transportation

(UDOT) road project. The Simon Bymaster investigation provides additional information on the number of earthquakes and displacement per earthquake on the Fort Pearce section in Utah.

Purpose and Scope of Work

The purpose of the investigations presented in this volume was to develop new geologic and paleoseismic information for the Washington fault zone in Utah, and in particular for the part of the fault zone which trends through the St. George metropolitan area (figure 2). The scope of work included:

(1) 1:50,000-scale surficial geologic mapping of the Washington fault zone in Utah and northernmost Arizona (Knudsen this volume). This included a review of geologic literature, maps, aerial photographs, and other imagery available for the Washington fault zone, and particularly data related to previous paleoseismic investigations and geologic mapping of the fault.

(2) Paleoseismic trenching of a faulted alluvial fan near Dutchman Draw in Arizona to develop new information on paleoearthquake timing, displacement, and recurrence for the Fort Pearce section (Lund and others this volume). This task included preparation of site topographic and geologic maps, scarp profiling, trenching, and radiocarbon and optically stimulated luminescence (OSL) dating of carbon and sediment samples from trenches.

(3) Geochemical correlation and radiometric dating ($^{40}Ar/^{39}Ar$) of displaced mafic volcanic flows in Arizona to determine long-term (early to middle Quaternary) vertical-slip-rate estimates for the southern part of the Fort Pearce section and northern end of the Sullivan Draw section (Lund and Knudsen this volume).

(4) Synthesis of results from a surface-fault-rupture-hazard investigation conducted on the Fort Pearce section by SBI for the UDOT (Simon and others this volume). The SBI investigation evaluates the surface-fault-rupture hazard to a proposed freeway alignment and three elevated freeway interchanges that are part of a new state highway in the St. George metropolitan area.

This new information, along with earthquake recurrence and vertical slip-rate estimates derived from the paleoseismic data, help characterize the earthquake hazard presented by the Washington fault zone to the rapidly urbanizing St. George, Utah, metropolitan area.

Setting

In Utah, most earthquakes are associated with the Intermountain Seismic Belt (ISB) (Smith and Sbar, 1974; Smith and Arabasz, 1991), an approximately 150-km-wide, north-south trending zone of earthquake activity that extends from northern Montana to northwestern Arizona (figure 3). Since 1850, there have been at least 15 earthquakes of magnitude (**M**) 5.5 or greater within the ISB (University of Utah Seismograph Stations [UUSS], 2012). Included among those events are Utah's two largest historical earthquakes, the estimated **M** 6.5 1902

Richfield earthquake, and the **M** 6.6 1934 Hansel Valley earthquake, which produced Utah's only historical surface faulting (figure 3). In an average year, Utah experiences more than 700 earthquakes, but most are too small to be felt (UUSS, 2012). Moderate-magnitude earthquakes (**M** 5.5 – 6.5) happen in Utah on average every seven years (UUSS, 2012), the most recent being the M_L 5.8 St. George earthquake on September 2, 1992 (Christenson, 1995; figure 3). Large-magnitude earthquakes (**M** 6.5 – 7.5) occur much less frequently in Utah, but geologic evidence shows that most areas of the state within the ISB, including the St. George metropolitan area, have experienced large surface-faulting earthquakes in the Holocene (Lund and others, 2007, 2008b).

Historical surface faulting has not occurred in southwestern Utah, but the area has a pronounced record of seismicity. At least 20 earthquakes equal to or greater than **M** 4 have occurred in southwestern Utah over the past century (Christenson and Nava, 1992; UUSS, 2012), the largest being the estimated **M** 6 1902 Pine Valley earthquake (Williams and Tapper, 1953) and the M_L 5.8 1992 St. George earthquake (Christenson, 1995). The Pine Valley earthquake is pre-instrumental and poorly located, and therefore, is not associated with a recognized fault. However, the epicenter is west of the surface trace of the west-dipping Hurricane fault, so the earthquake may have occurred on that structure. Based chiefly on its epicentral location and focal mechanism, Pechmann and others (1995) concluded that the St. George earthquake could have resulted from buried slip on the Hurricane fault.

Despite a lack of historical surface faulting, geologic data for faults in southwestern Utah indicate a moderate rate of long-term Quaternary activity. Mid-Quaternary basalt flows are displaced more than 300 m in several locations and latest Quaternary and Holocene alluvial and colluvial deposits are displaced meters to tens of meters (Anderson and Christenson, 1989; Lund and others, 2007, 2008b). Prominent among the Quaternary faults in southwestern Utah are the Hurricane (Lund and others, 2007), Sevier (Lund and others, 2008a), and Washington fault zones.

WASHINGTON FAULT ZONE

Overview

The Washington fault zone is an approximately 97-km-long (straight line), down-to-the-west normal fault that trends from northern Arizona into the St. George, Utah, metropolitan area (figure 2; Biek and others, 2009). The Washington fault zone lies west of the longer, late Quaternary-active Hurricane fault (Lund and others, 2007; figure 1), and crosses much of the St. George metropolitan area before dying out north of Washington City. In Utah, displacement on the Washington fault zone decreases northward, in a sense opposite to the northward-increasing displacement of the Hurricane fault. According to Peterson (1983), the fault reaches its maximum displacement (about 670 m) 10 km south of the Utah-Arizona state line. Billingsley (1993) reported about 500 m of displacement at the state line, and Hayden (2005) estimated about 185 m of displacement south of Washington City in Utah.

Figure 2 shows the boundaries and section names as originally defined by Pearthree (1998). There has been no historical surface faulting on any of the sections, and based on the

paleoseismic information available prior to this investigation, Black and others (2003) assigned an age of < 15,000 years for the timing of the most recent surface-faulting paleoearthquake on the Fort Pearce (then Northern) section.

Evidence of Quaternary Surface Faulting

Although long suspected of being active, prior to this investigation little was known about the surface-faulting history of the Washington fault zone. Situated in the transition zone between the Colorado Plateau and Basin and Range physiographic provinces, the geomorphology of the St. George basin is dominated by erosion driven by the rapid incision of the Virgin River and its tributaries (figure 2). Consequently, fault scarps are chiefly preserved on bedrock along the fault zone in Utah. Many of those scarps are fault-line scarps created by erosional retreat of the soft bedrock. In such areas, the main fault trace is often buried by loose eolian sand. Because it is farther away from the large, actively incising drainages in Utah and has not been subject to urban development, the part of the Fort Pearce section that lies in Arizona preserves isolated fault scarps on latest Quaternary basin-fill deposits.

In Utah, a short subsidiary splay of the Fort Pearce section displaces the Washington basalt flow about 4.6 m. K-Ar dating by Best and others (1980) places the age of the flow at 1.7 $\pm$ 0.1 Ma. More recent $^{40}Ar/^{39}Ar$ dating of the flow yielded ages of 0.87 $\pm$ 0.04 and 0.98 $\pm$ 0.02 Ma (Biek, 2003). Timing of the earthquake(s) that displaced the basalt flow is unknown other than being younger than the age of the flow. Based on geomorphic relations observed elsewhere on what Pearthree (1998) then defined as the Northern section, he assigned a time of <130 ka for the most recent surface faulting. However, Anderson and Christenson (1989) profiled a 3.5-m-high fault scarp in Utah preserved on mixed colluvial and alluvial deposits near the Utah-Arizona border (point D on figure 2), and based on diffusion modeling estimated a late Quaternary age of about 15 ka for the scarp.

Previous Paleoseismic Investigations

In addition to the Anderson and Christenson (1989) scarp profile, Earth Sciences Associates, Inc. (ESA) trenched the Washington fault zone (Fort Pearce section) as part of a U.S. Soil Conservation Service (SCS; now Natural Resources Conservation Service) seismic-safety investigation of flood-retention structures in Utah (ESA, 1982; Bowman and others, 2011) (point E on figure 2). ESA reported a few inches of vertical displacement in "younger" deposits, but was unsure if this small displacement was fault related or the result of differential compaction of loose eolian sediments across the fault. However, ESA identified "older" deposits that were displaced about a meter and represent at least one and possibly more surface-faulting earthquakes (ESA, 1982). The absence of organic carbon or other datable material in their trenches prevented ESA from refining their relative age assessments beyond "younger" and "older" categories, which they estimated to be 5 to 10 ka and 10 to 25 ka, respectively.

In 2007, Applied Geotechnical Engineering Consultants, Inc. (AGEC) excavated five trenches to locate the buried trace of the Washington fault zone where it crosses a proposed subdivision in Washington City (Payton, 2007) (point C on figure 2). One trench produced an excellent exposure of the fault, and AGEC allowed the UGS to make a reconnaissance log of one trench wall, and collect samples for OSL dating. Results of the logging and dating indicated that

the fault zone has likely experienced at least three surface-faulting earthquakes in the past 76 kyr, the most recent possibly in Holocene time (Lund and others, 2008b). However, the UGS had less than two days to spend in the trench, and significant questions remained regarding both the number and timing of paleoearthquakes. In particular, the rupture from the most recent surface-faulting earthquake extended to within 25 cm of the ground surface through loose eolian sand. The rupture displaced a moderately developed soil Bk horizon, indicating that the event could be as young as Holocene. The trench was later reoccupied and logged in detail by SBI for the UDOT surface-fault-rupture-hazard investigation (Simon and others this volume).

REDUCING EARTHQUAKE LOSSES

Results of the new geologic mapping and paleoseismic investigations presented in this volume will help reduce losses from future earthquakes by permitting more accurate earthquake-hazard evaluations for hazard mitigation in the rapidly urbanizing St. George, Utah, metropolitan area. Results of these investigations better define the location, length, rates of activity, and earthquake magnitudes for the Washington fault zone in Utah. These data are critical for improving deterministic seismic-source characterization models and probabilistic earthquake-hazard analyses for the rapidly urbanizing St. George metropolitan area. Study results will also be used to update the U.S. Geological Survey's (USGS) *Quaternary Fault and Fold Database of the United States*, the UGS *Quaternary Fault and Fold Database of Utah*, and the USGS *National Seismic Hazards Maps* for Utah and Arizona. Additionally, the surficial geology map of the Fort Pearce and newly defined Washington Hollow sections better defines the fault's location, and will help planners, geologists, and engineers reduce surface-fault-rupture hazard to future development.

REFERENCES

Anderson, R.E., and Christenson, G.E., 1989, Quaternary faults, folds, and selected volcanic features in the Cedar City 1° x 2° quadrangle, Utah: Utah Geological and Mineral Survey Miscellaneous Publication 89-6, 29 p., 1 plate, scale 1:250,000.

Best, M.G., McKee, E.H., and Damon, P.E., 1980, Space-time-composition patterns of late Cenozoic mafic volcanism, southwestern Utah and adjoining areas: American Journal of Science, v. 280, p. 1035-1050.

Biek, R.F., 2003, Geologic map of the Harrisburg Junction quadrangle, Washington County Utah: Utah Geological Survey Map 191, 42 p., 2 plates, scale 1:24,000.

Billingsley, G.H., 1992, Geologic map of the Yellowhorse Flat quadrangle, northern Mohave County, Arizona: U.S. Geological Survey Open-File Report 92-442, scale 1:24,000.

Billingsley, G.H., 1993, Geologic map of the Wolf Hole Mountain and vicinity, Mohave County, northwestern Arizona: U.S. Geological Survey Miscellaneous Investigation Series Map I-2296, scale 1:31,680.

Black, B.D., Hecker, S., Hylland, M.D., Christenson, G.E., and McDonald, G.N., 2003, Quaternary fault and fold database and map of Utah: Utah Geological Survey Map 193DM, scale 1:50,000, CD.

Bowman, S.D, Young, B.W., and Unger, C.D., 2011, Paleoseismology of Utah Volume 21 – Compilation of 1982-83 seismic safety investigation reports of eight SCS dams in southwestern Utah (Hurricane and Washington fault zones) and low-sun-angle aerial photography, Washington and Iron Counties, Utah, and Mohave County, Arizona: Utah Geological Survey Open-File Report 583, 4 p., 6 DVD set, online at <http://geology.utah.gov/ghp/consultants/paleoseismic_series.htm>.

Christenson, G.E., editor, 1995, The September 2, 1992 M_L 5.8 St. George earthquake: Utah Geological Survey Circular 88, 41 p.

Christenson, G.E., and Nava, S.J., 1992, Earthquake hazards in southwestern Utah, *in* Harty, K.M., editor, Engineering and environmental geology of southwestern Utah: Utah Geological Association Publication 21, p. 123-137.

Earth Sciences Associates, 1982, Seismic safety investigation of eight SCS dams in southwestern Utah: Portland, Oregon, unpublished consultant's report for the U.S. Soil Conservation Service, variously paginated, 2 volumes.

Governor's Office of Planning and Budget, 2008, Population area and component of change: Demographic and Economic Analysis Section, online, < http://www.governor.utah.gov/dea/projections.html>, accessed September 30, 2011.

Hayden, J.M., 2005, Geologic map of the Washington Dome quadrangle, Washington County, Utah: Utah Geological Survey Map 209, 29 p. pamphlet, scale 1:24,000.

Lund, W.R., Hozik, M.J., and Hatfield, S.C., 2007, Paleoseismology of Utah Volume 14 - Paleoseismic investigation and long-term slip history of the Hurricane fault in southwestern Utah: Utah Geological Survey Special Study 119, 81 p., CD.

Lund, W.R., Knudsen, T.R., and Vice, G.S., 2008a, Paleoseismology of Utah Volume 16 - Paleoseismic reconnaissance of the Sevier fault, Kane and Garfield Counties, Utah: Utah Geological Survey Special Study 122, 37 p., CD.

Lund, W.R., Knudsen, T.R., Vice, G.S., and Shaw, L., 2008b, Geologic hazards and adverse construction conditions, St. George – Hurricane metropolitan area, Washington County, Utah: Utah Geological Survey Special Study 127, 105 p., DVD.

Payton, C.C., 2007, Surface fault rupture hazard study, proposed Zippy LLC, 47-acre site, Washington Fields, Washington City, Utah: Applied Geotechnical Engineering Consultants, Inc., Project Number 2070301, 15 p., 22 figures.

Pearthree, P.A., compiler, 1998, Quaternary fault data and map for Arizona: Arizona Geological Survey Open-File Report 98-24, 122 p., 1 plate in pocket, scale 1:750,000.

Pechmann, J.C., Arabasz, W.J., and Nava, S.J., 1995, Seismology, *in* Christenson, G.E., editor, The September 2, 1992 M_L 5.8 St. George earthquake, Washington County, Utah: Utah Geological Survey Circular 88, p. 1.

Peterson, S.M., 1983, The tectonics of the Washington fault zone, northern Mohave County, Arizona: Brigham Young University Geology Studies, v. 30, part 1, p. 83-94.

Smith, R.B., and Arabasz, W.J., 1991, Seismicity of the Intermountain seismic belt, *in* Slemmons, D.B., Engdahl, E.R., Zoback, M.D., and Blackwell, D.D., editors, Neotectonics of North America: Boulder, Colorado, Geological Society of America, Decade Map Volume, p. 185-228.

Smith, R.B., and Sbar, M.L., 1974, Contemporary seismicity in the Intermountain Seismic Belt: Geological Society of America Bulletin, v. 85, p. 1205-1218.

U. S. Census Bureau, 2011, State and county quickfacts: Online, <http://quickfacts.census.gov/qfd/states/49/4965330.html>, webpage last revised Tuesday, 18-Oct-2011 15:41:32 EDT, accessed November 3, 2011.

University of Utah Seismograph Stations, 2012, Regional earthquake information: Online, < http://www.quake.utah.edu/REGIONAL/eqfaq.htm>, accessed July 7, 2012.

Williams, J.S., and Tapper, M.L., 1953, Earthquake history of Utah: Bulletin of the Seismological Society of America, v. 43, p. 191-218.

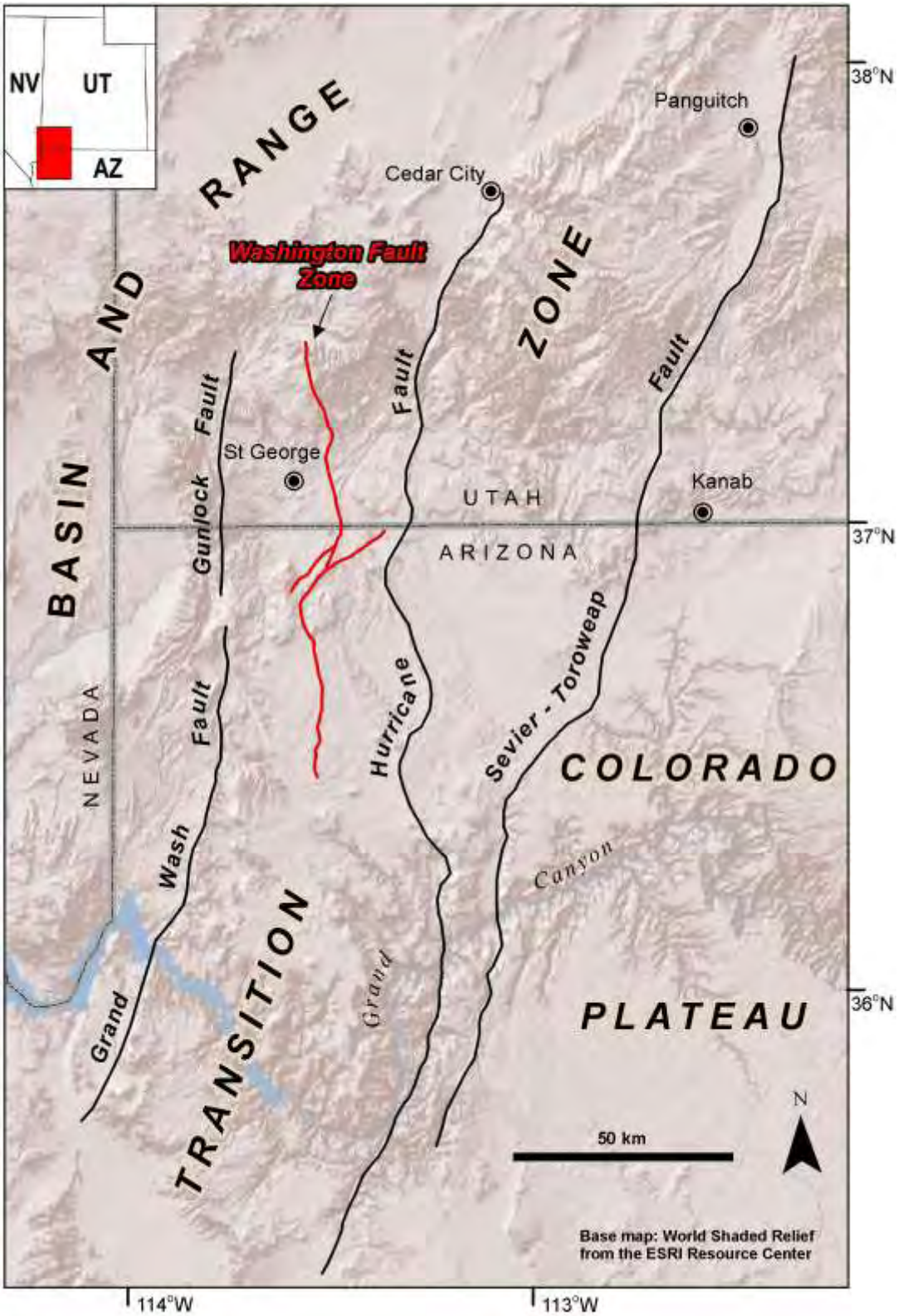

Figure 1. *Location of the Washington fault zone and other large Quaternary faults in southwestern Utah.*

Figure 2. *Washington fault zone study area showing fault sections as proposed by Pearthree (1988), UGS and UDOT trench locations, and the locations of earlier paleoseismic investigations. A = Dutchman Draw trench site, B = UDOT surface-fault-hazard investigation site, C = existing consultant's trench incorporated into the UDOT study, D = Anderson and Christenson (1988) scarp profile, E = ESA (1982) flood control structure investigation. Yellow shading indicates St. George and Washington City boundaries. Additional Quaternary faults are shown as gray lines.*

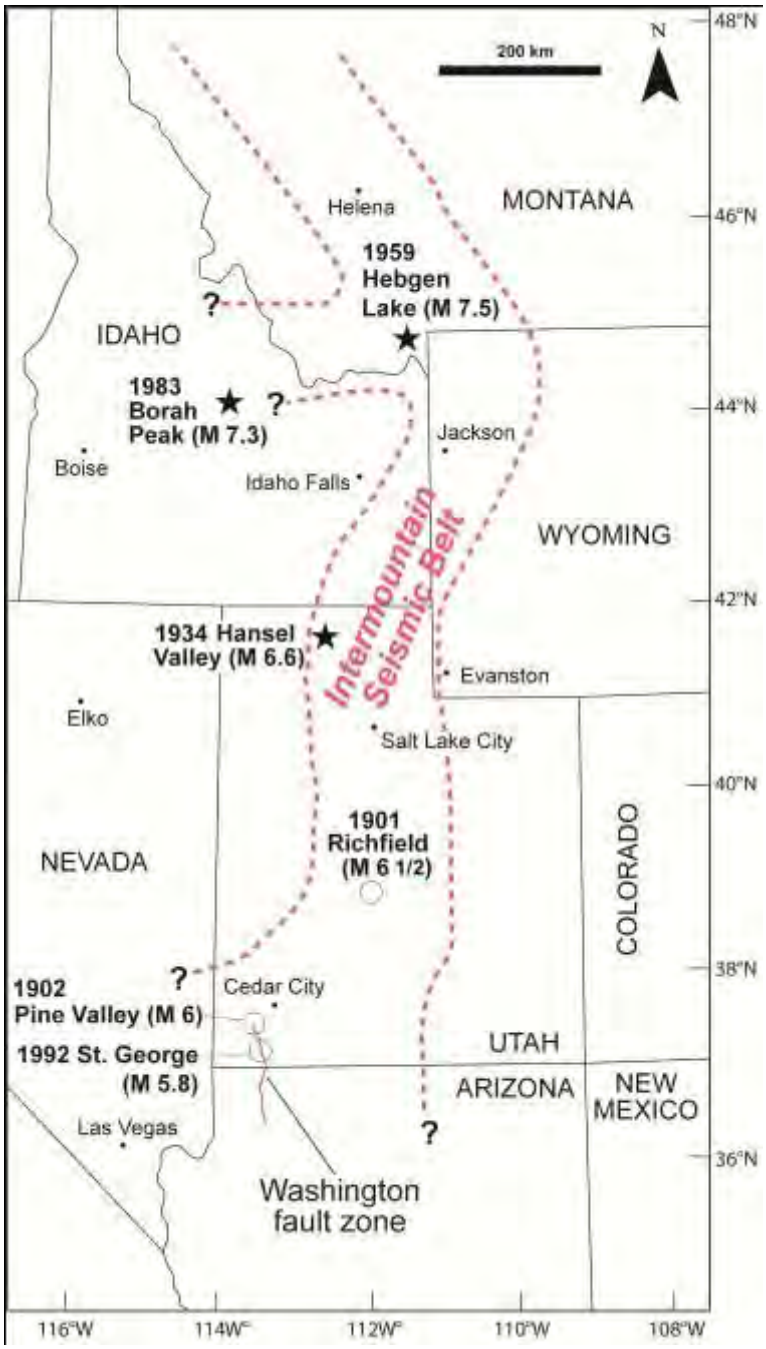

Figure 3. *Intermountain Seismic Belt and significant Utah historical earthquakes. Stars denote earthquakes that caused surface rupture. Note that the Washington fault zone is a west-dipping normal fault; therefore, the hypocenters of the 1902 Pine Valley and 1992 St. George earthquakes are most likely on the also west-dipping fault plane of the Hurricane fault, the surface trace of which lies several kilometers east of the Washington fault zone surface trace (see figure 1).*

SURFICIAL GEOLOGY OF THE FORT PEARCE AND WASHINGTON HOLLOW SECTIONS OF THE WASHINGTON FAULT ZONE, WASHINGTON COUNTY, UTAH, AND MOHAVE COUNTY, ARIZONA

by
Tyler R. Knudsen
Utah Geological Survey

CONTENTS

ABSTRACT....19
INTRODUCTION....20
PREVIOUS WORK....22
METHODS....23
GEOLOGY OF THE FORT PEARCE AND WASHINGTON HOLLOW SECTIONS OF THE WASHINGTON FAULT ZONE....24
Fort Pearce Section....24
Quail Hill to Fort Pearce Wash....24
Fort Pearce Wash to Washington City....26
Mokaac Strand....30
Dutchman Draw Strand....32
Washington Hollow Section....33
RELATION BETWEEN THE WASHINGTON FAULT ZONE AND OTHER TRANSITION ZONE FAULTS....35
SUMMARY....37
ACKNOWLEDGMENTS....38
REFERENCES....38

FIGURES

Figure 1. Washington fault zone and fault sections in southwestern Utah and northwestern Arizona as defined in this study....44
Figure 2. Lithologic column of geologic units that crop out in the map area....45
Figure 3. 7.5-minute geologic quadrangle map coverage of the Fort Pearce and Washington Hollow sections of the Washington fault zone....46
Figure 4. The Washington fault zone places Fossil Mountain Member over the younger Harrisburg Member....47
Figure 5. Obsequent fault scarp formed along the Washington fault zone....48
Figure 6. A splay of the Washington fault zone exposed in a stream cut....49
Figure 7. Oblique aerial view of a scarp formed in Triassic bedrock and Quaternary unconsolidated deposits....50
Figure 8. Oblique aerial view of fault scarp formed on the Washington lava flow....51
Figure 9. Splay of the Washington fault zone exposed in a stream cut north of Washington City....52
Figure 10. Major splay of the Washington fault zone within the Navajo Sandstone....53
Figure 11. Dutchman Draw fault exposed on the southwest flank of an unnamed mesa in Arizona....54
Figure 12. Summary of geologic mapping of the Washington fault zone and Washington Hollow fault between Interstate 15 and the Pine Valley Mountains....55
Figure 13. Joints of probable Cretaceous age near Washington Hollow that are unaffected by the Washington fault zone....56
Figure 14. Displacement map of faults in the Colorado Plateau-Basin and Range

transition zone in southwestern Utah and northwestern Arizona. 57
Figure 15. Schematic block diagram of the Colorado Plateau-Basin and Range transition zone in southwestern Utah and Northwestern Arizona. 58

PLATES

Plate 1. Surficial geologic map of the Fort Pearce and Washington Hollow sections of the Washington fault zone, Washington County, Utah, and Mohave County, Arizona.

APPENDIX

Appendix A – Description of map units 59

ABSTRACT

The 97-km-long Washington fault zone is one of several west-dipping normal faults in the structural and seismic transition between the Colorado Plateau and Basin and Range physiographic provinces. As defined by previous workers, the Northern section of the Washington fault zone extends from the southern margin of the St. George basin in northwestern Arizona northward into southwestern Utah and terminates near Washington City. New surficial geologic mapping reveals minor structures linking the Northern section of the Washington fault zone with the west-dipping Washington Hollow fault zone that extends north of Washington City and across the southwestern shoulder of the Pine Valley Mountains, indicating the two faults are part of the same tectonic structure. However, minimal displacement, structural complexity, and a 45° change in fault strike between the Washington Hollow and Washington fault zones indicate the Washington Hollow fault is likely a separate section of the Washington fault zone that I redefine as the Washington Hollow section. Because the previously defined Northern section is no longer the northernmost section of the Washington fault zone, to avoid confusion, I herein propose renaming the Northern section the Fort Pearce section. Geologic-map relations indicate the boundary of the Fort Pearce section with the Sullivan Draw section to the south is best placed near the head of Quail Canyon where a 50° change in strike is accompanied by a large change in vertical displacement along the fault. The lengths (straight line) of the newly defined Fort Pearce and Washington Hollow sections are 37 and 22 km, respectively.

The west-dipping Mokaac and Dutchman Draw faults, each about 16 km long, branch from the Fort Pearce section in Arizona, and have been discussed as separate faults or sections (Mokaac section) of the Washington fault zone in previous paleoseismic studies. Because the Dutchman Draw and Mokaac faults have the greatest displacement near their junction with the Fort Pearce section, and because they appear to have similar slip rates, I redefine the Dutchman Draw and Mokaac faults as strands of the Fort Pearce section of the Washington fault zone rather than individual faults or fault sections capable of independent earthquake rupture.

The surface expression of the Fort Pearce section is dominated by prominent bedrock escarpments up to 250 m high. The scarps are chiefly fault-line scarps created by erosional retreat of softer bedrock exposed in the fault hanging wall. Because the geomorphology of the St. George basin is dominated by erosion, fault scarps on unconsolidated deposits are rare and isolated. Detailed surficial mapping identified two previously unknown fault scarps formed on late Pleistocene to Holocene alluvial deposits in Arizona. One site is on the main strand of the Fort Pearce section and the other is on a subsidiary fault of the Mokaac splay of the Fort Pearce section. The remaining known scarps on unconsolidated deposits along the Fort Pearce section in Utah and Arizona appear to be bedrock cored. The Washington Hollow section has formed two scarps up to 8 m high on Pleistocene alluvial deposits; Holocene alluvial deposits are not displaced. The Washington Hollow section displaces a 1.2 Ma basalt flow 12 m, yielding a Pleistocene-Holocene vertical slip rate of 0.01 mm/yr.

Geologic-map patterns, slip budgets, and structural similarities among the Washington, Main Street, Hurricane, Grand Wash, and other lesser faults indicate that most or all transition-zone normal faults in the study area may be structurally linked and part of the same tectonic system. Several lines of evidence support a model where the Colorado Plateau-Basin and Range

boundary in this area initially developed along the Grand Wash fault in the early to middle Miocene. Beginning in the Pliocene, the locus of tensional stress migrated eastward eventually initiating movement on the Hurricane fault. Internal strain within the intervening block became great enough by the Pleistocene to create the Washington, Main Street, and other lesser faults. The nature of structural linkage among the transition zone faults and whether the faults sole into a regional master detachment remain unknown.

INTRODUCTION

The Washington fault zone is one of several north- to northeast-striking, west-dipping normal faults within the structural transition zone between the Colorado Plateau and Basin and Range physiographic provinces (figure 1). In terms of displacement and length, the Washington fault zone is a relatively minor structure compared to larger faults in the transition zone, namely the Hurricane and Sevier-Toroweap faults to the east, and the Grand Wash/Gunlock fault to the west. The Washington fault zone bisects the St. George structural block, which is bounded by these larger faults. The Washington fault zone extends for 97 km (straight line) from the southwest flank of the Pine Valley Mountains in southern Utah southward through the St. George Basin and into the Shivwits Plateau of northern Arizona (figure 1). In Utah, the fault trends directly through downtown Washington City and the rapidly urbanizing Washington Fields area, where the fault crosses the Virgin River and truncates the southwest part of the Sevier-age Virgin anticline. South of Washington City, the Washington fault zone parallels Warner Ridge until crossing Fort Pearce Wash near the Utah-Arizona border (figure 1). The fault continues into Arizona where it has formed high bedrock escarpments traversing the southern part of the St. George Basin. Farther south, the fault forms a conspicuous graben within the Shivwits Plateau.

Bedrock exposed along the Washington fault zone ranges in age from the Permian Queantoweap Sandstone to Quaternary basalt flows (figure 2; see appendix A for unit descriptions). The rock units represent an over 4000-m-thick section of chiefly marine and continental rock types that include limestone, mudstone, claystone, shale, sandstone, conglomerate, evaporite, and basalt. Previous workers reported maximum displacements on the Washington fault zone ranging from 500 m (Billingsley, 1992a) to 750 m (Anderson and Christenson, 1989) at, or just south of, the Utah-Arizona border. Displacement decreases northward to an estimated 455 m about 5 km north of the border (Hayden, 2005), and to about 210 m near Washington City (Willis and Higgins, 1995) before the fault bifurcates and becomes obscured within the thick Jurassic Navajo Sandstone. South of the displacement maximum, displacement decreases to about 400 m in the Quail Canyon area (Billingsley, 1990b), and to about 76 m near Wolf Hole Lake (Billingsley, 1990b) (figure 1). The fault displays minor offset (< 50 m) for another 30 km southward before dying out at the head of Sullivan Draw on the Shivwitz Plateau (Billingsley and Workman, 2000; Billingsley and Wellmeyer, 2003).

Previous workers have subdivided the Washington fault zone in Arizona into three sections based on amount of displacement and scarp morphology. Menges and Pearthree (1983) defined the Seegmuller Mountain section as extending from Quail Hill to the Utah-Arizona border (figure 1) (the spelling of Seegmiller Mountain varies from Seegmuller, Segmiller, to

Seegmiller, depending on publication or U.S. Geological Survey [USGS] quadrangle map; I use Seegmiller hereafter because it appears on the most recent USGS 7.5-minute quadrangle map). They defined the Sullivan Draw section extending south from Quail Hill to the fault's southern terminus near the head of Sullivan Draw on the Shivwitz Plateau. In Arizona, Menges and Pearthree (1983) defined a prominent fault that is subparallel to the Washington fault zone to the west as the Mokaac Wash section. The Mokaac Wash section has a maximum displacement of about 400 m near its junction with the main Washington fault zone about 5 km south of the Utah border. Pearthree (1998) renamed the Seegmuller segment the Northern section and the Mokaac Wash segment the Mokaac section. He left the Sullivan Draw section name unchanged. Since we discovered no likely section boundaries along the Washington fault zone from the Utah border north into Washington City (figure 1), we expand the definition of the Northern section to include that part of the fault in Utah. Additionally, since I define a new northernmost section of the Washington fault zone (Washington Hollow section) in this study (see below), I propose changing the name of the Northern section to the Fort Pearce section.

About 6 km south of the Mokaac/Fort Pearce section intersection, a second prominent fault branches from the Fort Pearce section and extends 16 km to the northeast (figure 1). Hamblin and Best (1970) first mapped the fault, which Menges and Pearthree (1983) later named the Yellowhorse Flat fault zone. Billingsley (1992a, 1992b) mapped the splay in greater detail and renamed it the Dutchman Draw fault. The fault has a maximum displacement of about 115 m near its intersection with the Fort Pearce section (Billingsley, 1992a). Displacement decreases to about 15 m at the Utah border shortly before being obscured by Quaternary surficial deposits. The structural relation between the Fort Pearce section and the Dutchman Draw fault is analogous to the relation between the Fort Pearce section and Mokaac strand (see above); I therefore redefine the Dutchman Draw fault as the Dutchman Draw strand of the Fort Pearce section.

North of Washington City, Willis and Higgins (1995) and Hacker [in preparation (a)] mapped the northwest-trending, west-dipping Washington Hollow fault traversing the southwest shoulder of the Pine Valley Mountains (1). Willis and Higgins (1995) estimated the fault has about 150 m of displacement, and they discussed the possibility that the fault may connect to the Washington fault zone through a wide breccia zone in Washington Hollow (figure 1). Results of this mapping show the Washington Hollow and Washington fault zones are parts of the same fault zone, and I herein define the Washington Hollow fault as the northernmost section of the Washington fault zone.

The accompanying 1:50,000-scale surficial geologic map (plate 1) provides new information on the location and length of young surface ruptures and the relative ages of displaced surficial deposits along the Fort Pearce and Washington Hollow sections of the Washington fault zone. This report and map can be used to better define the location of the Fort Pearce and Washington Hollow sections, their major strands, and their section boundaries, which will be useful to planners, geologists, and engineers involved in reducing surface-fault-rupture risk to future development.

PREVIOUS WORK

Dobbin (1939) named and mapped the Utah portion of the Washington fault zone as part of a structural-geologic study of the St. George area. He recognized three key fault characteristics: (1) the fault displaces the Cretaceous Virgin anticline, (2) fault displacement in Utah increases southward into Arizona, and (3) the fault, in places, consists of multiple splays. Cook (1960) included the Washington fault zone on his geologic map of Washington County, and reported an estimated 2500 ft (760 m) of throw at the state line. The Washington fault zone appears on Hintze's (1963) *Geologic Map of Southwestern Utah* and Stokes and Heylmun's (1963) tectonic map of southwestern Utah. A regional gravity survey and Bouguer gravity anomaly map by Cook and Hardman (1967) shows only a minor deflection of gravity contours across the fault, consistent with a mostly bedrock-against-bedrock fault with thin surficial cover on the downthrown block. Hamblin (1970a) described the Washington fault zone as a "small-scale version" of the Hurricane fault, noting that the two faults have parallel surface traces with salients and reentrants at roughly the same latitudes. He also noted that the fault zone cuts a Tertiary basalt flow (newly acquired $^{40}Ar/^{39}Ar$ radiometric ages indicate an early Quaternary age for this basalt flow; see Lund and Knudsen this volume) on the south side of Seegmiller Mountain, and that most of the relief across the fault is due to differential erosion rather than tectonic displacement. Hamblin and Best's (1970) photogeologic map accompanying their field-trip road log of the St. George Basin-Shivwits Plateau region, provides the earliest detailed mapping of the Washington fault zone in Arizona. Hamblin (1963, 1970b), Best and Brimhall (1970), and Best and Hamblin (1970) distinguished and described basalt flows in the western Grand Canyon region based on relative age and geochemistry, providing a framework for developing relative timing relations for the Washington and nearby faults. Best and others (1980) and Wenrich and others (1995) refined relative basalt ages in the western Grand Canyon region with K-Ar radiometric dating. Cordova (1978) mapped a portion of the Washington fault zone near Washington City as part of a groundwater investigation of the Navajo Sandstone in Utah.

As part of a seismic-safety investigation of several U.S. Soil Conservation Service (now Natural Resources Conservation Service) dams in southwestern Utah, Earth Sciences Associates, Inc. (ESA, 1982; Bowman and others, 2011) excavated several trenches across Washington-fault-zone-related lineaments at Gypsum Wash dam east of Washington Fields in Utah (plate 1). Based on soil development and stratigraphy, ESA estimated relative ages of faulted Quaternary deposits and concluded that the Washington fault zone at Gypsum Wash has had late Pleistocene movement and likely Holocene movement.

Peterson (1983) produced the only previous study that focused solely on the Washington fault zone. His detailed structural analysis and accompanying map cover the fault zone in Arizona from the state line to Wolf Hole Lake. Major conclusions of his report include: (1) basalts of at least two different ages are displaced by the fault zone (Stage I and II flows of Hamblin [1963]), (2) south of the state line, several splays comprise a 4-km-wide fault zone where "maximum displacement commonly shifts from one fault plane to another," (3) the fault planes, where exposed, are steeply west dipping, (4) slickensides show nearly pure dip-slip movement, (5) differential erosion caused by juxtaposition of units with differing mechanical properties is the main factor controlling scarp development rather than fault displacement, (6) although both normal and reverse drag is common along the fault, reverse drag is more

extensive, and (7) in more brittle rocks, reverse drag is expressed as antithetic faulting and graben formation.

Christenson and Deen (1983) mapped portions of the Washington fault zone near St. George and Washington City for their report on the engineering geology of that area. They recognized that subsidiary faults displace the Washington basalt flow on the west end of Washington Black Ridge.

Menges and Pearthree (1983) prepared a neotectonic map for Arizona that includes the Washington fault zone. Based on multiple scarp profiles, landform analysis of bedrock scarps, and the estimated ages of faulted and unfaulted geologic units, they concluded that the most recent faulting from near the Utah-Arizona border to the intersection with the Dutchman Draw fault is late Pleistocene or younger. South of the fault intersection, they estimated the most recent faulting to be middle Pleistocene or younger. Their inset map of the fault zone implies that several scarps are developed on "alluvial piedmonts" including one about 2 km north of the Utah border. Analysis of scarp profiles from these sites yielded scarp ages ranging from late Pleistocene to early Holocene.

As part of an inventory of Quaternary structures in the Cedar City 1° x 2° quadrangle, Anderson and Christenson (1989) made a reconnaissance study of the Washington fault zone in Utah. They reported rake angles of striations ranging from pure dip-slip to 50° south, indicating possible sinistral (left lateral) movement, and identified portions of the fault that are east dipping, indicating a local reverse sense of movement. They concluded that a prominent fault scarp north of Interstate 15 in Washington City is due largely to differential erosion rather than to tectonic movement, which indicates that little displacement has occurred on that portion of the fault in late Quaternary time. South of Washington City, they profiled a scarp developed in a thin mixed alluvial-colluvial deposit, and by comparing the profile to Lake Bonneville shoreline scarps with similar morphologies, estimated the scarp age as late Pleistocene.

The Washington fault zone and major splays have been mapped at 1:24,000 scale in Arizona by Billingsley (1990a, 1990b, 1991a, 1991b, 1992a, 1992b). Recent 1:24,000-scale geologic mapping by the Utah Geological Survey (UGS) of the Washington Dome (Hayden, 2005), St. George (Hayden and Willis, 2011), Harrisburg Junction (Biek, 2003), and Washington (Willis and Higgins, 1995) quadrangles includes portions of the trace of the Washington fault zone in Utah.

METHODS

The *Surficial Geologic Map of the Fort Pearce and Washington Hollow Sections of the Washington Fault Zone, Washington County, Utah, and Mohave County, Arizona* that accompanies this report (plate 1) combines new surficial geologic mapping accomplished for this study and bedrock geology compiled from existing geologic quadrangle maps (figure 3). Because the pre-existing geologic mapping did not focus primarily on late Cenozoic surface faulting, our new map emphasizes late Cenozoic unconsolidated deposits and volcanic rocks, and their relation to displacement on the Fort Pearce and Washington Hollow sections of the

Washington fault zone. The primary aerial photography sets used for mapping were 1981 1:24,000-scale a.m. and p.m. low-sun-angle photos (ESA, 1982, compiled by Bowman and others, 2011), 1983 1:24,000-scale color photos (IntraSearch, 1983), and 2002 Bureau of Land Management 1:24,000-scale color photos (Bureau of Land Management, 2002).

GEOLOGY OF THE FORT PEARCE AND WASHINGTON HOLLOW SECTIONS OF THE WASHINGTON FAULT ZONE

Fort Pearce Section

Quail Hill to Fort Pearce Wash

Previous workers placed the Sullivan Draw-Fort Pearce section boundary at Quail Hill (Menges and Pearthree, 1983; Pearthree, 1998) (figure 1), where there is a significant change in the Washington fault zone's surface expression. South of Quail Hill, the fault zone is near the base of the east-facing slope of Wolf Hole Mountain. North of Quail Hill, the fault defines an increasingly higher, west-facing escarpment formed on Permian Kaibab limestone. The change in morphology at Quail Hill is likely caused by differential erosion of rocks with varying resistance to erosion on opposite sides of the fault. South of Quail Hill, the easily eroded Harrisburg Member of the Permian Kaibab Formation is in fault contact with the equally weak and easily eroded Shnabkaib Member of the Triassic Moenkopi Formation, resulting in little relief across the fault. Escarpment formation in that area is controlled by differential erosion of the resistant Pliocene Wolf Hole lava flow which caps Wolf Hole Mountain to the west (plate 1). North of Quail Hill, the Washington fault zone juxtaposes resistant limestone of the Fossil Mountain Member of the Kaibab Formation in the footwall against colluvium- and alluvium-mantled, easily eroded shale of the Harrisburg Member and Moenkopi Formation in the hanging wall. Differential erosion along the fault has formed a west-facing escarpment that rises from no relief at Quail Hill to 250 m high at a prominent bend in the fault less than 3 km to the north. The fault's 50° change in strike from north-northwest to north-northeast at the bend is accompanied by a rhombic pattern of secondary faults in the footwall.

Since the change in scarp morphology at Quail Hill is due chiefly to differential erosion, and has no apparent tectonic implications, I propose that the Fort Pearce-Sullivan Draw section boundary be placed at the prominent fault bend 3 km to the north. The fault bend is also coincident with where Billingsley (1990b) showed an abrupt north-to-south decrease in fault displacement from 167 m at a point about 0.8 km north of the bend to 122 m about 1 km south of the bend.

North of the fault bend, escarpment height increases to about 300 m. The main fault trace is positioned about midway up the cliff face and is poorly exposed due to partial cover by colluvium and slope-wash deposits. Where exposed, the fault plane is nearly vertical and, in some places, dips steeply to the east (Billingsley, 1993). About 4.5 km northeast of the bend, a short section (~ 170 m long) of the fault appears to have vertically displaced alluvial and

colluvial deposits (Qca) up to 1.5 m (station 1, plate 1). However, the deposits appear to be only a few meters thick and the scarp is likely bedrock cored at shallow depth.

About 5 km northeast of the fault bend a 5-km-long by 0.5-km-wide lava flow remnant ($Tbqd_1$) in the fault hanging wall is in fault contact with Harrisburg Member in the fault footwall (plate 1). The hanging-wall basalt acts as a protective caprock that preserves nearly a full section of Moenkopi Formation above the otherwise stripped Kaibab surface below. There, the large topographic escarpment along the fault (~ 300 m high) is shifted to the western edge of the flow remnant with essentially no scarp development along the fault itself (Peterson, 1983). The flow has been interpreted by previous workers (e.g., Billingsley and Workman, 2000; Downing and others, 2001) to be a displaced remnant of the 2.4 Ma (see Lund and Knudsen this volume) Seegmiller Mountain flow, which caps Seegmiller Mountain on the fault footwall to the south. However, a new $^{40}Ar/^{39}Ar$ age of 2.9 Ma obtained for the flow as part of this investigation (sample QD1 on plate 1; Lund and Knudsen this volume) indicates the elevated flow remnant is significantly older and therefore cannot be part of the Seegmiller Mountain flow. Additionally, Billingsley's (1990a, 1993) mapping and plate 1 show a vent area ($Tbqdc_1$ on plate 1) within the flow remnant indicating a local source for the flow.

Near the north end of the remnant flow, the Dutchman Draw fault branches to the northeast from the Washington fault zone which continues to the north-northeast. Since results of this mapping indicate the Dutchman Draw fault is better defined as a strand of the Fort Pearce section rather than as an independent fault (see Dutchman Draw discussion below), hereafter, it is called the Dutchman Draw strand.

North of the intersection with the Dutchman Draw strand, the Fort Pearce section consists of one to three closely spaced splays that have formed steep cliffs on the Kaibab Formation. Starting at a point about 2 km north of the intersection with the Dutchman Draw strand, the westernmost splay forms a nearly continuous 1- to 2-m-high bedrock fault scarp extending to the north for about 3 km. This splay places colluvium-mantled, older alluvial-fan deposits against the Kaibab Formation. The scarp appears sharp and relatively young on aerial photography, but is less well-expressed in the field due to partial cover by colluvium and slope-wash deposits. The fault is well exposed in several drainages, revealing a steeply east-dipping fault plane (figure 4). One possibility for the apparent reverse sense of faulting is that the steeply west-dipping fault at depth may take advantage of pre-existing east-dipping fracture sets within resistant Kaibab limestone as the fault projects to the surface. Several slickenlines exposed in the fault zone indicate nearly pure dip-slip movement. This area exhibits the greatest stratigraphic offset documented anywhere along the Fort Pearce section, with the Fossil Mountain Member of the Kaibab Formation in fault contact with the upper red member of the Moenkopi Formation, resulting in a maximum throw of about 660 m (Peterson, 1983).

Near Dutchman Draw (figure 1), the Fort Pearce section consists of two sub-parallel splays that have produced moderately high bedrock escarpments about 300 m apart. The eastern splay is chiefly a bedrock fault juxtaposing various members of the Kaibab and Moenkopi Formations. Short sections (< 300 m) of the eastern splay are overlain by unfaulted, mid-Pleistocene to Holocene colluvium/slope-wash (Qca) and pediment deposits (Qap).

The western splay generally defines a bedrock-alluvium contact between a moderately high bedrock escarpment to the east and a broad alluvial plain to the west. About 0.6 km south of Dutchman Draw, the eastern splay displaces a late Pleistocene to Holocene alluvial fan (Qaf_2) for a distance of approximately 100 m (plate 1). The scarp is up to 4 m high and is the location of a detailed UGS paleoseismic trenching investigation (Lund and others this volume).

The Mokaac fault joins the Fort Pearce section from the southwest near Dutchman Draw (plate 1). Since results of this mapping show that the Mokaac section (Pearthree, 1998) is better defined as a strand of the Fort Pearce section rather than as an independent fault section (see Mokaac Fault discussion below), hereafter, it is called the Mokaac strand.

Several mafic lava flow remnants ($Qbdd_1$ and $Qbdd_2$) cap low mesas (12-60 m high) west of the Fort Pearce section near Dutchman Wash. The flow remnants overlie upper members of the Moenkopi Formation and the Triassic Chinle Formation. Although the flow remnants have not been dated, new geochemical analyses (Lund and Knudsen this volume) indicate likely correlations between the flow remnants west of Dutchman draw and flows to the south and southeast on the footwall of the Fort Pearce section. The remnants northwest of the Mokaac strand ($Qbdd_1$) appear to be correlative with either the 1.75 Ma ($^{40}Ar/^{39}Ar$) West Mesa or the 1.28 Ma ($^{40}Ar/^{39}Ar$) East Mesa (Qbe) lava flows about 5-8 km to the southeast (Lund and Knudsen this volume). The flow remnant bounded by the Mokaac strand and Fort Pearce section ($Qbdd_2$ on plate 1) appears to be correlative to the 2.4 Ma ($^{40}Ar/^{39}Ar$) Seegmiller Mountain flow (Qbs), more than 9 km to the south (plate 1; Lund and Knudsen this volume). These correlations allow calculation of long-term vertical-slip-rate estimates across all three strands (main, Mokaac, Dutchman Draw) of the Fort Pearce section; slip rate calculations are discussed in Lund and Knudsen (this volume).

Near the displaced alluvial fan, a significant change in escarpment morphology and near-fault bedrock deformation coincides with a change in the dominant geologic unit exposed in the fault footwall. South of the displaced fan, the main fault escarpment exposes the resistant Fossil Mountain Member of the Kaibab Formation and is over 100 m high. A narrow zone of footwall normal drag is expressed as closely spaced, down-to-the-west subsidiary faults in rhombic to anastomosing patterns. North of the displaced fan, the main escarpment consists of easily eroded, gypsiferous mudstone and siltstone of the Harrisburg Member of the Kaibab Formation and the lower red member of the Moenkopi Formation, resulting in an escarpment height typically less than 30 m. A narrow zone of footwall fault drag is expressed in generally unfaulted bedrock that exhibits sharp monoclinal folding and near-vertical bedding in exposures close to the fault zone.

North of the displaced fan, the main trace of the Fort Pearce section is typically buried beneath alluvial deposits, but for short distances (< 500 m) is expressed as a bedrock-against-bedrock fault, or bedrock-against-alluvium contact. Displaced unconsolidated deposits are not mapped again for several kilometers into Utah.

Fort Pearce Wash to Washington City

Just north of Fort Pearce Wash near the Utah-Arizona border (figure 1), the Fort Pearce section makes a 35° bend to the west and trends N. 14° W. Hayden (2005) estimated normal

separation at the border to be 500 m. The regional dip of strata north of Fort Pearce Wash is generally to the east as part of the eastern limb of the Cretaceous Virgin anticline. Normal down-to-the-west drag in the fault footwall superimposed on the regional east-dipping Moenkopi strata has produced a narrow anticline that parallels the fault. In a number of places, anticlinal closure has been attained east of the fault zone (Hayden, 2005) (Punchbowl and Beehive Domes, plate 1).

Near the fault bend about 1 km north of the border, a 1- to 2-m-high and 240-m-long, east-facing obsequent fault scarp has formed where soft mudstones of the middle red member of the Moenkopi Formation in the fault footwall have eroded faster than mixed alluvial and eolian deposits (unit Qae) in the hanging wall to the west (figure 5; station 2, plate 1).

North of the obsequent scarp, the fault zone resumes a west-facing scarp configuration. The scarp maintains a 2- to 14-m-high and steep (30-45°) geometry for about 7 km where the Shnabkaib Member of the Moenkopi Formation in the footwall is in fault contact with easily eroded mudstone of the Moenave Formation and mixed alluvial and eolian deposits in the hanging wall. The continuous and prominent scarp is most likely a fault-line scarp produced by differential erosion rather than surface faulting—a conclusion also reached by previous investigators (e.g., Peterson, 1983; Anderson and Christenson, 1989; Hayden, 2005).

At a point about 3 km north of the border, the Fort Pearce section bifurcates into several splays for a distance of less than 350 m (station 3, plate 1). A stream cut exposes a splay that places vertical upper red member Moenkopi strata in fault contact with highly deformed alluvial and eolian deposits (figure 6). The unconsolidated deposits are deformed in a 3-m-wide zone that includes shears, antithetic faulting, and rotated clasts. The faulted unconsolidated deposits have weak carbonate soil morphology and are estimated to be late Pleistocene to early Holocene in age. The faulted units have been beveled and covered by unfaulted stream deposits that are estimated to be middle to late Holocene in age. No scarp is present at the surface.

A bouldery mixed colluvial and alluvial deposit (map unit Qcao) appears to be vertically displaced 3.5 m by the fault about 1.5 km south of the Washington Fields-Warner Valley Road junction (Anderson and Christenson, 1989; Hayden, 2005; station 4, plate 1; figure 7). The scarp is less than 30 m long where formed on Quaternary sediments, but continues to the north and south where it is developed on the Shnabkaib Member. Stream cuts across the scarp reveal that it is bedrock cored, and that the overlying mixed colluvial and alluvial deposit is generally less than 1 m thick. Anderson and Christenson (1989) profiled the scarp and found the slope angle and height comparable to those of a 13,000-year-old Lake Bonneville shoreline, and therefore estimated that the scarp formed in the late Pleistocene. Since the scarp is continuous with the prominent bedrock scarp to the south, which I and others (including Anderson and Christenson, 1989) consider an erosional fault-line scarp, I conclude that the scarp, while appearing to be developed on Quaternary sediments, is actually the result of differential erosion of the underlying bedrock rather than surface fault rupture. Therefore, I consider Anderson and Christenson's (1989) age estimates erroneous. The thin mantle of unconsolidated material, which includes abundant Shinarump boulders up to 1 m in diameter, draped over the scarp may have slowed scarp formation locally since less than 100 m to the south, the scarp quadruples in height to about

14 m where the Dinosaur Canyon Member of the Moenave Formation in the footwall is in fault contact with the Shnabkaib Member of the Moenkopi Formation in the hanging wall.

Near Warner Valley Road, the Fort Pearce section consists of several west-dipping splays. Low bedrock scarps indicate the presence of the splays, but I observed no definitive displacement of Quaternary deposits. In 2009, Simon Bymaster, Inc. excavated 13 trenches to evaluate the surface-fault-rupture hazard to part of a proposed Utah Department of Transportation (UDOT) freeway alignment and three elevated interchanges that were either astride or near surface traces of the Fort Pearce section (see plate 1 for trench locations). Simon Bymaster, Inc. excavated 11 trenches along the westernmost splays near Warner Valley Road, and two additional trenches to the north near the Gypsum Wash flood-control dam (plate 1). See Simon and others (this volume) for details of their surface-fault-hazard investigation.

North of Warner Valley Road and in the vicinity of the Gypsum Wash dam, the expression of the Fort Pearce section becomes more subdued and is mapped as a concealed fault (plate 1). Aside from a few short (< 125 m long) bedrock scarps, any fault scarps formed on Quaternary deposits that may have existed in this area are now obscured by dam construction. As part of a seismic-safety investigation of the Gypsum Wash dam, ESA (1982) excavated several trenches (see plate 1 for trench locations) across photolineaments near the dam's foundation. ESA excavated two trenches across what they considered a "major trace" of the fault zone and exposed a near-vertical shear plane displacing gypsiferous shale bedrock, an "older alluvial fan" deposit, and an overlying "younger alluvial fan" deposit. The absence of datable material in the trenches prevented ESA from refining their relative age assessments (which were based on soil development) beyond their "younger" and "older" categories, which they estimated to be 5000-10,000 years old and 10,000-25,000 years old, respectively. The bedrock was displaced below the floor of the trench in the fault hanging wall, indicating a minimum displacement of 1.2 m. The fault displaced young alluvium above the bedrock about 5 cm before dying out within 0.6 m of the ground surface. ESA stated that the 5 cm of displacement in the young alluvium could be either tectonic or due to differential compaction across the fault plane. Trenches excavated farther west revealed several east- and west-dipping faults that offset stratified late Pleistocene "older alluvium" up to several feet. Overlying "young alluvium" estimated to be Holocene in age was unfaulted. ESA (1982) found no datable material to constrain rupture timing, but concluded that the Washington fault zone at Gypsum Wash has had late Pleistocene and likely Holocene movement.

North of Gypsum Wash dam, the Fort Pearce section truncates the southern nose of the Washington Dome portion of the Virgin anticline. At the intersection, a heavily dissected bedrock escarpment formed on the Harrisburg Member of the Kaibab Formation and lower Moenkopi Formation strata is about 450 m long. The exact position of the fault in this area was unknown until Applied Geotechnical and Engineering Consultants (AGEC) excavated five trenches across the concealed trace of the fault zone near the bedrock escarpment as part of a surface-fault-rupture-hazard investigation for a proposed residential development (see plate 1 for trench locations). Trench T-1 exposed the main trace of the fault zone. The UGS made a brief reconnaissance investigation of the exposed fault and collected several samples of colluvial/eolian sand from within, above, and below what were interpreted to be faulting-related colluvial wedge deposits and submitted them to the Optically Stimulated Luminescence (OSL)

Geochronology Laboratory at Utah State University for age analysis. Results of reconnaissance logging and OSL analysis indicated that the Fort Pearce section has likely experienced at least three surface-faulting earthquakes at this site since 76 ka, the most recent possibly in latest Pleistocene time (Lund and others, 2008). The trench, which remained open for several years, was later logged in detail by Simon Bymaster, Inc., as part of their surface-fault-rupture-hazard investigation for UDOT (Simon and others this volume).

North of Washington Dome, the Fort Pearce section traverses the eastern margin of Washington Fields—a relatively flat, low-lying agricultural area south of the Virgin River that is rapidly being converted to residential development. Any surficial expression of the fault that may have existed in this area has been destroyed, and the main fault is mapped as concealed beneath Quaternary deposits (Qae) (plate 1).

A 1.5-km-long, west-dipping, subsidiary fault splay exposed in Moenkopi strata parallels the main Fort Pearce section less than 0.5 km east of Washington Fields. The subsidiary splay has formed a well-defined, linear bedrock scarp where the middle red member of the Moenkopi Formation is in fault contact with the Virgin Limestone Member to the east. The escarpment is clearly visible on 1983 color aerial photos, but has been destroyed by residential development in recent years. Additionally, the 1983 aerial photos show a 25-m-long section of the scarp developed in mixed alluvial and eolian deposits (Qae; station 5, plate 1). Because the subsidiary splay is buried by the same map unit immediately to the north, it is likely that the Quaternary sediments forming the scarp are unfaulted and draped over a preexisting bedrock scarp rather than displaced by surface faulting.

North of the Virgin River, the Fort Pearce section is mapped as concealed where it parallels the linear western end of Washington Black Ridge. Highly deformed mudstones and sandstones of the Chinle Formation exposed in road cuts along Washington Field Road indicate that the main fault is likely coincident with the roadway at the base of the ridge.

Washington Black Ridge is capped by the Washington lava flow, which has $^{40}Ar/^{39}Ar$ radiometric ages of 0.87 and 0.98 Ma (Biek and others, 2009). The flow erupted from a cinder cone 5 km north of Washington City, flowed south along the ancestral Grapevine Wash, and then flowed west along the ancestral Virgin River (plate 1). The downstream termination of the flow coincides with the main trace of the Fort Pearce section, and is within 500 m of the north-to-south-flowing Mill Creek drainage. Anderson and Christenson (1989) proposed three possible explanations for the Washington flow's termination: (1) the distal end of the flow has been displaced down to the west by the Washington fault zone and subsequently buried by alluvium, (2) the western continuation of the flow has been eroded away by Mill Creek, and (3) the flow terminated at its present location and never extended across the fault. I researched the Utah Division of Water Right's water-well database (Utah Division of Water Rights, 2011) for wells drilled along the projected downthrown continuation of the Washington flow near Mill Creek. Drillers' logs for two water wells immediately west of Mill Creek in the SW1/4NW1/4 section 23, T. 42 S., R. 15 W. and the NW1/4SW1/4 section 23, T. 42 S., R. 15 W., Salt Lake Base Line and Meridian (see plate 1 for approximate locations) show unconsolidated alluvium to a depth of 30 m. If the Washington flow is present beyond Mill Creek, it is more than 30 m below the surface, which would result in more than 90 m of displacement when compared to the flow

capping Washington Black Ridge which stands an additional 60 m above stream level. I consider the evidence inconclusive for any of the three flow termination scenarios proposed by Anderson and Christenson (1989).

Four subsidiary fault splays 0.5 km east of the main Fort Pearce section displace the Washington flow up to 4.5 m (Anderson and Christenson, 1989; Hayden, 2005; figure 8). Two of the smaller scarps have been destroyed by residential development in recent years.

The Fort Pearce section is obscured by development where it traverses through Washington City; however, late 1930s-era aerial photos (Utah Automated Geographic Reference Center, 2012a) show that the main trace defines the western edge of a low, poorly defined, mostly bedrock escarpment through the town.

Near Interstate 15, the Fort Pearce section consists of three parallel, northwest-trending splays that form prominent but discontinuous scarps. The western splay is considered the main fault because it juxtaposes Kayenta Formation and Navajo Sandstone indicating about 200 m of stratigraphic separation, and because that splay has substantial footwall and hanging-wall deformation associated with it. In contrast, the middle and eastern splays are wholly contained within the Kayenta Formation, and appear to have only a few tens of meters of displacement.

Despite sharp, up to 8-m-high scarps formed on all three splays near Interstate 15, I consider scarp formation there to result from differential erosion rather than fault rupture. Anderson and Christenson (1989) investigated the middle splay and concluded that the scarp is the result of accelerated erosion of hanging-wall bedrock that has been weakened by groundwater seepage from springs and intense fracturing rather than surface faulting. I agree with their assessment, which explains the anomalously short length (~ 400 m) of the 8-m-high scarp.

Just north of a residential development, an ephemeral stream incises a scarp formed on the middle splay and exposes the fault, which dips 65° southwest and juxtaposes middle parts of the Kayenta Formation (figure 9; station 6, plate 1). The faulted bedrock has been beveled by erosion, and is covered with about 0.5 m of moderately indurated sand with a strongly-developed pedogenic carbonate soil horizon (Qecl) estimated to be middle to late Pleistocene in age (Anderson and Christenson, 1989; Willis and Higgins, 1995). The calcic sand unit is unbroken, indicating that this part of the fault zone has likely not ruptured since at least the late Pleistocene.

North of Washington City, the Fort Pearce section continues to bifurcate as it enters an area of densely jointed Navajo Sandstone. Beyond the Washington City water tanks (plate 1) fault displacement is contained entirely within the homogeneous Navajo Sandstone and becomes difficult to map. Closely spaced joint sets that parallel the fault splays are difficult to differentiate from faults on aerial photos (figure 10). Also complicating mapping in this area are large sheets of eolian sand that bury the fault exposures. The Fort Pearce section can be traced with some confidence to near the cinder cone that produced the Washington flow (unit Qbwc on plate 1), before it becomes obscured in a zone of northwest-trending fractures.

Mokaac Strand

The 16-km-long Mokaac strand lies to the west of and is subparallel with the Fort Pearce section of the Washington fault zone. Similar to the Fort Pearce section, the Mokaac strand dips to the west and has created a prominent escarpment capped by Kaibab Formation limestone. The escarpment height reaches about 180 m near the midpoint of the fault. Stratigraphic separation on the fault increases from about 60 m near its southern end where it is partially obscured by landslides on the eastern flank of Mokaac Mountain, to 390 m before merging with the Fort Pearce section to the north (Billingsley, 1990a).

Starting near the Quail Hill Road intersection with the Mokaac strand (plate 1), a 5-km-long, fairly continuous fault scarp formed on resistant Permian bedrock runs northeast along the base of the escarpment and defines a bedrock-alluvium/colluvium contact. The fault scarp is up to 4 m high and is commonly covered with a thin mantle of colluvium. Billingsley (1990a, 1993) indicated two locations along the scarp where Holocene alluvium and talus are displaced up to 3.7 m. I could not find any scarps developed in unconsolidated deposits that are not bedrock cored along the central and southern Mokaac strand.

At its northern end, the Mokaac strand juxtaposes various non-resistant members of the Moenkopi and Chinle Formations, and has a subdued to nonexistent surface expression. The fault appears to displace and possibly tilt lava flows near Dutchman Draw (plate 1; see Lund and Knudsen this volume for a discussion of displaced lava flows) before merging with the Fort Pearce section. A subsidiary, sub-parallel fault splay south of the main Mokaac strand has produced a 3- to 5-m-high scarp on the Shnabkaib Member of the Moenkopi Formation, and just to the north, on late Pleistocene to early Holocene mixed alluvial and eolian deposits (Qae; station 9, plate 1). The part of the scarp developed in unconsolidated deposits is about 0.5 km long and has a maximum height of about 3 m. A stream cut through the scarp exposes a footwall composed of Shnabkaib bedrock covered with 2 to 3 m of alluvium; the site appears amenable to trenching. The subsidiary splay continues into a low mesa capped by a mafic volcanic flow, and appears to displace the flow a few meters, before dying out.

There is no obvious indication of a rupture barrier between the Mokaac strand and Fort Pearce section. With maximum displacement on the Mokaac strand near its junction with the Fort Pearce section, the two faults have most likely shared earthquake ruptures in the past. The fault's relatively short length (16 km) supports the inference that the Mokaac strand is accommodating slip originating on the Fort Pearce section rather than generating its own earthquakes. Based on the branching geometry of the Mokaac strand with the Fort Pearce section, it is possible that the Mokaac strand only ruptures during southward-propagating fault rupture on the Fort Pearce section. Additionally, the two faults have similar scarp morphologies, and both have displaced late Pleistocene-Holocene alluvial-fan deposits, thus indicating similar rates of activity. For these reasons, I consider the Mokaac strand to be part of the Fort Pearce section rather than a separate fault section capable of independent earthquake rupture as proposed by Pearthree (1998). My interpretation is based on the distribution of maximum fault displacements and apparent similar rates of activity. Detailed paleoseismic trench data are necessary to definitively show that the two faults have or have not ruptured synchronously in the past.

Dutchman Draw Strand

From its junction with the Fort Pearce section (plate 1), the Dutchman Draw strand trends northeast and has formed a 120-m-high escarpment in resistant limestone of the Permian Kaibab Formation. Stratigraphic separation near the fault junction is about 115 m and decreases to the north (Billingsley, 1992a). Like other high escarpments along the Washington fault zone, prominent escarpments along the Dutchman Draw strand are likely chiefly the result of differential erosion.

The Dutchman Draw strand consists of two splays near Joe Blake Hill (plate 1). The southern splay vertically displaces the 1.28 Ma ($^{40}Ar/^{39}Ar$; Lund and Knudsen this volume) East Mesa lava flow (Qbe) about 45 m. The underlying Kaibab-Moenkopi contact appears to be displaced roughly the same amount, indicating that faulting on the southern splay likely initiated after flow emplacement (Billingsley, 1992a).

Northeast of Joe Blake Hill, the Dutchman Draw strand is partially obscured by landslide and alluvial deposits. The fault is again well displayed on the south flank of an unnamed lava-flow-capped mesa where the Shnabkaib Member of the Moenkopi Formation is downthrown against the middle red member (plate 1, figure 11). The basalt capping the mesa is in the fault hanging wall and could be the downthrown distal remnant of an unnamed volcanic flow on the fault footwall that issued from a volcanic center 2.5 km to the east (Lund and Knudsen this volume). If the two outcrops are correlative, the flow has been displaced up to 80 m across the Dutchman Draw strand. Although the age of the unnamed flow has not been determined, cross-cutting relations exposed on the west flank of the mesa indicate the flow postdates at least some movement on the Dutchman Draw strand. Normal drag in the hanging wall has folded the Shnabkaib and upper red members up to 20° to the north. The flat-lying basalt truncates the underlying folded strata indicating that folding and faulting initiated prior to lava deposition (figure 11).

Northeast of the unnamed mesa, there is no apparent relief across the Dutchman Draw strand for several kilometers. However, the fault is well expressed on aerial photos, where the red and white “bacon stripes” of the Shnabkaib Member of the Moenkopi Formation in the footwall are in fault contact with the middle red member.

Stratigraphic separation on the Dutchman Draw strand decreases significantly near Fort Pearce Wash, where the Shinarump Conglomerate Member of the Chinle Formation is displaced about 15 m. In the northern bank of the wash, the Petrified Forest Member of the Chinle Formation is in fault contact with the Shinarump Conglomerate. This is the northernmost definitive exposure of the Dutchman Draw strand that I could find. Billingsley and Graham (2003) mapped a 250-m-long fault scarp on older alluvium north of Fort Pearce Wash. I consider this subdued scarp to be a bedrock scarp with a thin veneer of alluvial deposits (unit Qat_3) draped over the top. Although Billingsley and Graham (2003) extended the Dutchman Draw strand as a concealed fault to the Utah border, Hayden (2004) did not map a fault in the adjoining 7.5-minute quadrangle (The Divide) in Utah. I found no evidence for continuing the Dutchman Draw strand into Utah, although there is substantial alluvial/eolian cover in the area that may obscure the fault trace. Both west- and east-dipping faults are present along the projection of the

Dutchman Draw strand 3.5 km north of the Utah border at Sand Mountain (plate 1). Although not exposed in the intervening interval, it is possible the Dutchman Draw strand connects with the faults at Sand Mountain. At least two of the larger Sand Mountain faults displace the approximately 1 Ma (Biek and others, 2009) Grass Valley flow up to 76 m before merging with the nearby Hurricane fault.

Less than 3 km east of where the Dutchman Draw strand approaches the Utah-Arizona border, Hayden (2004) mapped the down-to-the-west Warner Valley fault between Sand Mountain and the Hurricane Cliffs (plate 1). She reported a maximum stratigraphic separation of 550 m on the approximately 5-km-long fault, and stated that the fault quickly dies out in northern Arizona. Geologic maps of this area in Arizona (Billingsley, 1992b; Billingsley and Workman, 2000; this study) show no southern continuation of the Warner Valley fault, indicating that the fault likely does die out abruptly just after entering Arizona. The apparent en-echelon right step between the Warner Valley fault and Dutchman Draw strand may indicate that these faults are part of the same fault system (Lund and others, 2008). This is supported by Hamblin and Best (1970) who mapped the two faults in an en-echelon relation near the state line. Although obscured by alluvial fans emanating from the Hurricane Cliffs, the Warner Valley fault likely merges with the Hurricane fault.

Although the Dutchman Draw strand has been mapped and discussed separately from the Washington fault zone in previous studies, I consider the Dutchman Draw strand to be part of the Fort Pearce section of the Washington fault zone. Much like the Mokaac strand, displacement on the Dutchman Draw strand increases toward its junction with the Fort Pearce section, indicating the Dutchman Draw strand most likely accommodates slip from the Fort Pearce section rather than being independently active. This inference is supported by the relatively short length (16 km) of the Dutchman Draw strand, and similar rates of Quaternary activity as indicated by similar scarp morphologies among the two faults. Based on the branching geometry of the Dutchman Draw strand with the Fort Pearce section, it is possible that the Dutchman Draw strand only ruptures during northward-propagating fault rupture on the Fort Pearce section.

Washington Hollow Section

A 5-km-long zone of fractures and joints extends to the northwest from the Washington flow cinder cone near the end of the Fort Pearce section of the Washington fault zone. This fracture zone trends into the Washington Hollow fault—a west-dipping normal fault with about 150 m of stratigraphic separation (Willis and Higgins, 1995). Some previous workers have mapped a continuous fault through Washington Hollow connecting the Washington and Washington Hollow faults, while others have mapped them as separate faults (figure 12). A prominent northeast-trending joint set at approximately right angles to the proposed connector fault through Washington Hollow parallels the Cretaceous Virgin anticline and other Sevier-age compressional structures, indicating a likely Sevier age for the joints. The joint set is therefore likely older than the more recent normal faulting, and is clearly visible on aerial photos where it persists with little or no displacement across the proposed connecting fault in Washington Hollow (figure 13), indicating that if a connecting fault does exist, it either has minimal offset,

or has pure dip-slip movement, in which case the displaced vertical joints would appear continuous across the fault in map view.

I mapped an approximately located, small-displacement fault in Washington Hollow (plate 1) since there is evidence for structural deformation there including brecciation, 1.5-3-m-wide crushed zones, and minor-displacement faulting (Willis and Higgins, 1995) along lineaments that have geometries similar to the two larger faults. Although I placed the fault along one of the more prominent fracture zones, strain has likely been distributed over a relatively wide zone rather than on a single master fault. This zone links the Fort Pearce section of the Washington fault zone and Washington Hollow fault, and I consider this zone of diffuse and low displacement a boundary between two separate fault sections, and therefore map the Washington Hollow fault as a section (Washington Hollow section) of the Washington fault zone, and I refer to it as the Washington Hollow section hereafter.

The following lines of evidence indicate a probable section boundary between the Washington Hollow and Fort Pearce sections near the Washington flow vent: (1) the fault exhibits increased structural complexity where it bifurcates into several smaller splays; such structural complexities are often associated with seismogenic segment boundaries, (2) net displacement across the Fort Pearce section appears to decrease significantly near the Washington flow vent with no single fault or shear zone accommodating more than a few 10s of meters of displacement, and (3) the fault displays a 45° change in strike near the vent. The Washington Hollow section from the Washington flow cinder cone to the fault's terminus west of Pine Valley is 22 km long (straight-line).

The Washington Hollow section is clearly expressed at the head of Washington Hollow where it displaces varicolored strata of the Jurassic Temple Cap and Carmel Formations. Farther north the fault juxtaposes red Tertiary Claron Formation against the pale yellow and brown Cretaceous Iron Springs Formation.

The Washington Hollow section has displaced Quaternary unconsolidated deposits in at least two places. The fault forms a scarp (station 7, plate 1) on a linear, relatively thin Pleistocene alluvial-fan deposit (Qafo; Biek and others, 2009; Hacker, in preparation [a]) that caps a high ridge dividing Spring Hollow from Cottonwood Creek. The scarp is 3 to 4 m high and less than 50 m long. North of Grass Knoll, where the fault consists of three to four splays, an east-dipping splay forms a 6- to 8-m-high, 600-m-long scarp on a Pleistocene alluvial-fan deposit (Qafo) 0.8 km west of Quaking Aspen spring (station 8, plate 1; Hacker, in preparation [a]; Biek and others, 2009).

From Cedar Bench to Truman Bench, the Washington Hollow section and subsidiary splays have displaced five different lava flows that range in age from about 450 ka to 1.2 ka (plate 1; Biek and others, 2009), indicating middle Pleistocene or younger fault movement. I observed the greatest displacement on the fault at Cedar Bench just beyond the western map boundary, where a northeast-trending subsidiary fault displaces the 1.2 Ma ($^{40}Ar/^{39}Ar$ plateau age [UGS unpublished data]) Cedar Bench lava flow up to 12 m, yielding an early Pleistocene-Holocene vertical slip rate of 0.01 mm/yr.

The Washington Hollow section dies out on the northern flank of Saddle Mountain where it cannot be traced into the 0.6 Ma ($^{40}Ar/^{39}Ar$ plateau age [UGS unpublished data]) Lark Canyon flow to the north (plate 1; Biek and others, 2009; Hacker, in preparation [b]).

RELATION BETWEEN THE WASHINGTON FAULT ZONE AND OTHER TRANSITION ZONE FAULTS

Although my mapping focused on the northernmost two sections of the Washington fault zone (the Fort Pearce and herein defined Washington Hollow sections), the fault's branching pattern and close spatial relation with other nearby transition zone faults prompts questions about how these faults formed and how they may interact. A regional view of the various faults and fault zones comprising the transition zone in southwestern Utah and northwestern Arizona reveals a pattern where many of the faults are en echelon, intersect, form rhombic patterns, and have salients and reentrants at similar latitudes (figure 14). Geologic mapping also shows that all major and many minor faults within the transition zone displace Quaternary alluvial deposits (Billingsley and Workman, 2000). Structural patterns and similar relative rates of activity indicate many or all normal-displacement transition zone faults may be structurally linked and part of the same fault system.

The 87-km-long, west-dipping Main Street fault zone maintains a closely spaced (~ 5 km) en echelon relation with the Sullivan Draw section of the Washington fault zone for nearly 40 km (figure 14). Hamblin (1970a) and Peterson (1983) considered the Washington and Main Street faults to be part of the same fault system. Billingsley's geologic map of the Littlefield 30' x 60' quadrangle shows a southwest-dipping, northwest-trending fault splay with 70 m of vertical displacement and associated monocline branching from the Sullivan Draw section of the Washington fault zone and intersecting the Grand Wash fault (figure 14). Therefore, it appears the Washington fault zone and Grand Wash faults are structurally linked at the surface. Other significant but lesser faults (in terms of displacement and length) in the transition zone at this latitude include the Gyp Pocket, Sunshine Trail, and Sunshine fault zones (Pearthree, 1998; Billingsley and Workman, 2000) that occupy a large reentrant of the Hurricane fault (Hurricane Valley) (figure 14) and are considered subsidiary to the Hurricane fault (Pearthree, 1998). Hamblin (1970a) noted that these lesser faults are concave toward the Hurricane fault and suggested that they are the result of complex hanging-wall deformation being translated over a curved Hurricane fault plane. The easternmost strand of the Sunshine fault zone is parallel to, and lies within 1 km of the Main Street fault and defines the eastern edge of the Main Street horst (figure 14); these closely spaced structures are likely linked at depth. Additionally, results of this mapping (see previous section) indicate that the Washington, Dutchman Draw, Warner Valley, Hurricane, and additional minor faults may all be linked or nearly linked at the surface.

Schramm (1994) proposed a regional fault system linking the Grand Wash, Washington, and Hurricane faults. She used the following lines of evidence to support a displacement transfer zone or regional scale relay ramp bounded by the Hurricane and Grand Wash faults (figure 15) that may be linked at depth with a subhorizontal detachment:

1. The faults have similar geometries.

2. Displacement on the Grand Wash and Hurricane faults increases in opposite directions along strike, consistent with transfer of slip between the two faults (figure 15).

3. Quaternary unconsolidated deposits and basalt flows are displaced by the Hurricane, Washington, and Gunlock-Grand Wash fault, indicating that they all have been active in the Quaternary.

4. Although the earthquake record in this area of the transition zone is incomplete, scattered seismic activity across the region has been attributed to all three faults, indicating all are seismically active.

While Schramm (1994) viewed the Hurricane, Washington, and Grand Wash faults as being contemporaneously active, timing data from subsequent studies indicate that these faults have been active sequentially with some overlap. Movement on the Grand Wash fault initiated in the early or middle Miocene (Bohannon and others, 1993; Billingsley and Workman, 2000), and the fault attained nearly all of its stratigraphic separation by the end of the Miocene (Lucchitta, 1987; Wenrich and others, 1995; Pearthree, 1998). Pleistocene displacement appears to be only a few meters, and Holocene deposits are unfaulted (Pearthree, 1998). Conversely, equal displacement of a 3.6 Ma basalt flow and underlying bedrock near Mt. Trumbull (figure 14) indicates movement on the Hurricane fault initiated in the Pliocene or later (Billingsley and Workman, 2000). Similar relations between basalt flows of various ages and other structures in the transition zone led Billingsley and Dyer (2003) to conclude that the Washington and Main Street fault zones and lesser faults between the Main Street and Hurricane faults (Gyp Pocket, Sunshine, and Sunshine Trail faults) became active during or since the Pleistocene. All major faults and most minor structures east of the Grand Wash fault have been active in the Holocene since Holocene alluvium has been displaced by the Hurricane fault (e.g., Billingsley and Dyer, 2003; Amoroso and others, 2004; Lund and others, 2007), the Washington fault zone (this study), and most lesser structures (Main Street, Sunshine, Sunshine Trail, and Gyp Pocket faults) occupying the Shivwitz Plateau east of the Washington fault zone (Billingsley and Dyer, 2003).

I favor a model where a narrow Colorado Plateau-Basin and Range transition zone initiated along the Grand Wash fault in early to middle Miocene time. By the Pliocene, the generally east-west tensional stress field had migrated eastward and movement on the Grand Wash fault nearly ceased as the Hurricane fault began to develop, possibly along older pre-existing structures (Huntoon, 1990; Billingsley and Wellmeyer, 2003). By Pleistocene time, the internal strain of the intervening block between the Hurricane and Grand Wash faults (the St. George-Shivwitz block) was great enough to form the Washington, Main Street, and other minor fault zones. A west-to-east transfer of strain is also consistent with the fact that basalt flows generally young from west to east, with basalt flows in the Grand Wash trough ranging from 4-6 Ma and flows in the Uinkaret volcanic field typically being less than 850 ka (Wenrich and others, 1995; Billinglsey and Workman, 2000).

While geologic-map relations are permissive of structural linkage between many faults in the transition zone in southwestern Utah and northwestern Arizona, it remains unclear if the

faults sole into a master detachment at depth, which might permit simultaneous sympathetic rupture of several faults. As an alternative, Schramm (1994) suggested that transition zone faults may simply die out at depth and that mechanical and geometric continuity is accomplished by internal strain of intervening fault blocks. Additional data and analyses are needed to further evaluate the existence of a regional transfer zone involving the Grand Wash, Hurricane, and Washington faults.

SUMMARY

New surficial geologic mapping of the Fort Pearce and Washington Hollow sections of the Washington fault zone determined or confirmed the following:

1. Similar geometries and amounts of displacement among the Washington and Washington Hollow fault zones, as well as minor structures bridging the distance between the two faults, indicate that they are both part of the same fault zone. However, minimal displacement and structural complexity north of Washington City near the Washington flow cinder cone indicate the Washington Hollow fault is likely a separate section of the Washington fault zone, and I therefore redefine the Washington Hollow fault as the Washington Hollow section of the Washington fault zone.

2. Since the Northern section, as defined by previous workers (Pearthree, 1998), is no longer the northernmost section of the Washington fault zone, I herein renaming it the Fort Pearce section of the Washington fault zone.

3. Since displacement on both the Mokaac section (Pearthree, 1998) and Dutchman Draw faults increases toward their junctures with the Fort Pearce section, and because all three faults have similar scarp morphologies indicating similar rates of activity, I believe that the three faults most often rupture contemporaneously. The Mokaac strand may be more likely to rupture during southward-propagating fault rupture on the Fort Pearce section, and the Dutchman Draw strand may be more likely to rupture during northward-propagating fault rupture. I consider the Mokaac and Dutchman Draw faults to be major strands of the Fort Pearce section, and herein define them as such.

4. The Fort Pearce-Sullivan Draw section boundary is best placed near the head of Quail Canyon where a 50° change in strike is accompanied by an abrupt change in vertical displacement along the fault.

5. The lengths (straight line) of the newly defined Fort Pearce and Washington Hollow sections are 37 and 22 km, respectively.

6. Due to high rates of erosion in the St. George Basin, fault scarps developed in unconsolidated deposits are rare and isolated. Only two discontinuous scarps formed on unconsolidated alluvium suitable for paleoseismic trenching were discovered on the Fort Pearce section; both are in Arizona. One site is on the main strand of the Fort Pearce section near Dutchman Draw and was subsequently trenched (see Lund and others this

volume). The second scarp is formed on a subsidiary splay of the Mokaac strand of the Fort Pearce section.

7. Several other scarps formed on unconsolidated deposits along the Fort Pearce section described in previous studies are bedrock cored and likely not suitable for trenching investigations.

8. Prominent bedrock escarpments up to 250 m high along the Fort Pearce section are chiefly the result of differential erosion rather than tectonic displacement.

9. Normal faults comprising the Colorado Plateau-Basin and Range transition zone in southwestern Utah and northwestern Arizona may be structurally linked. Similar geometries, structural styles, rates of activity, as well as evidence for transfer of strain among the Grand Wash, Hurricane, Washington, Main Street, and other faults indicate all of the faults may be part of a single regional transfer fault system. Several lines of evidence support a model where the Colorado Plateau-Basin and Range boundary in this area developed along the Grand Wash fault in Miocene time, then beginning in the Pliocene, the locus of strain migrated eastward, initiating development of the Hurricane fault. Internal strain within the intervening block became great enough by the Pleistocene to create the Washington, Main Street, and other lesser faults.

10. Although surficial geologic mapping indicates that transition zone faults in southwestern Utah and northwestern Arizona are likely linked or nearly linked at the surface, additional data and analyses are necessary to evaluate the possibility that the faults sole into a single regional detachment.

ACKNOWLEDGMENTS

I am grateful to William Lund, Robert Biek, and Grant Willis with the UGS, and Peter Rowley of Geologic Mapping, Inc., for advice, discussions, and information concerning this geologic map. Thoughtful reviews by Christopher DuRoss, Steven Bowman, and Michael Hylland (UGS) greatly improved this map and text. Corey Unger with assistance from Jay Hill, both with the UGS, did the cartography.

REFERENCES

Amoroso, L., Pearthree, P.A., and Arrowsmith, J.R., 2004, Paleoseismology and neotectonics of the Shivwits section of the Hurricane fault, northwestern Arizona: Bulletin of the Seismological Society of America, v. 94, no. 5, p. 1919-1942.

Anderson, R.E., and Christenson, G.E., 1989, Quaternary faults, folds, and selected volcanic features in the Cedar City 1° x 2° quadrangle, Utah: Utah Geological and Mineral Survey Miscellaneous Publication 89-6, 29 p.

Best, M.G., and Brimhall, W.H., 1970, Late Cenozoic basalt types in the western Grand Canyon region, *in* Hamblin, W.K., and Best, M.G., editors, The western Grand Canyon region: Utah Geological Society Guidebook to the Geology of Utah, no. 23, p. 57-74.

Best, M.G., and Hamblin, W.K., 1970, Implications of tectonism and volcanism in the western Grand Canyon, *in* Hamblin, W.K., and Best, M.G., editors, The western Grand Canyon region: Utah Geological Society Guidebook to the Geology of Utah, no. 23, p. 75-79.

Best, M.G., McKee, E.H., and Damon, P.E., 1980, Space-time composition patterns of late Cenozoic mafic volcanism, southwestern Utah and adjoining areas: American Journal of Science, v. 280, p. 1035-1050.

Biek, R.F., 2003, Geologic map of the Harrisburg Junction quadrangle, Washington County, Utah: Utah Geological Survey Map 191, 42 p., 2 plates, scale 1:24,000.

Biek, R.F., Rowley, P.D., Hayden, J.M., Hacker, D.B., Willis, G.C., Hintze, L.F., Anderson, R.E., and Brown, K.D., 2009, Geologic map of the St. George and east part of the Clover Mountains 30' x 60' quadrangles, Washington and Iron Counties, Utah: Utah Geological Survey Map 242, 101 p., 2 plates, scale 1:100,000.

Billingsley, G.H., 1990a, Geologic map of the Lizard Point quadrangle, northern Mohave County, Arizona: U.S. Geological Survey Open-File Report 90-643, scale 1:24,000.

Billingsley, G.H., 1990b, Geologic map of the Wolf Hole Mountain East quadrangle, northern Mohave County, Arizona: U.S. Geological Survey Open-File Report 90-644, scale 1:24,000.

Billingsley, G.H., 1991a, Geologic map of the Sullivan Draw South quadrangle, northern Mohave County, Arizona: U.S. Geological Survey Open-File Report 91-559, scale 1:24,000.

Billingsley, G.H., 1991b, Geologic map of the Sullivan Draw North quadrangle, northern Mohave County, Arizona: U.S. Geological Survey Open-File Report 91-558, scale 1:24,000.

Billingsley, G.H., 1992a, Geologic map of the Yellowhorse Flat quadrangle, northern Mohave County, Arizona: U.S. Geological Survey Open-File Report 92-442, scale 1:24,000.

Billingsley, G.H., 1992b, Geologic map of the Rock Canyon quadrangle, northern Mohave County, Arizona: U.S. Geological Survey Open-File Report 92-449, scale 1:24,000.

Billingsley, G.H., 1993, Geologic map of the Wolf Hole Mountain and vicinity, Mohave County, northwestern Arizona: U.S. Geological Survey Miscellaneous Investigations Series Map I-2296, scale 1:31,680.

Billingsley, G.H., and Dyer, H.C., 2003, Geologic map of the upper Hurricane Wash and vicinity, Mohave County, northwestern Arizona: U.S. Geological Survey Miscellaneous Field Studies Map MF-2410, 23 p., scale 1:31,680.

Billingsley, G.H., and Graham, S.E., 2003, Geologic map of the lower Hurricane Wash and vicinity, Mohave County, northwestern Arizona: U.S. Geological Survey Miscellaneous Field Studies Map MF-2396, 27 p., scale 1:31,680.

Billingsley, G.H., and Wellmeyer, J.L., 2003, Geologic map of the Mount Trumbull 30' x 60' quadrangle, Mohave and Coconino Counties, northwestern Arizona: U.S. Geological Survey Geologic Investigations Series I-2766, scale 1:100,000.

Billingsley, G.H., and Workman, J.B., 2000, Geologic map of the Littlefield 30' x 60' quadrangle, Mohave County, northwestern Arizona: U.S. Geological Survey Geologic Investigations Series Map I-2628, Version 1.0, 25 p., 2 plates, scale 1:100,000.

Bohannon, R.G., Grow, J.A., Miller, J.J., and Blank, R.H., Jr., 1993, Seismic stratigraphy and tectonic development of Virgin River depression and associated basins, southeastern Nevada and northwestern Arizona: Geological Society of America Bulletin, v. 105, no. 4, p. 501-520.

Bowman, S.D, Young, B.W., and Unger, C.D., 2011, Paleoseismology of Utah Volume 21 – Compilation of 1982-83 seismic safety investigation reports of eight SCS dams in southwestern Utah (Hurricane and Washington fault zones) and low-sun-angle aerial photography, Washington and Iron Counties, Utah, and Mohave County, Arizona: Utah Geological Survey Open-File Report 583, 4 p., 6 DVD set, available online at http://geology.utah.gov/ghp/consultants/paleoseismic_series.htm.

Bureau of Land Management, 2002, Stereoscopic color aerial photographs, project AZ-02-AC, scale 1:24,000.

Christenson, G.E., and Deen, R.D., 1983, Engineering geology of the St. George area, Washington County, Utah: Utah Geological and Mineral Survey Special Studies 58, 32 p., 2 plates.

Cook, E.F., 1960, Geologic atlas of Utah, Washington County: Utah Geological and Mineralogical Survey Bulletin 70, 119 p.

Cook, K.L., and Hardman, E., 1967, Regional gravity survey of the Hurricane fault area and Iron Springs District, Utah: Geological Society of America Bulletin, v. 78, p. 1063-1076.

Cordova, R.M., 1978, Ground-water conditions in the Navajo Sandstone in the central Virgin River basin, Utah: Utah Division of Water Rights Technical Publication 61, 66 p., plate in pocket, scale 1:250,000.

Dobbin, C.E., 1939, Geologic structure of St. George district, Washington County, Utah: American Association of Petroleum Geologists Bulletin, v. 23, no. 2, p. 121-144.

Downing, R.F., Smith, E.I., Orndorff, R.L., Spell, T.L., and Zanetti, K.A., 2001, Imaging the Colorado Plateau – Basin and Range transition zone using basalt geochemistry, geochronology, and geographic information systems, *in* Erskine, M.C., Faulds, J.E., Bartley, J.M., and Rowley, P.D., editors, The geologic transition, High Plateaus to Great Basin—a symposium and field guide (The Mackin Volume): Utah Geological Association and Pacific Section of the American Association of Petroleum Geologists, Utah Geological Association Publication 30, p. 127-154.

Earth Sciences Associates, 1982, Seismic safety investigation of eight SCS dams in southwestern Utah: Portland, Oregon, unpublished consultant's report for the U.S. Soil Conservation Service, variously paginated, 2 volumes.

Hacker, D.B., in preparation (a), Geologic map of the Saddle Mountain quadrangle, Washington County, Utah: Utah Geological Survey Map, scale 1:24,000.

Hacker, D.B., in preparation (b), Geologic map of the Central East quadrangle, Washington County, Utah: Utah Geological Survey Map, scale 1:24,000.

Hamblin, W.K., 1963, Late Cenozoic basalts of the St. George basin, Utah, *in* Heylmun, E.B., editor, Geology of the southwestern transition between the Basin-Range and Colorado Plateau, Utah: Intermountain Association of Petroleum Geologists, Guidebook to the Geology of Southwestern Utah, p. 84-89.

Hamblin, W.K., 1970a, Structure of the western Grand Canyon region, *in* Hamblin, W.K., and Best, M.G., editors, The western Grand Canyon region: Utah Geological Society Guidebook to the Geology of Utah, no. 23, p. 3-20.

Hamblin, W.K., 1970b, Late Cenozoic basalt flows of the western Grand Canyon, *in* Hamblin, W.K., and Best, M.G., editors, The western Grand Canyon region: Utah Geological Society Guidebook to the Geology of Utah, no. 23, p. 21-37.

Hamblin, W.K., and Best, M.G., 1970, Road log, *in* Hamblin, W.K., and Best, M.G., editors, The western Grand Canyon region: Utah Geological Society Guidebook to the Geology of Utah, no. 23, p. 93-153.

Hayden, J.M., 2004, Geologic map of The Divide quadrangle, Washington County, Utah: Utah Geological Survey Map 197, 31 p. pamphlet, scale 1:24,000.

Hayden, J.M., 2005, Geologic map of the Washington Dome quadrangle, Washington County, Utah: Utah Geological Survey Map 209, 29 p. pamphlet, scale 1:24,000.

Hayden, J.M., and Willis, G.C., 2011, Geologic map of the St. George 7.5' quadrangle, Washington County, Utah: Utah Geological Survey Map 251, 19 p., 2 plates, scale 1:24,000.

Hintze, L.F., 1963, Geologic map of southwestern Utah, *in* Intermountain Association of Petroleum Geologists Guidebook, 12th Annual Field Conference: Utah Geological and Mineralogical Survey, 1 sheet, scale 1:250,000.

Huntoon, P.W., 1990, Phanerozoic structural geology of the Grand Canyon, *in* Beus, S.S., and Morales, M., editors, Grand Canyon geology: Oxford, New York, Oxford University Press, and Flagstaff, Arizona, Museum of Northern Arizona Press, p. 261-310.

IntraSearch, 1983, Stereoscopic color aerial photographs, roll 3214, project no. 3214, frames 95-126, scale 1:24,000.

Lucchitta, I., 1987, The mouth of the Grand Canyon and edge of the Colorado Plateau in the upper Lake Mead area, Arizona, *in* Beus, S.S., editor, Geological Society of America Centennial Field Guide - Rocky Mountain Section, v. 2, p. 365-370.

Lund, W.R., Hozik, M.J., and Hatfield, S.C., 2007, Paleoseismology of Utah Volume 14 — Paleoseismic investigation and long-term slip history of the Hurricane fault in southwestern Utah: Utah Geological Survey Special Study 119, 81 p., CD.

Lund, W.R., Knudsen, T.R., Vice, G.S., and Shaw, L., 2008, Geologic hazards and adverse construction conditions, St. George – Hurricane metropolitan area, Washington County, Utah: Utah Geological Survey Special Study 127, 105 p., 14 plates, DVD.

Menges, C.M., and Pearthree, P.A., 1983, Map of neotectonic (latest Pliocene-Quaternary) deformation in Arizona: Arizona Geological Survey Open-File Report 83-22, 48 p., 4 plates.

Pearthree, P.A., compiler, 1998, Quaternary fault data and map for Arizona: Arizona Geological Survey Open-File Report 98-24, 122 p., 1 plate in pocket, scale 1:750,000.

Peterson, S.M., 1983, The tectonics of the Washington fault zone, northern Mohave County, Arizona: Brigham Young University Geology Studies, v. 30, part 1, p. 83-94.

Schramm, M.E., 1994, Structural analysis of the Hurricane fault in the transition zone between the Basin and Range Province and the Colorado Plateau, Washington County, Utah: University of Nevada at Las Vegas, M.S. thesis, 90 p.

Stokes, W.L., and Heylmun, E.B., 1963, Tectonic history of southwestern Utah, *in* Heylmun, E.B., editor, Guidebook to the geology of southwestern Utah: Intermountain Association of Petroleum Geologists Guidebook 12, p. 19-25.

Utah Automated Geographic Reference Center, 2012a, Black and white Soil Conservation Service (SCS) historical aerial imagery acquired in the late 1930s, viewed using AGRC's SGID Image Server for ArcMap: Online, <http://gis.utah.gov/data/utah-sgid-image-server/>, accessed October 2012.

Utah Automated Geographic Reference Center, 2012b, 2006 National Agriculture Imagery Program (NAIP) 1 meter orthophotography: Online, <http://gis.utah.gov/data/aerial-photography/2006-naip-1-meter-color-orthophotography>, accessed November 2012.

Utah Division of Water Rights, 2011, Well information program: Online, <http://www.waterrights.utah.gov/cgi-bin/wellview.exe?Startup>, accessed November 2011.

Utah Geological Survey and New Mexico Geochronology Research Laboratory, 2007, $^{40}Ar/^{39}Ar$ geochronology results from the Antelope Peak, Central East, Goldstrike, Page Ranch, and Saddle Mountain quadrangles, Utah: Utah Geological Survey Open-File Report 508, variously paginated, http://geology.utah.gov/online/analytical_data.htm.

Wenrich, K.J., Billingsley, G.H., and Blackerby, B.A., 1995, Spatial migration and compositional changes of Miocene-Quaternary magmatism in the Western Grand Canyon: Journal of Geophysical Research, v. 100, p. 10,417-10,440.

Willis, G.C., and Higgins, J.M., 1995, Interim geologic map of the Washington quadrangle, Washington County, Utah: Utah Geological Survey Open-File Report 324, 90 p., scale 1:24,000.

Figure 1. *Washington fault zone showing fault sections in southwestern Utah and northwestern Arizona as defined in this study. Yellow shading indicates St. George and Washington City boundaries. Additional Quaternary faults are shown as gray lines. Fault section boundaries are based on results of this study; see Lund (this volume) for section boundaries as defined by earlier workers.*

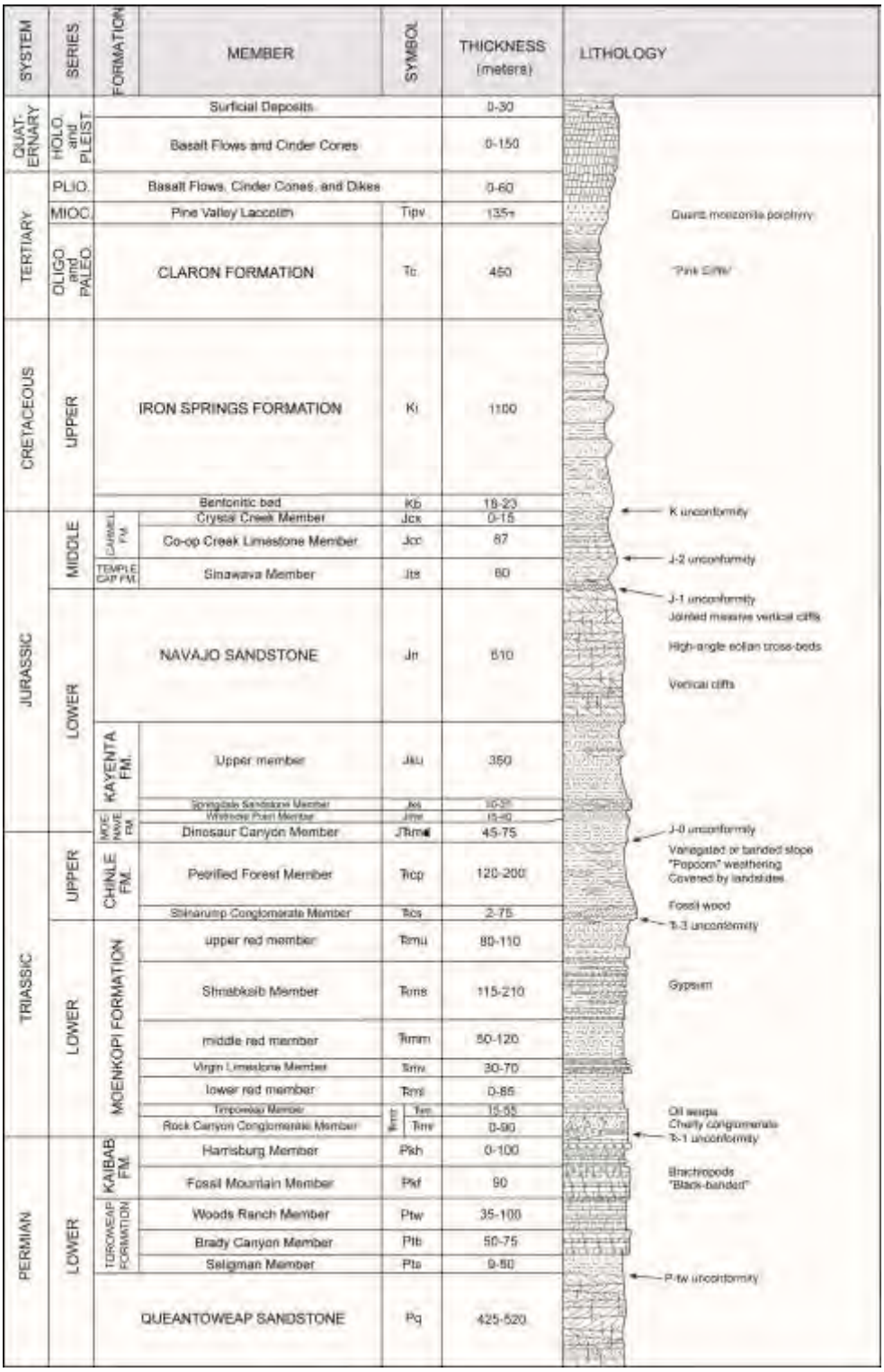

Figure 2. *Lithologic column of geologic units that crop out in the map area. Modified from Biek and others (2009).*

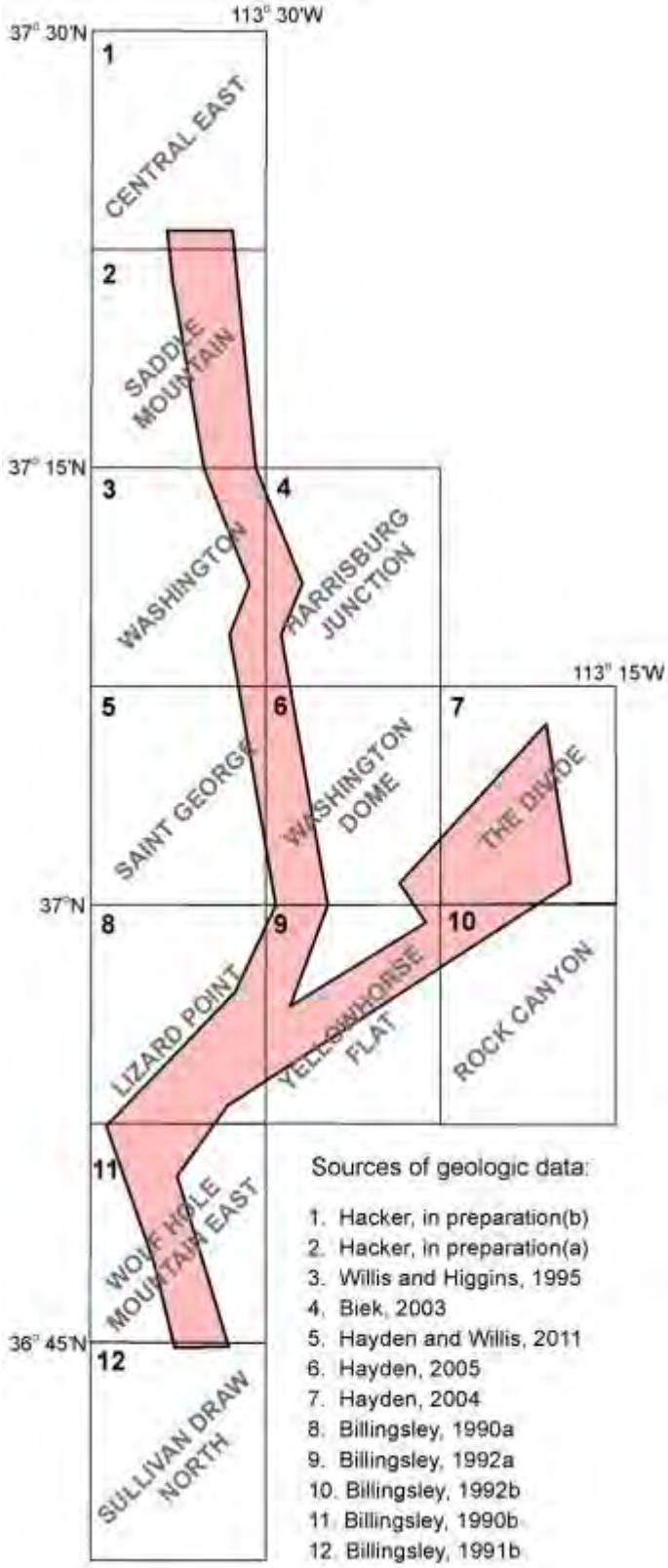

Figure 3. *7.5-minute geologic quadrangle map coverage of the Fort Pearce and Washington Hollow sections of the Washington fault zone.*

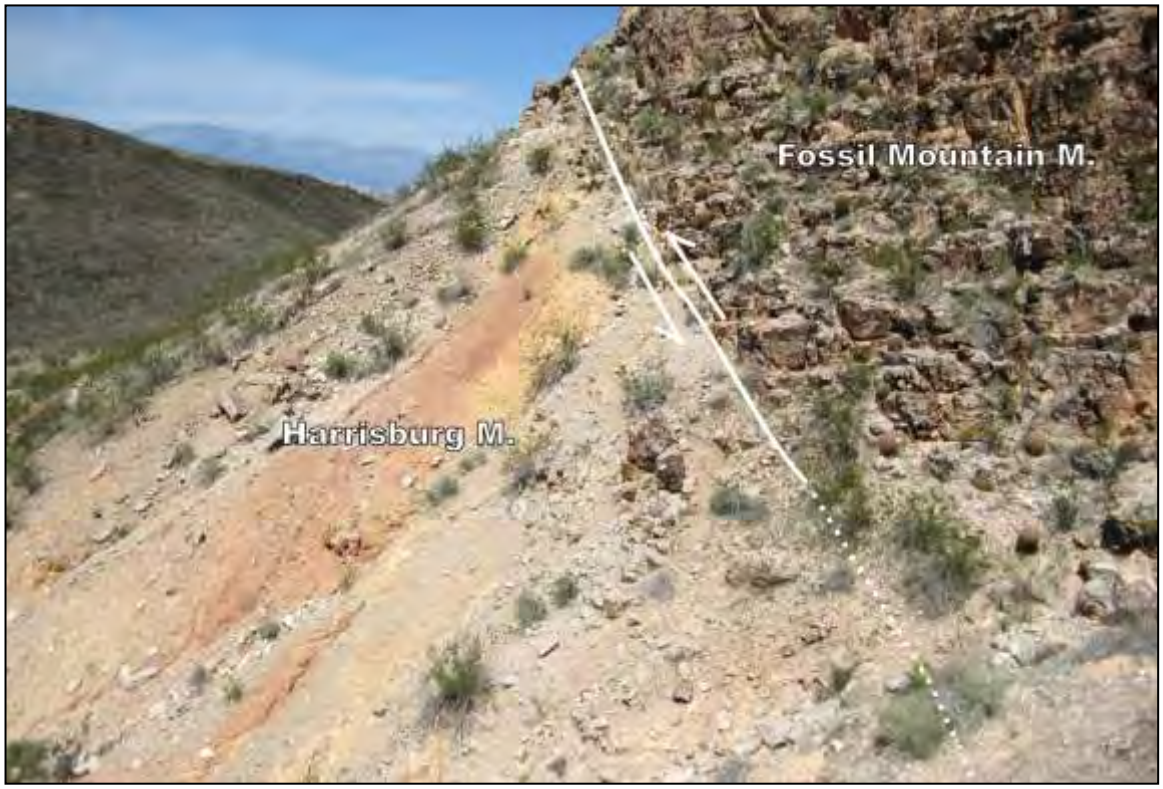

Figure 4. *The Washington fault zone places Fossil Mountain Member of the Kaibab Formation over the younger Harrisburg Member (reverse sense faulting) about 9 km south of the Utah-Arizona state line. View is to the north.*

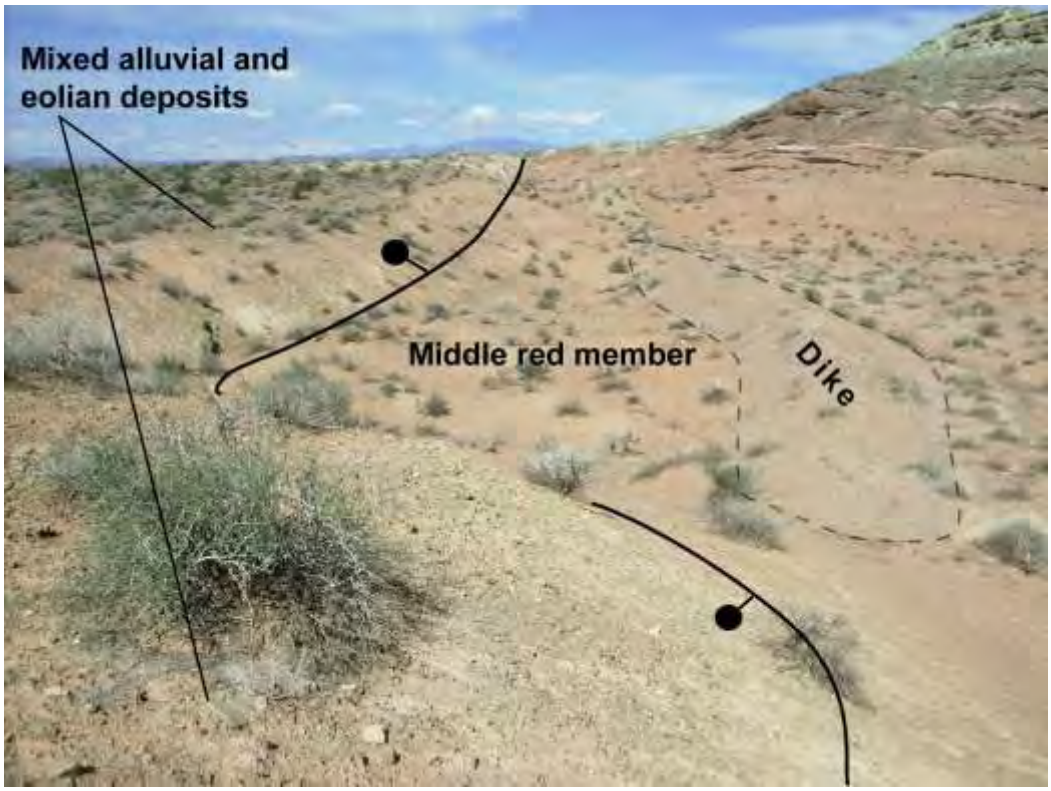

Figure 5. *Obsequent fault scarp formed along the Washington fault zone between unconsolidated basin-fill deposits and the middle red member of the Moenkopi Formation north of Fort Pearce Wash. View is to the north*.

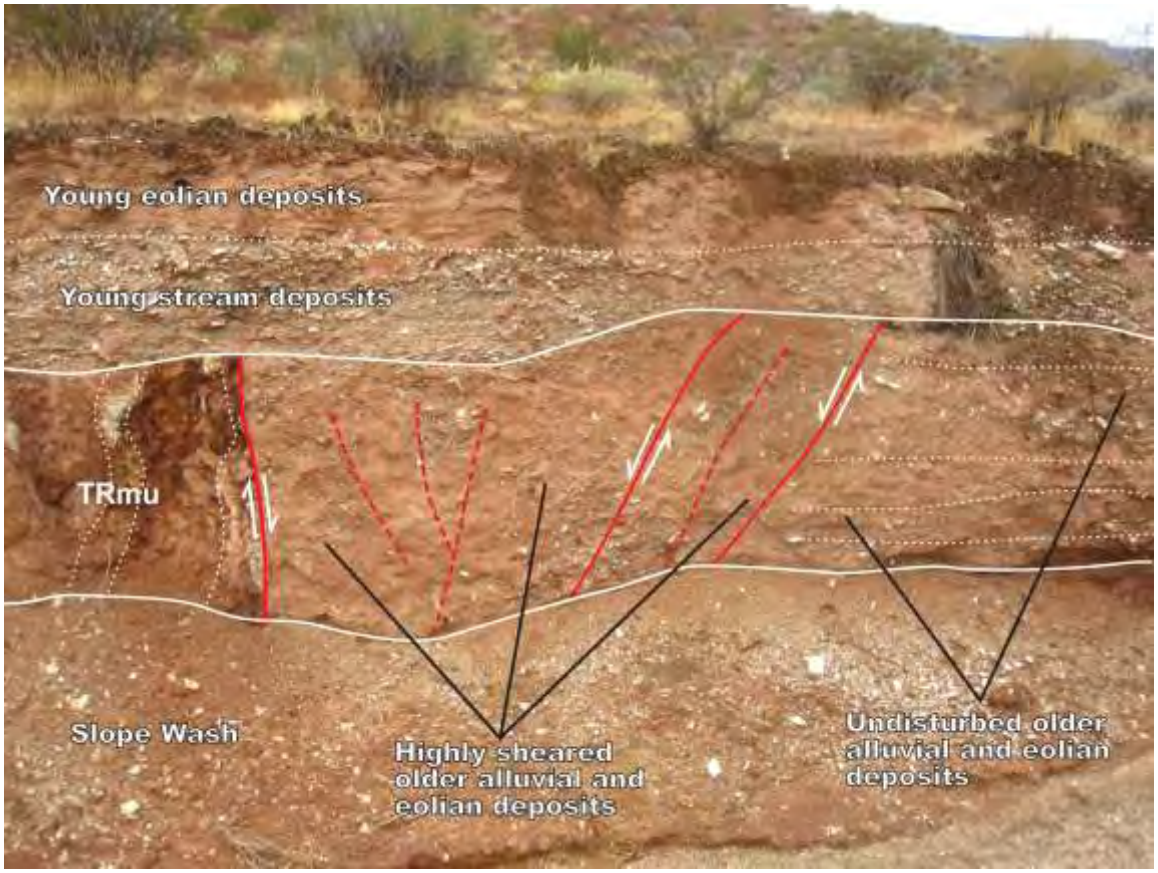

Figure 6. *A splay of the Washington fault zone exposed in a stream cut about 1 km north of the Utah state line. TRmu, Triassic upper red member of the Moenkopi Formation. Note the beveled surface formed by erosion on the Moenkopi bedrock. View is to the south.*

***Figure** 7. Oblique aerial view to the east of a scarp formed in Triassic bedrock and Quaternary unconsolidated deposits 1.5 km south of the Washington Fields-Warner Valley Road junction. Undated photo acquired by Pictometry International and viewed using Microsoft's Bing Maps software (http://www.bing.com/maps/). Qac, Quaternary mixed alluvium and colluvium; Qcao, Quaternary older mixed colluvium and alluvium; TRmu, Triassic upper red member of the Moenkopi Formation; TRms, Triassic Shnabkaib Member of the Moenkopi Formation.*

Figure 8. *Oblique aerial view to the east of fault scarp formed on the Washington lava flow. Scarp is 4.5 m high. Undated photo acquired by Pictometry International and viewed using Microsoft's Bing Maps software (http://www.bing.com/maps/).*

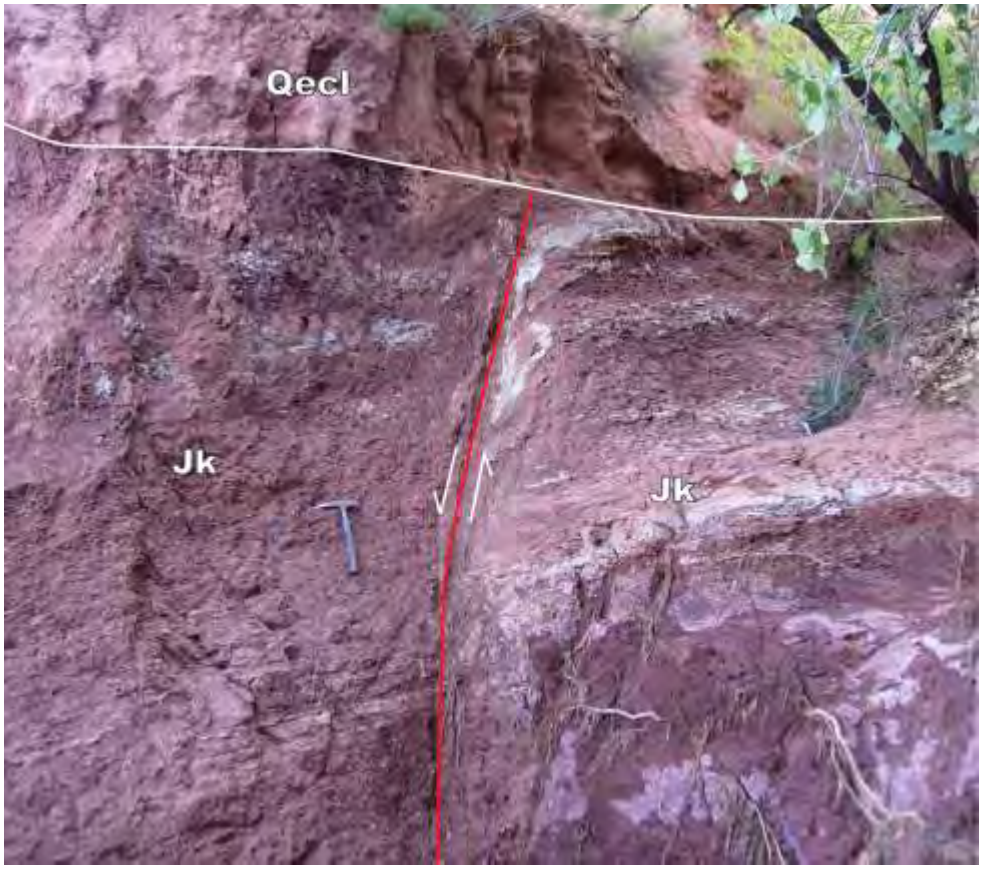

Figure 9. *Splay of the Washington fault zone exposed in a stream cut north of Washington City. Note the minor fault drag in the Kayenta Formation (Jk), and the unbroken Pleistocene carbonate-cemented sand (Qecl) covering the fault.*

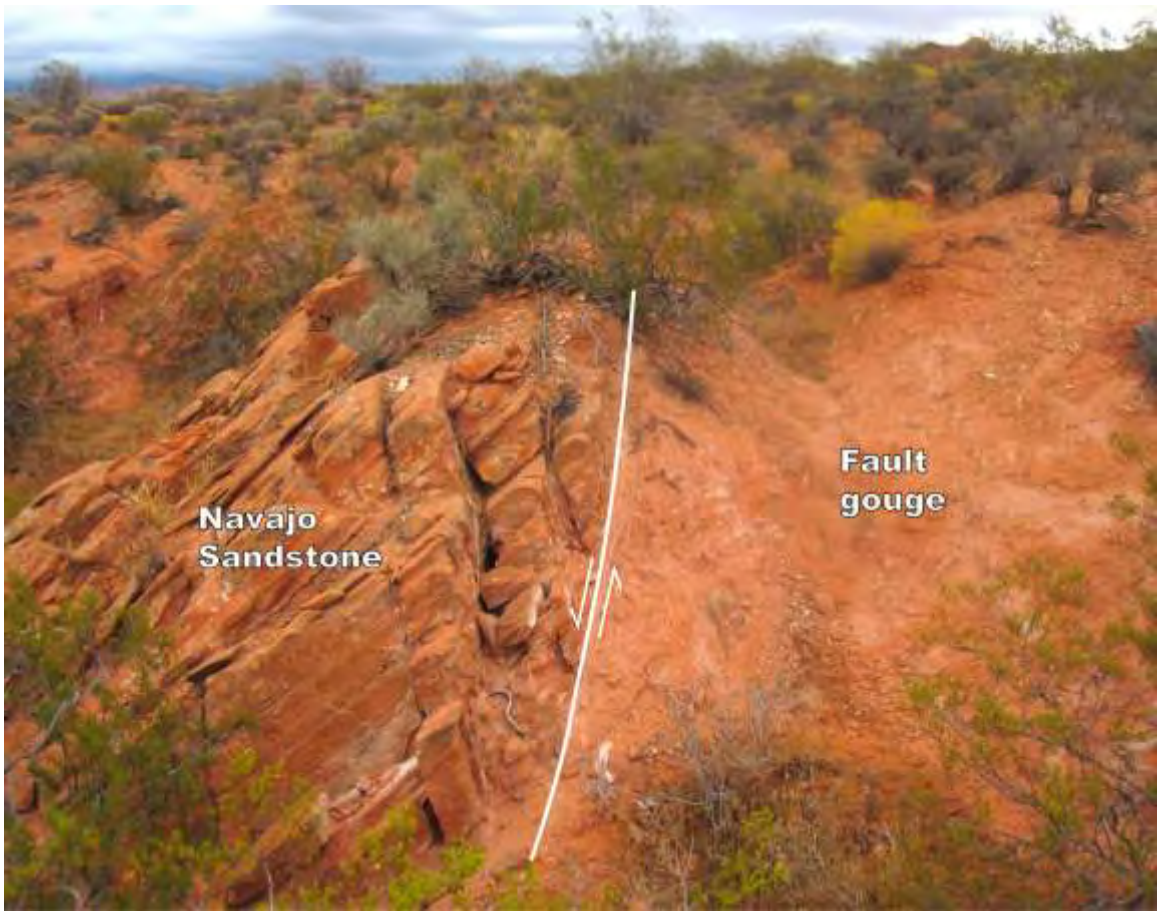

Figure 10. *Major splay of the Washington fault zone within the Navajo Sandstone north of Washington City. This structure appears similar to many nearby sub-parallel joints visible on aerial photos. Only after a field visit and documentation of fault-related features (fault drag on hanging wall and wide zone of fault gouge in footwall) was this structure identified as a fault. View to the north.*

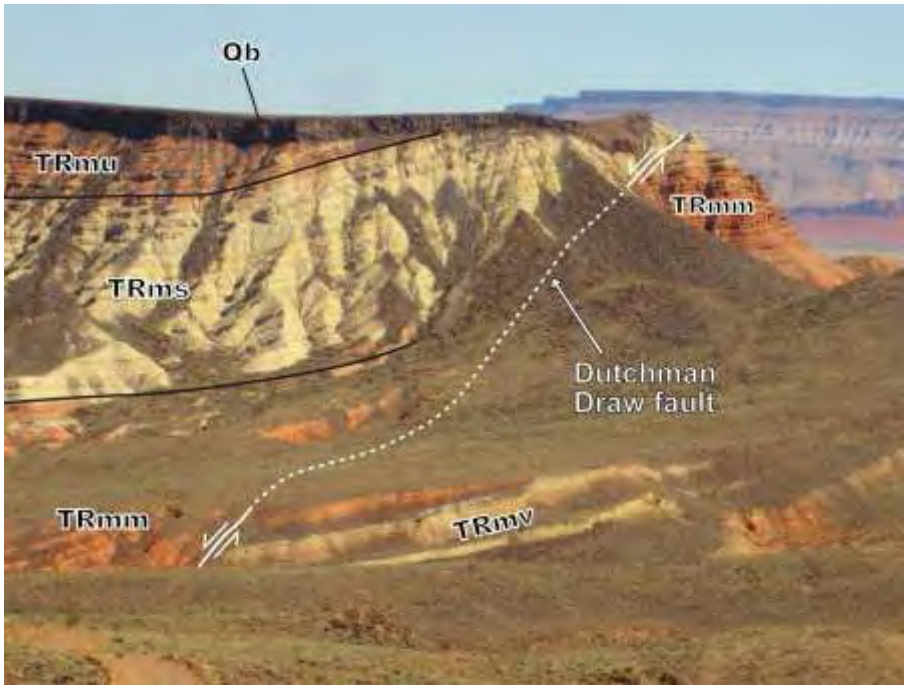

Figure 11. *Dutchman Draw fault exposed on the southwest flank of an unnamed mesa in Arizona. Truncation of fault-drag folding by Quaternary lava flow (Qb) indicates faulting initiated prior to deposition of the flow. View is to the northeast. Trmu, Triassic upper red member of the Moenkopi Formation; TRmm, Triassic middle red member of the Moenkopi Formation; TRms, Triassic Shnabkaib Member of the Moenkopi Formation; TRmv, Triassic Virgin Limestone Member of the Moenkopi Formation.*

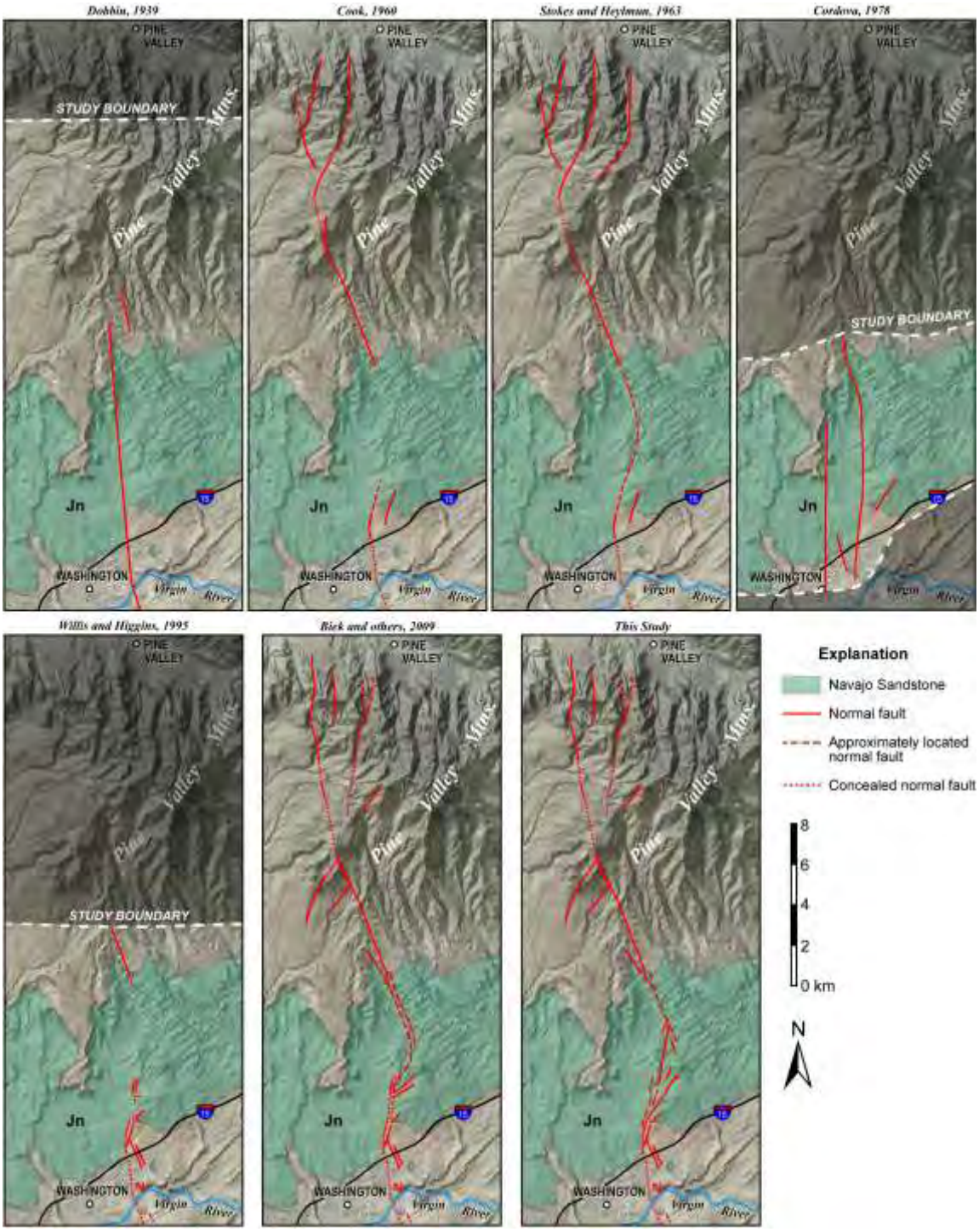

Figure 12. *Summary of geologic mapping of the Washington fault zone and Washington Hollow fault between Interstate 15 and the Pine Valley Mountains. See References section for complete citations.*

Figure 13. *Joints of probable Cretaceous age (dashed blue lines) near Washington Hollow that are unaffected by the Washington fault zone (WFZ). Base map is 2006 National Agriculture Imagery Program (NAIP) orthophotography (Utah Automated Geographic Reference Center, 2012b).*

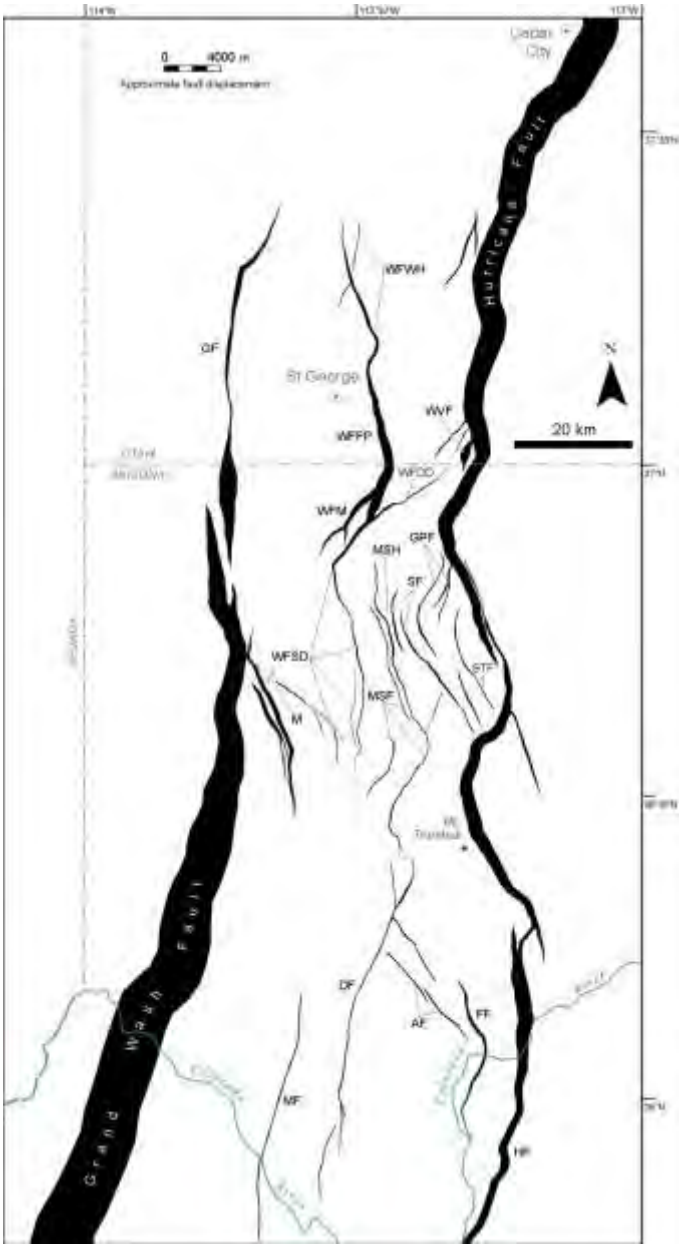

Figure 14. *Displacement map of faults in the Colorado Plateau-Basin and Range transition zone in southwestern Utah and northwestern Arizona. Fault widths are proportional to vertical fault displacement as indicated by alternating scale. WFWH, Washington Hollow section of the Washington fault zone; GF, Gunlock fault; WFFP, Fort Pearce section of the Washington fault zone; WVF, Warner Valley fault; WFDD, Dutchman Draw strand of the Fort Pearce section of the Washington fault zone; WFM, Mokaac strand of the Fort Pearce section of the Washington fault zone; GPF, Gyp Pocket fault zone; MSH, Main Street horst; SF, Sunshine fault zone; WFSD, Sullivan Draw section of the Washington fault zone; STF, Sunshine Trail fault zone; MSF, Main Street fault; M, southwest-dipping monocline; DF, Dellenbaugh fault; AF, Andrus fault; FF, Froggy fault; MF, Merriwhitica fault; HF, Hurricane fault.*

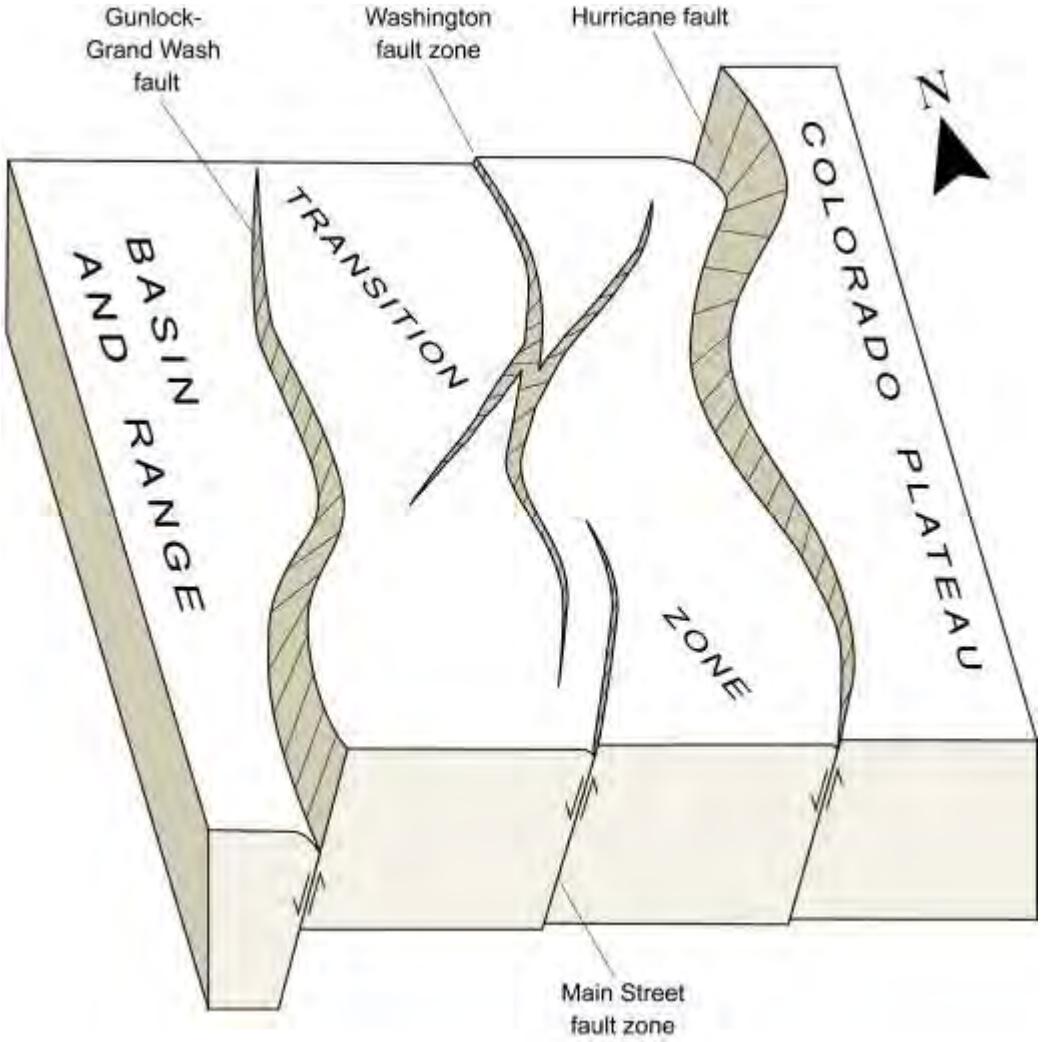

Figure 15. *Schematic block diagram of the Colorado Plateau-Basin and Range transition zone in southwestern Utah and northwestern Arizona. Displacement decreases on the Gunlock-Grand Wash fault as displacement increases on the Hurricane fault, indicating strain may have transferred from the west side of the transition zone to the east side through time. Modified from Schramm (1994). Not to scale.*

UTAH GEOLOGICAL SURVEY
a division of
Utah Department of Natural Resources

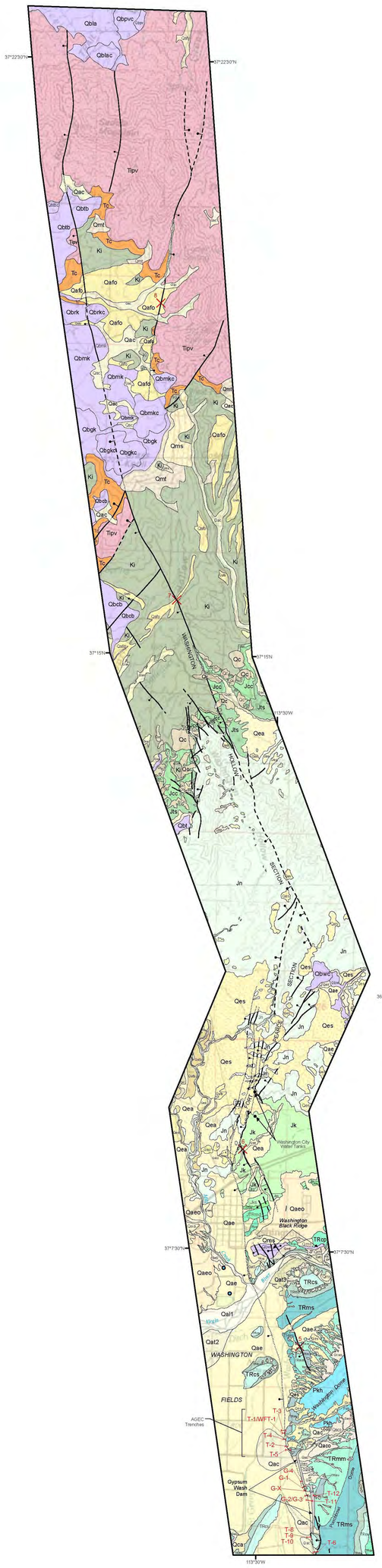

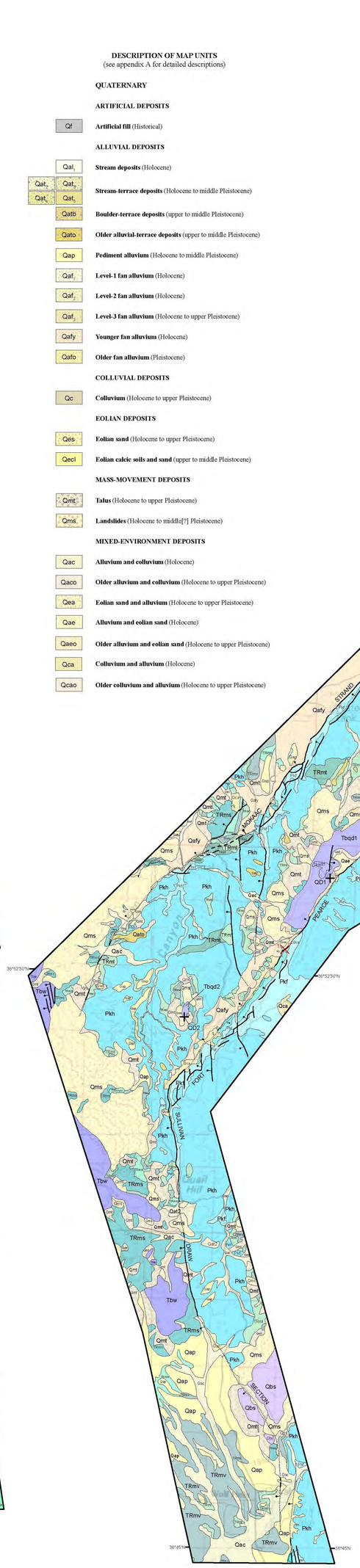

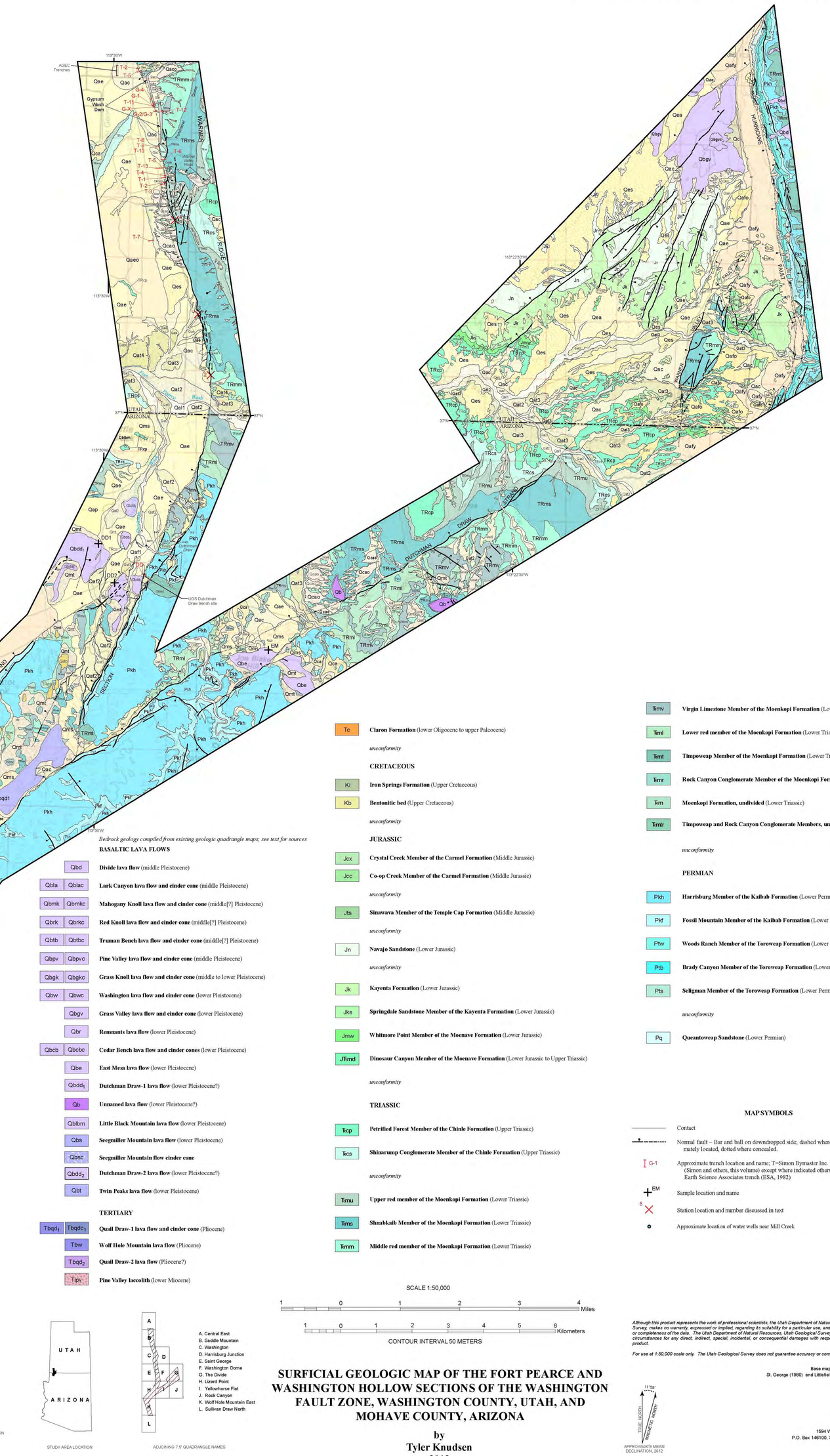

DESCRIPTION OF MAP UNITS

(see appendix A for detailed descriptions)

QUATERNARY

ARTIFICIAL DEPOSITS

- Qf — **Artificial fill** (Historical)

ALLUVIAL DEPOSITS

- Qal_1 — **Stream deposits** (Holocene)
- Qat_2, Qat_3, Qat_4, Qat_5 — **Stream-terrace deposits** (Holocene to middle Pleistocene)
- Qatb — **Boulder-terrace deposits** (upper to middle Pleistocene)
- Qato — **Older alluvial-terrace deposits** (upper to middle Pleistocene)
- Qap — **Pediment alluvium** (Holocene to middle Pleistocene)
- Qaf_1 — **Level-1 fan alluvium** (Holocene)
- Qaf_2 — **Level-2 fan alluvium** (Holocene)
- Qaf_3 — **Level-3 fan alluvium** (Holocene to upper Pleistocene)
- Qafy — **Younger fan alluvium** (Holocene)
- Qafo — **Older fan alluvium** (Pleistocene)

COLLUVIAL DEPOSITS

- Qc — **Colluvium** (Holocene to upper Pleistocene)

EOLIAN DEPOSITS

- Qes — **Eolian sand** (Holocene to upper Pleistocene)
- Qecl — **Eolian calcic soils and sand** (upper to middle Pleistocene)

MASS-MOVEMENT DEPOSITS

- Qmt — **Talus** (Holocene to upper Pleistocene)
- Qms — **Landslides** (Holocene to middle[?] Pleistocene)

MIXED-ENVIRONMENT DEPOSITS

- Qac — **Alluvium and colluvium** (Holocene)
- Qaco — **Older alluvium and colluvium** (Holocene to upper Pleistocene)
- Qea — **Eolian sand and alluvium** (Holocene to upper Pleistocene)
- Qae — **Alluvium and eolian sand** (Holocene)
- Qaeo — **Older alluvium and eolian sand** (Holocene to upper Pleistocene)
- Qca — **Colluvium and alluvium** (Holocene)
- Qcao — **Older colluvium and alluvium** (Holocene to upper Pleistocene)

Bedrock geology compiled from existing geologic quadrangle maps; see text for sources

BASALTIC LAVA FLOWS

- Qbd — **Divide lava flow** (middle Pleistocene)
- Qbla, Qblac — **Lark Canyon lava flow and cinder cone** (middle Pleistocene)
- Qbmk, Qbmkc — **Mahogany Knoll lava flow and cinder cone** (middle[?] Pleistocene)
- Qbrk, Qbrkc — **Red Knoll lava flow and cinder cone** (middle[?] Pleistocene)
- Qbtb, Qbtbc — **Truman Bench lava flow and cinder cone** (middle[?] Pleistocene)
- Qbpv, Qbpvc — **Pine Valley lava flow and cinder cone** (middle Pleistocene)
- Qbgk, Qbgkc — **Grass Knoll lava flow and cinder cone** (middle to lower Pleistocene)
- Qbw, Qbwc — **Washington lava flow and cinder cone** (lower Pleistocene)
- Qbgv — **Grass Valley lava flow and cinder cone** (lower Pleistocene)
- Qbr — **Remnants lava flow** (lower Pleistocene)
- Qbcb, Qbcbc — **Cedar Bench lava flow and cinder cones** (lower Pleistocene)
- Qbe — **East Mesa lava flow** (lower Pleistocene)
- $Qbdd_1$ — **Dutchman Draw-1 lava flow** (lower Pleistocene?)
- Qb — **Unnamed lava flow** (lower Pleistocene?)
- Qblbm — **Little Black Mountain lava flow** (lower Pleistocene)
- Qbs — **Seegmiller Mountain lava flow** (lower Pleistocene)
- Qbsc — **Seegmiller Mountain flow cinder cone**
- $Qbdd_2$ — **Dutchman Draw-2 lava flow** (lower Pleistocene?)
- Qbt — **Twin Peaks lava flow** (lower Pleistocene)

TERTIARY

- $Tbqd_1$, $Tbqdc_1$ — **Quail Draw-1 lava flow and cinder cone** (Pliocene)
- Tbw — **Wolf Hole Mountain lava flow** (Pliocene)
- $Tbqd_2$ — **Quail Draw-2 lava flow** (Pliocene?)
- Tipv — **Pine Valley laccolith** (lower Miocene)
- Tc — **Claron Formation** (lower Oligocene to upper Paleocene)

unconformity

CRETACEOUS

- Ki — **Iron Springs Formation** (Upper Cretaceous)
- Kb — **Bentonitic bed** (Upper Cretaceous)

unconformity

JURASSIC

- Jcx — **Crystal Creek Member of the Carmel Formation** (Middle Jurassic)
- Jcc — **Co-op Creek Member of the Carmel Formation** (Middle Jurassic)

unconformity

- Jts — **Sinawava Member of the Temple Cap Formation** (Middle Jurassic)

unconformity

- Jn — **Navajo Sandstone** (Lower Jurassic)

unconformity

- Jk — **Kayenta Formation** (Lower Jurassic)
- Jks — **Springdale Sandstone Member of the Kayenta Formation** (Lower Jurassic)
- Jmw — **Whitmore Point Member of the Moenave Formation** (Lower Jurassic)
- JTrmd — **Dinosaur Canyon Member of the Moenave Formation** (Lower Jurassic to Upper Triassic)

unconformity

TRIASSIC

- TRcp — **Petrified Forest Member of the Chinle Formation** (Upper Triassic)
- TRcs — **Shinarump Conglomerate Member of the Chinle Formation** (Upper Triassic)

unconformity

- TRmu — **Upper red member of the Moenkopi Formation** (Lower Triassic)
- TRms — **Shnabkaib Member of the Moenkopi Formation** (Lower Triassic)
- TRmm — **Middle red member of the Moenkopi Formation** (Lower Triassic)
- TRmv — **Virgin Limestone Member of the Moenkopi Formation** (Lower Triassic)
- TRml — **Lower red member of the Moenkopi Formation** (Lower Triassic)
- TRmt — **Timpoweap Member of the Moenkopi Formation** (Lower Triassic)
- TRmr — **Rock Canyon Conglomerate Member of the Moenkopi Formation** (Lower Triassic)
- TRm — **Moenkopi Formation, undivided** (Lower Triassic)
- TRmtr — **Timpoweap and Rock Canyon Conglomerate Members, undivided** (Lower Triassic)

unconformity

PERMIAN

- Pkh — **Harrisburg Member of the Kaibab Formation** (Lower Permian)
- Pkf — **Fossil Mountain Member of the Kaibab Formation** (Lower Permian)
- Ptw — **Woods Ranch Member of the Toroweap Formation** (Lower Permian)
- Ptb — **Brady Canyon Member of the Toroweap Formation** (Lower Permian)
- Pts — **Seligman Member of the Toroweap Formation** (Lower Permian)

unconformity

- Pq — **Queantoweap Sandstone** (Lower Permian)

MAP SYMBOLS

- Contact
- Normal fault – Bar and ball on downdropped side; dashed where approximately located, dotted where concealed.
- G-1 — Approximate trench location and name; T=Simon Bymaster Inc. trench (Simon and others, this volume) except where indicated otherwise; G= Earth Science Associates trench (ESA, 1982)
- EM — Sample location and name
- 8 — Station location and number discussed in text
- Approximate location of water wells near Mill Creek

STUDY AREA LOCATION

A. Central East
B. Saddle Mountain
C. Washington
D. Harrisburg Junction
E. Saint George
F. Washington Dome
G. The Divide
H. Lizard Point
I. Yellowhorse Flat
J. Rock Canyon
K. Wolf Hole Mountain East
L. Sullivan Draw North

ADJOINING 7.5' QUADRANGLE NAMES

SCALE 1:50,000

1 0 1 2 3 4 Miles

1 0 1 2 3 4 5 6 Kilometers

CONTOUR INTERVAL 50 METERS

SURFICIAL GEOLOGIC MAP OF THE FORT PEARCE AND WASHINGTON HOLLOW SECTIONS OF THE WASHINGTON FAULT ZONE, WASHINGTON COUNTY, UTAH, AND MOHAVE COUNTY, ARIZONA

by
Tyler Knudsen
2012

Although this product represents the work of professional scientists, the Utah Department of Natural Resources, Utah Geological Survey, makes no warranty, expressed or implied, regarding its suitability for a particular use, and does not guarantee accuracy or completeness of the data. The Utah Department of Natural Resources, Utah Geological Survey, shall not be liable under any circumstances for any direct, indirect, special, incidental, or consequential damages with respect to claims by users of this product.

For use at 1:50,000 scale only. The Utah Geological Survey does not guarantee accuracy or completness of data.

Base map from U.S. Geological Survey
St. George (1980) and Littlefield (1987) 30'x60' quadrangles.

Projection: UTM zone 12
Datum: NAD 83

GIS: Tyler Knudsen
Cartography: Corey D. Unger

Utah Geological Survey
1594 West North Temple, Suite 3110
P.O. Box 146100, Salt Lake City, UT 84114-6100
(801) 537-3300
geology.utah.gov

APPROXIMATE MEAN DECLINATION, 2012

APPENDIX A
DESCRIPTION OF MAP UNITS

Quaternary Deposits

Artificial deposits

Qf Artificial fill (Historical) – Borrow material and engineered fill used to construct flood-control dams, retaining ponds, and roadbeds.

Alluvial deposits

Qal_1 Stream deposits (Holocene) – Stratified, moderately to well-sorted gravel, sand, silt, and clay deposited in larger active drainages; includes small alluvial-fan and colluvial deposits, and minor terraces less than 3 m above modern base level; 0 to 10 m thick.

$Qat_{2\text{-}5}$ Stream-terrace deposits (Holocene to middle Pleistocene) – Stratified, moderately to well-sorted gravel, sand, silt, and clay that forms level to gently sloping terraces above modern drainages; subscripts denote relative heights above the current drainage (and approximate ages); level 2 deposits are about 3 to 9 m, level 3 deposits are about 9 to 15 m, level 4 deposits are 15 to 25 m, and level 5 deposits are about 25 to 32 m above adjacent drainages; 0 to 20 m thick.

Qatb Boulder-terrace deposits (upper to middle Pleistocene) – Poorly to moderately sorted sand- to boulder-sized material forming poorly developed terraces; clasts are mostly basalt; terraces are at several levels from 6 to 60 m above Mill Creek and Washington Hollow drainages; 0 to 6 m thick.

Qato Older alluvial-terrace deposits (upper to middle Pleistocene) – Moderately sorted sand to boulder deposits that form isolated, gently north-sloping surfaces within the uplifted structural block east of the Mokaac fault; clasts are chiefly from an adjacent remnant of the Seegmiller Mountain flow; found about 25 to 45 m above adjacent drainages; 0 to 10 m thick.

Qap Pediment alluvium (Holocene to middle Pleistocene) – Poorly sorted, subangular to rounded, silt- to boulder-sized alluvial deposits that form a locally resistant cap over eroded bedrock surfaces; 0 to 24 m thick.

Qaf_1 Level-1 fan alluvium (Holocene) – Poorly to moderately sorted, subangular to rounded, boulder- to clay-sized sediment deposited at the mouth of Dutchman Draw and other nearby active washes that have cut through the Washington fault escarpment; deposited principally by debris flows and debris floods on active depositional surfaces; about 3 to 9 m thick.

Qaf_2 Level-2 fan alluvium (Holocene) – Poorly to moderately sorted, subangular to rounded, boulder- to clay-sized sediment deposited at the mouth of Dutchman Draw and other nearby washes that have cut through the Washington fault escarpment; deposited principally by debris flows and debris floods, and typically forms inactive surfaces incised by active drainages; about 3 to 12 m thick.

Qaf_3 Level-3 fan alluvium (Holocene to upper Pleistocene) – Similar to level-2 fan alluvium, but clasts have more pronounced desert varnish coating; forms inactive surfaces 3 to 10 m above younger alluvial-fan deposits; about 3 to 15 m thick.

Qafy Younger fan alluvium (Holocene) – Poorly to moderately sorted, non-stratified, subangular to subrounded, boulder- to clay-sized sediment deposited at the mouths of streams and washes; forms both active depositional surfaces (Qaf_1 equivalent) and low-level inactive surfaces incised by small streams (Qaf_2 equivalent) undivided here; deposited principally by debris flows and debris floods, but colluvium locally constitutes a significant part of the deposits; about 3 to 20 m thick.

Qafo Older fan alluvium (Pleistocene) – Poorly to moderately sorted, non-stratified, subangular to subrounded, boulder- to clay-sized sediment with moderately developed calcic soils (hardpan or caliche); forms broad, gently sloping, deeply dissected surfaces about 5 to 20 m above adjacent active drainages; deposited principally by debris flows and debris floods; about 3 to 20 m thick.

Colluvial deposits

Qc Colluvium (Holocene to upper Pleistocene) – Poorly sorted, angular, clay- to boulder-size, locally derived sediment deposited principally by slope wash and soil creep; locally includes talus, alluvium, and eolian sand too small to map separately; gradational with talus; includes older colluvium now incised by adjacent drainages; generally less than 6 m thick.

Eolian deposits

Qes Eolian sand (Holocene to upper Pleistocene) – Well-sorted, fine- to medium-grained, well-rounded, frosted quartz sand; sand is recycled principally from the Navajo Sandstone and Kayenta Formation; locally forms small dunes; locally capped by thick calcic soils (hardpan or caliche); typically less than 6 m thick.

Qecl Eolian calcic soils and sand (upper to middle Pleistocene) – Thick pedogenic carbonate (hardpan or caliche) mixed with minor to moderate amounts of eolian sand (Qes); mapped in areas where most eolian sands have been stripped off, leaving calcic-soil caps covering bedrock; 0 to 6 m thick.

Mass-movement deposits

Qmt Talus (Holocene to upper Pleistocene) – Poorly sorted, angular boulders and finer grained interstitial sediment deposited principally by rock fall on and at the base of steep slopes; typically grades downslope into colluvium where impractical to differentiate the two; also includes alluvium in the bottom of washes; generally less than 9 m thick.

Qms Landslides (Holocene to middle[?] Pleistocene) – Very poorly sorted, clay- to boulder-size, locally derived material deposited principally by rotational slump processes; commonly

characterized by hummocky topography, numerous subdued internal scarps, and chaotic bedding attitudes; thickness highly variable.

Mixed-environment deposits

Qac, Qaco Alluvium and colluvium (Holocene to upper Pleistocene) – Poorly to moderately sorted, clay- to boulder-size, locally derived sediments deposited in swales and small drainages; gradational with alluvial and colluvial deposits; older deposits (Qaco) form incised, inactive surfaces up to about 6 meters above modern drainages; generally less than 6 m thick.

Qea Eolian sand and alluvium (Holocene to upper Pleistocene) – Well-sorted, fine- to medium-grained eolian sand reworked by alluvial processes, and poorly to moderately sorted gravel, sand, and silt deposited in small channels; generally less than 6 m thick.

Qae, Qaeo Alluvium and eolian sand (Holocene to upper Pleistocene) – Moderately sorted gravel, sand, and silt deposited in small channels and on alluvial flats, and well-sorted, fine- to medium-grained eolian sand locally reworked by alluvial processes; younger deposits (Qae) form active depositional surfaces, whereas older deposits (Qaeo) typically form incised, inactive surfaces; generally less than 9 m thick.

Qca, Qcao Colluvium and alluvium (Holocene to upper Pleistocene) – Poorly sorted, angular to rounded, fine-grained to boulder-sized material deposited on broad, moderate slopes; deposited by slope wash, debris flow, and slope creep processes and lack well-defined drainage patterns; locally includes talus, eolian, or alluvial deposits; younger deposits (Qca) form active depositional surfaces whereas older deposits (Qcao) are inactive and deeply incised; 0 to 10 m thick.

Basaltic lava flows

Qbd Divide lava flow (middle Pleistocene) – Dark-gray, fine-grained basalt to basanite with small olivine phenocrysts; forms lava cascade over Hurricane Cliffs; yielded an $^{40}Ar/^{39}Ar$ age of 0.41 ± 0.08 Ma (Hayden, 2004a); lava flow is generally 5 to 12 m thick.

Qbla, Qblac Lark Canyon lava flow and cinder cone (middle Pleistocene) – Dark-gray basalt (Qbla) with small olivine phenocrysts; erupted from a vent at a cinder cone (Qblac) about 3 km southwest of Pine Valley; yielded an $^{40}Ar/^{39}Ar$ plateau age of 0.61 ± 0.04 Ma (0.64 ± 0.04 Ma isochron) (UGS and New Mexico Geochronology Research Laboratory [NMGRL], 2007) and a K-Ar age of 0.56 ± 0.06 Ma (Best and others, 1980); lava flow is generally 6 to 12 m thick.

Qbmk, Qbmkc Mahogany Knoll lava flow and cinder cone (middle[?] Pleistocene) – Dark-gray basalt (Qbmk) with small olivine phenocrysts; erupted from vents at cinder cones (Qbmkc) on the southwest flank of the Pine Valley Mountains; yielded a K-Ar age of 1.2 ± 0.1 Ma (Best and others, 1980), but based on geomorphic expression, is believed to be younger and of comparable age to nearby lava flows that are about 600 ka (Biek and others, 2009); lava flow is generally 6 to 12 m thick.

Qbrk, Qbrkc Red Knoll lava flow and cinder cone (middle[?] Pleistocene) – Gray andesite to trachyandesite (Qbrk) that erupted from a vent at a cinder cone (Qbrkc) on the southwest flank of the Pine Valley Mountains; yielded a low-confidence $^{40}Ar/^{39}Ar$ integrated age of 0.45 ± 0.86 Ma (1.12 ± 0.50 Ma isochron) (UGS and NMGRL, 2007), but based on geomorphic expression is probably about 450 to 700 ka (Biek and others, 2009); lava flow is generally 9-18 m thick.

Qbtb, Qbtbc Truman Bench lava flow and cinder cone (middle[?] Pleistocene) – Dark-gray basalt to trachybasalt (Qbtb) with small olivine phenocrysts; erupted from a vent at a cinder cone (Qbtbc) on the southwest flank of the Pine Valley Mountains; probably about 450 to 700 ka based on comparison with nearby flows (Biek and others, 2009); lava flow is generally 6 to 12 m thick.

Qbpv, Qbpvc Pine Valley lava flow and cinder cone (middle Pleistocene) – Dark-gray basaltic lava flows (Qbpv) with small olivine phenocrysts; erupted from a number of vents at cinder cones (Qbpvc) west of Pine Valley; yielded an $^{40}Ar/^{39}Ar$ plateau age of 0.67 ± 0.07 Ma (0.67 ± 0.08 Ma isochron) (UGS and NMGRL, 2007); lava flow is generally 6 to 12 m thick.

Qbgk, Qbgkc Grass Knoll lava flow and cinder cone (middle to lower Pleistocene) – Dark-gray basalt to trachybasalt (Qbgk) with small olivine phenocrysts; erupted from a vent at the Grass Knoll cinder cone (Qbgkc) on the southwest flank of the Pine Valley Mountains; yielded an $^{40}Ar/^{39}Ar$ integrated age of 1.02 ± 0.36 Ma (1.20 ± 0.17 Ma isochron) (UGS and NMGRL, 2007); lava flow is generally 6 to 12 m thick.

Qbw, Qbwc Washington lava flow and cinder cone (lower Pleistocene) – Medium- to dark-gray to dark-greenish-gray, fine-grained basanite to picobasalt (Qbw) with abundant clinopyroxine and olivine phenocrysts; erupted from a vent at a cinder cone (Qbwc) about 5 km northeast of Washington; yielded $^{40}Ar/^{39}Ar$ ages of 0.87 ± 0.04 and 0.98 ± 0.02 Ma (Biek, 2003a), which fit well with regional incision rates (Willis and Biek, 2001), but Best and others (1980) reported an anomalously old K-Ar age of 1.7 ± 0.1 Ma for this flow; lava flow is 8 to 11 m thick except near its source, where it is as much as 30 m thick.

Qbgv Grass Valley lava flow and cinder cone (lower Pleistocene) – Dark-gray, fine- to medium-grained trachybasalt to basalt (Qbgv) with small olivine phenocrysts; erupted from a vent at a deeply eroded cinder cone (Qbgvc) about 11 km south of Hurricane; yielded an $^{40}Ar/^{39}Ar$ plateau age of 1.09 ± 0.09 Ma (0.966 ± 0.030 Ma preliminary isochron) (UGS unpublished data); lava flow is several meters thick.

Qbr Remnants lava flow (lower Pleistocene) – Dark-brownish-black to dark-gray, medium-grained basanite with small olivine phenocrysts; vertically displaced by the Hurricane fault about 440 m; yielded preferred $^{40}Ar/^{39}Ar$ plateau ages of 1.06 ± 0.03 Ma (1.07 ± 0.08 Ma isochron) and 0.94 ± 0.04 Ma (0.94 ± 0.05 Ma isochron) (Hayden, 2004a) and an anomalous $^{40}Ar/^{39}Ar$ plateau age of 1.47 ± 0.34 Ma (1.12 ± 0.50 Ma isochron) (Lund and others, 2001, 2007a); typically about 12 m thick.

Qbcb, Qbcbc Cedar Bench lava flow and cinder cones (lower Pleistocene) – Dark-greenish-gray to brownish-black trachybasalt (Qbcb) with small phenocrysts of clinopyroxine and olivine;

yielded an $^{40}Ar/^{39}Ar$ plateau age of 1.23 ± 0.01 Ma (UGS unpublished data); erupted from vents at two overlapping cinder cones (Qbcbc) about 19 km north of St. George; flow is displaced by minor splays of the Washington Hollow fault; lava flow is typically 3 to 9 m thick, but as much as about 30 m thick where it fills paleotopography.

Qbe East Mesa lava flow (lower Pleistocene) – Dark-gray, fine-grained trachybasalt with small olivine phenocrysts; yielded an $^{40}Ar/^{39}Ar$ plateau age of 1.28 ± 0.01 Ma (this study) and a K-Ar age of 1.4 ± 0.25 Ma (Wenrich and others, 1995); vertically displaced about 45 m by a splay of the Dutchman Draw fault; thickness varies from about 9 to 55 m.

$Qbdd_1$ Dutchman Draw-1 lava flow (lower Pleistocene?) – Dark-gray, fine-grained trachybasalt with small olivine phenocrysts; caps a series of low hills north of the Mokaac strand of the Washington fault and west of Dutchman Draw; geochemical analyses indicate a possible correlation with either the East Mesa or West Mesa lava flow (Lund and Knudsen this volume); less than 12 m thick.

Qb Unnamed lava flow (lower Pleistocene?) – Dark-gray, fine-grained basalt with small olivine phenocrysts; likely similar in age to the East Mesa flow based on flow morphology; up to 45 m thick.

Qblbm Little Black Mountain lava flow (lower Pleistocene) – Dark-gray, fine-grained olivine basalt; only a small remnant caps Little Black Mountain; yielded a K-Ar age of 1.7 ± 0.4 Ma (Wenrich and others, 1995); less than 12 m thick.

Qbs Seegmiller Mountain lava flow (lower Pleistocene) – Dark-gray, fine-grained basalt with small olivine and augite phenocrysts; vertically displaced by the Sullivan Draw section of the Washington fault by as much as 85 m; erupted from a number of probable source areas east of the map area (Billingsley, 1993); yielded an $^{40}Ar/^{39}Ar$ plateau age of 2.3 ± 0.02 Ma (this study), an anomalous $^{40}Ar/^{39}Ar$ total gas age of 4.17 ± 0.18 Ma (Downing and others 2001), and K-Ar ages of 2.35 ± 0.31 Ma and 2.44 ± 0.51 Ma (Reynolds and others, 1986); thickness varies from 10 to 60 m.

$Qbdd_2$ Dutchman Draw-2 lava flow (lower Pleistocene?) – Dark-gray, fine-grained basalt with small olivine phenocrysts; caps a series of low ridges and hills west of the Washington fault and south of Dutchman Wash; geochemical analyses indicate a possible correlation with the Seegmiller Mountain flow (Lund and Knudsen this volume); lava flow is 3 to 12 m thick.

Qbt Twin Peaks lava flow (lower Pleistocene) – Dark-gray to dark-brownish-gray basaltic trachyandesite with large plagioclase and quartz, and small olivine and clinopyroxene phenocrysts; yielded a $^{40}Ar/^{39}Ar$ plateau age of 2.43 ± 0.02 Ma (UGS unpublished data); lava flow is generally about 6 to 24 m thick.

Tertiary Deposits

$Tbqd_1$, **$Tbqdc_1$** Quail Draw-1 lava flow and cinder cone (Pliocene) – Dark-gray, fine-grained Hawaiite basalt with small olivine crystals; caps mesa west of Quail Draw near the intersection of the main and Dutchman Draw strands of the Fort Pearce section of the Washington fault; erupted from a vent at a cinder cone ($Tbqdc_1$) marked by light-red basaltic cinder and scoria (Billingsley, 1993); yielded an $^{40}Ar/^{39}Ar$ plateau age of 2.8 ± 0.01 Ma (this study) and an $^{40}Ar/^{39}Ar$ plateau age of 3.32 ± 0.04 Ma (Downing and others 2001); generally less than 20 m thick.

Tbw Wolf Hole Mountain lava flow (Pliocene) – Dark-gray to brownish-black olivine basalt capping Wolf Hole Mountain; erupted from several vents on Wolf Hole Mountain just west of the map area (Billingsley, 1993); yielded a K-Ar age of 3.1 ± 0.4 Ma (Wenrich and others, 1995); between 25 and 50 m thick in the map area.

$Tbqd_2$ Quail Draw-2 lava flow (Pliocene?) – Dark-gray, fine-grained basalt with small olivine crystals; caps small, isolated mesa west of Quail Draw; map relations indicate a possible correlation with the Wolf Hole Mountain lava flow; lava flow is about 8 m thick.

Tipv Pine Valley laccolith (lower Miocene) – Locally flow layered, medium-gray quartz monzonite porphyry with medium- to coarse-grained phenocrysts of plagioclase, pyroxene, biotite, and sanadine; groundmass is fine-grained to microscopic plagioclase, quartz, and pyroxene; yielded a K-Ar age on biotite of 20.9 ± 0.6 Ma (McKee and others, 1997), and $^{40}Ar/^{39}Ar$ ages of 20.47 ± 0.04 and 20.63 ± 0.12 Ma from a sample collected from the base of the laccolith, and 20.32 ± 0.12 and 20.46 ± 0.05 Ma from a sample collected 150 m above the base (Rowley and others, 2006).

Tc Claron Formation (lower Oligocene to upper Paleocene) – Interbedded mudstone, siltstone, sandstone, conglomerate, and limestone; mudstone is orangish red to reddish brown; sandstone is light-brown, medium- to coarse-grained, cross-bedded to structureless litharenite; about 450 m thick in the southwestern Pine Valley Mountains.

unconformity

Cretaceous

Ki Iron Springs Formation (Upper Cretaceous) – Interbedded, ledge-forming, calcareous, cross-bedded, fine- to medium-grained sandstone, siltstone, and mudstone; contains a few coquina beds, minor carbonaceous shale, and uncommon pebbly sandstone; about 1100 m thick in the Pine Valley Mountains.

Kb Bentonitic bed (Upper Cretaceous) – Pale-gray to pinkish-gray, bentonitic clay and minor siltstone and fine-grained sandstone; nonresistant and poorly exposed; 18-23 m thick.

unconformity

Jurassic

Jcx Crystal Creek Member of the Carmel Formation (Middle Jurassic) – Reddish-brown, thin-bedded, poorly exposed sandstone and mudstone; 0 to 15 m thick.

Jcc Co-op Creek Member of the Carmel Formation (Middle Jurassic) – Pale-gray, pale-greenish-gray, or pale-yellowish-gray, interbedded limestone, sandstone, and mudstone; fossiliferous; thin uniform bedding; about 87 m thick.

unconformity

Jts Sinawava Member of the Temple Cap Formation (Middle Jurassic) – Dark-reddish-brown to pale-gray, slope-forming mudstone, claystone, and gypsum; contains several white, gray, and pink alabaster gypsum beds as much as 3 m thick; about 60 m thick.

unconformity

Jn Navajo Sandstone (Lower Jurassic) – Pale-yellowish-gray to moderate-grayish-red, well-sorted, fine- to medium-grained quartz sandstone; grains are well rounded and frosted; prominent eolian cross-beds; strongly jointed; about 610 m thick.

unconformity

Jk Kayenta Formation (Lower Jurassic) – Moderate- to dark-reddish-brown, thin- to thick-bedded siltstone, fine-grained sandstone, and mudstone with planar, low-angle, and ripple cross-stratification; cross-cutting gypsum veinlets are common; about 350 m thick.

Jks Springdale Sandstone Member of the Kayenta Formation (Lower Jurassic) – Pale-reddish-brown to grayish-yellow, fine- to medium-grained, cross-bedded sandstone with interbedded light-purplish-gray siltstone near the middle; weathers to rounded ledges; typically 30 to 35 m thick.

Jmw Whitmore Point Member of the Moenave Formation (Lower Jurassic) – Greenish-gray claystone interbedded with pale-brown to pale-red, thin-bedded siltstone with several 8- to 120-cm-thick beds of light-greenish-gray dolomitic limestone that contains algal structures and fossil fish scales; nonresistant and poorly exposed; ranges from about 15 to 40 m thick.

JTRmd Dinosaur Canyon Member of the Moenave Formation (Lower Jurassic to Upper Triassic) – Interbedded moderate-reddish-brown siltstone and pale-reddish-brown to grayish-red, fine-grained, thin-bedded sandstone with laminated cross-beds; forms ledgy slopes; 45 to 75 m thick.

unconformity

Triassic

TRcp Petrified Forest Member of the Chinle Formation (Upper Triassic) – Varicolored, typically gray to purple mudstone, claystone, and siltstone, lesser white to yellow-brown sandstone and pebbly sandstone, and minor chert and nodular limestone; petrified wood is common; commonly forms landslides; about 120 to 200 m thick.

TRcs Shinarump Conglomerate Member of the Chinle Formation (Upper Triassic) – Grayish-orange to moderate-yellowish brown, medium- to coarse-grained sandstone, pebbly sandstone, and lesser pebbly conglomerate; forms prominent cliffs, hogbacks and mesas; ranges from 2 to 75 m thick.

unconformity

TRmu Upper red member of the Moenkopi Formation (Lower Triassic) – Moderate-reddish-orange to moderate-reddish-brown, mostly thin- to medium-bedded siltstone, mudstone, and fine-grained sandstone with planar, low-angle, and ripple cross-stratification; typically 80 to 110 m thick.

TRms Shnabkaib Member of the Moenkopi Formation (Lower Triassic) – Forms "bacon-striped," ledgy slopes of laminated to thin-bedded, gypsiferous, pale-red to moderate-reddish-brown mudstone and siltstone, resistant, white to greenish-gray gypsum, and minor thin, laminated, light-gray dolomite beds; thickens northwesterly across the map area from 115 to 210 m.

TRmm Middle red member of the Moenkopi Formation (Lower Triassic) – Interbedded, slope-forming, laminated to thin-bedded, moderate-reddish-brown to moderate-reddish-orange siltstone, mudstone, and fine-grained sandstone with thin interbeds and veinlets of greenish-gray to white gypsum; thickens northeasterly across map area from about 50 to 120 m.

TRmv Virgin Limestone Member of the Moenkopi Formation (Lower Triassic) – Light-gray, light-olive-gray, and yellowish-brown limestone and silty limestone that typically forms three to four thin, resistant ledges that are separated by slopes of white to pale-yellow, red, and blue-gray, thin-bedded gypsum and gypsiferous siltstone; generally thickens northward across map area from about 30 to 70 m.

TRml Lower red member of the Moenkopi Formation (Lower Triassic) – Interbedded, slope-forming, laminated to thin-bedded, moderate-reddish-brown mudstone, siltstone, and fine-grained sandstone with local, thin, laminated light-olive-gray gypsum beds and veinlets; thickness ranges from 0 to 85 m.

TRmt Timpoweap Member of the Moenkopi Formation (Lower Triassic) – Lower part consists of light-brown-weathering, light-gray to grayish-orange, thin- to thick-bedded limestone and cherty limestone; upper part consists of grayish-orange, thin- to thick-bedded, slightly calcareous, fine-grained sandstone, siltstone, and mudstone; varies from 15 to 55 m thick.

TRmr Rock Canyon Conglomerate Member of the Moenkopi Formation (Lower Triassic) – Pebble to cobble, clast-supported conglomerate that contains subrounded to rounded chert clasts set in a pinkish-gray to very pale orange, calcareous, medium- to coarse-grained sandstone matrix; also includes a widespread, but thin, well-cemented breccia; conglomerate and breccia clasts are predominantly chert and limestone derived from underlying Kaibab Formation; fills paleovalleys; thickness ranges from 0 to about 90 m.

TRm Moenkopi Formation, undivided (Lower Triassic) – West-dipping, fault-bounded blocks of lower, middle, or upper red strata along the Hurricane fault.

TRmtr Timpoweap and Rock Canyon Conglomerate Members, undivided (Lower Triassic) – Mapped undivided in Arizona.

unconformity

Permian

Pkh Harrisburg Member of the Kaibab Formation (Lower Permian) – Upper part consists mainly of slope-forming, red and gray, gypsiferous siltstone, sandstone, gray gypsum, and thin-bedded gray limestone; medial part consists of an upper dark-brown-weathering cherty limestone bed and a lower light-gray, thick-bedded, sandy limestone bed separated by thin-bedded gypsiferous sandstone; lower part consists of slope-forming, light-red, fine- to medium-grained gypsiferous siltstone and sandstone, interbedded with gray, medium-grained, thin-bedded limestone and gray to white, thick-bedded gypsum. Thickness varies from 0 to 100 m.

Pkf Fossil Mountain Member of the Kaibab Formation (Lower Permian) – Lithologically uniform, light-gray, thick-bedded, fossiliferous limestone and cherty limestone; “black-banded” due to abundant reddish-brown to black ribbon chert and irregular chert nodules; maintains uniform thickness of about 90 m.

Ptw Woods Ranch Member of the Toroweap Formation (Lower Permian) – Laterally variable, interbedded, yellowish-gray to light-gray, laminated to thin-bedded dolomite and similarly bedded black chert, massive gypsum, yellowish-orange gypsiferous mudstone and siltstone, and limestone; thickness varies from 35 to 100 m due to dissolution of gypsum.

Ptb Brady Canyon Member of the Toroweap Formation (Lower Permian) – Light- to medium-gray, medium- to coarse-grained, thick-bedded, fossiliferous limestone and cherty limestone; ribbon chert and irregular chert nodules locally make up 30 to 40% of the rock; 50 to 75 m thick.

Pts Seligman Member of the Toroweap Formation (Lower Permian) – Forms slopes of yellowish-brown to grayish-orange, thin-bedded, planar-bedded, fine- to medium-grained sandstone and minor siltstone with brown-weathering nodular chert; thickness ranges from 9 to 50 m.

unconformity

Pq Queantoweap Sandstone (Lower Permian) – Yellowish-brown, pale-orange, and grayish-orange, thick-bedded, cross-bedded, fine- to medium-grained sandstone that weathers to a conspicuous stair-step topography; about 425 to 520 m thick.

UTAH GEOLOGICAL SURVEY
DUTCHMAN DRAW SITE PALEOSEISMIC INVESTIGATION, FORT PEARCE SECTION, WASHINGTON FAULT ZONE, MOHAVE COUNTY, ARIZONA

by
William R. Lund, Tyler R. Knudsen, Christopher B. DuRoss, and Greg N. McDonald
Utah Geological Survey

CONTENTS

ABSTRACT 73
INTRODUCTION 74
GEOLOGIC SETTING 74
TRENCHING 75
North Trench 75
Stratigraphy 75
Structure 77
South Trench 77
Stratigraphy 77
Structure 78
Numerical Ages 79
Radiocarbon Ages 79
Optically Stimulated Luminescence Ages 80
PALEOSEISMOLOGY 81
Number of Earthquakes 81
Earthquake Timing and Recurrence 83
Earthquake Timing 83
Earthquake Recurrence 83
Vertical Displacement 84
Scarp Profiles 84
Displaced Trench Stratigraphy 85
Colluvial-Wedge Thickness 85
Vertical Slip Rate 86
Paleoearthquake Magnitude Estimates 86
Anderson and others (1996) – SRL for All Fault Types and SR 87
Stirling and others (2002) – Censored Instrumental SRL Relation 88
Wesnousky (2008) – SRL All Fault Types 88
Summary 88
STUDY RESULTS 89
ACKNOWLEDGEMEMTS 90
REFERENCES 90

FIGURES

Figure 1. Dutchman Draw trench site on the main strand of the Fort Pearce section of the Washington fault zone. 93
Figure 2. Dutchman Draw trench site area geologic map showing the location of paleoseismic trenches and scarp profiles. 94
Figure 3. Fault scarp formed on a late Quaternary alluvial fan at the Dutchman Draw trench site. 95
Figure 4. Dutchman Draw trench site geologic and topographic map 96
Figure 5. Dutchman Draw trench site scarp profile #2 97

Figure 6. Dutchman Draw trench site scarp profile #3 97

TABLES

Table 1. AMS radiocarbon age results for carbon samples from the Dutchman Draw site trenches, Arizona 98
Table 2. OSL age results for sediment samples from the Dutchman Draw site trenches, Arizona 98
Table 3. Radiocarbon and OSL ages used in OxCal v. 4.1.7 to model earthquake timing at the Dutchman Draw site, Arizona 99
Table 4. Earthquake timing and recurrence (one seismic cycle) at the Dutchman Draw site, Arizona.....99

PLATE

Plate 1. Stratigraphic and structural relations exposed in trenches at the Dutchman Draw trench site, Fort Pearce section, Washington fault zone, Arizona.....

APPENDICES

Appendix A – Dutchman Draw site trench geologic unit descriptions 100
Appendix B – Examination of bulk soil and AMS radiocarbon analysis of carbon from the Dutchman Draw trenches, Washington fault zone, Arizona.....101
Appendix C – USU Luminescence Laboratory OSL ages, Dutchman Draw trench site, Washington fault zone, Arizona.....115
Appendix D – Dutchman Draw trench site OxCal model 121

ABSTRACT

The Utah Geological Survey conducted a paleoseismic trenching investigation to develop new information on paleoearthquake timing and displacement for the Fort Pearce section of the late-Quaternary-active Washington fault zone in southwestern Utah. Those data, along with the earthquake recurrence and vertical slip-rate estimates derived from them, can be used to improve both deterministic seismic-source characterization models and probabilistic earthquake-hazard analyses in the rapidly urbanizing St. George, Utah, metropolitan area. The data will also be used to update the U.S. Geological Survey's *Quaternary Fault and Fold Database of the United States*, the Utah Geological Survey's *Quaternary Fault and Fold Database and Map of Utah,* and the *National Seismic Hazard Maps* for Utah and Arizona.

Stratigraphic and structural relations exposed in two trenches excavated across a fault scarp formed on a late Quaternary alluvial fan near Dutchman Draw in Arizona, revealed evidence for two surface-faulting earthquakes on the main strand of the Fort Pearce section. OxCal modeling of a combination of radiocarbon and optically stimulated luminescence ages constrain the timing of the earthquakes to the Holocene, one at about 7.7 ± 2.4 ka (P2) and the other at about 1.0 ± 0.6 ka (P1) (rounded to the nearest 100 years, two-sigma uncertainty). The closed-seismic-cycle recurrence interval between the two earthquakes (also modeled with OxCal) is 6.6 ± 2.4 kyr. Additionally, the trenches revealed indirect stratigraphic evidence permissive of, but not conclusive for, at least one latest Pleistocene earthquake that may have occurred between 13.8 ± 1.2 and 17.1 ± 1.4 ka. If a P3 earthquake did occur in that time interval, and the P2 earthquake occurred at 7.7 ± 2.4 ka, the length of the resulting P3–P2 recurrence interval would range from about 2.5 to 13.2 kyr, with a median value at about 7.9 kyr. The P2-P1 recurrence interval of 6.6 ± 2.4 kyr is within one sigma of the possible P3–P2 median value, suggesting that the P2–P1 recurrence interval may be generally representative of the average surface-faulting recurrence on the Fort Pearce section during latest Quaternary time.

We obtained net vertical displacement estimates at the Dutchman Draw site from a combination of scarp profiles, displaced stratigraphy exposed in trenches, and scarp free-face heights extrapolated from colluvial-wedge thicknesses. Displacements ranged from about 1.0 m (P1) to 2.4 m (P2). There are significant caveats associated with all three displacement estimation methods at the Dutchman Draw site; therefore, we consider the displacement values poorly constrained best estimates. The vertical slip rate for the P2–P1 recurrence interval (6.6 ± 2.4 kyr) and the P1 net vertical displacement (1.0-1.2 m) is 0.11-0.29 mm/yr (average 0.2 mm/yr). This slip-rate range represents only the most recent closed seismic cycle, and should be treated with caution if used to extrapolate the long-term behavior of the Fort Pearce section.

Using multiple regression relations recommended by the Working Group on Utah Earthquake Probabilities to estimate M_w for various rupture scenarios for the Fort Pearce section resulted in magnitude estimates ranging from M_w 6.7 to 7.1, depending on the regression used and length of surface rupture. Available paleoseismic information is insufficient to fully characterize all possible Fort Pearce section rupture scenarios, but our limited analysis shows that the Fort Pearce section is likely to produce future earthquakes of $M_w \geq 7$, with average recurrence intervals of several thousand years.

INTRODUCTION

The purpose of this paleoseismic trenching investigation was to develop new information on paleoearthquake timing and displacement for the Fort Pearce (formerly Northern; Knudsen this volume) section of the late-Quaternary-active Washington fault zone in southwestern Utah. Those data, along with the earthquake recurrence and vertical slip-rate estimates derived from them can be used to improve both deterministic seismic-source characterization models and probabilistic earthquake-hazard analyses in the rapidly urbanizing St. George metropolitan area of Washington County, Utah. The data will also be used to update the U.S. Geological Survey's *Quaternary Fault and Fold Database of the United States* (http://earthquake.usgs.gov/hazards/qfaults), the Utah Geological Survey's (UGS) *Quaternary Fault and Fold Database and Map of Utah*, and the *National Seismic Hazard Maps* (http://earthquake.usgs.gov/hazards/index.php) for Utah and Arizona.

The Washington fault zone is one of several north-south trending, down-to-the-west Quaternary normal faults that define the boundary between the Colorado Plateau and Basin and Range physiographic provinces in northern Arizona and southwestern Utah (Lund, this volume). Based on structural and geomorphic criteria, Pearthree (1998) subdivided the Washington fault zone from south to north into the Sullivan Draw, Mokaac, and Northern sections (Lund, this volume). The Northern section, redefined as the Fort Pearce section by Knudsen (this volume), trends into the St. George metropolitan area, and scarps on unconsolidated basin-fill deposits and soft bedrock are evidence of late Quaternary surface faulting; therefore, the Fort Pearce section is considered active and capable of producing future large, damaging earthquakes.

Recognizing the earthquake hazard presented by the Fort Pearce section to the St. George metropolitan area, the UGS initiated a 1:50,000-scale surficial geologic mapping project (Knudsen this volume) to better define the Fort Pearce section's location, boundaries, and geometry. While conducting the mapping, the UGS identified an isolated fault scarp formed on a latest Quaternary alluvial fan near Dutchman Draw south of the Utah–Arizona border (figure 1). After site evaluation that include three-dimensional (3-D) tomographic seismic profiling (Shengdong Liu, University of Utah Department of Geology and Geophysics, written communication, 2008), the UGS excavated and logged two trenches across the scarp, and excavated a third trench several meters west of the scarp to explore for possible antithetic faulting inferred from the seismic profiles. The two scarp trenches exposed the fault zone and associated fault-related geologic deposits that provide new information on the timing, recurrence, and displacement of the two most recent surface-faulting earthquakes on the main strand of the Fort Pearce section, and indirect evidence for a possible third, older earthquake. The third trench did not uncover evidence of antithetic faulting and was not logged.

GEOLOGIC SETTING

The Dutchman Draw trench site is approximately 6 km south of the Utah-Arizona border near the southern end of the Fort Pearce section (figure 1). We selected the site based on

interpretation of 1:24,000-scale, color aerial photographs (Knudsen this volume) and a field reconnaissance along the fault in Utah and Arizona. The site is about 0.6 km south of Dutchman Draw (figure 1) at the mouth of a small unnamed ephemeral drainage where the fault displaces a late Quaternary alluvial fan (figure 2). The fault scarp is 2 to 4 m high (figure 3), and is continuous across the fan for approximately 100 m. The scarp is expressed as a single trace across most of the site before bifurcating to form two subparallel strands near its southern end (figure 4). There is no surface evidence of antithetic faulting. North and south of the site, scarps are formed on bedrock, but at the site, a stream cut dissects the fault scarp and exposes alluvial deposits that are at least 4 m thick in the fault footwall. The 3-D seismic profiling (Shengdong Liu, University of Utah Department of Geology and Geophysics, written communication, 2008) showed that the scarp is not bedrock cored, and that unconsolidated alluvial-fan deposits extend to a depth of several meters on the fault hanging wall. A second, subparallel fault trace to the east is well expressed in bedrock, but geologic mapping (Knudsen this volume) shows that it does not displace Holocene/latest Quaternary unconsolidated deposits. Because the site is on the remote southern part of the Fort Pearce section, it has received minimal human-caused disturbance.

TRENCHING

We excavated three trenches (North, South, and West) at the Dutchman Draw site (figures 2 and 4 and plate 1). The North and South trenches were roughly parallel, about 5 m apart, and normal to the main fault scarp. Both trenches exposed the fault zone and associated geologic units. Detailed trench logging demonstrated that the geologic units were common to both trenches (plate 1). We excavated the West trench in the fault hanging wall about 30 m west of the main fault scarp (figure 2) to explore for possible antithetic faulting indicated by the 3-D tomographic seismic profiles; however, no antithetic faults were discovered and we did not log the West trench.

We established meter-scale horizontal and vertical grid systems in the North and South trenches, and measured both horizontal and vertical distances from the east end of the North trench (plate 1). The grid system in the shorter South trench was tied to the grid system in the longer Northern trench; consequently, the east end of the South trench grid corresponds to horizontal station 13 in the North trench and is numbered accordingly on plate 1. We logged the North and South trenches at a scale of 1:20 using a total station instrument (Trimble TTS 500) to measure geologic control points.

North Trench

Stratigraphy

The North trench exposed nine geologic units, with units 1 and 4 further subdivided into “a” and “b” subunits (plate 1; appendix A). Units 8 and 9 were the only units exposed in the fault footwall; unit 9 was not exposed on the fault hanging wall. Unit 9, the oldest stratigraphic unit in the trench, consists of steeply dipping to overturned red mudstone, siltstone, and fine sandstone bedrock of the Triassic Moenkopi Formation. Unit 8 unconformably overlies unit 9

creating an angular unconformity, and consists of strongly indurated (chiefly gypsum cemented), coarse-grained, massively bedded alluvial sediments (appendix A). Because of its thickness, massive bedding, and strong cementation, we interpret unit 8 as an undifferentiated "alluvial-fan" deposit that likely consists of numerous individual debris-flow and debris-flood deposits; however, we were unable to map any stratigraphically continuous subunits in unit 8. The upper part of unit 8 yielded an optically stimulated luminescence (OSL) age of 48.66 ± 3.74 ka (see the Numerical Ages section below and appendices B and C for details regarding the radiocarbon [^{14}C] and OSL ages obtained from the North and South trenches).

The fault zone in the North trench contained tilted and sheared blocks of unit 8 (see Structure section below), but unit 8 was not present elsewhere in the fault footwall. Unit 8 is in fault contact with unit 7, a strongly indurated, coarse-grained, massively bedded debris-flow deposit (plate 1, appendix A). Unit 6 was of limited extent in the North trench, but was thicker and more extensive in the South trench. Unit 6 is a moderately indurated, coarse-grained, thick-bedded debris-flow deposit. Unit 5 conformably overlies units 6, 7, and 8 in the fault hanging wall, and is a weakly indurated, coarse-grained debris-flow deposit. Units 5 through 9 predate the penultimate surface-faulting earthquake (P2) at the Dutchman Draw site.

Unit 4 consists of the colluvial-wedge (unit 4a) and associated crack-fill (unit 4b) deposits formed by fault-scarp erosion following the P2 earthquake. We obtained three stratigraphically consistent ^{14}C ages (6900-6200 cal yr. B.P., 4420-4250 cal yr. B.P., and 4150-4300 (92.7%) and 4330-4360 (2.7%) cal yr B.P. [2σ)]; appendix B) from weakly organic, fine-grained horizons in unit 4a (plate 1). An OSL sample from near the bottom of the P2 colluvial wedge (plate 1) yielded an anomalously young age of 3.03 ± 0.34 ka when compared with the three stratigraphically consistent ^{14}C ages (see discussion regarding why numerical ages may be out of stratigraphic order in the Numerical Ages section below).

Unit 3 is a loosely indurated debris-flow deposit (appendix A), which conformably overlies unit 5 but does not overlie unit 4. Because units 3 and 4 occupy the same relative stratigraphic position in the North trench, and because there are no numerical ages available for unit 3, it is not known if unit 3 is older, younger, or contemporaneous with unit 4. However, based on stratigraphic position, deposition of unit 3 likely occurred close in time to deposition of unit 4.

Unit 2 is a loose to moderately indurated, chiefly coarse-grained debris-flow/debris-flood deposit (appendix A) that directly overlies unit 4, and therefore post-dates the P2 earthquake. Unit 2 is overlain by unit 1a, the colluvial-wedge deposit formed by fault-scarp erosion following the most recent surface-faulting earthquake (P1). A thin, weakly developed paleosol (buried A horizon soil) formed on unit 2 is preserved beneath unit 1a (s2 on plate 1). Charcoal from the paleosol yielded a ^{14}C age of 1530-1280 cal yr B.P. The ^{14}C age from the charcoal is in correct stratigraphic order with the three older ^{14}C ages from unit 4a (P2 colluvial wedge). Unit 1b is a crack-fill deposit related to the P1 earthquake (plate 1).

Other than the s2 paleosol, no other paleosols were recognized in the North trench. A modern soil (sm) is forming at the ground surface on unit 8 in the fault footwall and on units 1a and 2 on the fault hanging wall (plate 1).

Structure

In the North trench, faulting was restricted to a 3-m-wide zone between horizontal stations (h) 15 and 18 (plate 1). The main fault (NF1) intersected the trench bottom at about station h-15.7, and consisted of a steeply dipping main trace with minor secondary strands that locally gave the fault a bifurcated character. The upper part of NF1 dipped steeply to the east, before changing to a west dip with increasing depth in the trench. At about station h-16.8 (bottom of trench), the first of three interconnected, small-displacement, east-dipping, high-angle reverse faults (NF2–NF4) formed a zone of secondary faulting that was about a meter wide at its greatest extent.

Two colluvial-wedge deposits (units 1a and 4a) and associated crack-fill deposits (units 1b and 4b) that formed adjacent to NF1 by post-earthquake fault scarp erosion provide stratigraphic evidence for two surface-faulting earthquakes (P1 and P2) on the Fort Pearce section. Units 8 and 9 have been displaced beneath the bottom of the trench in the fault hanging wall. Units 5, 6, and 7 are displaced by the three small reverse faults (NF2–NF4). Evidence for reverse faulting extending above unit 5 was poorly expressed, and it is possible that the reverse faults were only active during the P2 earthquake. Unit 2, which overlies the P2 colluvial wedge and underlies the P1 colluvial wedge, was only displaced by NF1 during the P1 earthquake.

Geologic units 2 through 7 either were never deposited on the fault footwall or were removed by one or more episodes of post-earthquake erosion. Given that units 2 and 5 were exposed on the footwall in the South trench just 5 m distant (plate 1), erosion seems a likely explanation for their absence on the North trench footwall.

South Trench

Stratigraphy

The South trench exposed eight geologic units (plate 1) that correspond with the stratigraphic units in the North trench (plate 1; appendix A). Unit 9 (Moenkopi Formation bedrock) was not present in the South trench. As in the North trench, we divided units 1 and 4 into “a” and “b” subunits. Additionally, unit 8, the oldest stratigraphic unit in the South trench, displayed better developed bedding than did the same unit in the North trench; consequently, we divided unit 8 in the South trench into four subunits (8a–8d; plate 1 and appendix A). Unit 8 is a strongly indurated (chiefly gypsum cemented), mostly coarse-grained, thick-bedded alluvial-fan deposit confined to the footwall of the main fault in the South trench (see Structure section below). Unit 8b yielded an OSL age of 54.07 ± 4.07 ka (plate 1).

Rotated and sheared blocks of what we interpret to be unit 8 were present in the South trench fault zone (see Structure section below); however, the blocks were highly sheared making positive identification of the geologic unit from which they were derived difficult. Unit 8 was not exposed in the fault hanging wall. Unit 7, a strongly indurated, coarse-grained, massively bedded debris-flow deposit (plate 1; appendix A), is in fault contact with unit 8. Unit 7 yielded an OSL age of 30.75 ± 2.21 ka in the North trench, making unit 7 at least 23.3 kyr younger than

unit 8 in the South trench. Unit 6 is a moderately indurated, coarse-grained debris-flow deposit that conformably overlies unit 7. A sample from near the top of unit 6 yielded an OSL age of 17.10 ± 1.38 ka (plate 1), making unit 6 about 13.7 kyr younger than unit 7. Units 6 and 7 were only exposed in the fault hanging wall. Unit 5 is a coarse-grained, weakly indurated debris-flow deposit, and is the oldest geologic unit present on both sides of the main fault in the South trench. A sample from near the top of unit 5 in the fault hanging wall yielded an OSL age of 13.80 ± 1.18 ka (plate 1), making unit 5 about 3.3 ka younger than unit 6. Unit 5 overlies units 6 and 8 in the fault hanging wall and units 8a and 8b in the fault footwall. Units 5 through 8 predate the P2 earthquake.

Unit 4 consists of the colluvial-wedge (unit 4a) and associated crack-fill (unit 4b) deposits formed by erosion of the P2 earthquake fault scarp (see the North trench Stratigraphy section for details of the ^{14}C ages associated with unit 4). Unit 3 is a loosely indurated debris-flow deposit confined to the main fault hanging wall that conformably overlies unit 5, but does not overlie unit 4 (plate 1). Because units 3 and 4 occupied the same relative stratigraphic position in the South trench, and because there are no numerical ages available for unit 3, it is not known if unit 3 is older, younger, or contemporaneous with unit 4. However, based on stratigraphic position, deposition of unit 3 likely occurred close in time to deposition of unit 4.

Unit 2 is a loose to moderately indurated, chiefly coarse-grained debris-flow/debris-flood deposit that overlies unit 4 (plate 1), and therefore is younger than the P2 earthquake. Unit 2 yielded an OSL age of 4.22 ± 0.27 ka, which is younger than the youngest ^{14}C age obtained from the underlying P2 colluvial wedge (unit 4a) in the North trench, thus the OSL age is in correct stratigraphic sequence with the older ^{14}C ages. Erosion either prior to or contemporaneously with deposition of unit 2 truncated the upper part of the P2 colluvial wedge (unit 4a). Unit 2 is overlain by unit 1a, the P1 earthquake colluvial wedge (plate 1); therefore, unit 2 predates the P1 earthquake. Unit 2 is also present on the fault footwall, where it overlies units 8a and 5, and is displaced by P1 faulting on a secondary fault zone (see Structure section below). Erosion, either prior to or contemporaneously with deposition of unit 2, locally removed unit 5 from the fault footwall. Unit 1b is a crack-fill deposit related to the P1 earthquake (plate 1).

We identified no other paleosols or other organic-bearing units in the South trench. A modern soil (sm) is forming at the ground surface on units 1a and 2.

Structure

The South trench exposed three fault zones: a main, west-dipping zone (SF1) at about station h-17.8 (bottom of trench); a secondary, west-dipping zone (SF2) at about station h-13.5 (bottom of trench); and an east-dipping, small displacement reverse fault (SF3) west of the main fault zone at about station h-20 (bottom of trench) (plate 1).

Fault zone SF1 consists of a near-vertical to west-dipping principal shear and two interconnected, small-displacement, subsidiary reverse faults. Two colluvial-wedge deposits (units 1a and 4a) and associated crack-fill deposits (units 1b and 4b) that formed adjacent to SF1 provide evidence for two surface-faulting earthquakes on the Northern section. Fault zone SF1 displaced unit 8 down-to-the-west to below the bottom of the trench in the fault hanging wall.

Units 6 and 7 are exposed in the hanging wall of the main fault, but not in the footwall. In the footwall, units 2 and 5 directly overlie unit 8, indicating that units 6 and 7 were either (1) eroded from the footwall most likely following an earlier surface-faulting earthquake, or (2) were only deposited on the fault hanging wall, possibly by debris flows whose flow paths were controlled by a preexisting fault scarp on the displaced alluvial-fan surface. Unit 5 has been displaced by two surface-faulting paleoearthquakes (P1 and P2), and unit 2 by one paleoearthquake (P1).

Fault zone SF2 is in the footwall of the main fault zone, and represents a wide, debris-filled void across which the P1 earthquake produced a few tens of centimeters of displacement (plate 1). Fault zone SF2 displaces units 5 and 8 (both pre-P2 earthquake geologic units) and unit 2 (a post-P2 earthquake geologic unit) by roughly the same amount, indicating that SF2 was only active during the P1 earthquake. The fissure formed along SF2 is exceptionally wide for a fault with such small displacement. Additionally, between SF1 and SF2 there were several well-developed cracks also related to the P1 earthquake (plate 1). The cracks exhibited little or no vertical displacement, but some have open voids formed along them. Open voids are also present along both the SF1 and SF2 fault zones. We interpret the voids as evidence that the P1 earthquake is a geologically young event, and that there has not been sufficient time for the voids to collapse or completely fill with debris since the P1 earthquake.

Fault zone SF3 is a moderate- to high-angle reverse fault that bifurcates upward (plate 1). Fault zone SF3 displaces unit 5 tens of centimeters. Evidence that SF3 displaces units 2 and 3 is poorly expressed, and if such displacement did occur, it was significantly less than the displacement produced in unit 5. Therefore, SF3 was active during the P2 earthquake, but less so, if at all, during the P1 earthquake.

Numerical Ages

Geologic units in the North and South trenches yielded a combination of ^{14}C and OSL ages (briefly discussed above in the Stratigraphy sections) that helped constrain both the ages of the units and the timing of the two most recent surface-faulting earthquakes at the Dutchman Draw site.

Radiocarbon Ages

We found no datable organic material in the South trench, and no macroscopic charcoal in the North trench. However, the North trench did expose three thin, weakly organic stringers of fine-grained sediment within the P2 colluvial wedge (unit 4a), and a thin, weakly organic paleosol (s2) formed on unit 2 and buried by the P1 colluvial wedge (unit 1a; plate 1). Because all four horizons were thin (a few cm to 10 cm thick) and only weakly organic, we sampled them through their entire thickness to ensure that we collected sufficient material for ^{14}C dating. The likely origin of the organic colluvial-wedge stringers is erosion of pre-existing carbon-bearing material on the upthrown side of the fault following the P2 earthquake. The s2 paleosol was forming on unit 2 (a debris-flow deposit) at the time of the P1 earthquake, and was down dropped by the earthquake and subsequently buried by P1 colluvial-wedge sediment.

We submitted four bulk organic sediment samples from the North trench to PaleoResearch Institute (PRI) for separation and identification of plant macrofossils (appendix B). Sample NT-RC1 yielded charcoal consisting of Salicaceae (willow family) and unidentified hardwood (wood from a broad-leaved flowering tree or shrub but too small for further identification). Sample NT-RC2 also yielded unidentified hardwood charcoal. Samples NT-RC3 and NT-RC4 both provided microcharcoal suitable for dating, but which could not be identified to family or genus. Following preparatory treatment of the charcoal (appendix B), PRI submitted the four charcoal samples to the Keck Carbon Cycle Accelerator Mass Spectrometry Facility at the University of California, Irvine, for accelerator mass spectrometry (AMS) ^{14}C dating. Table 1 presents the results of the PRI sample processing and subsequent AMS radiocarbon dating. The resulting age estimates are reported both as radiocarbon years before present (RCYBP) and as one- and two-sigma calendar calibrated ages (cal yr. BP). The four ^{14}C ages are in correct stratigraphic order (plate 1).

Bioturbation, the mixing of younger or older carbon within an unconsolidated geologic unit by burrowing animals and/or root mixing, can result in anomalously young or old ^{14}C ages that are out of stratigraphic order. Additionally, reworking of older detrital carbon into a younger unconsolidated geologic deposit by erosion and redeposition of a pre-existing A horizon soil or other carbon-bearing deposit may yield an age that is too old and likewise stratigraphically inconsistent. We tried to minimize these dating uncertainties to the extent possible given the limited size of the organic-bearing horizons in the North trench (our sampling largely depleted the organic stringers in the P2 colluvial wedge and the most organic parts of the s2 paleosol), by avoiding collecting samples near obviously burrowed or otherwise bioturbated areas. Although not a guarantee that carbon mixing has not occurred, the fact that the four ^{14}C ages from the North trench are in proper age/stratigraphic order gives us confidence that the sampled deposits were not significantly contaminated by younger or older carbon. Additionally, during trench logging we observed little evidence of burrowing or other bioturbation in the sampled geologic units.

Optically Stimulated Luminescence Ages

We collected seven OSL samples at the Dutchman Draw site: three from the North trench and four from the South trench (plate 1). We conducted the sampling in accordance with Utah State University Luminescence Laboratory (USULL) sampling protocol (http://www.usu.edu/geo/luminlab/how2osl.pdf), and submitted the samples to USULL for OSL dating. See appendix C for details of USULL sample processing and dating procedures. Table 2 presents the OSL age estimates.

Optically stimulated luminescence determines the last time quartz or feldspar grains were exposed to sunlight (see USULL website at http://www.usu.edu/geo/luminlab/whatis.html for details of the OSL dating technique). As sediment is transported, it is exposed to sunlight and zeroed of any previous luminescence signal. If insufficient sunlight exposure occurs, the quartz or feldspar grains may retain a luminescence signal that results in an OSL age that is too old. Similarly, OSL ages may be affected by bioturbation if material with a young OSL signal is carried downward into older unconsolidated geologic units by burrowing or root mixing. Sample NT-OSL3 has an age that is too young given its stratigraphic context and the multiple stratigraphically consistent ^{14}C ages obtained from the same unit. A possible explanation for the

anomalously young age is bioturbation of more recently deposited sediment downward into older material. The other OSL ages from the North and South trenches are in correct stratigraphic order.

PALEOSEISMOLOGY

Number of Earthquakes

Geologic units 1a, 1b, 4a, and 4b in both the North and South trenches (see Stratigraphy sections above; plate 1) provide direct stratigraphic evidence (tectonic colluvial-wedge and crack-fill deposits) for two Holocene surface-faulting earthquakes on the main strand of the Fort Pearce section of the Washington fault zone. New geologic mapping performed for this study (Knudsen this volume) has redefined the Mokaac section (Pearthree, 1988) as a strand of the Fort Pearce section. Likewise, our new mapping has redefined the Dutchman Draw fault (previously mapped as an independent structure; Pearthree [1988]) as also a strand of the Fort Pearce section. There are no paleoseismic data for either the Mokaac or Dutchman Draw strands to quantify the number or timing of past surface-faulting earthquakes on those structures. However, given their comparatively short lengths (both 16 km long) and the fact that they connect to the Fort Pearce section main strand, but not to each other (plate 1), we consider it most likely that the strands rupture coseismicly with the main strand of the Fort Pearce section and are not independent earthquake sources that rupture either separately or together.

In the absence of paleoseismic data for the Mokaac and Dutchman Draw strands, it is not known whether both strands rupture during all Fort Pearce section earthquakes, or if they rupture less frequently (i.e., due to geometrical constraints, the Dutchman Draw strand may rupture only during northward propagating earthquakes, while the Mokaac strand may rupture only during southward propagating earthquakes; Knudsen this volume). It may also be possible that an earthquake initiating at the south end of the main strand may divert onto the Dutchman Draw strand and not rupture the main strand farther north. Likewise, an earthquake initiating at the north end of the main strand may rupture southward and divert onto the Mokaac strand and not rupture the main strand farther south. Determining which of these scenarios (or others possible on this geometrically complex fault) may occur requires acquiring additional paleoseismic trenching information for the Mokaac and Dutchman Draw strands.

Based on the results of our trenching at the Dutchman Draw site on the Fort Pearce section main strand, we believe that the two surface-faulting earthquakes identified there represent a minimum number of surface-faulting earthquakes on the Fort Pearce section during the Holocene. In particular, southward-propagating earthquakes that may have diverted onto the Mokaac strand would not appear in the geologic record at the Dutchman Draw site. Again, while not beyond all possibility, we consider a Mokaac-strand or Dutchman Draw-strand independent rupture, or a combined Mokaac- and Dutchman Draw-strand coseismic rupture (which would also require rupture of 6 km of the main Fort Pearce strand) to be unlikely, but additional paleoseismic information is required to confirm or refute that supposition.

The South trench contained additional indirect stratigraphic evidence for at least one possible latest Pleistocene surface-faulting earthquake. There, units 6 and 7 are present on the main fault hanging wall, but not on the footwall (plate 1). On the hanging wall, units 6 and 7 are overlain by units 2, 3, and 5 which consist of younger debris-flow deposits. Units 2 and 5 are also present on the fault footwall where they overlie unit 8. Those stratigraphic relations show that either units 6 and 7 were removed by erosion from the footwall prior to deposition of units 2 and 5, or alternatively, that units 6 and 7 were never deposited on the footwall. We consider the non-deposition scenario unlikely because units 6 and 7 are thick and continuous on the hanging wall and extend to the main fault zone (see Stratigraphy section above). Neither unit 6 nor 7 shows evidence of pinching out toward the fault zone, which would support a non-deposition scenario on the fault footwall. Instead, both units maintain their thickness to the fault zone where they are sheared and displaced by faults. Because unit 5 overlies units 6 and 7 on the hanging wall, but overlies unit 8 on the footwall, units 6 and 7 were likely eroded from the footwall prior to deposition of unit 5. Surface faulting that left units 6 and 7 at an elevated position and exposed to erosion on the fault footwall, but at a lower elevation and protected from erosion on the fault hanging wall, could account for the stratigraphic relations observed in the South trench. Because unit 5 has been displaced by both the P1 and P2 earthquakes, and units 6 and 7 had to have been down faulted prior to deposition of unit 5 to create the stratigraphic relations observed in the South trench, any earthquake(s) that caused units 6 and 7 to be eroded from the footwall and preserved on the hanging wall must be older than the P2 earthquake. Based on OSL ages of units 6 (17.10 ± 1.38 ka) and 5 (13.80 ± 1.18 ka), the older surface faulting would have occurred in the latest Pleistocene between about 17.1 and 13.8 ka. Evidence not supporting an older earthquake scenario is the absence of colluvial-wedge deposits representing older event(s) in the North or South trenches.

Stratigraphic evidence for older surface faulting is not well expressed in the North trench, where units 2 and 5 are not present on the fault footwall. Where exposed on the hanging wall, units 2 and 5 show evidence of thinning toward the fault zone, implying that they were pinching out in that direction (plate 1). However, unit 5 does overlie what we interpret to be a sheared block of unit 8 in the fault zone. Units 6 and 7 are also absent from the fault footwall and present on the hanging wall, where they do not show evidence of thinning toward the fault zone. A possible explanation for these stratigraphic relations is that an older surface-faulting earthquake resulted in erosion of units 6 and 7 from the footwall and their preservation on the hanging wall. At a later time, the P3 scarp or other irregularity in the alluvial-fan surface that either was not present or not well expressed at the South trench influenced the flow paths of the debris flows that deposited units 2 through 5 and limited their deposition to the fault hanging wall. Conversely, since unit 5 does overlie unit 8 in the fault zone, it is possible that unit 5 and possibly unit 2 were deposited on the footwall after an older earthquake, but were subsequently removed by erosion following the P2 earthquake.

OSL ages from the North and South trenches show that geologic units deposited prior to the P2 earthquake range in age from at least 54.07 ka to 13.80 ka (plate 1; table 2). Unconformable contacts between several of those units represent intervals of either non-deposition or erosion. For example, the contact between units 5 and 8b in the South trench footwall represents a hiatus of about 40.3 kyr, and evidence presented above indicates that the upper unit 8a contact is likely an erosional surface. Similarly, the contact between units 6 and 7

represents a hiatus of about 13.7 kyr, and the contact between units 4a and 5 a hiatus of as much as 7.6 kyr. Clearly, long periods of time elapsed between episodes of sediment deposition on the alluvial fan at the Dutchman Draw site. What remains unclear is how much erosion occurred in those long intervals that may have been earthquake driven, and how much, if any, stratigraphic evidence of older surface-faulting earthquakes may have been eroded away.

Earthquake Timing and Recurrence

Earthquake Timing

We used OxCal radiocarbon calibration and analysis software (version 4.1.7; Bronk Ramsey, 2010; using the IntCal09 radiocarbon age calibration curve [Reimer and others, 2009]) to model the timing of the P1 and P2 earthquakes and the duration of the closed seismic interval between the earthquakes (appendix D). The OxCal software (Bronk Ramsey, 2009) probabilistically models the time distribution of undated events (such as earthquakes) by incorporating stratigraphic ordering information for radiocarbon and luminescence ages (Bronk Ramsey, 2008) obtained from our trenches. We report earthquake time ranges, and elapsed time between earthquakes with two-sigma confidence intervals. Note that we report OSL ages as the mean and two-sigma uncertainty rounded to the nearest century in thousands of calendar years before the sample processing date (2009–2010). In discussing the OSL ages, we do not account for the ~ 60-year difference in the OSL sample age versus the reference standard for ^{14}C (1950). This difference is minor compared to the OSL age uncertainties, and is accounted for in modeling of earthquake times in OxCal.

OxCal modeling of ^{14}C and OSL ages from the Dutchman Draw site constrains the timing of the P2 and P1 earthquakes to the Holocene, P2 at about 7.7 ± 2.4 ka and P1 at about 1.0 ± 0.6 ka. Table 3 shows the ^{14}C and OSL ages that we modeled in OxCal to constrain earthquake timing. Ages older than 13.8 ka (see table 2) were not used in the OxCal model because they do not impose significant constraints on earthquake timing within the stratigraphic context provided by the trenches. We rounded all ages to the nearest 10 years for use in the OxCal model.

Table 4 shows the earthquake timing resulting from OxCal modeling at the Dutchman Draw site. All results are rounded to the nearest 100 years.

Earthquake Recurrence

The elapsed time between the P2 and P1 earthquakes represents a single closed seismic cycle (recurrence interval) for the Fort Pearce section of the Washington fault zone. The length of a seismic cycle represents the time required following a large stress-release earthquake (P2) for a fault to re-accumulate sufficient strain to generate a second large earthquake (P1) on the same fault section. The recurrence interval when compared with the elapsed time since the most recent surface-faulting earthquake (MRE) gives an indication of where a fault lies in its current seismic cycle. However, the paleoearthquake timing information from the Dutchman Draw site is limited and only constrains the length of the most-recent seismic cycle for the main trace of the Fort Pearce section. The recurrence interval modeled by OxCal between the P2 and P1 earthquakes is 6.6 ± 2.4 kyr (table 4), and the elapsed time since P1 is 1.0 ± 0.6 ka, indicating

that the Fort Pearce section at the Dutchman Draw site is likely early in its current seismic cycle. However, we do not know whether the P2–P1 recurrence interval approximates the average long-term recurrence of surface-faulting on the Fort Pearce section, or if it represents an outlier, a recurrence interval that is significantly longer or shorter than the long-term average recurrence. Therefore, while the single recurrence interval and MRE elapsed time at the Dutchman Draw site represent significant new paleoseismic information for the Fort Pearce section, caution is advised when using those data to extrapolate the long-term behavior of the section.

As a matter for speculation, stratigraphic relations in the South trench are permissive of, but do not provide conclusive evidence for, at least one latest Pleistocene surface-faulting earthquake (see Number of Earthquakes section above). If a single older surface-faulting earthquake (P3) did occur sometime between 17.10 ± 1.38 ka and 13.80 ± 1.18 ka (see Earthquake Timing section above), and the P2 earthquake occurred at 7.7 ± 2.4 ka, the resulting P3–P2 recurrence interval would range from about 2.5 [12.6 ka – 10.1 ka) to 13.2 kyr [18.5 ka – 5.3 ka), with a median value at about 7.9 kyr (all values rounded to the nearest hundred years). By way of comparison, the P2–P1 mean recurrence of 6.6 kyr is 1.3 kyr from the P3–P1 possible mean recurrence of 7.9 kyr, or nearly within the P2–P1 one-sigma range (± 1.2 kyr), thus suggesting that the P2–P1 recurrence interval may be generally representative of the average surface-faulting recurrence on the Fort Pearce section during latest Pleistocene–Holocene time. Again, evidence for a P3 (or possibly more) surface-faulting earthquake is not conclusive, and the length of a possible P3–P2 recurrence interval remains speculative.

Vertical Displacement

Scarp Profiles

We measured three profiles across the Dutchman Draw fault scarp (figures 2 and 4) using a survey-grade GPS (Trimble R8 GNSS) instrument. Profile 1 crossed the southern, bifurcated end of the scarp (figure 4) and immediately encountered uneven gullied terrain on the footwall alluvial-fan surface, which made projecting the surface slope back to the fault zone speculative. For that reason, profile 1 was not suitable for vertical offset analysis.

Profile 2 (figure 5) was the longest profile, extending 280 m from west of any anticipated antithetic faulting on the fault hanging wall, through the future location of the North trench, and as far east on the footwall alluvial-fan surface as possible before encountering gullied terrain. At profile 2, the scarp height was 3.7 m and the vertical surface offset (minimum net vertical slip) was 2.8 m (figure 5). Later excavation of the North trench confirmed that the scarp was not bedrock cored, as was indicated by 3-D tomography. The scarp-height and surface-offset measurements obtained from profile 2 are minimum values because material eroded from the scarp has buried the original alluvial-fan surface on the hanging wall to an unknown depth.

The profile 3 scarp is cored by bedrock (figure 4). The scarp height is 4.5 m and the vertical surface offset is 3.9 m (figure 6), both significantly larger than values obtained from profile 2 where the scarp is formed in alluvium. This variation may reflect differences in the way bedrock and alluvial scarps degrade over time, or the bedrock scarp may record more

paleoearthquakes (see discussion of possible older surface-faulting earthquakes above). For that reason, we do not consider profile 3 suitable for vertical offset analysis.

Displaced Trench Stratigraphy

When geologic units in a trench are well exposed on both sides of a fault, it is possible to determine net vertical slip across the fault by projecting the same unit contact from the footwall and hanging wall to the main fault and measuring the vertical distance (displacement) between them. Measurement reliability is improved when (1) the unit contact is relatively smooth and dips (slopes) at the same angle on both sides of the fault, (2) the portions of the contact selected for projection are outside any zone of tilting or deformation associated with faulting, and (3) a sufficient length of contact is exposed on both sides of the fault to ensure that the projections can be aligned to accurately reflect the continuation of the contact to the fault zone. All of these conditions are problematic in the Dutchman Draw trenches.

The North trench (plate 1) did not expose geologic units common to both the footwall and hanging wall; therefore, trench stratigraphy could not be used to determine net vertical slip across the fault. In the South trench, units 2 and 5 are present on both sides of the fault; however, (1) both units have been affected by post-faulting erosion making their contacts undulatory and irregular, (2) exposures of both units on the footwall east of fault SF2 (and therefore outside the fault displacement zone) are limited (plate 1), and (3) the slopes of the contacts on either side of the main fault are different, indicating that in addition to being affected by erosion, the units also may be affected by fault-related deformation. Given these caveats, we consider the measurements of net vertical slip based on displaced stratigraphy in the South trench to be "rough estimates" only and not precise measurements of net vertical displacement.

Unit 5 has been displaced by both the P1 and P2 earthquakes. Projecting the unit 5 upper contact to the main fault from (1) east of fault SF2 on the footwall, and (2) west of the small reverse faults (SF3) in the hanging wall resulted in a "best estimate" vertical net slip of about 2.3 m for two earthquakes. Projections of the unit 5 lower contact from the hanging wall and footwall to the main fault zone were at such widely divergent angles that a reliable estimate of net slip could not be made. Unit 2 has been displaced by only the P1 earthquake. Projecting the unit 2 lower contact from the footwall and hanging wall to the fault zone resulted in a net vertical displacement "best estimate" for the P1 earthquake of about 1 m.

Colluvial-Wedge Thickness

Ostenna (1984) stated that ". . . for large displacements, the thicknesses of the colluvial wedge preserved should approach half the initial free face height." Numerous factors can affect the height of a surface-faulting scarp free face, but in general, in the absence of antithetic faulting or significant back-rotation or drag along the fault, free face height can be used as a rough proxy for fault slip during a surface-faulting earthquake (McCalpin, 2009). The logs for the North and South trenches (plate 1) show that the P1 and P2 colluvial wedges are not the same size. In both trenches, the P2 wedge is both thicker and longer in cross section than the P1 wedge. The P2 wedge in the North trench has been somewhat affected by erosion and is much affected by erosion in the South trench. The thickness of the P2 colluvial wedge in the North trench is 1.2

m, which implies an initial free face height of about 2.4 m. The P2 wedge in the South trench is too modified by erosion to provide a good measurement of wedge thickness. The P1 wedge in the North trench is 0.5 m thick, and in the South trench is 0.6 m thick, implying an initial free-face height of 1.0 to 1.2 m. The colluvial-wedge thicknesses in the trenches show that the P2 earthquake produced approximately twice as much slip as the P1 earthquake. However, we consider both measurements poorly constrained and to represent only approximate values of net vertical slip for the P1 and P2 earthquakes.

Vertical Slip Rate

Slip rate provides a measure of fault activity; generally the higher the slip rate, the more active the fault. Slip rates may be calculated horizontally (typical for strike-slip faults), vertically (typical for normal-slip faults), or in a down-dip direction (net slip) when the fault's dip at depth is known. A vertical slip rate measures how fast two sides of a fault are slipping vertically relative to one another, and is commonly determined from vertically offset features whose ages are known. It is preferable to calculate slip rates for "closed" seismic cycles. A vertical slip rate for a closed seismic cycle is calculated by dividing per event net vertical displacement by the length of the previous recurrence interval.

The new paleoseismic information obtained at the Dutchman Draw site defines one closed seismic cycle (P2–P1 mean recurrence interval = 6.6 ± 2.4 kyr) on the main strand of the Fort Pearce section. The "best estimate" vertical displacement resulting from the P1 earthquake determined from the South trench is 1.0–1.2 m; therefore, the vertical slip rate for the most recent closed seismic cycle is:

$$1000 \text{ to } 1200 \text{ mm}/6.6 \pm 2.4 \text{ kyr} = 0.11\text{-}0.29 \text{ mm/yr}$$

Where sufficient data are available, it is preferred to calculate an average slip rate that incorporates multiple closed seismic cycles and cumulative net vertical slip to provide a more stable measure of long-term fault activity. Since that is not possible at the Dutchman Draw site, caution is advised when using the single closed-seismic-cycle vertical slip rate reported here to extrapolate the long-term behavior of the Fort Pearce section. Also note that this slip rate is applicable only to the main strand of the Fort Pearce section and does not include slip that may have occurred on the Mokaac or Dutchman Draw stands due to coseismic rupture.

Paleoearthquake Magnitude Estimates

Paleoearthquake magnitude estimates are typically based on magnitude scaling relations that variously incorporate surface rupture length (SRL), fault rupture area (RA), or slip rate (SR). The proper relations for calculating paleoearthquake magnitudes within a particular tectonic regime has been and continues to be a topic of active research and discussion (e.g., see Lund [2012] and Stirling and Goded [2012]). The Working Group on Utah Earthquake Probabilities (WGUEP) (Wong and others, 2011, 2012), which at the time of this report is conducting an ongoing project to develop time-independent and time-dependent earthquake forecasts for the Wasatch Front region (see http://geology.utah.gov/ghp/workgroups/wguep.htm), has performed a rigorous analysis of magnitude scaling relations to determine which relations are appropriate for

their study region (includes portions of the Basin and Range and Middle Rocky Mountain physiographic provinces). The WGUEP grouped the faults in their study area into category A, B, and C faults based on decreasing availability/reliability of paleoseismic data. Based on the WGUEP fault category criteria, the Fort Pearce section of the Washington fault zone is a category B fault—reliable displacement and slip-rate data from a single site. The paleomagnitude scaling relations currently recommended by the WGUEP for category B faults are:

- Anderson and others (1996) – SRL for all fault types and SR
- Stirling and others (2002) – Censored instrumental SRL relation
- Wesnousky (2008) – SRL all fault types

Although the WGUEP is still a work in progress, based on their careful evaluation of available scaling relations, we adopt the current WGUEP fault category B relations for this investigation.

All three scaling relations rely on SRL in total or part to determine paleomagnitude estimates. For this study we use two SRL values (straight line tip-to-tip length) representing three possible rupture scenarios on the Fort Pearce section. The three rupture scenarios are:

- 37 km – (a) Fort Pearce section end to end. Includes any coseismic rupture on the sub-parallel Mokaac and Dutchman Draw strands. (b) Northern tip of the Fort Pearce section to the southern tip of the Mokaac strand.
- 25 km – Southern tip of the Fort Pearce section to the northern tip of the Dutchman Draw strand.

Although not considered further here because we consider the possibility unlikely, a rupture scenario that includes the Mokaac and Dutchman Draw sections (each 16 km long) and the intervening portion of the Fort Pearce section main strand (6 km) would be 38 km long. Paleomagnitude estimates for this scenario would be very similar (slightly larger) than those reported for the two 37-km-long rupture scenarios described above.

Anderson and others (1996) – SRL for All Fault Types and SR

Anderson and others (1996) developed a regression for moment magnitude ($M_{w)}$ as a function of SRL and SR using observations from 43 worldwide earthquakes for which SR was reported. Their results showed that inclusion of fault slip rate reduced the misfit between predicted and observed values of M_w as compared to regressions based of SRL alone. We used the SR determined at the Dutchman Draw trench site to calculate M_w with the Anderson and others (1996) relation; however, as noted above, the Dutchman Draw SR represents (1) only the most recent closed seismic cycle on the Fort Pearce section, (2) the vertical displacement for that cycle is poorly constrained, and (3) the slip is only representative of the Fort Pearce section main strand and does not include possible coseismic slip on the Mokaac or Dutchman Draw strands.

The Anderson and others (1996) SRL and SR relation is:

$$M_{w} = 5.12 + (1.16 * \log SRL) - (0.2 * \log SR)$$

Using SRLs of 25 and 37 km and SRs ranging from 0.11 to 0.29 mm/yr (see Vertical Slip Rate section above) results in M_{max} values ranging from M_w 6.9 to 7.1 (rounded to the nearest 0.1 magnitude unit).

As noted by Anderson and others (1996), their relation demonstrates that the largest earthquakes occur on the slowest slipping faults for a given SRL.

Stirling and others (2002) – Censored Instrumental SRL Relation

Stirling and others (2002) developed their censored instrumental SRL relation to compare pre-instrumental (pre-1900) and prehistoric earthquake magnitudes with those for instrumental surface-faulting earthquakes to understand why the Wells and Coppersmith (1994) regressions systematically underestimate the magnitudes of many large-magnitude earthquakes (Stirling and Goded, 2012). Stirling and others (2002) expanded and updated the all-fault-type Wells and Coppersmith (1994) earthquake dataset, and systematically removed (censored) small SRL events from the dataset. The results were significantly larger magnitudes than those obtained from the Wells and Coppersmith (1994) regressions (Stirling and Goded, 2012).

The Stirling and others (2002) censored instrumental SRL relation is:

$$M_{w} = 5.88 + (0.8 * \log SRL)$$

Using SRLs of 25 and 37 km results in M_{max} values ranging from M_w 7.0 to 7.1 (rounded to the nearest 0.1 magnitude unit).

Wesnousky (2008) – SRL All Fault Types

Wesnousky (2008) developed a SRL all-fault-type regression using a dataset of 37 worldwide, surface-rupturing, continental earthquakes with rupture lengths greater than 15 km and for which there were both maps and measurements of coseismic displacement along the strike of the rupture (Stirling and Goded, 2012).

The Wesnousky (2008) SRL all-fault-type relation is:

$$Mw = 5.30 + (1.02 * \log SRL)$$

Using SRLs of 25 and 37 km results in M_{max} values ranging from M_w 6.7 to 6.9 (rounded to the nearest 0.1 magnitude unit).

Summary

Using the multiple paleomagnitude regressions recommended by the WGUEP to determine M_w for various rupture scenarios of the Fort Pearce section of the Washington fault zone resulted in earthquake magnitude estimates ranging from M_w 6.7 to 7.1, depending on the regression relation used and the SRL value selected. Available paleoseismic data are not sufficient to fully characterize all the possible rupture scenarios for the Fort Pearce section; however, it is clear from the limited analysis above that the Fort Pearce section is likely capable of generating $M_w \geq 7$ earthquakes in the future.

STUDY RESULTS

Results of trenching at the Dutchman Draw site provide the following new paleoseismic information for the Fort Pearce section of the Washington fault zone:

1. The Fort Pearce section has experienced at least two surface-faulting paleoearthquakes during the Holocene, one in the middle Holocene at about 7.7 ± 2.4 ka (P2) and the other in the late Holocene at about 1.0 ± 0.6 ka (P1).

2. The resulting single, closed-seismic-cycle recurrence interval (P2–P1 earthquakes) is 6.6 ± 2.4 kyr. It is unknown if this recurrence interval approximates the long-term average recurrence of large surface-faulting earthquakes on the Fort Pearce section. This recurrence interval represents only the most recent closed seismic cycle, and should be treated with caution if used to extrapolate the long-term behavior of the Fort Pearce section.

3. There is indirect stratigraphic evidence in the trenches permissive of at least one latest Pleistocene earthquake that may have occurred between 13.8 ± 1.2 and 17.1 ± 1.4 ka; however, any resulting tectonic colluvial-wedge deposits have either been removed by erosion or faulted below the bottom of the trenches.

4. It can be speculated that if a single P3 surface-faulting earthquake did occur between 13.8 ± 1.2 and 17.1 ± 1.4 ka, and the P2 earthquake occurred at 7.7 ± 2.4 ka, the length of the resulting P3–P2 recurrence interval would range from about 2.5 to 13.2 kyr, with a median value at about 7.9 kyr. The P2–P1 recurrence interval is 6.6 ± 2.4 kyr, placing it within one-sigma (1.2 kyr) of the possible P3–P2 median value at 7.9 kyr, thus suggesting that the P2–P1 recurrence interval may be generally representative of the average surface-faulting recurrence on the Fort Pearce section during latest Pleistocene–Holocene time.

5. Net vertical displacement estimates at the Dutchman Draw site range from about 1.0 m (P1) to 2.4 m (P2). We obtained these estimates from a combination of scarp profiles, displaced trench stratigraphy, and scarp free-face heights extrapolated from colluvial-wedge thicknesses. There are significant caveats associated with all three methods and we consider these displacement values poorly constrained "best estimates."

6. The vertical slip rate for the P2–P1 recurrence interval (6.6 ± 2.4 kyr) and a P1 net vertical displacement (1.0–1.2 m) is 0.11–0.29 mm/yr. This slip-rate range is representative of only the most recent closed seismic cycle on the main strand of the Fort Pearce section at the Dutchman Draw site, and should be treated with caution if used to extrapolate the long-term behavior of the Fort Pearce section.

7. Multiple magnitude regression relations provide paleomagnitude estimates at the Dutchman Draw site ranging from M_w 6.7 to 7.1, depending on the regression relation and the SRL value selected. The regression relations demonstrate that the Fort Pearce section of the Washington fault zone is likely capable of producing future **M** $\geq$ 7 earthquakes.

ACKNOWLEDGEMENTS

The authors thank Philip Pearthree and Jeri Young, Arizona Geological Survey, and Tony Crone, U.S. Geological Survey, for their visits to the Dutchman Draw trench site and insightful comments on the geologic relations exposed in the trenches. We thank Rosenberg Associates for funding the radiocarbon dates obtained for the Dutchman Draw North trench. We also thank Professor Gerald Schuster, University of Utah Department of Geology and Geophysics, and his graduate student Shengdong Liu for performing the 3-D tomographic seismic profiling of the fault scarp at the Dutchman Draw site.

REFERENCES

Anderson, J.G., Wesnousky, S.G., and Stirling, M.W., 1996, Earthquake size as a function of fault slip rate: Bulletin of the Seismological Society of America, v. 86, no. 3, p. 683-690.

Biek, R.F., Rowley, P.D., Hayden, J.M., Hacker, D.B., Willis, G.C., Hintze, L.F., Anderson, R.E., and Brown, K.D., 2009, Geologic map of the St. George and east part of the Clover Mountains 30' x 60' quadrangles, Washington and Iron Counties, Utah: Utah Geological Survey Map 242, 101 p., 2 plates, scale 1:100,000.

Birkeland, P.W., Machette, M.N., and Haller, K.M., 1991, Soils as a tool for applied Quaternary research: Utah Geological and Mineral Survey Miscellaneous Publication 91-3, 63 p.

Bronk Ramsey, C., 2005, OxCal Program, v. 3.1, Radiocarbon Accelerator Unit, University of Oxford, UK; Online, <https://c14.arch.ox.ac.uk/oxcal.html>.

Bronk Ramsey, C., 2008, Depositional models for chronological records: Quaternary Science Reviews, v. 27, no. 1-2, p. 42–60.

Bronk Ramsey, C., 2009, Bayesian analysis of radiocarbon dates: Radiocarbon, v. 51, no. 1, p. 337–360.

Bronk Ramsey, C., 2010, OxCal Program, v. 4.1.7, Radiocarbon Accelerator Unit, University of Oxford, UK; Online, <https://c14.arch.ox.ac.uk/oxcal.html>.

GretagMacbeth, 2000, Munsell Soil Color Charts, year 2000 revised washable edition: GretagMacBeth, New Windsor, New York, variously paginated.

Lund, W.R., editor, 2012, Basin and Range Province Earthquake Working Group II—Recommendations to the U.S. Geological Survey National Seismic Hazard Mapping Program for the 2014 update of the National Seismic Hazard Maps: Utah Geological Survey Open-File Report 591, 17 p.

McCalpin, J.P., 2009, Chapter 3 – Paleoseismology in extensional tectonic environments, *in* McCalpin, J.P., editor, Paleoseismology (2nd edition): Burlington, Mass., Academic Press (Elsevier), p. 171-269.

Ostenaa, D., 1984, Relationships affecting estimates of surface fault displacement based on scarp-derived colluvial deposits [abs.]: Geological Society of America, Abstracts with Programs, v. 16, no. 5, p. 327.

Pearthree, P.A., compiler, 1998, Quaternary fault data and map for Arizona: Arizona Geological Survey Open-File Report 98-24, 122 p., 1 plate in pocket, scale 1:750,000.

Reimer, P.J., Baillie, M.G.L., Bard, E., Bayliss, A., Beck, J.W., Blackwell, P.G., Bronk Ramsey, C., Buck, C.E., Burr, G.S., Edwards, R.L., Friedrich, M., Grootes, P.M., Guilderson, T.P., Hajdas, I., Heaton, T.J., Hogg, A.G., Hughen, K.A., Kaiser, K.F., Kromer, B., McCormac, F.G., Manning, S.W., Reimer, R.W., Richards, D.A., Southon, J.R., Talamo, S., Turney, C.S.M., van der Plicht, J., and Weyhenmeyer, C.E., (2009), IntCal09 and Marine09 radiocarbon age calibration curves, 0-50,000 years cal BP: Radiocarbon, v. 51, no. 4, p. 1111-1150.

Stirling, M.W., and Goded, T., 2012, Magnitude scaling relationships, GEM Faulted Earth and Regionalisation Global Components: GNS Science Miscellaneous Series 42, 40 p., available online at http://www.nexus.globalquakemodel.org.

Stirling, M., Rhoades, D., and Berryman, K., 2002, Comparison of earthquake scaling relations derived from data of the instrumental and preinstrumental era: Bulletin of the Seismological Society of America, v. 92, no. 2, pp. 812-830.

Wells, D.L., and Coppersmith, K.J., 1994, New empirical relationships among magnitude, rupture length, rupture width, rupture area, and surface displacement: Bulletin of the Seismological Society of America, v. 84, no. 4, p. 974-1002.

Wesnousky, S.G., 2008, Displacement and geometrical characteristics of earthquake surface ruptures—Issues and implications for seismic-hazard analysis and the process of

earthquake rupture: Bulletin of the Seismological Society of America, v. 98, no. 4, p. 1609-1632.

Wong, I., Lund, W., DuRoss, C., Arabasz, W., Pechmann, J., Crone, A., Luco, N., Personius, S., Petersen, M., Olig, S., and Schwartz, D., 2011, The Working Group on Utah Earthquake Probabilities (WGUEP) – background and goals [abs.]: Seismological Research Letters, v. 82, no. 2, p. 345–346.

Wong, I., Lund, W., DuRoss, C., Thomas, P., Arabasz, W., Crone, A., Hylland, M., Luco, N., Olig, S., Pechmann, J., Personius, S., Petersen, M., Schwartz, D., and Smith, R., 2012, Forecasting large earthquakes along the Wasatch Front, Utah [abs]: AEG News, 2012 Annual Meeting Program with Abstracts, v. 55, p. 85.

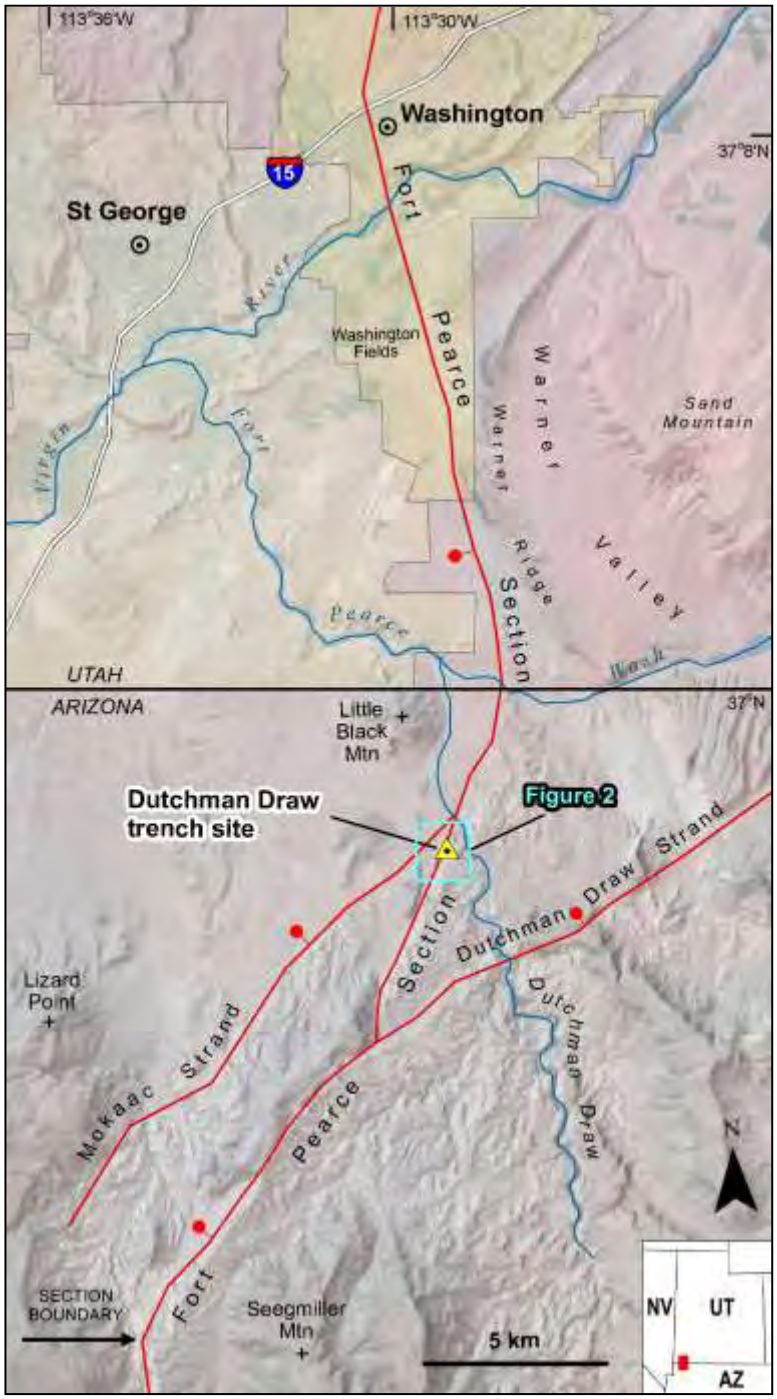

Figure 1. *Dutchman Draw trench site on the main strand of the Fort Pearce section of the Washington fault zone. Base map consists of Microsoft Bing Maps aerial imagery and World Shaded Relief Map from the ESRI Resource Center.*

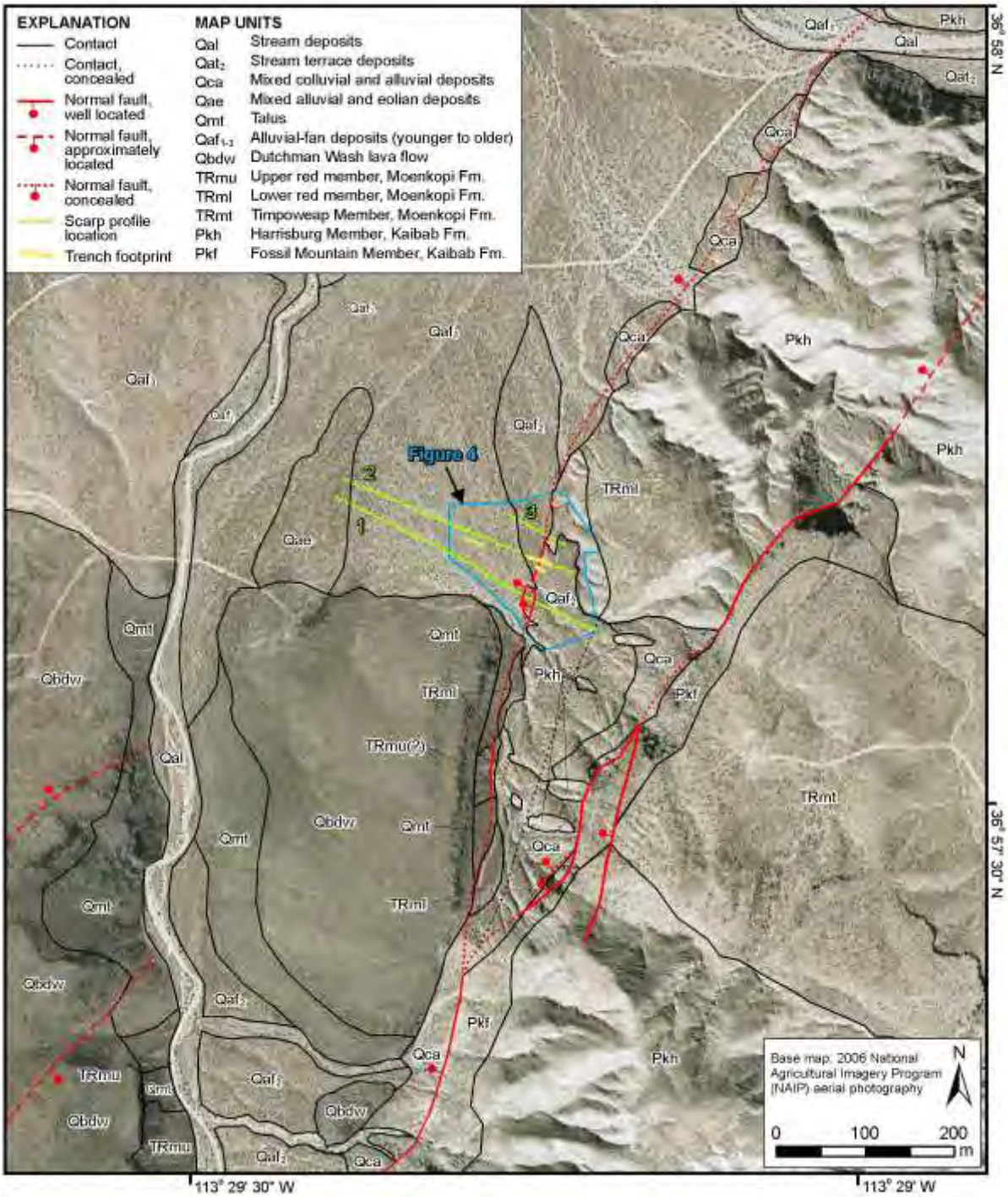

Figure 2. *Dutchman Draw trench site area geologic map showing the location of paleoseismic trenches and scarp profiles.*

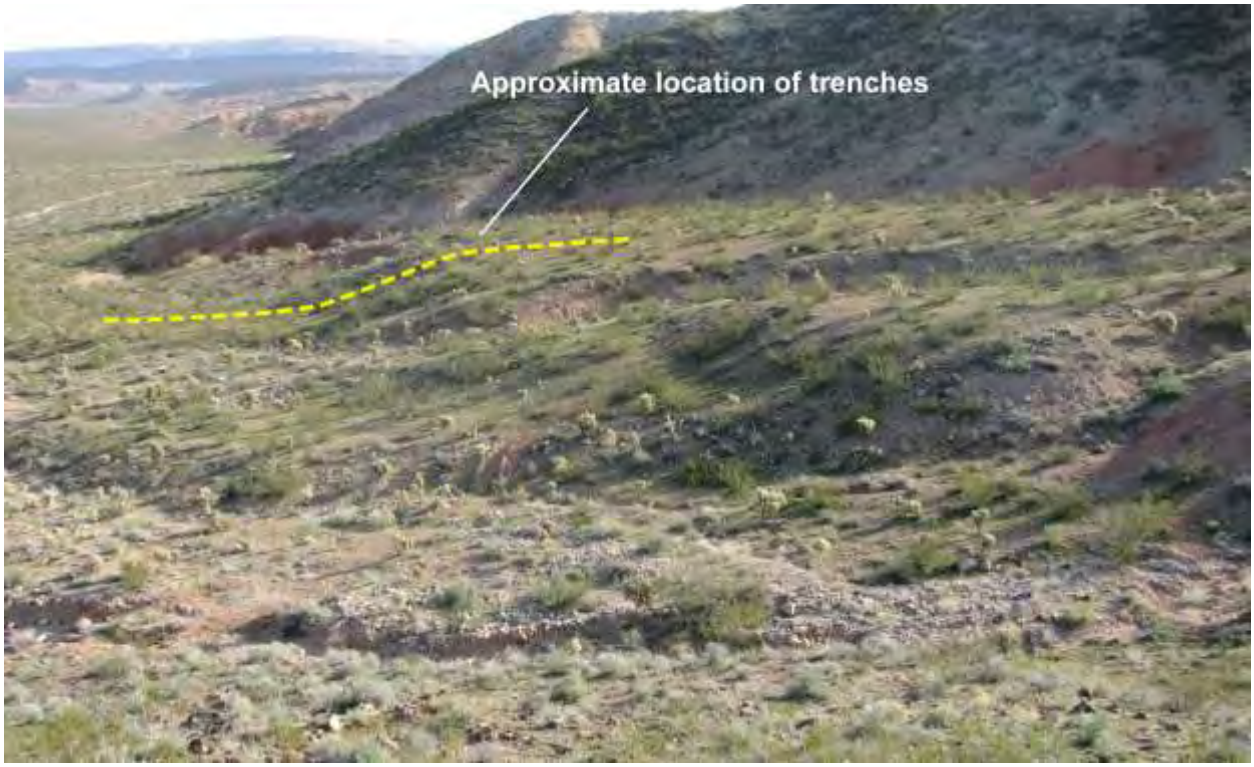

Figure 3. *Fault scarp (identified by yellow line) formed on a late Quaternary alluvial fan at the Dutchman Draw trench site. View to the north.*

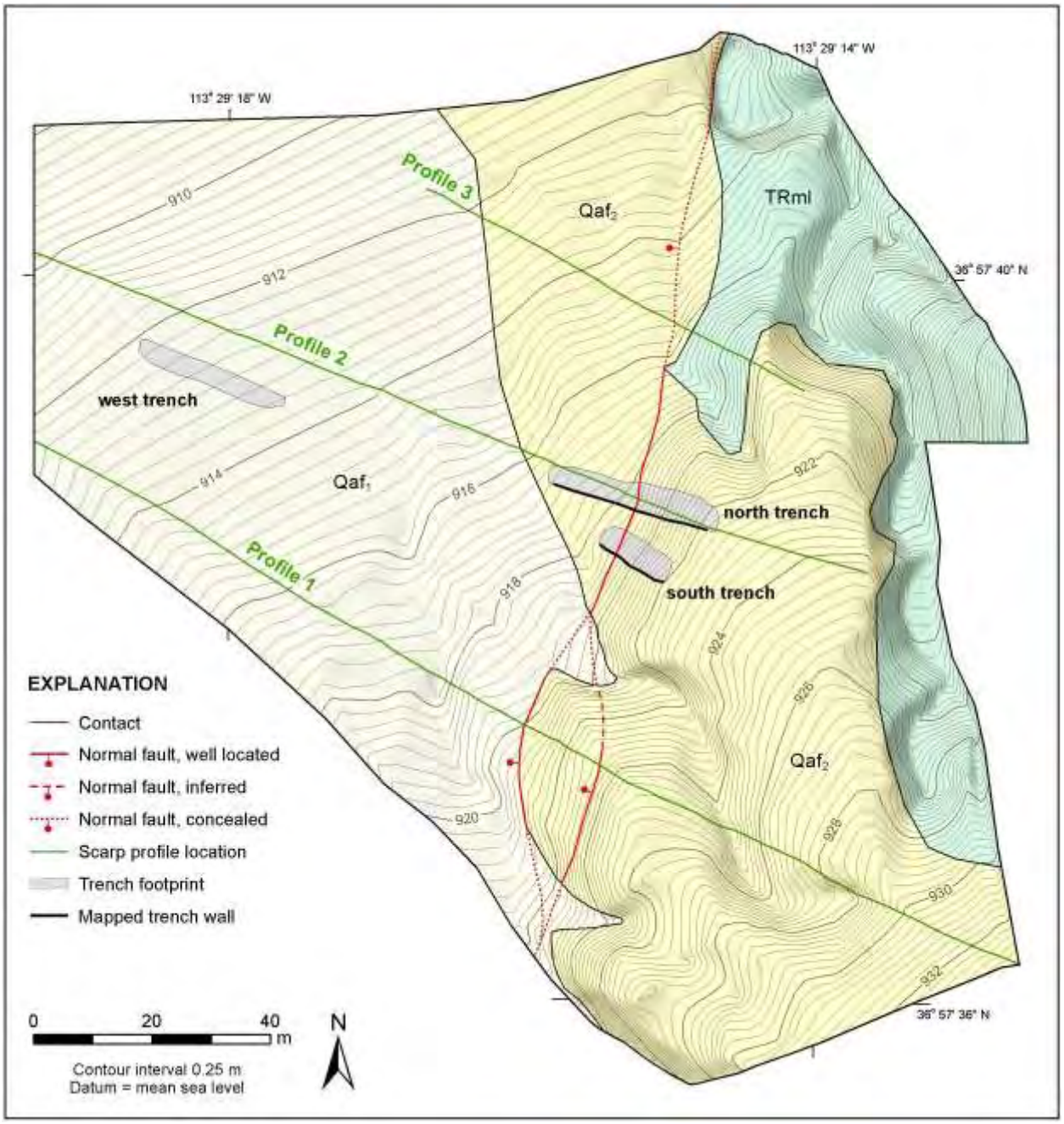

Figure 4. *Dutchman Draw trench site geologic and topographic map; topography mapped summer 2009. See figure 2 for explanation of geologic units.*

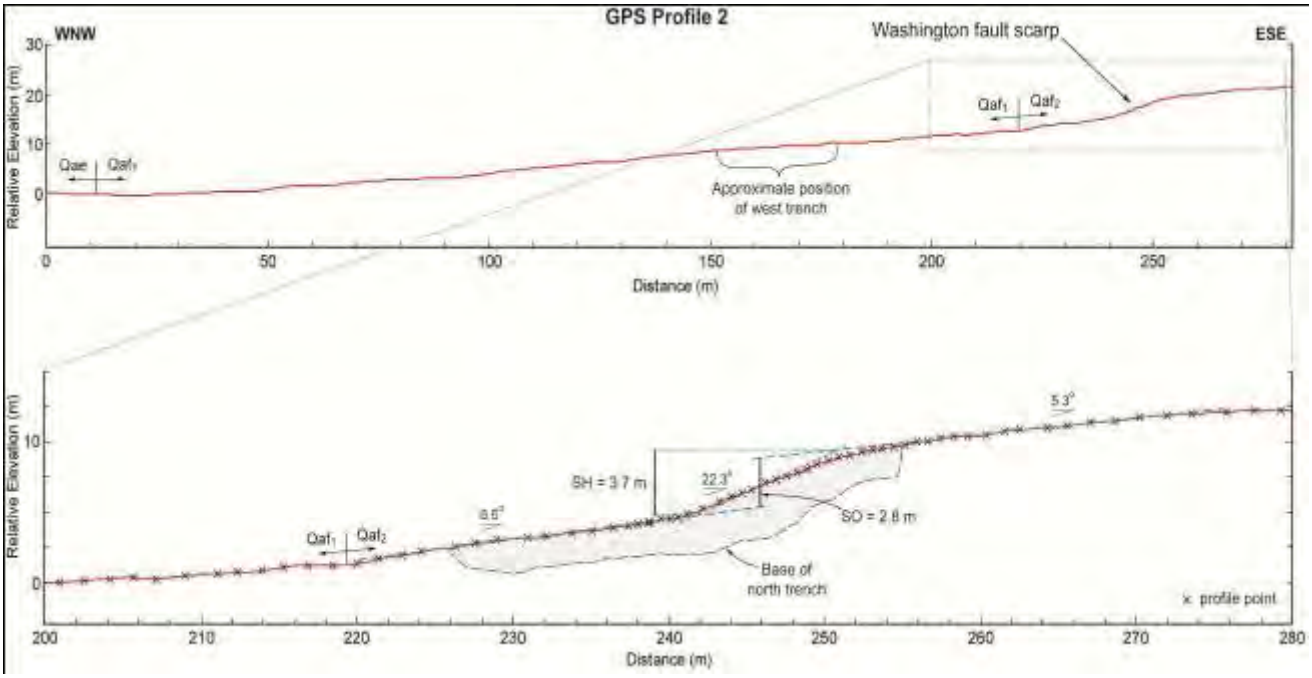

Figure 5. *Dutchman Draw trench site scarp profile #2; profile measured summer 2009. See figure 2 for explanation of geologic units. View to the north.*

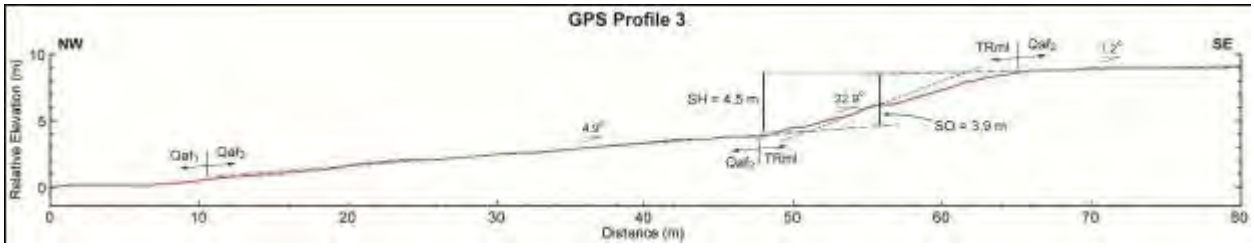

Figure 6. *Dutchman Draw trench site scarp profile #3; profile measured summer 2009. See figure 2 for explanation of geologic units. View to the north.*

Table 1. *AMS radiocarbon age results for carbon samples from the Dutchman Draw site trenches, Arizona. Samples analyzed at the Keck Carbon Cycle AMS Facility at the University of California, Irvine.*

Sample No.	Sample Identification	Geologic Unit	AMS ^{14}C Age[1] RCYBP[3]	One-sigma Calibrated Age[2] (68.2%) cal yr B.P.[3]	Two-sigma Calibrated Age[2] (95.4%) cal yr B.P.
PRI-09-61-NT-RC1	Salicaceae and unidentified hardwood charcoal	4a P2 colluvial wedge	5720 ± 150	6680-6390 (61.7%) 6370-6320 (6.5 %)	6900-6200
PRI-09-61-NT-RC2	Unidentified hardwood charcoal	s2 paleosol on unit 2	1480 ± 70	1490-1470 (2.7%) 1420-1300 (65.5%)	1530-1280
PRI-09-61-NT-RC3	Microcharcoal	4a P2 colluvial wedge	3905 ± 20	4420-4350 (42.1%) 4330-4290 (26.1%)	4420-4250
PRI-09-61-NT-RC4	Microcharcoal	4a P2 colluvial wedge	3830 ± 20	4290-4270 (2.5%) 4250-4220 (22.1%) 4210-4150 (43.6%)	4360-4330 (2.7%) 4300-4150 (92.1%)

[1]Reported in radiocarbon years at one standard deviation measurement precision (68.2%), corrected for ^{13}C.
[2]PRI utilized OxCal3.10 (Bronk Ramsey, 2005) for radiocarbon age calibration (see appendix C for details).
[3]BP = before 1950 for both RCYBP and cal yr B.P. ages.

Table 2. *OSL age results for sediment samples from the Dutchman Draw site trenches, Arizona. Samples analyzed at the Utah State University Luminescence Laboratory.*

Sample Number	Trench	Geologic Unit	OSL Age (ka)
NT-OSL1*	North	7 Debris-flow deposit	30.75±2.21
NT-OSL2*	North	8 Debris-flow deposit	48.66+3.74
NT-OSL3*	North	4b P2 Colluvial wedge	3.02±0.34
ST-OSL1*	South	2 Debris-flow deposit	4.22+0.27
ST-OSL2**	South	7 Debris-flow deposit	17.10±1.38
ST-OSL3**	South	8b Debris-flow deposit	54.07±4.07
ST-OSL4**	South	5 Debris-flow deposit	13.80±1.18

OSL ages do not require calendar calibration, and are reported here as years before present; present being either 2009 (*) or 2010 (**) depending on when the laboratory performed the analyses.

Table 3. *Radiocarbon and OSL ages used in OxCal v. 4.1.7 (Bronk Ramsey, 2010; Reimer and others, 2009) to model earthquake timing at the Dutchman Draw site, Arizona.*

Sample Number	Trench	AMS ^{14}C Age (^{14}C BP[1])	OSL Age (ka)	Calibrated Age[2,3] ± Two Sigma (cal yr B.P.)	Median[4] (cal yr B.P.)	Mode[5] (cal yr B.P.)
NT-RC1	North	5720 ± 150		6540 ± 340	6530	6490
NT-RC2	North	1480 ± 70		1390 ± 140	1380	1360
NT-RC3	North	3905 ± 20		4350 ± 80	4350	4360
NT-RC4	North	3830 ± 20		4220 ± 100	4220	4180
ST-OSL1	South		4.22 ± 0.27	4160 ± 540	4160	4160
ST-OSL2	South		17.10 ± 1.38	17,040 ± 2760	17,040	17,050
ST-OSL4	South		13.80 ± 1.18	13,020 ± 2360	13,020	13,040

[1]Carbon 14 years before present; present = 1950. [2]Calender years before present; present = 1950. [3]Mean ± two-sigma (two standard deviations). Reported ages are unmodelled values. [4]Value that separates the higher half of the sample from the lower half. [5]Value that occurs most frequently in the data set, i.e., the peak of the probability density function for the age value.

Table 4. *Earthquake timing and recurrence (one seismic cycle) at the Dutchman Draw site, Arizona.*

	Mean ± Two-Sigma[1]	Median[2]	Mode[3]	95.4% Probability
P1 Earthquake	1000 ± 600	1100	1300	1500 – 400
P2 Earthquake	7700 ± 2400	7300	6700	10,200 – 6200
P2 – P1 Interval	6600 ± 2400	6300	7800	9300 – 4900

[1]All values in table reported as cal yr. BP (present = 1950). [2]Value that separates the higher half of the sample from the lower half. [3]Value that occurs most frequently in the data set, i.e., the peak of the probability density function.

UTAH GEOLOGICAL SURVEY
a division of
Utah Department of Natural Resources

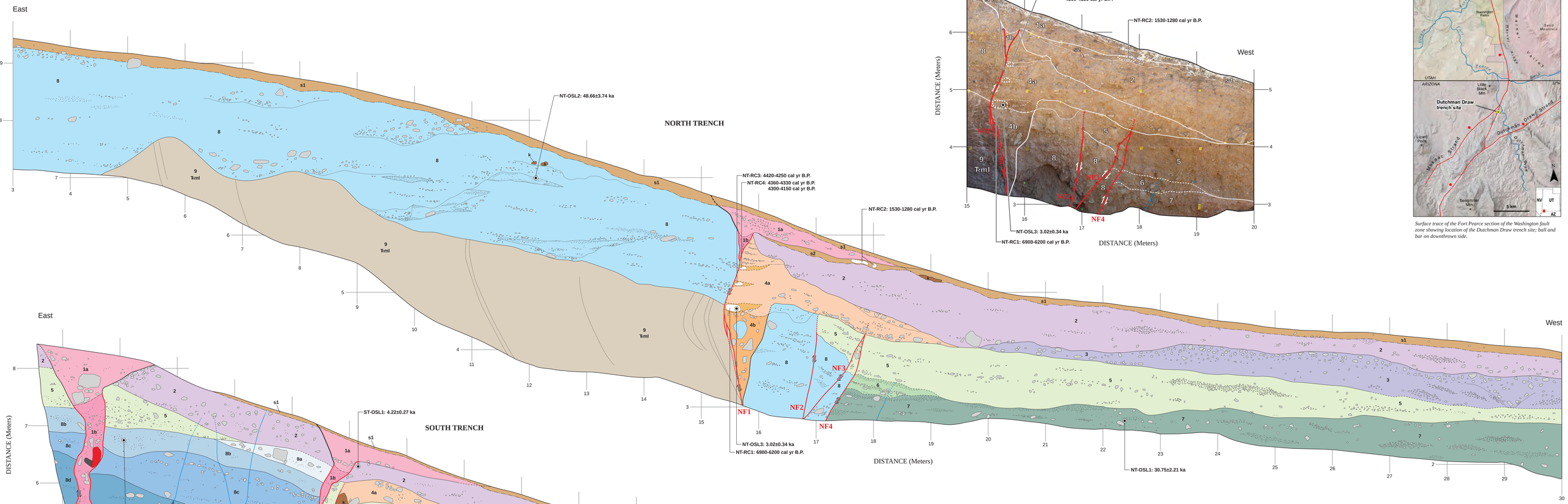

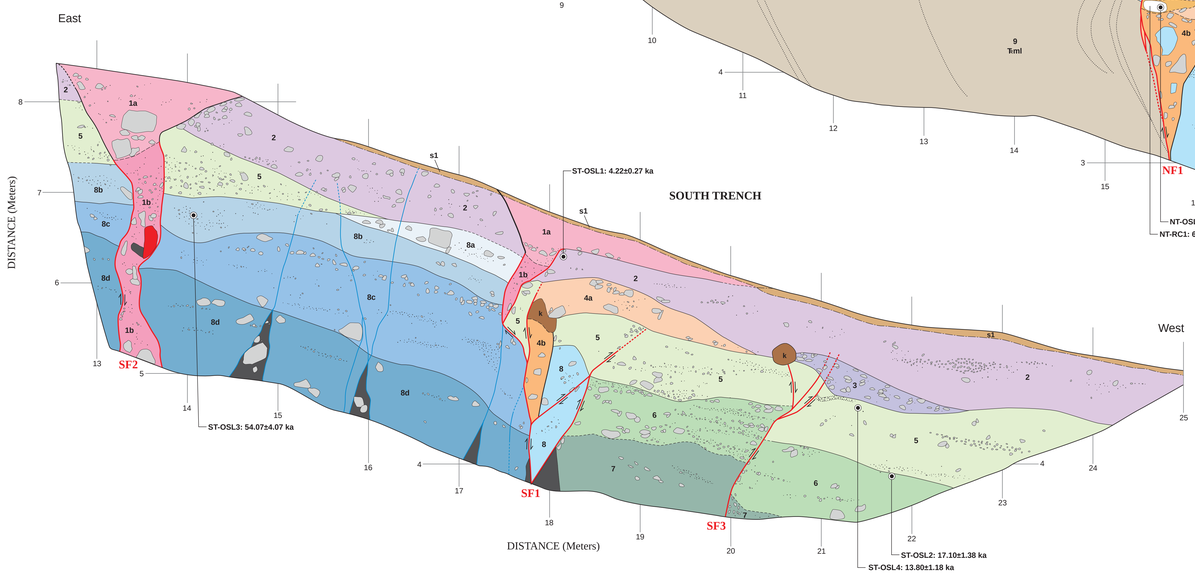

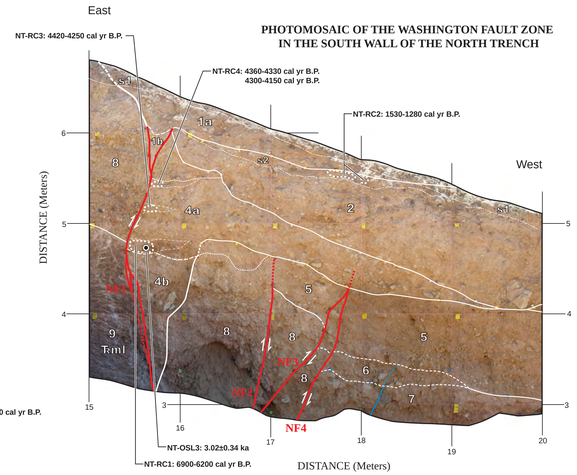

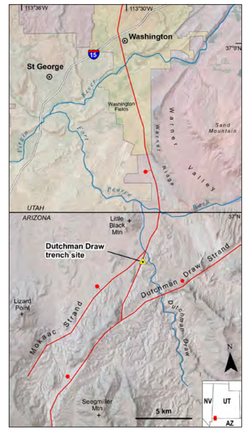

Surface trace of the Fort Pearce section of the Washington fault zone showing location of the Dutchman Draw trench site; ball and bar on downthrown side.

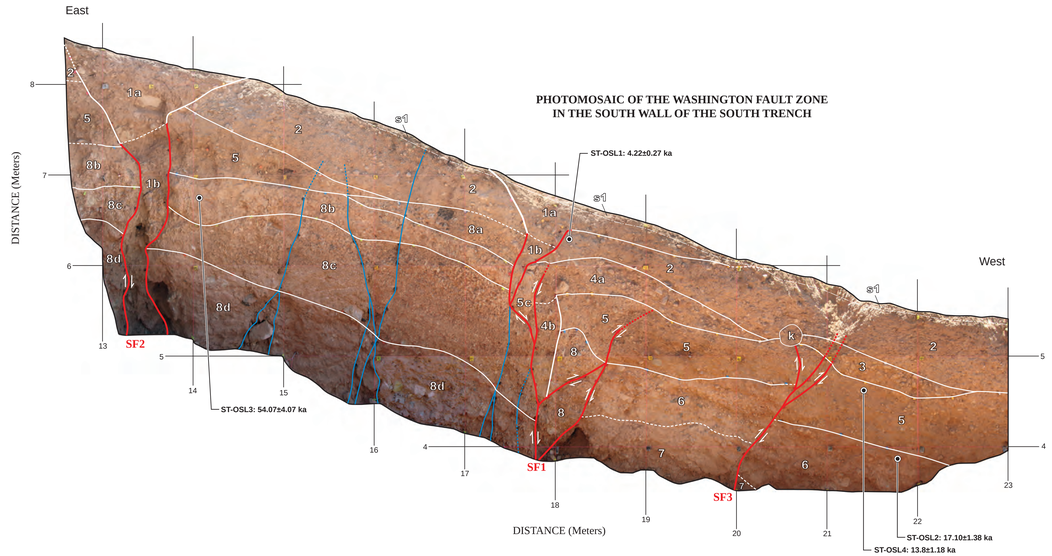

EXPLANATION

- s1 — Soil horizon; s1=modern soil, s2=buried soil horizon
- Weakly organic sediment in unit 4
- k — Infilled burrow (krotovina)
- Block in colluvial unit
- Block of unit 8 in colluvial unit
- Open void
- Bulk sample for radiocarbon analysis
- Sample for OSL dating
- Gravel
- Sand and silt
- Contact; well located, dashed where indistinct
- Contact above scarp-colluvial crack fill
- Intra-unit bedding
- Base of modern or buried soil organic material
- Fault; arrows indicate direction of relative movement; dashed where indistinct
- Eroded fault-scarp free face; dashed where indistinct
- Fissure wall
- Fracture
- 1a / 1b — Scarp colluvium (paleoearthquake P1) (1a) colluvium (1b) crack fill
- 2 — Debris-flow and debris-flood deposits
- 3 — Debris-flow deposit
- 4a / 4b — Scarp colluvium (paleoearthquake P2) (4a) colluvium (4b) crack fill
- 5 — Debris-flow deposit
- 6 — Debris-flow deposit
- 7 — Debris-flow deposit
- 8 (8a, 8b, 8c, 8d) — Strongly indurated (chiefly gypsum-cemented) debris-flow and stream deposits
- 9 (Ŧml) — Mudstone and siltstone of the lower red member of the Triassic Moenkopi Formation

NOTES

Stratigraphic units and soils are described in appendix A.

Bulk-soil samples (e.g., NT-RC1) and radiocarbon ages (e.g., 6900-6200 cal yr B.P.) are summarized in appendix B.

Optically stimulated luminescence samples (e.g., NT-OSL1) and ages (e.g., 30.75±2.21 ka) are summarized in appendix C.

Although this product represents the work of professional scientists, the Utah Department of Natural Resources, Utah Geological Survey, makes no warranty, expressed or implied, regarding its suitability for a particular use. The Utah Department of Natural Resources, Utah Geological Survey, shall not be liable under any circumstances for any direct, indirect, special, incidental, or consequential damages with respect to claims by users of this product.

STRATIGRAPHIC AND STRUCTURAL RELATIONS EXPOSED IN TRENCHES AT THE DUTCHMAN DRAW TRENCH SITE, FORT PEARCE SECTION, WASHINGTON FAULT ZONE, ARIZONA

by William R. Lund, Tyler R. Knudsen, Christopher B. DuRoss, and Greg N. McDonald

APPENDIX A
DUTCHMAN DRAW SITE TRENCH GEOLOGIC UNIT DESCRIPTIONS

Unit	Genesis	Color[1]		Texture[2] (wt. percent)			Max. Clast (cm)	Density/ Consistency[3]	Clast/Matrix Supported[4]	Cementation			Lower Boundary	Soil Development Thickness (cm)	North Trench		South Trench	
		Dry	Moist	Fines	Sand	Gravel				Strength	Type	Morphology[5]			Footwall	Hanging Wall	Footwall	Hanging Wall
1_a	P1 colluvium	7.5YR6/4	7.5YR4/6	30	50	20	20	low	–	none	–	I	clear	weak A horizon, <10 cm	–	x	–	x
1_b	P1 crack fill	7.5YR6/4	7.5YR4/6	30	50	20	10	low	–	none	–	?	abrupt	none	–	x	–	x
2	debris flow	7.5YR6/4	7.5YR4/6	20	35	45	15	low	matrix	weak	carbonate	I+	clear/gradual	weak A horizon, 10-15 cm	–	x	x	x
3	debris flow	7.5YR6/4	7.5YR4/4	15	25	60	20	low	variable	weak	carbonate	I+	clear	none	–	x	–	–
4_a	P2 colluvium	7.5YR7/3	7.5YR5/4	20	25	55	20	low	clast	weak	carbonate	I+	clear	none	–	x	–	x
4_b	P2 crack fill	7.5YR7/3	7.5YR5/4	30	30	40	10	low	matrix	weak	carbonate	?	abrupt	none	–	x	–	x
5	debris flow	7.5YR6/4	7.5YR5/6	20	50	30	15	loose/low	matrix	weak	carbonate	I+	abrupt	none	–	x	x	x
6	debris flow	7.5YR7/4	7.5YR5/6	20	50/30	30/50	20	medium	variable	moderate	gypsum	II-	clear	none	–	–	–	x
7	debris flow	7.5YR8/4	7.5YR6/6	50	35	15	10	hard	na	strong	gypsum	II+	not exposed	none	–	–	–	x
8	old alluvial fan undifferentiated	7.5YR7/4	7.5YR5/6	20	30	50	15	high	variable	strong	gypsum	II+	not exposed	none	–	–	–	x
8_a	old alluvial fan	5YR7/4	5YR6/6	20	30	50	20	high	variable	strong	gypsum	II+	clear	none	–	–	x	–
8_b	old alluvial fan	5YR7/4	5YR6/6	25	60	15	5	high	–	strong	gypsum	II+	abrupt	none	–	–	x	–
8_c	old alluvial-fan	5YR5/6	5YR4/6	25	50	25	35	high	–	strong	gypsum	II+	abrupt	none	–	–	x	–
8_d	old alluvial-fan	5YR5/6	5YR4/6	30	60	10	35	high	–	strong	gypsum	II+	not exposed	none	–	–	x	–
9	Moenkopi Fm.	10R3/4	10R3/4	–	–	–	–	–	–	–	–	–	not exposed	none	x	–	–	–

[1]Munsell Soil Color Chart year 2000 revised edition (GretagMacbeth, 2000). [2]Textural information may not be representative of entire unit due to vertical and horizontal lithological heterogeneity. Clast sizes: fines (silt and clay), < 0.074mm (#200 sieve); sand, > 0.074 mm <4.76 mm (# 4 sieve); gravel, 4.76 mm-76 mm (3 in.); cobbles, 76 mm-305 mm (12 in.); boulders > 305 mm. Weight percentage reported for clast-size fractions are field estimates. [3]Density terms (loose-high) describe coarse-grained units (> 50% retained on the #200 sieve) and consistency terms (very soft-hard) describe fine-grained units (< 50% retained on the #200 sieve). [4]Visual estimate for units with ≥ 30% gravel content. [5]Cement morphology stages follow table A-6 in UGS Miscellaneous Publication 91-3 (Birkeland and others, 1991). Morphology stages are used descriptively only and do not imply pedogenic development.

APPENDIX B
EXAMINATION OF BULK SOIL AND AMS RADIOCARBON ANALYSIS OF CARBON FROM THE DUTCHMAN DRAW TRENCHES, WASHINGTON FAULT ZONE, ARIZONA
(Analyses performed by Paleo Research Institute, Golden, Colorado)

EXAMINATION OF BULK SOIL AND AMS RADIOCARBON ANALYSIS OF MATERIAL FROM THE DUTCHMAN DRAW TRENCH SITE ON THE WASHINGTON FAULT, ARIZONA

By

Kathryn Puseman

With Assistance from
R. A. Varney

PaleoResearch Institute
Golden, Colorado

PaleoResearch Institute Technical Report 09-61

Prepared For

Utah Geological Survey (Microcharcoal Recovery)
Salt Lake City, Utah

and

Rosenberg Associates (AMS Radiocarbon Dating)
St. George, Utah

November 2009

INTRODUCTION

A total of four bulk soil samples from the Dutchman Draw Trench site on the Washington Fault in northwest Arizona were examined to recover organic fragments suitable for radiocarbon analysis. These samples were recovered from soil stringers in the PE wedge, as well as from paleosol beneath the Most Recent Event (MRE) wedge in the North paleoseismic trench. Botanic components and detrital charcoal were identified, and potentially radiocarbon datable material was separated. Two of the samples did not yield sufficient macroscopic charcoal for dating; therefore, they were processed to recover microscopic charcoal to obtain a radiocarbon date.

METHODS

Flotation and Charcoal Identification

After removing calcium carbonates with hydrochloric acid (10%), the samples were screened through a 250 micron mesh sieve. The material remaining in the screen was retained for macroscopic examination, while the material that passed through the screen was saved for possible microscopic charcoal extraction. The dried screen contents were examined under a binocular microscope at a magnification of 10x. Charcoal fragments were separated from the water-screened sample matrix, broken to expose a fresh cross-section, and examined under a binocular microscope at a magnification of 70x.

Macrofloral remains, including charcoal, were identified using manuals (Core, et al. 1976; Martin and Barkley 1961; Panshin and Zeeuw 1980; Petrides and Petrides 1992) and by comparison with modern and archaeological references. Because charcoal and possibly other botanic remains were to be submitted for radiocarbon dating, clean laboratory conditions were used during flotation and identification to avoid contamination. All instruments were washed between samples, and samples were protected from contact with modern charcoal.

Microcharcoal Extraction

The next step is to recover microscopic charcoal from sediments for the purpose of obtaining an AMS radiocarbon age. Microscopic charcoal fragments are far superior to humates because they provide dates with the same precision as those obtained from larger pieces of charcoal, with the single exception that the individual pieces of microscopic charcoal are not identified to taxon. A chemical extraction technique based on that used for pollen, and relying upon heavy liquid extraction, has been modified to recover microscopic charcoal for the purpose of obtaining an AMS radiocarbon age. Two of the samples did not yield sufficient macroscopic charcoal for radiocarbon dating; therefore, the fraction of the sample that passed through the 250 micron mesh sieve during initial screening was further processed to obtain microscopic charcoal.

The samples were rinsed until neutral, then a small quantity of sodium hexametaphosphate was added to each sample, which was then filled with reverse osmosis, deionized (RODI) water and allowed to settle according to Stoke's Law. After two hours the

supernatant, containing clay, was poured off and the samples were rinsed with RODI water three more times, being allowed to settle according to Stoke's Law to remove more clays. Once the clays had been removed, the samples were freeze dried. Sodium polytungstate (SPT), with a density of 1.8, was used for the flotation process. The samples were mixed with SPT and centrifuged at 1500 rpm for 10 minutes to separate organic from inorganic remains. The supernatant containing pollen, organic remains, and microscopic charcoal was decanted. Sodium polytungstate again was added to the inorganic fraction to repeat the separation process until all visible charcoal had been recovered. The charcoal was recovered from the sodium polytungstate and rinsed thoroughly with RODI water. At this stage, the microcharcoal samples joined the macroscopic charcoal samples for chemistry pre-treatment.

AMS Radiocarbon Dating

Wood and charcoal samples submitted for radiocarbon dating are identified and weighed prior to selecting subsamples for pre-treatment. The remainder of each su sa l e that roceed s to re-treat ent if there is an is e r anentl curated at aleoResearch. he su sa l e selected for re-treat ent is first su ected to hot (at least) h drochloric acid (HCl), with rinses to neutral between each HCl treatment, until the supernatant is clear. This removes iron compounds and calcium carbonates that would hamper removal of humate compounds later. Next the samples are subjected to 5% potassium hydroxide (KOH) to remove humates. Once again, the samples are rinsed to neutral and re-acidified with pH 2 HCl between each KOH step. This step is repeated until the supernatant is clear, signaling removal of all humates. After humate removal, each sample is made slightly acidic and left that way for the next step. Charcoal samples (but not wood samples) are subjected to a concentrated, hot nitric acid bath, which removes all modern and recent organics. This treatment is not used on unburned or partially burned wood samples because it oxidizes the submitted sample of unknown age.

ach su itted sa l e is then freeze-dried using a acuu s ste freezing out all oisture at - . ach indi idual sa l e is co i ned with cu r ic o ide (uO) and ele en tal silver (Ag^o) in a quartz tube, then flame sealed under vacuum.

Standards and laboratory background samples also are treated in the same manner as the wood and charcoal sa l es of unknown age. A radiocar o n “dead” UA wood l ank fro Alaska that is more than 70,000 years old (currently beyond the detection capabilities of AMS) is treated using the same chemical processing as the samples of unknown age in order to calibrate the laboratory correction factor. Standards of known age, such as Two Creeks wood that dates to 11,400 RCYBP and others from the Third International Radiocarbon Intercomparison (TIRI), are also processed simultaneously to establish the laboratory correction factor. Each wood standard is run in a quantity similar to the submitted samples of unknown age and sealed in a quartz tube after the requisite pre-treatment.

Once all the wood standards l anks and su itted sa l es of unknown age are re ared and sealed in their indi idual uartz tu es the are co u sted at soaked for an extended period of time at that temperature, and then slowly allowed to cool to enable the chemical reaction that extracts carbon dioxide ($C0_2$) gas.

Following this last step, all samples of unknown age, the wood standards, and the laboratory backgrounds are sent to the Keck Carbon Cycle AMS Facility at the University of California, Irvine, where the $C0_2$ gas is processed into graphite. The graphite in these samples

is then placed in the target and run through the accelerator, which produces the numbers that are converted into the radiocarbon date presented in the data section. Dates are presented as conventional radiocarbon ages, as well as calibrated ages using Intcalc04 curves on Oxcal version 3.10.

RADIOCARBON REVIEW

When interpreting radiocarbon dates from non-annuals such as trees and shrubs, it is important to understand that the radiocarbon date reflects the age of that portion of the tree/shrub when it stopped exchanging carbon with the atmosphere, not necessarily the date that the tree/shrub died or was burned. Trees and shrubs grow bigger each year from the cambium, where a new layer or ring of cells is added each year. During photosynthesis new cells take in atmospheric carbon dioxide, which includes radiocarbon. The radiocarbon taken in will reflect the radiocarbon present in the atmosphere during that season of growth. Once the sapwood in a tree has been converted into heartwood, the metabolic process stops for that inner wood. Once this happens, no new carbon atoms are acquired, and the radiocarbon that is present starts to decay. Studies have shown that there is little to no movement of carbon-bearing material from one ring to another. As a result, wood from different parts of the tree will yield different radiocarbon dates. The outer rings exhibit an age close to the cutting or death date of the tree, while the inner rings will reflect the age of the tree. Because the younger, outer rings burn off first when a log or branch is burned, it is the older, inner rings that typically are what is left remaining in a charcoal assemblage (Puseman 2009; Taylor 1987).

DISCUSSION

The Dutchman Draw Trench site is located on the Washington Fault in northwest Arizona. Samples were collected from three soil stringers in the PE wedge, as well as from paleosol beneath the MRE wedge. Sample NT-RC-1 was taken from the lower soil stringer in the PE wedge (Table 1). This sample yielded small fragments of Salicaceae and unidentified hardwood charcoal weighing a total of 0.0006 g. This charcoal reflects a woody member of the willow family and possibly another type of hardwood (Tables 2 and 3). Recovery of a few charred insect fecal pellets suggests that some of the burned wood contained insects. An AMS radiocarbon date of 5720 ± 150 RCYBP (PRI-09-61-NT-RC1) was returned for the combined charcoal, with a two-sigma calibrated age range of 6900-6200 CAL yr. BP (Table 4, Figure 1). Sample RC1 also yielded a moderate amount of uncharred rootlets from modern plants, a few uncharred bone fragments, and two snail shell fragments.

Sample NT-RC-3 was collected from the middle soil stringer in the PE wedge, while sample NT-RC-2 represents the upper soil stringer. No macroscopic charcoal fragments were present in either of these two samples; therefore, AMS radiocarbon dates were obtained on microscopic charcoal (microcharcoal) recovered from this sample. Sample NT-RC-3 yielded a date of 3905 ± 20 RCYBP (PRI-09-61-NT-RC3) and a two-sigma calibrated age range of 4420-4250 CAL yr. BP (Figure 2). Sample NT-RC-4 from the upper soil stringer yielded a date of 3830 ± 20 RCYBP (PRI-09-61-NT-RC4). This date calibrates to 4360-4330 and 4300-4150 CAL yr. BP at the two-sigma level (Figure 3).

Paleosol from beneath the MRE wedge was collected as sample NT-RC-2. This sample contained 16 fragments of hardwood charcoal too small for identification weighing 0.0009 g. A $\delta^{13}C$ value of -9.9 $^{o}/_{o}$ reported as part of the AMS dating process, suggests that this hardwood charcoal represents a wood with a C4 photosynthetic pathway, such as *Atriplex* (saltbush). The hardwood charcoal returned a date of 1480 ± 70 RCYBP (PRI-09-61-NT-RC2), with a two-sigma calibrated age range of 1530-1280 CAL yr. BP (Figure 4). A moderate amount of uncharred rootlets from modern plants, several insect chitin fragments, and numerous worm casts also were noted.

SUMMARY AND CONCLUSIONS

Examination of bulk samples from the Dutchman Draw trench site resulted in recovery of macroscopic and microscopic charcoal submitted for AMS radiocarbon dating. Pieces of willow family and unidentified hardwood charcoal from the lowest soil stringer in the PE wedge returned a date of 5720 ± 150 BP. Microscopic charcoal extracted from samples NT-RC-3 (middle soil stringer) and NT-RC-4 (upper stringer) yielded dates of 3905 ± 20 BP and 3830 ± 20 BP, respectively. A date of 1480 ± 70 BP was returned for unidentified hardwood charcoal from paleosol beneath the MRE wedge.

TABLE 1
PROVENIENCE DATA FOR SAMPLES FROM THE DUTCHMAN DRAW TRENCH SITE, ARIZONA

Sample No.	Provenience/ Description	Analysis
NT-RC-1	Sediment from lower soil stringer in PE Wedge	Macrofloral AMS ^{14}C Date
NT-RC-3	Sediment from middle soil stringer in PE Wedge	Macrofloral Microcharcoal AMS ^{14}C Date
NT-RC-4	Sediment from upper soil stringer in PE Wedge	Macrofloral Microcharcoal AMS ^{14}C Date
NT-RC-2	Sediment from paleosol beneath MRE wedge in alluvial fan	Macrofloral AMS ^{14}C Date

TABLE 2
MACROFLORAL REMAINS FROM THE DUTCHMAN DRAW TRENCH SITE, ARIZONA

Sample No.	Identification	Part	Charred W	Charred F	Uncharred W	Uncharred F	Weights/ Comments
NT-RC-1	Liters Floated						1.00 L
	Light Fraction Weight						0.57 g
	FLORAL REMAINS:						
	Rootlets					X	Moderate
	CHARCOAL/WOOD:						
	Salicaceae and Unidentified hardwood - small**	Charcoal		X			0.0006 g
	NON-FLORAL REMAINS:						
	Bone					X	Few
	Insect fecal pellet		X	X			Few
	Rock/Gravel					X	Few
	Snail shell					2	
NT-RC-3	Liters Floated						0.20 L
	Light Fraction Weight						0.42 g
	FLORAL REMAINS:						
	Rootlets					X	Few
	NON-FLORAL REMAINS:						
	Rock/Gravel					X	Moderate
NT-RC-4	Liters Floated						0.40 L
	Light Fraction Weight						0.30 g
	FLORAL REMAINS:						
	Rootlets					X	Moderate
	NON-FLORAL REMAINS:						
	Rock/Gravel					X	Numerous
NT-RC-2	Liters Floated						1.00 L
	Light Fraction Weight						6.70 g
	FLORAL REMAINS:						
	Rootlets					X	Moderate
	CHARCOAL/WOOD:						
	Unidentified hardwood - small**	Charcoal		16			0.0009 g

Table 2 Continued

Sample No.	Identification	Part	Charred		Uncharred		Weights/ Comments
			W	F	W	F	
NT-RC-2	NON-FLORAL REMAINS						
	Insect	Chitin				37	
	Rock/Gravel					X	Moderate
	Worm casts				X	X	Numerous

W = Whole
F = Fragment
X = Presence noted in sample
L = Liters
g = grams
** = Submitted for AMS radiocarbon dating

TABLE 3
INDEX OF MACROFLORAL REMAINS RECOVERED FROM
THE DUTCHMAN DRAW TRENCH SITE, ARIZONA

Scientific Name	Common Name
CHARCOAL/WOOD:	
Salicaceae	Willow family
Unidentified hardwood - small	Wood from a broad-leaved flowering tree or shrub, fragments too small for further identification

TABLE 4
RADIOCARBON RESULTS FOR SAMPLES FROM
THE DUTCHMAN DRAW TRENCH SITE, ARIZONA

Sample No.	Sample Identification	AMS ^{14}C Date*	1-sigma Calibrated Date (68.2%)	2-sigma Calibrated Date (95.4%)
PRI-09-61-NT-RC1	Salicaceae and unidentified hardwood charcoal	5720 ± 150 RCYBP	6680-6390 6370-6320 CAL yr. BP	6900-6200 CAL yr. BP
PRI-09-61-NT-RC3	Microcharcoal	3905 ± 20 RCYBP	4420-4350 4330-4290 CAL yr. BP	4420-4250 CAL yr. BP
PRI-09-61-NT-RC4	Microcharcoal	3830 ± 20 RCYBP	4290-4270 4250-4220 4210-4150 CAL yr. BP	4360-4330 4300-4150 CAL yr. BP
PRI-09-61-NT-RC2	Unidentified hardwood charcoal	1480 ± 70 RCYBP	1490-1470 1420-1300 CAL yr. BP	1530-1280 CAL yr. BP

* Reported in radiocarbon years at 1 standard deviation measurement precision (68.2%), corrected for $\delta^{13}C$

FIGURE 1. PRI RADIOCARBON AGE CALIBRATION

Laboratory Number: PRI-09-61-NT-RC1
Sample Identification: Salicaceae and unidentified hardwood charcoal
Conventional AMS ^{14}C Date: 5720 ± 150 RCYBP
1-sigma Calibrated Date (68.2%): 6680-6390; 6370-6320 CAL yr. BP
2-sigma Calibrated Date (95.4%): 6900-6200 CAL yr. BP

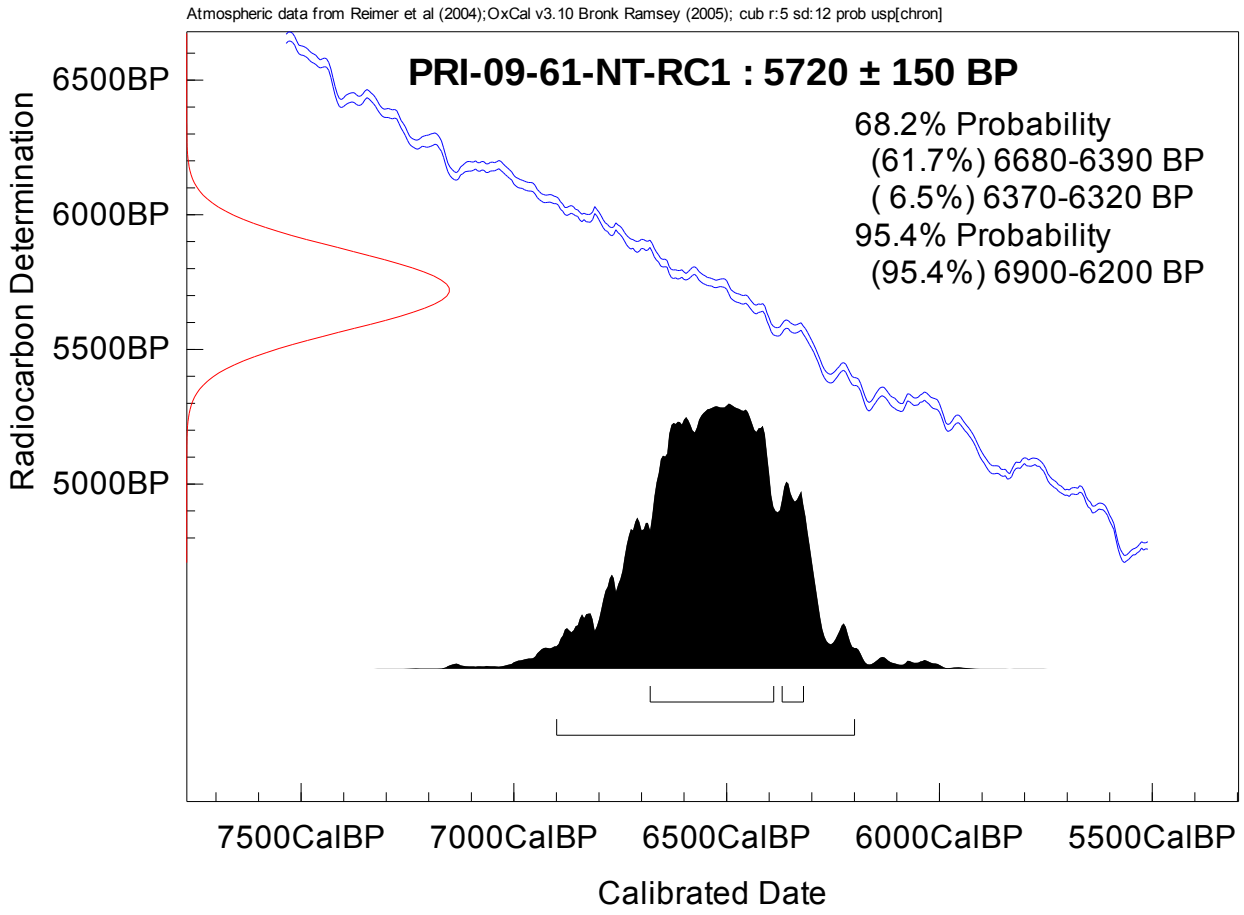

Intercept Statement. PaleoResearch Institute utilizes OxCal3.10 (Bronk Ramsey, 2005) for radiocarbon calibration, which is a probability-based method for determining conventional ages. We prefer this method over the intercept-based alternative because it provides our clients with a calibrated date that reflects the probability of its occurrence within a given distribution (reflected by the amplitude (height) of the curve), as opposed to individual point estimates (Telford 2004). As a result, the probability-based method offers more stability to the calibrated values than those derived from intercept-based methods that are subject to adjustments in the calibration curve (Telford 2004).

References

Telford, R. J., E. Heegaard, and H. J. B. Birks, 2004, *The Holocene* 14(2), pp. 296-298.

FIGURE 2. PRI RADIOCARBON AGE CALIBRATION

Laboratory Number: PRI-09-61-NT-RC3
Sample Identification: Microcharcoal
Conventional AMS ^{14}C Date: 3905 ± 20 RCYBP
1-sigma Calibrated Date (68.2%): 4420-4350; 4330-4290 CAL yr. BP
2-sigma Calibrated Date (95.4%): 4420-4250 CAL yr. BP

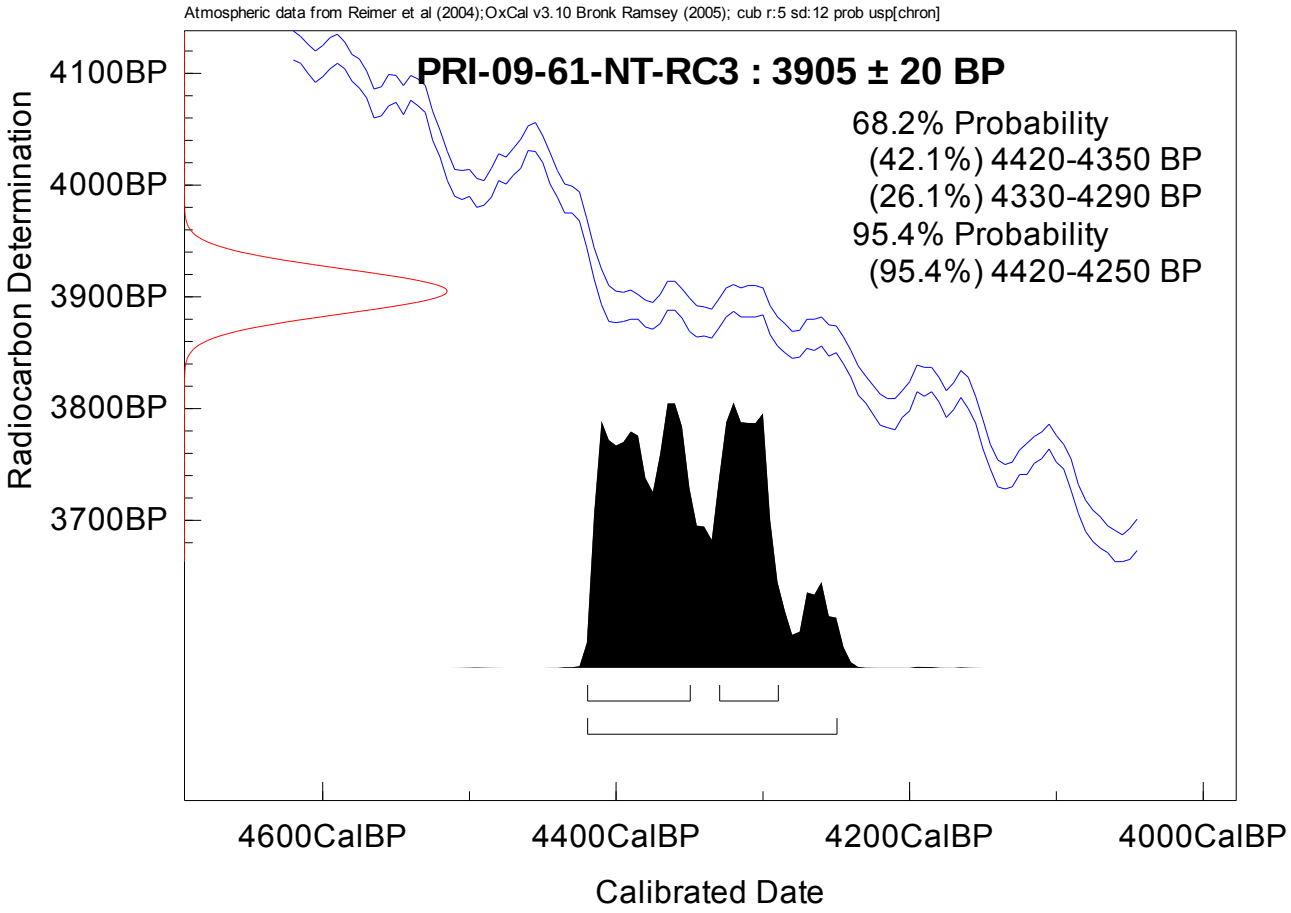

Intercept Statement. PaleoResearch Institute utilizes OxCal3.10 (Bronk Ramsey, 2005) for radiocarbon calibration, which is a probability-based method for determining conventional ages. We prefer this method over the intercept-based alternative because it provides our clients with a calibrated date that reflects the probability of its occurrence within a given distribution (reflected by the amplitude (height) of the curve), as opposed to individual point estimates (Telford 2004). As a result, the probability-based method offers more stability to the calibrated values than those derived from intercept-based methods that are subject to adjustments in the calibration curve (Telford 2004).

References

Telford, R. J., E. Heegaard, and H. J. B. Birks, 2004, *The Holocene* 14(2), pp. 296-298.

FIGURE 3. PRI RADIOCARBON AGE CALIBRATION

Laboratory Number: PRI-09-61-NT-RC4
Sample Identification: Microcharcoal
Conventional AMS ^{14}C Date: 3830 ± 20 RCYBP
1-sigma Calibrated Date (68.2%): 4290-4270; 4250-4220; 4210-4150 CAL yr. BP
2-sigma Calibrated Date (95.4%): 4360-4330; 4300-4150 CAL yr. BP

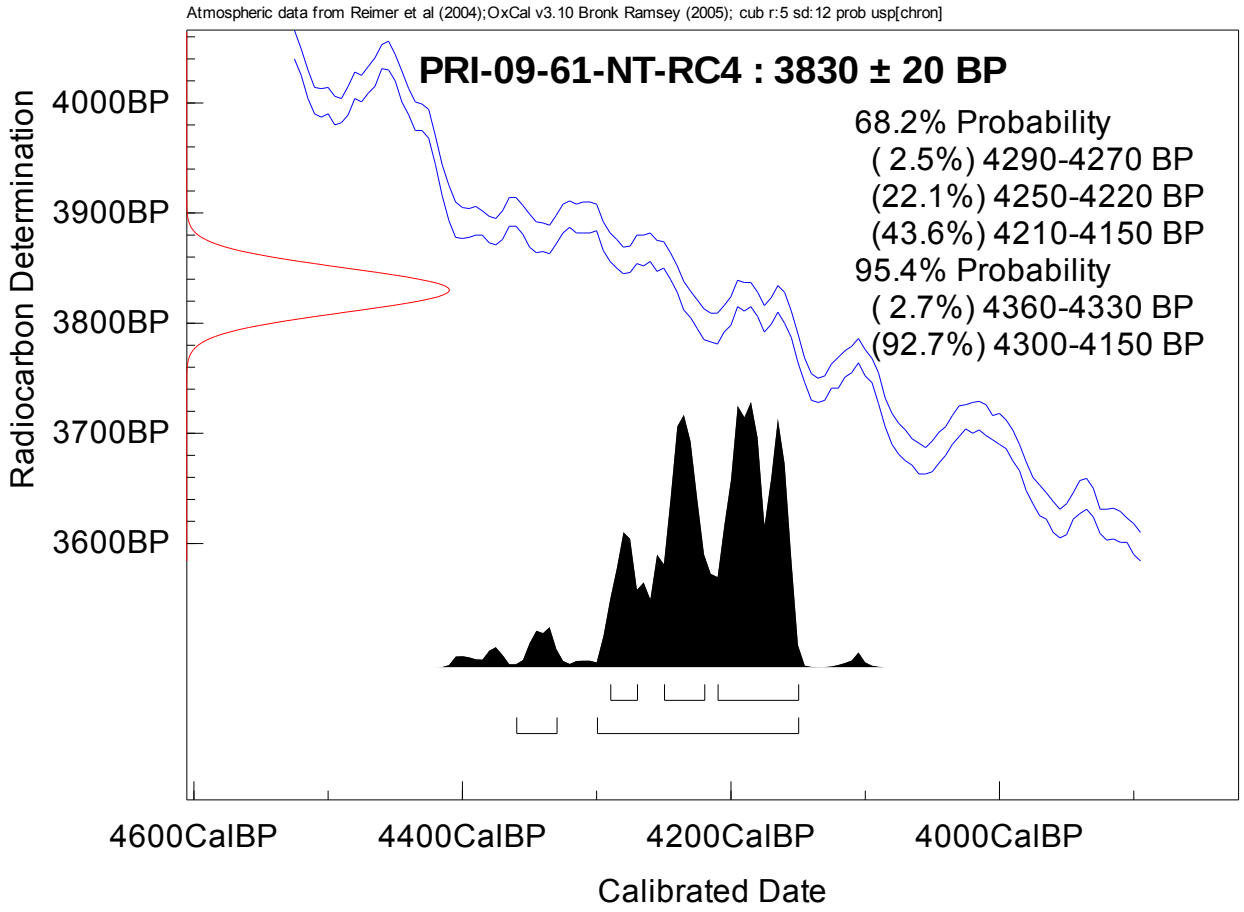

Intercept Statement. PaleoResearch Institute utilizes OxCal3.10 (Bronk Ramsey, 2005) for radiocarbon calibration, which is a probability-based method for determining conventional ages. We prefer this method over the intercept-based alternative because it provides our clients with a calibrated date that reflects the probability of its occurrence within a given distribution (reflected by the amplitude (height) of the curve), as opposed to individual point estimates (Telford 2004). As a result, the probability-based method offers more stability to the calibrated values than those derived from intercept-based methods that are subject to adjustments in the calibration curve (Telford 2004).

References

Telford, R. J., E. Heegaard, and H. J. B. Birks, 2004, *The Holocene* 14(2), pp. 296-298.

FIGURE 4. PRI RADIOCARBON AGE CALIBRATION

Laboratory Number: PRI-09-61-NT-RC2
Sample Identification: Unidentified hardwood charcoal
Conventional AMS ^{14}C Date: 1480 ± 70 RCYBP
1-sigma Calibrated Date (68.2%): 1490-1470; 1420-1300 CAL yr. BP
2-sigma Calibrated Date (95.4%): 1530-1280 CAL yr. BP

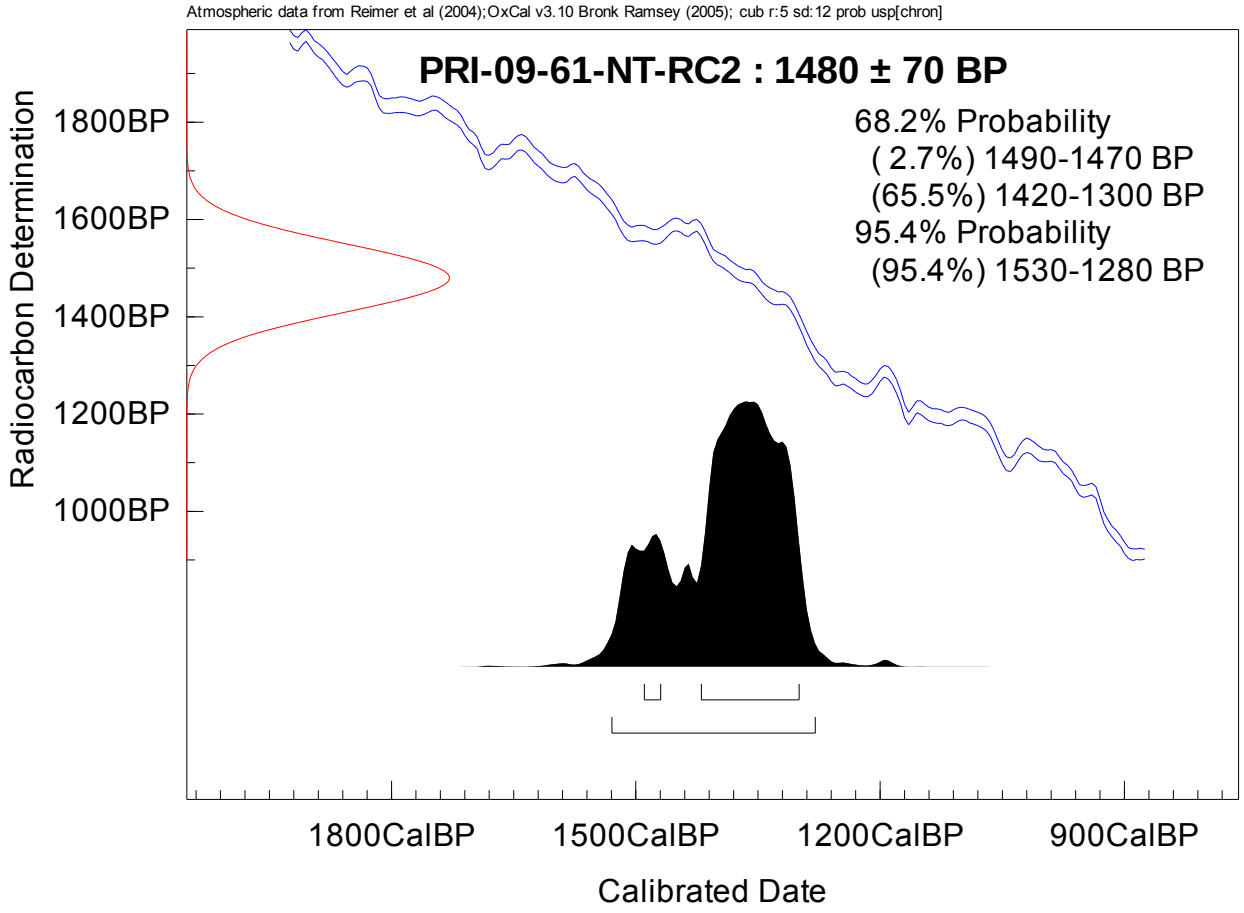

Intercept Statement. PaleoResearch Institute utilizes OxCal3.10 (Bronk Ramsey, 2005) for radiocarbon calibration, which is a probability-based method for determining conventional ages. We prefer this method over the intercept-based alternative because it provides our clients with a calibrated date that reflects the probability of its occurrence within a given distribution (reflected by the amplitude (height) of the curve), as opposed to individual point estimates (Telford 2004). As a result, the probability-based method offers more stability to the calibrated values than those derived from intercept-based methods that are subject to adjustments in the calibration curve (Telford 2004).

References

Telford, R. J., E. Heegaard, and H. J. B. Birks, 2004, *The Holocene* 14(2), pp. 296-298.

REFERENCES CITED

Puseman, Kathryn

2009 Choose Your Wood Wisely: Bigger Isn't Always Better. Paper presented at the Ninth Biennial Rocky Mountain Anthropological Conference, Western State College of Colorado, Gunnison.

Taylor, R. E.

1987 *Radiocarbon Dating: An Archaeological Perspective*. Academic Press, Inc., Orlando.

Telford, R.J., E. Heegaard, and H.J.B. Birks

2004 The Intercept is a Poor Estimate of a Calibrated Radiocarbon Age. *The Holocene* 14(2):296-298.

APPENDIX C
UTAH STATE UNIVERSITY
LUMINESCENCE LABORATORY OSL AGES,
DUTCHMAN DRAW TRENCH SITE,
WASHINGTON FAULT ZONE, ARIZONA

USU LUMINESCENCE LABORATORY
1770 north research park way, suite 123, north logan, ut, 84341

FINAL OSL AGE REPORT

Project: Washington Fault, Utah Geological Survey **Project #:** 068
Scientists: William Lund
Report by: Tammy Rittenour
Date: 01 September 2010

OSL Age Information[1]

USU #	Sample #	Location	Num. of aliquots[2]	Equivalent Dose[3] (De), Gy	Dose Rate (Gy/ka)	OSL Age[4] (ka)
NT-OSL 1	USU-554	unit 5b, hanging wall	**26** (35)	51.52 ± 6.08	1.68 ±0.07	**30.75 ± 2.21**
NT-OSL 2	USU-555	unit 5, foot wall	**26** (33)	55.72 ± 8.36	1.10 ±0.05	**48.66 ± 3.74**
NT-OSL 3	USU-556	fault scarp colluv, P2	**23** (35)	6.92 ± 1.59	2.30 ±0.10	**3.02 ± 0.34**
ST-OSL 1	USU-557	btwn P2 and P1 colluv	**25** (31)	7.53 ± 0.07	1.78 ±0.08	**4.22 ± 0.27**
ST-OSL 2	USU-788	South trench, unit 5a	**22** (31)	25.06 ± 5.11	1.47 ± 0.07	**17.10 ± 1.38**
ST-OSL 3	USU-789	South trench, unit 5e	**24** (40)	57.18 ± 9.33	1.06 ± 0.05	**54.07 ± 4.07**
ST-OSL 4	USU-790	South trench, unit 4	**20** (32)	17.20 ± 4.31	1.25 ± 0.06	**13.80 ± 1.18**

[1]Age analysis using the single-aliquot regenerative-dose procedure of Murray and Wintle (2000) on 1-mm small-aliquots (SA) of quartz sand.

[2]Number of aliquots used for age calculation, number of aliquots measured in parentheses.

[3]De calculated using the central age model of Galbraith et al (1999), error on De is 1 standard deviation.

[4]Error on age includes random and systematic errors calculated in quadrature.

Dose Rate Information[1]

USU #	Sample #	Depth (m)	Grain size (µm)	*In-situ* H_2O%[2]	U (ppm)	Th (ppm)	K_2O%	Rb_2O (ppm)	Cosmic[3] (Gy/ka)
NT-OSL 1	USU-554	2.0	90-150	1.0%	1.8±0.1	3.3±0.3	1.06±0.03	41.6±1.7	0.19±0.02
NT-OSL 2	USU-555	0.68	90-150	0.3%	1.3±0.1	1.9±0.2	0.57±0.01	21.8±0.9	0.23±0.02
NT-OSL 3	USU-556	1.9	90-150	0.9%	1.9±0.1	5.8±0.5	1.59±0.04	61.4±2.5	0.19±0.02
ST-OSL 1	USU-557	0.46	90-150	1.4%	1.7±0.1	4.3±0.4	1.08±0.03	49.0±2.0	0.23±0.02
ST-OSL 2	USU-788	2.25	90-125	2.0%	1.6±0.1	3.2±0.3	0.84±0.02	33.7±1.3	0.18±0.02
ST-OSL 3	USU-789	1.5	75-150	0.6%	0.9±0.1	1.9±0.2	0.61±0.02	22.6±0.9	0.20±0.02
ST-OSL 4	USU-790	1	75-150	1.0%	1.6±0.1	2.5±0.2	0.58±0.01	21.5±0.9	0.22±0.02

[1]Radioelemental concentrations determined by ICP-MS and ICP-AES techniques from ALS Chemex, dose rate is derived from concentrations by conversion factors from Aitken (1985) and Adamiec and Aitken (1998).

[2]Assumed 3±3%wt H_2O for USU-554:-557 and *in-situ* ±3%wt H_2O for USU-788:-790 to represent moisture content over burial history.

[3]Contribution of cosmic radiation to the dose rate was calculated by using sample depth, elevation, and longitude/latitude following Prescott and Hutton (1994).

Equivalent dose distributions: Probability density functions

USU-554

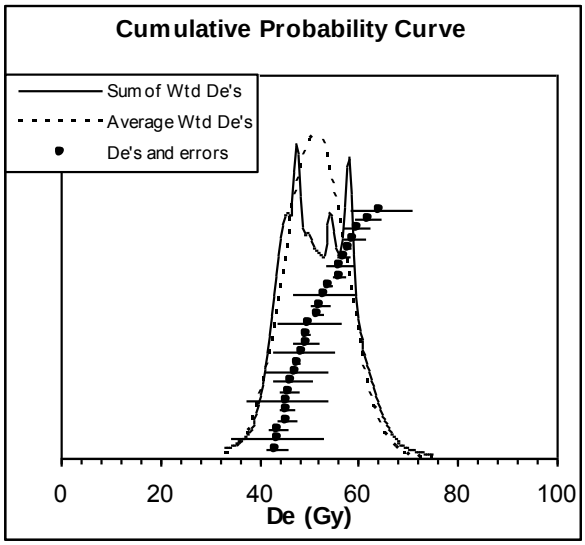

USU-555

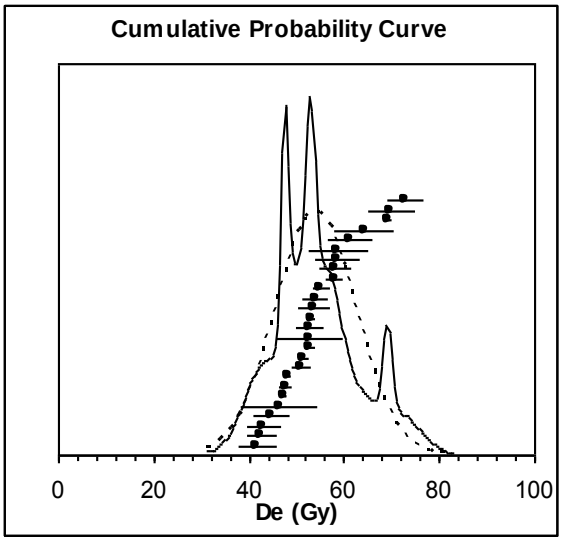

USU-556

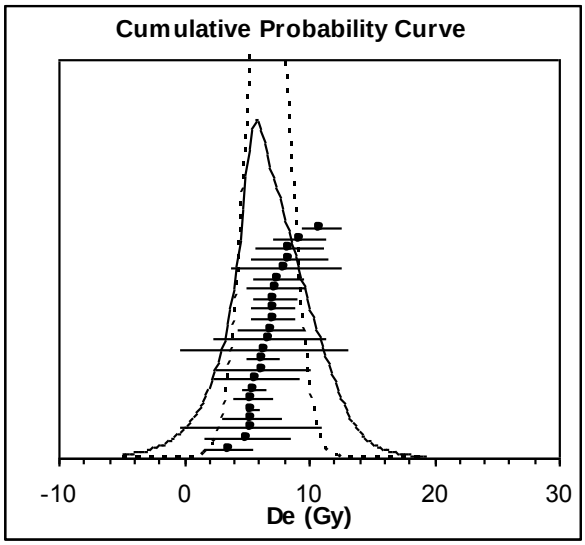

USU-557

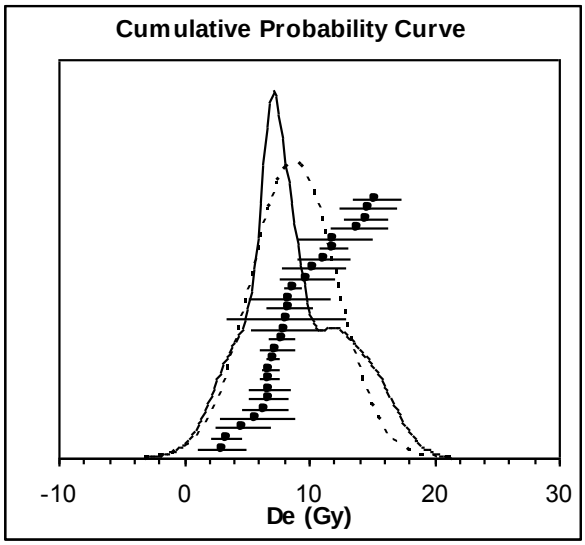

Equivalent dose distributions: Probability density functions (con't)

USU-788

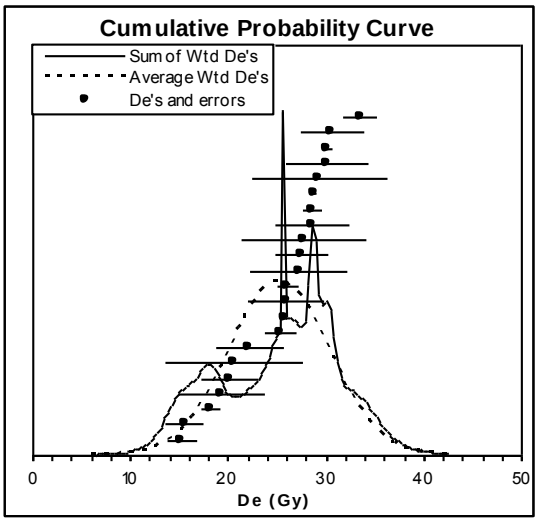

USU-789

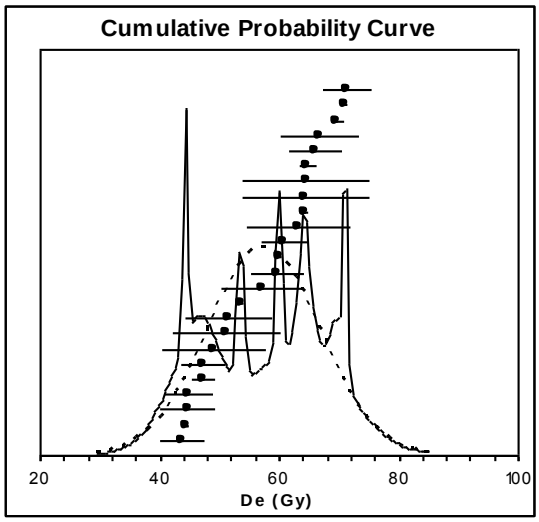

USU-790

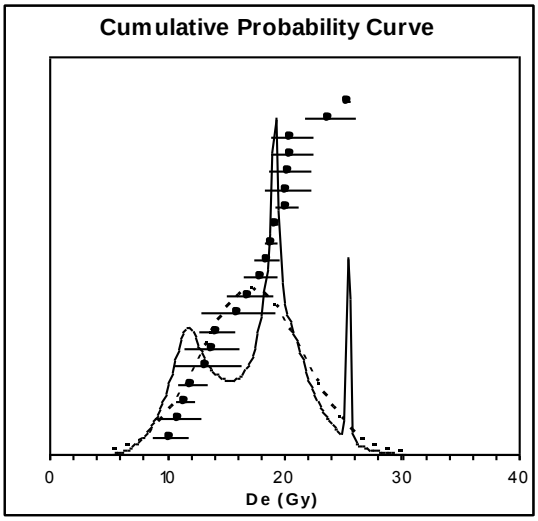

Procedures for sample processing and age analysis:

All samples were opened and processed under dim amber safelight conditions within the lab. Sample processing follows standard procedures involving sieving, gravity separation and acid treatments with HCl and HF to isolate the quartz component of a narrow grain-size range, usually 90-150 µm*. The purity of the samples is checked by measurement with infra-red stimulation to detect the presence of feldspar. Sample processing procedures follow those outlined in Aitken (1998) and described in Rittenour et al. (2003, 2005).

The USU Luminescence Lab follows the latest single-aliquot regenerative-dose (SAR) procedures for dating quartz sand (Murray and Wintle, 2000, 2003; Wintle and Murray, 2006). The SAR protocol includes tests for sensitivity correction and brackets the equivalent dose (De) the sample received during burial by irradiating the sample at five different doses (below, at, and above the De, plus a zero dose and a repeated dose to check for recuperation of the signal and sensitivity correction). The resultant data are fit with a saturating exponential curve from which the De is calculated on the mean, Central Age Model (CAM) or the Minimum Age Model (MAM) of Galbraith et al. (1999) or Juyal et al. (2006), depending on the distribution of De results and evidence for partial bleaching*. In cases where the samples have significant positive skew, ages are calculated based on a MAM. OSL age is reported at 1σ or 2σ standard error* and is calculated by dividing the De (in grays, gy) by the environmental dose rate (gy/ka) that the sample has been exposed to during burial.

Dose-rate calculations were determined by chemical analysis of the U, Th, K and Rb content using ICP-MS and ICP-AES techniques by ALS Chemex, Elko NV and conversion factors from Aitken (1985) and Adamiec and Aitken (1998). The contribution of cosmic radiation to the dose rate was calculated using sample depth, elevation, and latitude/longitude following Prescott and Hutton (1994). Dose rates are calculated based on water content, sediment chemistry, and cosmic contribution (Aitken, 1998).

Under the collaborative agreement to analyze samples at the USU Luminescence Lab, please consider including Dr. Rittenour as a co-author on resultant publications. Contact me for additional information and help with describing the OSL technique when you plan your publication.

Dr. Tammy Rittenour

Director
USU Luminescence Lab
1770 N Research parkway, suite 123
North Logan, UT 84341

Assistant Professor
Department of Geology, Utah State University
4505 Old Main Hill
Logan, UT 84322-4505

tammy.rittenour@usu.edu
ph (435) 213-5756, fax (435) 797-1588
http://www.usu.edu/geo/luminlab/

* these parameters are sample dependant, see first page of report for specific sample information

References cited:

Adamiec, G., Aitken, M., 1998. Dose-rate conversion factors: update. Ancient TL 16, 37-50.

Aitken, M.J. 1985: Thermoluminescence Dating: New York, Academic Press, 359 p.

Aitken, M.J. 1998: An Introduction to Optical Dating: The dating of Quaternary sediments by the use of photon-stimulated luminescence. New York, Oxford University Press, 267 p.

Galbraith, R.F., Roberts, R.G., Laslett, G.M., Yoshida, H., Oleey, J.M., 1999. Optical dating of single and multiple grains of quartz from Jinmium Rock Shelter, northern Australia: Part I, experimental design and statistical models. Archaeometry 41, 339-364.

Goble, R.J. and Rittenour, T.M., 2006, A linear modulation OSL study of the unstable ultrafast component in samples from glacial lake Hitchcock, Massachusetts, USA: Ancient TL 24, 37-46.

Juyal, N., Chamyal, L.S., Bhandari, S., Bhushan, R., Singhvi, A.K., 2006. Continental record of the southwest monsoon during the last 130 ka: evidence from the southern margin of the Thar Desert, India. Quaternary Science Reviews 25, 2632-2650.

Prescott, J. R., Hutton, J.T., 1994. Cosmic ray contributions to dose rates for luminescence and ESR dating: Radiation Measurements 23, 497-500.

Murray, A.S., Wintle, A.G., 2000. Luminescence dating of quartz using an improved single aliquot regenerative-dose protocol. Radiation Measurements 32, 57-73.

Murray, A.S., Wintle, A.G., 2003. The single aliquot regenerative dose protocol: potential for improvements in reliability. Radiation Measurements 37, 377-381.

Olley, J.M., Pietsch, T., Roberts, R.G., 2004. Optical dating of Holocene sediments from a variety of geomorphic settings using single grains of quartz: Geomorphology 60, 337-358.

Rittenour, T.M., Goble, R.J., Blum, M.D., 2003, An Optical Age Chronology of Fluvial Deposits in the Northern Lower Mississippi Valley: Quaternary Science Reviews, v. 22, p. 1105-1110.

Rittenour, T.M., Goble, R.J., Blum, M.D., 2005, Development of an OSL chronology for late Pleistocene channel belts in the lower Mississippi valley: Quaternary Science Reviews, v.24, p.2539-2554.

Rittenour, T.M. 2008. Luminescence dating of fluvial deposits: applications to geomorphic, palaeoseismic and archaeological research. Boreas, 37, 613-635.

Wintle, A.G. Murray, A.S., 2006, A review of quartz optically stimulated luminescence characteristics and their relevance in single-aliquot regenerative protocols: Radiation Measurements, v. 41, p. 369-391.

APPENDIX D
DUTCHMAN DRAW TRENCH SITE
OXCAL MODEL

The OxCal model for the Dutchman Draw trench site was created using OxCal calibration and analysis software version 4.1.7 (Bronk Ramsey, 2010), and the IntCal09—Northern Hemisphere calibration curve of Reimer and others (2009). The model includes "C_Date" for luminescence ages, "R_Date" for radiocarbon ages, and "Boundary" for undated events (paleoearthquakes). The model components are arranged in sequence based on the stratigraphic position of the luminescence and radiocarbon samples. The "Difference P2–P1" command computes the two-sigma recurrence interval between the P1 and P2 paleoearthquakes. The "Difference MRE elapse time" command computes the elapsed time since the most recent surface-faulting earthquake (P1) to 2011" The model is in reverse stratigraphic order (oldest ages at the top), following the order in which the ages and events are evaluated in OxCal.

```
Plot()
 {
  Sequence("Washington fault OxCal Model, Version 3")
  {
   Boundary("Sequence start");
   C_Date("OSLS2 17.1",-15091,1380);
   C_Date("OSLS4 13.1",-11071,1180);
   Zero_Boundary("1");
   Boundary("P2 earthquake");
   R_Date("R1 6540+/-340",5720,150);
   R_Date("R3 4350+/-80",3905,20);
   R_Date("R4 4220+/-100",3830,20);
   C_Date("OSLS1 4.2",-2211,270);
   R_Date("R2 1390+/-140",1480,70);
   Boundary("P1 earthquake");
   Zero_Boundary("2");
   Boundary("Begin historical record",1847 AD);
   C_Date("2011",2011,0);
  };
  Page( );
  Difference("P2-P1", "P2", "P1");
  Difference("MRE elapse time", "2011", "P1");
 };
```

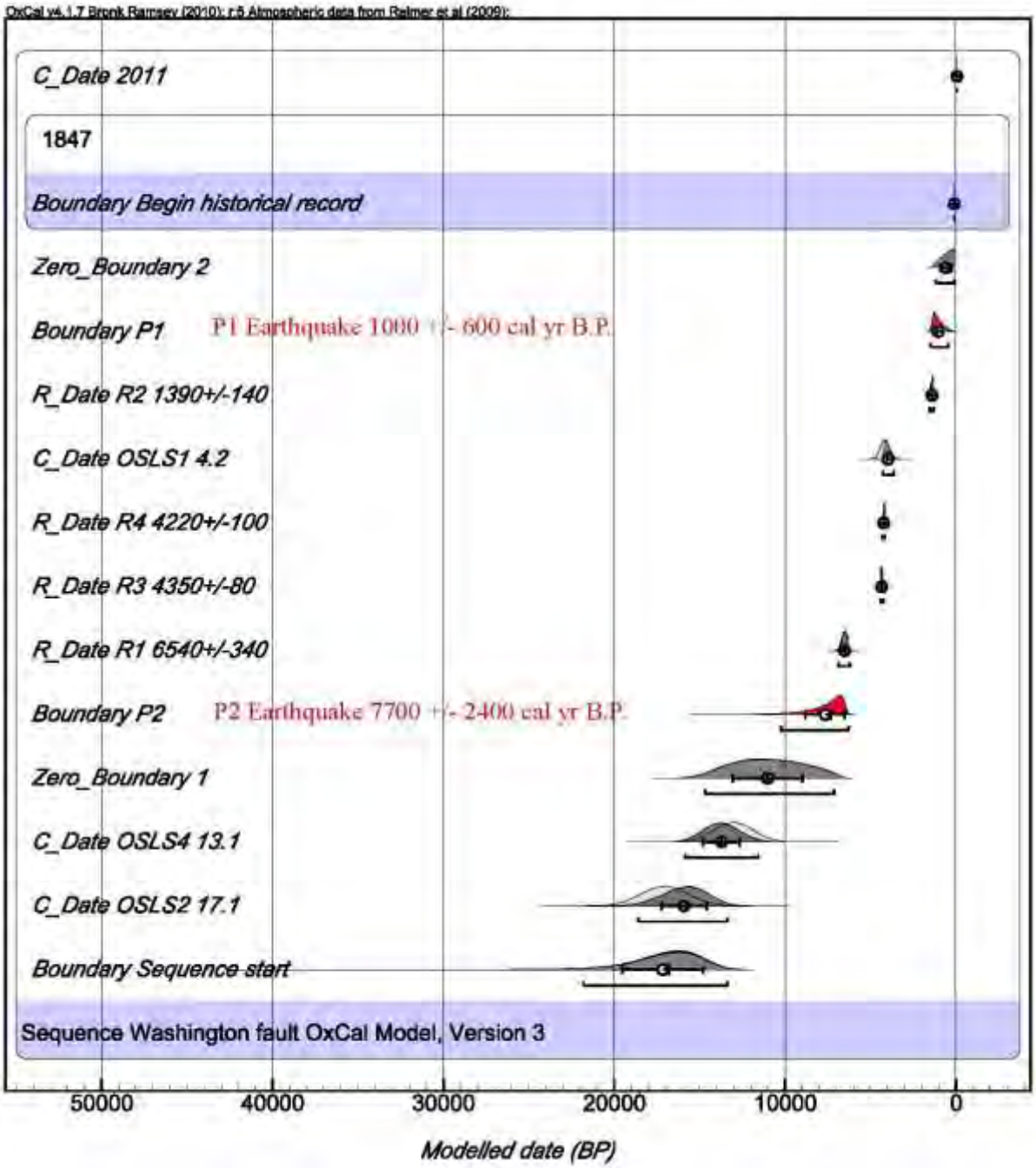

Stratigraphic ordering and age controls for the Dutchman Draw site using OxCal v. 4.1.7 (Bronk Ramsey, 2010) and the IntCal09—Northern Hemisphere calibration curve of Reimer and others (2009). Probability density functions are for radiocarbon and luminescence ages and the modeled paleoearthquake time ranges (two-sigma). Light gray shaded areas represent pre-modeling distributions; dark-gray areas represent modeled distributions using stratigraphic ordering information. Horizontal bars show two-sigma age ranges for post-modeling distributions.

LONG-TERM VERTICAL SLIP-RATE ESTIMATES FROM DISPLACED MAFIC VOLCANIC FLOWS, FORT PEARCE AND SULLIVAN DRAW SECTIONS, WASHINGTON FAULT ZONE, MOHAVE COUNTY, ARIZONA

by

William R. Lund and Tyler R. Knudsen

CONTENTS

ABSTRACT....126
INTRODUCTION....127
Purpose and Scope of Work....127
Geologic Setting....127
Previous Investigations....127
GEOCHEMISTRY....128
^{40}AR/^{39}AR RADIOMETRIC AGES....128
VOLCANIC FLOW CORRELATION....129
VERTICAL SLIP-RATE ESTIMATES....130
DISCUSSION....131
CONCLUSIONS....132
ACKNOWLEDGEMENTS....133
REFERENCES....133

FIGURES

Figure 1. Mafic volcanic flow remnants along the southern part of the Fort Pearce section and northern end of the Sullivan Draw section of the Washington fault zone, Mohave County, Arizona....135
Figure 2. Classification of mafic volcanic rock samples collected along the southern part of the Fort Pearce section and northern end of the Sullivan Draw section of the Washington fault zone, Mohave County, Arizona....136
Figure 3. Sections of the Hurricane and Washington fault zones....137

TABLES

Table 1. Radiometric ages available for mafic volcanic flows along southern part of the Fort Pearce section and northern end of the Sullivan Draw section of the Washington fault zone in Arizona prior to this investigation.... 138
Table 2. Newly acquired ^{40}Ar/^{39}Ar radiometric ages for mafic volcanic flows along the southern part of the Fort Pearce section and northern end of the Sullivan Draw section of the Washington fault zone. 138
Table 3. Long-term vertical-slip-rate estimates for southern part of the Fort Pearce section and northern end of the Sullivan Draw section of the Washington fault zone in Arizona determined from displaced volcanic flows....139

APPENDICES

Appendix – A Geochemical analyses of mafic volcanic rock samples from the footwall and hanging wall of the Washington fault zone, Mohave County, Arizona....140
Appendix – B Variation diagrams of mafic volcanic rock samples from the footwall and hanging wall of the Washington fault zone, Mohave County, Arizona....143

Appendix – C $^{40}Ar/^{39}Ar$ radiometric ages of mafic volcanic rock samples from the footwall and hanging wall of the Washington fault zone, Mohave County, Arizona.....147

ABSTRACT

The Utah Geological Survey conducted an investigation of mafic volcanic flow remnants along the southern part of the Fort Pearce section and extreme northern end of the Sullivan Draw section of the Washington fault zone in Arizona. The purpose of the investigation was to determine if flow remnants on the upthrown and downthrown sides of the sections are geochemically (trace elements and major oxides) correlative, and if so, obtain radiometric ages ($^{40}Ar/^{39}Ar$) for the correlative remnants and combine the new age information with flow displacement estimates to calculate long-term (early to middle Quaternary) vertical slip rates for the sections. New long-term slip-rate estimates will help improve seismic source zone characterization models for the fault sections, and provide important information for future probabilistic seismic hazard analyses in southwestern Utah and northwestern Arizona.

Earlier workers speculated that some or all of the volcanic flows along the Fort Pearce (formerly Northern) and Sullivan Draw sections of the Washington fault zone in northern Arizona are correlative across the fault. The close physical proximity of displaced flow remnants permits little doubt that the Seegmiller Mountain and East Mesa flows are displaced by the Sullivan Draw and Fort Pearce (Dutchman Draw strand) sections, respectively; however, evidence that other flows are correlative across the fault has been lacking. Our new geochemical analyses, radiometric ages, and geologic mapping provide evidence that a likely correlation exists across the fault between either the East or West Mesa flows (but not both) and the Dutchman Draw-1 flow remnant. A possible correlation also exists between the Seegmiller Mountain flow and the Dutchman Draw-2 flow remnant. The correlation with the Dutchman Draw-1 remnant captures the vertical slip across the entire Fort Pearce section (main, Mokaac, and Dutchman Draw strands). The displaced northwestern end of the East Mesa flow provides a vertical-slip-rate estimate for only one splay of the multi-splay Dutchman Draw strand. The southwestern end of the Seegmiller Mountain flow is displaced across the Sullivan Draw section, and provides a vertical-slip-rate estimate for the extreme northern end of that section.

The correlation of the East and West Mesa flows with the Dutchman Draw-1 flow remnant resulted in vertical-slip-rate estimates of 0.23 and 0.31 mm/yr, respectively. Only one of those estimates can be correct because the East and West Mesa flows are not correlative with each other. The possible correlation between the Seegmiller Mountain flow and the Dutchman Draw-2 flow remnant provides a vertical-slip-rate estimate for the main strand of the Fort Pearce section of 0.27 mm/yr. The vertical-slip-rate estimate for the Sullivan Draw section is 0.04 mm/yr, and the slip-rate estimate for one splay of the Dutchman Draw strand is also 0.04 mm/yr.

The composite long-term (middle Quaternary) vertical-slip-rate estimate for the Fort Pearce section of 0.23–0.31 mm/yr is generally compatible with the vertical slip rate determined from paleoseismic data at the Dutchman Draw trench site for the most recent closed seismic cycle on the main strand of the Fort Pearce section of 0.11–0.29 mm/yr (mean 0.20 mm/yr). The Seegmiller Mountain–Dutchman Draw-2 long-term vertical-slip-rate estimate for the main strand of the Fort Pearce section of 0.27 mm/yr also matches well with the Dutchman Draw trench site single seismic cycle rate. A long-term Fort Pearce-section slip rate of ~0.3 mm/yr is also generally compatible with the long-term vertical slip rate of the Shivwitz section of the Hurricane fault zone to the east.

INTRODUCTION

Purpose and Scope of Work

The Utah Geological Survey conducted an investigation of mafic volcanic flow remnants along the southern part of the Fort Pearce (formerly Northern; see Knudsen this volume) section and at the extreme northern end of the Sullivan Draw section of the Washington fault zone in Arizona (figure 1). The purpose of the investigation was to determine if the flow remnants on the upthrown and downthrown sides of the sections are correlative, and if so, combine that information with remnant age and displacement information to calculate long-term (early to middle Quaternary) vertical slip rates for the sections.

The investigation scope of work included:

- Collecting eight samples from selected flow remnants for geochemical analysis (appendix A), and analyzing the geochemical data using IgPet software to classify the remnants by rock type (figure 2) and establish potential geochemical correlations using trace element and major oxide variation diagrams (appendix B).

- Collecting four samples from the potentially correlative flow remnants for $^{40}Ar/^{39}Ar$ radiometric age analysis (appendix C).

- Combining the new and existing age information with flow displacement estimates to calculate long-term vertical-slip-rate estimates for the sections.

The resulting new long-term slip-rate estimates will improve seismic source zone characterization models for the fault sections, and provide important information for future probabilistic seismic hazard analyses in southwestern Utah and northwestern Arizona.

Geologic Setting

Lund (this volume) summarizes the general geologic setting of southwestern Utah and provides an overview of the Washington fault zone. Knudsen (this volume) provides details of the surficial geology along the Fort Pearce section, and more general information on the geology of the adjacent Sullivan Draw section. Readers interested in greater information about the geology of the Fort Pearce section are directed to those reports, and to the surficial geologic map and the reference lists accompanying them.

Figure 1 shows the relation of mafic volcanic flow remnants to the southern part of the Fort Pearce section and northern end of the Sullivan Draw section in Arizona. The figure also shows the locations of geochemical and radiometric age analyses conducted for this investigation, and the locations of previously existing flow remnant radiometric age information. It is important to note on figure 1 that cinder cone sources for the mafic volcanic flows are present on both the fault footwall and hanging wall.

Previous Investigations

Numerous workers (e.g., Hamblin and Best, 1970; Petersen, 1983; Billingsley and Workman, 2000; Billingsley and Graham, 2003) mapped mafic volcanic flows (figure 1) on both the southeast (upthrown) and northwest (downthrown) sides of the Fort Pearce section of the Washington fault zone in northern Arizona, and speculated that some of the volcanic flows are displaced by the Washington fault zone. Erosion of the soft sedimentary rocks on which the more resistant flows were extruded has left the flows as mostly isolated remnants capping hills and mesas (inverted topography) on both sides of the fault. Aerially extensive flow remnants cap Seegmiller Mountain (SF), West Mesa (WM), and East Mesa (EM) on the fault footwall. Smaller remnants either within or northwest of the fault zone on the fault hanging wall are present near Quail Draw (Quail Draw-1 [QD1] and Quail Draw-2 [QD2]), Joe Blake Hill (EM), Little Black Mountain (LBM), and at a cluster of low hills west of Dutchman Draw (Dutchman Draw-1 [DD1] and Dutchman Draw-2 [DD2]) (figure 1). The close physical proximity of displaced flow remnants permits little doubt that the Seegmiller Mountain and East Mesa flows are offset across the Sullivan Draw section and the Dutchman Draw strand of the Fort Pearce section, respectively; however, evidence that other flows are correlative across the fault has been lacking.

Recognizing the nature of the inverted topography created by the volcanic flows, Hamblin (1963, 1970) used the height of the flows above the current elevation of the Virgin River in the St. George basin as a proxy for flow age. Wenrich and others (1995) obtained a pair of K-Ar radiometric ages for the Seegmiller Mountain flow, and individual K-Ar ages for the Wolf Hole Mountain, Little Black Mesa, East Mesa, and West Mesa flows (figure 1, table 1). Downing and others (2001) obtained an $^{40}Ar/^{39}Ar$ total gas age for the Seegmiller Mountain flow, and an $^{40}Ar/^{39}Ar$ plateau age for the Quail Draw-1 flow remnant which they interpreted to be displaced Seegmiller Mountain flow.

GEOCHEMISTRY

We collected eight samples from mafic volcanic flows along the southern part of the Fort Pearce section and northern end of the Sullivan Draw section in Arizona for geochemical analysis (figure 1). The GeoAnalytical Lab at Washington State University (http://www.sees.wsu.edu/Geolab/index.html) analyzed the samples; results of the geochemical analyses are presented in appendix A.

Robert Biek (Utah Geological Survey, written communication, 2012) used the geochemical data to classify the rock types of the eight samples using the igneous rock classification system of LeBas and others (1986). Samples DD1, EM, QD1, and WM classify as trachybasalt and samples DD2, LBM, QD2, and SF classify as basalt (figure 2). Biek also plotted correlation diagrams to compare combinations of trace elements and major oxides (Rb vs. Sr, Sr vs. Zr, Ba vs. Cr, Nd vs. Nb, TiO_2 vs. P_2O_5, TiO_2 vs. SiO_2) between samples (appendix B). The correlation diagrams show a strong geochemical affinity between samples DD1, EM, and WM, and a possible affinity between samples DD2, QD1, and SF (R. Biek, Utah Geological Survey, written communication, 2012).

$^{40}AR/^{39}AR$ RADIOMETRIC AGES

We collected four samples for $^{40}Ar/^{39}Ar$ radiometric age analysis at locations EM, QD1, SF, and WM (figure 1). The New Mexico Geochronology Research Laboratory (http://geoinfo.nmt.edu/labs/argon/home.html) at the New Mexico Institute of Mining and Technology analyzed the samples; the resulting age estimates are shown in table 2. The sample analysis spectra are presented in appendix C.

Comparison of the new $^{40}Ar/^{39}Ar$ ages (table 2) with pre-existing radiometric ages (table 1) shows that:

1. The new $^{40}Ar/^{39}Ar$ age for the East Mesa flow is younger than but overlaps in time with the Wenrich and others (1995) K-Ar age for that flow.

2. The new $^{40}Ar/^{39}Ar$ age for the West Mesa flow is younger than and does not overlap in time with the Wenrich and others (1995) K-Ar age for that flow.

3. The new $^{40}Ar/^{39}Ar$ age for the Seegmiller Mountain flow is about 1.85 myr younger than the Downing and others (2001) $^{40}Ar/^{39}Ar$ age for that flow, but the new age does overlap in time with the two Wenrich and others (1995) K-Ar ages for the flow. The reason for the large discrepancy between the new and old $^{40}Ar/^{39}Ar$ ages for the Seegmiller Mountain flow is unknown.

4. The Downing and others (2001) $^{40}Ar/^{39}Ar$ age for the Quail Draw-1 flow remnant is about 540 kyr older than the newly acquired $^{40}Ar/^{39}Ar$ age for that flow, and the uncertainty limits for the two ages do not overlap.

VOLCANIC FLOW CORRELATION

Trace element and major oxide correlation diagrams (appendix B) show a strong geochemical affinity between the Dutchman Draw-1 flow remnant on the Fort Pearce section hanging wall and the East Mesa and West Mesa flows on the fault footwall (figure 1). Although less pronounced, the correlation diagrams also indicate a possible correlation between the Seegmiller Mountain flow on the fault footwall and the Dutchman Draw-2 and Quail Draw-1 flow remnants on the fault hanging wall (R. Biek, Utah Geological Survey, written communication, 2012) (figure 1).

The $^{40}Ar/^{39}Ar$ and K-Ar radiometric ages available for the volcanic flows (tables 1 and 2) provide additional insight regarding flow correlations across the fault. Although the East and West Mesa flows have a strong geochemical affinity and overlapping K-Ar ages, the new $^{40}Ar/^{39}Ar$ ages for those flows are significantly different, and their uncertainty limits do not overlap. Billingsley and Graham (2003) mapped the geology of lower Hurricane Wash and vicinity, and showed that the East and West Mesa flows are sourced from different volcanic centers. Similar geochemistry but significantly different ages for the two flows implies that the flows were likely derived from the same magma source, but were erupted at different times (as much as 60 kyr apart). Therefore, we conclude that the East and West Mesa flows are separate geologic units and are not directly correlative. A radiometric age is not available for the Dutchman Draw-1 flow remnant to help define its relation to the East and West Mesa flows. The Dutchman Draw-1 remnant is geochemically similar to both the East and West Mesa flows,

but in the absence of a radiometric age to further clarify the relation, the remnant could correlate with either flow, but not with both.

Geochemistry is also permissive of a possible correlation between the Seegmiller Mountain flow on the fault footwall, and the Quail Draw-1 and Dutchman Draw-2 flow remnants on the fault hanging wall (R. Biek, Utah Geological Survey, written communication, 2012) (appendix B). However, neither the K-Ar ages nor the $^{40}Ar/^{39}Ar$ ages available for the Seegmiller Mountain flow overlap in time with the two Quail Draw-1 flow radiometric ages (tables 1 and 2). So once again, geochemistry shows that the flows likely share the same magma source, but their ages indicate that the flows were erupted at different times and are not directly correlative. The Dutchman Draw-2 flow remnant is geochemically similar to both the Seegmiller Mountain and Quail Draw-1 flows, but lacking a radiometric age to better define the correlation, the Dutchman Draw-2 remnant could be correlative with either of the former, but not both.

One splay of the multi-splay Dutchman Draw strand displaces the northwestern end of the East Mesa flow, and the Sullivan Draw section displaces the northwestern end of the Seegmiller Mountain flow (figure 1). In both instances, the displaced flows are closely adjacent to each other, and are clearly correlative.

Based on the geochemistry, radiometric ages, and geologic relations of the volcanic flows on the footwall and hanging wall of the Fort Pearce section in Arizona, we conclude that a likely correlation exists between either the East or West Mesa flows and the Dutchman Draw-1 flow remnant, and that possible correlation exists between either the Seegmiller Mountain or Quail Draw-1 flow and the Dutchman Draw-2 flow remnant (figure 1). The East/West Mesa – Dutchman Draw-1 correlation encompasses the entire vertical slip across the Fort Pearce section (main, Dutchman Draw, and Mokaac strands). The possible Seegmiller Mountain – Dutchman Draw-2 correlation encompasses the slip only on the main strand of the Fort Pearce section. A Quail Draw-1–Dutchman Draw-2 correlation provides no information on fault slip since both flow remnants are on the hanging wall of the Fort Pearce section main trace. The displaced northwestern end of the East Mesa flow provides only a partial slip rate for the Dutchman Draw strand of the Fort Pearce section, since the flow is only displaced across a single splay of the multi-splay strand. New UGS mapping (Knudsen this volume) shows that the southwestern end of the Seegmiller Mountain flow is displaced across the Sullivan Draw section, so the vertical-slip-rate estimate determined there applies to the entire section.

VERTICAL-SLIP-RATE ESTIMATES

New information on volcanic flow geochemistry, new and existing radiometric flow ages, and elevation data for displaced correlative flows allowed us to calculate vertical-slip-rate estimates for the Washington fault zone in northern Arizona (table 3). We obtained elevation data for the displaced flows from Google Earth color aerial imagery dated 10/2/2011. Elevations from Google Earth were obtained in feet and converted to meters; the resulting elevation in meters was then rounded to the nearest 10 m (table 3). The locations where we measured flow elevations were (1) carefully evaluated on aerial imagery (chiefly Google Earth color and black-and-white aerial photographs of multiple vintages) to avoid areas of landsliding or other topographic complications, and (2) the closest suitable points on the flow remnants to each other.

The horizontal distances separating some of the correlated points are measured in multiple kilometers (table 3). Based on new geologic mapping (Knudsen this volume), the flows originated in the east and flowed downslope to the west prior to faulting. Our vertical-slip-rate estimates do not take into account the effect of pre-faulting topography (i.e., the original elevation difference between our measuring points due to downslope flow movement). We have no way of determining the original pre-faulting elevation difference between our flow measuring points; however, we recognize that in some instances, the difference may amount to hundreds of meters, which would tend to make our vertical-slip-rate estimates maximum values. We also have no information regarding whether the flows cascaded over a pre-existing fault escarpment. For purposes of our calculations we assume that they did not. Conversely, the onset of surface faulting that displaced the flows began after an unknown period of time, possibly thousands to tens of thousands of years, after eruption of the flows. If the interval between flow eruption (age of the flow) and onset of faulting was significantly long, the shorter period of time over which displacement actually occurred would tend to make the slip-rate estimates minimum values since the estimates are based on flow age, not the interval since faulting commenced. The extent to which these affects may balance each other is unknown.

We calculated five long-term, vertical-slip-rate estimates for the Washington fault zone: two "composite" rates that incorporate the main, Mokaac, and Dutchman Draw strands of the Fort Pearce section (only one of which can be correct – see discussion in Volcanic Flow Correlation section above), one rate across only the main trace of the Fort Pearce section, one rate at the extreme northern end of the Sullivan Draw section, and a rate for one splay of the multiple-splay Dutchman Draw strand of the Fort Pearce section (table 3). The two composite vertical-slip-rate estimates for the Fort Pearce section are 0.23 and 0.31 mm/yr (only one correct, and both maximum estimates). The rate for the main strand of the Fort Pearce section is 0.27 mm/yr. The vertical-slip-rate estimate for the Sullivan Draw section is 0.04 mm/yr, significantly lower than the estimates for the adjacent Fort Pearce section. Because the Seegmiller Mountain flow remnants displaced across the Sullivan Draw section are directly adjacent to each other, the effect of downslope movement of the flow prior to faulting is negligible. The low Sullivan Draw slip rate may indicate that (1) slip on the Sullivan Draw section is generally lower than on the Fort Pearce section (Knudsen this volume), (2) slip dies out rapidly at the end of the section, but may be higher farther south on the section, or (3) fault drag or other unrecognized near-fault perturbation may be affecting the rate. The slip rate for the Dutchman Draw strand is also 0.04 mm/yr, but is limited to a single splay of that multi-splay strand, and therefore does not represent all of the slip across that strand. Again, the close proximity of the flow remnants on either side of the fault makes the effect of pre-faulting topography negligible.

DISCUSSION

The Fort Pearce section of the Washington fault zone lies several kilometers west of and generally parallel to the Shivwits section of the Hurricane fault (figure 3). Amoroso and others (2004) used the displaced Moriah Knoll basalt flow to calculate a maximum middle Quaternary (0.85 Ma) vertical slip rate of 0.15 to 0.25 mm/yr for the Shivwits section. Lund and others (2007) determined long-term vertical slip rates for the Ash Creek and Anderson Junction sections of the Hurricane fault (figure 3) from displaced volcanic flows; middle Quaternary (0.63 – 1.08 Ma) slip rates ranged from 0.37 to 0.57 mm/yr, and a late Quaternary (0.353 Ma) vertical slip rate from a displaced flow on the Anderson Junction section yielded a vertical slip rate of

0.21 mm/yr. Displacement increases northward on the Hurricane fault, so slip rates also increase in that direction, hence the generally higher long-term vertical slip rates for the Ash Creek (northern) and Anderson Junction (middle) sections than those for the Shivwits (southern) section.

The vertical slip rates reported by Amoroso and others (2004) and Lund and others (2007) were for individual sections of the Hurricane fault. Each of those sections (Shivwits, Ash Creek, and Anderson Junction) is from tens to hundreds of meters wide depending on fault complexity, but all three are generally discrete, north-trending fault traces without significant branches or other major perturbations along their length. Such is not the case for the Fort Pearce section of the Washington fault zone. The Sullivan Draw section and the main strand of the Fort Pearce section share a common boundary and form a generally linear, north-trending combined fault trace. However, the Mokaac and Dutchman Draw strands of the Fort Pearce section are both northeast trending and branch from the Fort Pearce section main strand at different points, creating subparallel relations with the main strand over most of their lengths (figure 3). The distribution and age of volcanic flows displaced across the Fort Pearce section allowed us to obtain a composite vertical-slip-rate estimate for the Fort Pearce section (main, Mokaac, and Dutchman Draw strands), a rate for the main strand of the Fort Pearce section only, and a rate for one splay of the Dutchman Draw strand. The individual long-term vertical slip rates for the three strands of the Fort Pearce section must be lower than the section's long-term combined rate. However, available data are not sufficient to determine how slip is partitioned among the three Fort Pearce section strands. It is instructive to note that the vertical slip rate determined from paleoseismic data for the most recent seismic cycle on the Fort Pearce section main strand is 0.11–0.29 mm/yr (Lund and others this volume), which brackets the long-term (middle Quaternary) rate determined for the Fort Pearce section main strand from displaced volcanic flows (table 3). Therefore, the single seismic cycle vertical slip rate resulting from the two Holocene surface-rupturing earthquakes on the Fort Pearce section main strand may be close to the long-term average slip rate for the main strand of the Fort Pearce section.

CONCLUSIONS

The principal conclusions resulting from this investigation of long-term vertical slip rates determined from displaced volcanic flows along the Fort Pearce and Sullivan Draw sections of the Washington fault zone include the following:

1. New information on trace element and major oxide geochemistry combined with new and existing radiometric flow ages allowed correlation of some mafic volcanic flows across the Washington fault zone in Arizona. Elevation differences obtained from Google Earth imagery for the correlated flows displaced across the fault, combined with the flow ages permitted calculation of five vertical-slip-rate estimates for the Fort Pearce and Sullivan Draw sections. The estimates include two composite slip rates across the main, Mokaac, and Dutchman Draw strands of the Fort Pearce section (0.23 and 0.31 mm/yr [only one correct – see Discussion section]), a rate across the main trace of the Fort Pearce section (0.27 mm/yr), a rate for the northern end of the Sullivan Draw section (0.04 mm/yr), and a rate across one splay of the multi-splay Dutchman Draw strand (0.04 mm/yr).

2. The vertical-slip-rate estimates do not account for differences in elevation between displaced flow remnants due to pre-faulting topography. In instances where flows traveled long distances downslope following their eruption, the pre-faulting elevation difference between flow remnants may have amounted to hundreds of meters. Differences in pre-fault topography would tend to make the vertical-slip-rate estimates maximum values. It is unknown if some flows cascaded across pre-existing fault scarps.

3. Timing of the onset of surface faulting following eruption of the volcanic flows is unknown, but was possibly thousands to tens of thousands of years after emplacement of the flows, which would tend to make the slip-rate estimates minimum values.

4. Vertical-slip-rate estimates determined from displaced volcanic flows along the Fort Pearce section of the Washington fault zone show that the long-term (middle Quaternary) vertical slip rate on the Fort Pearce section has likely been ~ 0.3 mm/yr. The long-term vertical slip rate estimate for the Fort Pearce section is roughly comparable with the vertical slip rate reported by Amoroso and others (2004) for the Shivwits section of the Hurricane fault, and about a factor of 1.5 smaller than the middle Quaternary slip rates reported by Lund and others (2008) for the Anderson Junction and Ash Creek sections of the Hurricane fault.

ACKNOWLEDGMENTS

We thank Robert Biek, UGS Geologic Mapping Program, for classifying the mafic volcanic rock samples collected along the southern part of the Fort Pearce section and northern end of the Sullivan Draw section, and for preparing the variation diagrams for those rock samples which allowed us to correlate volcanic flows across the Washington fault zone.

REFERENCES

Amoroso, L., Pearthree, P.A., and Arrowsmith, J.R., 2004, Paleoseismology and neotectonics of the Shivwits section of the Hurricane fault, northwestern Arizona: Bulletin of the Seismological Society of America, v. 94, no. 5, p. 1919-1942, doi: 10.1785/012003241.

Billingsley, G.H., and Graham, S.E., 2003, Geologic map of the lower Hurricane Wash and vicinity, Mojave County, northwestern Arizona: U.S. Geological Survey Miscellaneous Field Studies Map 2396, scale 1:31,680, available at <http://pubs.usgs.gov/mf/2003/2396/>.

Billingsley, G.H., and Workman, J.B., 2000, Geologic map of the Littlefield 30' x 60' quadrangle, Mojave County, northwestern Arizona: U.S. Geological Survey Geologic Investigations Series Map I-2628, scale 1:100,000, available at <http://pubs.usgs.gov/imap/i2628/>.

Downing, R.F., Smith, E.I., Orndorff, R.L., Spell, T.L., and Zanetti, K.A., 2001, Imaging the Colorado Plateau – Basin and Range transition zone using basalt geochemistry, geochronology, and geographic information systems, *in* Erskine, M.C., Faulds, J.E.,

Bartley, J.M., and Rowley, P.D., editors, The geologic transition, High Plateaus to Great Basin—a symposium and field guide (The Mackin Volume): Utah Geological Association and Pacific Section of the American Association of Petroleum Geologists, Utah Geological Association Publication 30, p. 127-154.

Hamblin, W.K., 1963, Late Cenozoic basalts of the St. George basin, Utah, *in* Heylmun, E.B., editor, Geology of the southwestern transition between the Basin-Range and Colorado Plateau, Utah: Intermountain Association of Petroleum Geologists, Guidebook to the Geology of Southwestern Utah, p. 84-89.

Hamblin, W.K., 1970, Late Cenozoic basalt flows of the western Grand Canyon, *in* Hamblin, W.K., and Best, M.G., editors, The western Grand Canyon region: Utah Geological Society Guidebook to the Geology of Utah, no. 23, p. 21-37.

Hamblin, W.K., and Best, M.G., 1970, Road log, *in* Hamblin, W.K., and Best, M.G., editors, The western Grand Canyon region: Utah Geological Society Guidebook to the Geology of Utah, no. 23, p. 93-153.

LeBas, M.J., LeMaitre, R.W., Streckeisen, A., and Zanettin, B., 1986, A chemical classification of volcanic rocks based on the total alkali-silica diagram: Journal of Petrology, v. 27, p. 745-750.

Lund, W.R., Hozik, M.J., and Hatfield, S.C., 2007, Paleoseismology of Utah Volume 14—Paleoseismic investigation and long-term slip history of the Hurricane fault in southwestern Utah: Utah Geological Survey Special Study 119, available online at < http://ugspub.nr.utah.gov/publications/special_studies/SS-119.pdf>.

Peterson, S.M., 1983, The tectonics of the Washington fault zone, northern Mohave County, Arizona: Brigham Young University Geology Studies, v. 30, part 1, p. 83-94.

Wenrich, K.J., Billingsley, G.H., and Blackerby, B.A., 1995, Spatial migration and compositional changes of Miocene-Quaternary magmatism in the Western Grand Canyon: Journal of Geophysical Research, v. 100, p. 10,417-10,440.

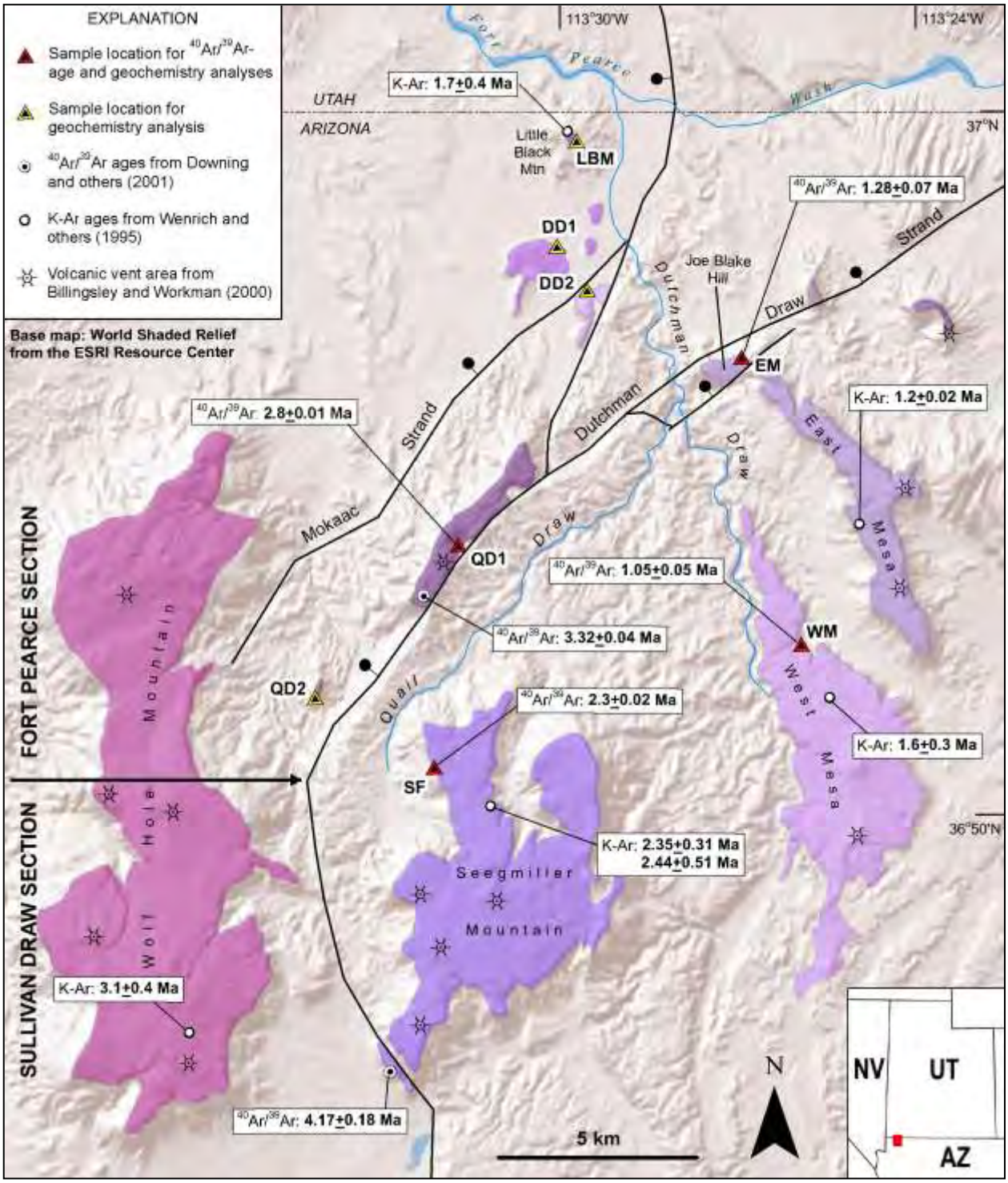

Figure 1. *Mafic volcanic flow remnants along the southern part of the Fort Pearce section and northern end of the Sullivan Draw section of the Washington fault zone, Mohave County, Arizona.*

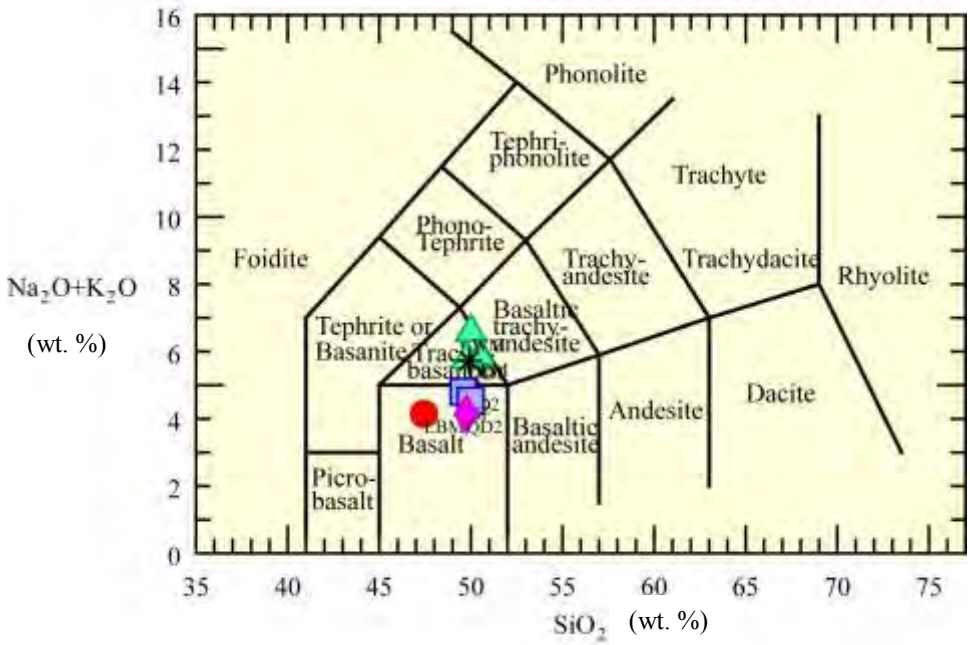

Figure 2. *Classification of mafic volcanic rock samples collected along the southern part of the Fort Pearce section and northern end of the Sullivan Draw section of the Washington fault zone, Mohave County, Arizona (after LeBas and others, 1986).* ▲ *= DD1, EM, WM;* ◆ *=QD2;* ■ *= DD2, SF;* ● *= LBM;* ✱ *= QD1*

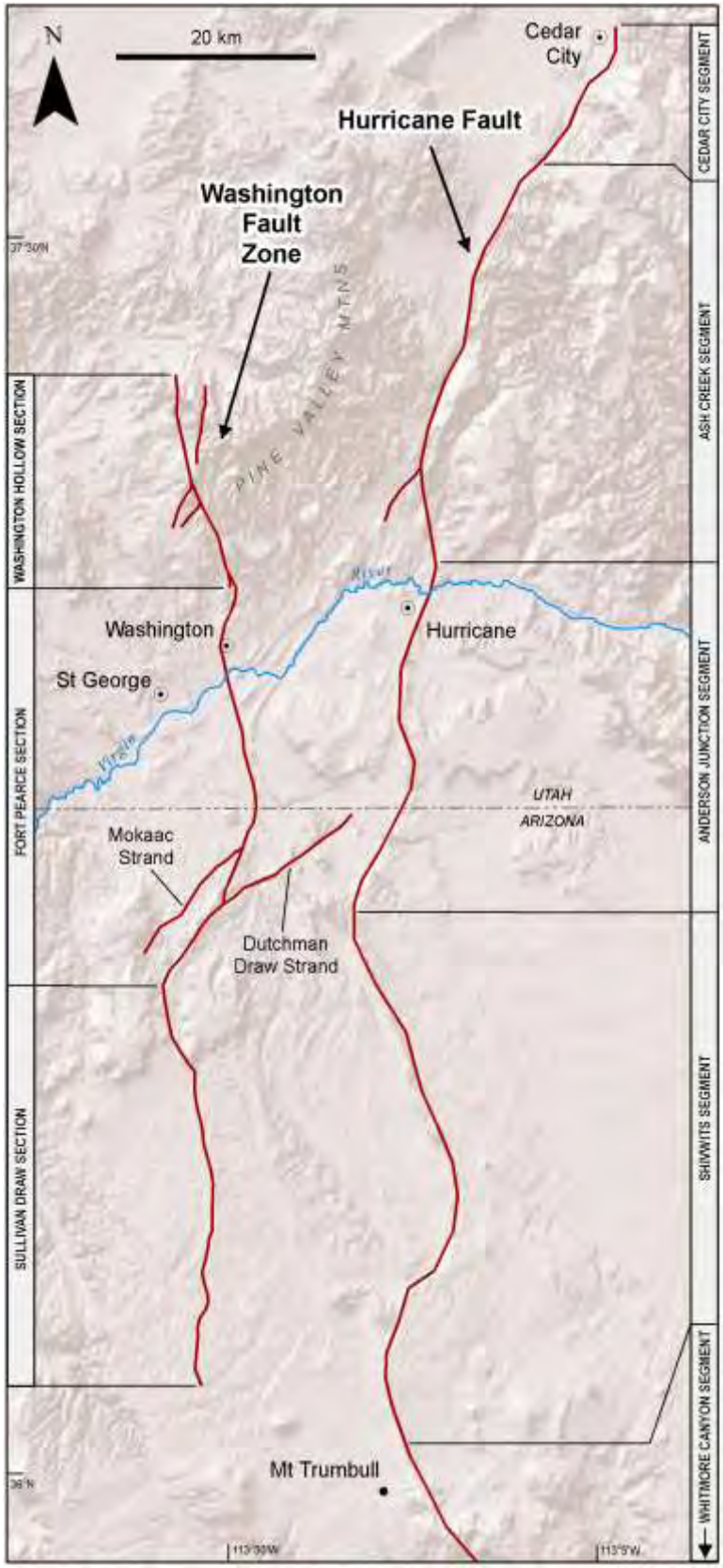

Figure 3. *Sections of the Hurricane and Washington (after Knudsen, this volume) fault zones.*

Table 1. *Radiometric ages available for mafic volcanic flows along southern part of the Fort Pearce section and northern end of the Sullivan Draw section of the Washington fault zone in Arizona prior to this investigation.*

Location[1]	Radiometric age (Ma)	Reference
East Mesa flow	1.4 ± 0.25 (K-Ar)	Wenrich and others (1995)
West Mesa flow	1.6 ± 0.3 (K-Ar)	Wenrich and others (1995)
Little Black Mountain flow	1.7 ± 0.4 (K-Ar)	Wenrich and others (1995)
Seegmiller Mountain flow	2.35 ± 0.31 and 2.44 ± 0.51 (K-Ar)	Wenrich and others (1995)
Wolf Hollow Mountain flow	3.1 ± 0.4 (K-Ar)	Wenrich and others (1995)
Quail Draw-1 flow	3.32 ± 0.04 ($^{40}Ar/^{39}Ar$)	Downing and others (2001)
Seegmiller Mountain flow	4.17 ± 0.18 ($^{40}Ar/^{39}Ar$)	Downing and others (2001)

[1]*See figure 1 for flow locations.*

Table 2. *Newly acquired $^{40}Ar/^{39}Ar$ radiometric ages for mafic volcanic flows along the southern part of the Fort Pearce section and northern end of the Sullivan Draw section of the Washington fault zone.*

Sample[1]	Location	$^{40}Ar/^{39}Ar$ Age[2] (Ma)
EM	East Mesa flow	1.211 ± 0.015
WM	West Mesa flow	1.05 ± 0.05
SF	Seegmiller Mountain flow	2.32 ± 0.02
QD1	Quail Draw-1 flow	2.779 ± 0.017

[1] *See figure 1 for sample locations .*[2]*Age analyses performed by the New Mexico Geochronology Research Laboratory – see appendix C.*

Table 3. *Long-term vertical-slip-rate estimates for southern part of the Fort Pearce section and northern end of the Sullivan Draw section of the Washington fault zone in Arizona determined from displaced volcanic flows.*

Correlated Flows	Elev. A[1] (m)	Elev. B[1] (m)	Elevation Difference (m)	Horizontal Distance[2] (km)	Radiometric Age[3] (Ma)	Vertical Slip Rate (mm/yr)	Vertical Slip Across
Seegmiller Mountain Flow – Dutchman Draw-2 Flow Remnant	1650	1020	630	9.2	2.32 ± 0.02	0.27[4]	Fort Pearce section main strand
West Mesa Flow– Dutchman Draw-1 Flow Remnant	1270	940	330	7.9	1.05 ± 0.05	0.31[4]	Fort Pearce section composite
East Mesa Flow – Dutchman Draw-1 Flow Remnant	1220	940	280	6.3	1.211 ± 0.015	0.23[4]	Fort Pearce section composite
East Mesa Flow – East Mesa Flow	1220	1170	50	Adjacent	1.211 ± 0.015	0.04	Dutchman Draw strand single splay
Seegmiller Mountain Flow - Seegmiller Mountain Flow	1800	1710	90	Adjacent	2.32 ± 0.02	0.04	Sullivan Draw section

[1]*Elevation obtained in feet from Google Earth imagery dated 10/2/2011. We converted elevations in feet to meters by dividing the elevations by 3.2808 feet and rounded the result to the nearest 10 m.* [2]*Straight line distance measured on Google Earth imagery dated 10/2/2011.* [3]*New* $^{40}Ar/^{39}Ar$ *radiometric ages obtained for this study (see appendix C). See table 1 for older radiometric ages available for some flows.* [4]*Horizontal distances between these correlated points are measured in multiple kilometers. Based on geologic mapping, the flows are thought to have originated in the east and then to have flowed downslope to the west prior to faulting. The reported slip rates do not take into account the effect of pre-faulting topography (i.e., original elevation difference between the two points due to the pre-faulting topography), so we consider the slip rates reported here to be maximum values. It is also assumed, but cannot be confirmed, that the flows did not cascade over a pre-existing fault escarpment.*

APPENDIX A

GEOCHEMICAL ANALYSES OF MAFIC VOLCANIC ROCK SAMPLES FROM THE FOOTWALL AND HANGING WALL OF THE WASHINGTON FAULT ZONE, MOHAVE COUNTY, ARIZONA

(Analyses performed by the GeoAnalytical Laboratory at Washington State University)

See figure 1 for sample locations

Geochemical analysis performed by the GeoAnalytical Lab at Washington State University (http://www.sees.wsu.edu/Geolab/index.html)

OXIDE/ELEMENT	SAMPLES							
	LBM	DD1	DD2	EM	WM	QD1	SF	QD2
Unnormalized Major Elements (Weight %):								
SiO2	46.55	48.00	48.74	49.39	49.30	49.18	49.41	49.35
TiO2	2.063	2.012	1.772	1.965	2.071	1.775	1.591	1.717
Al2O3	12.06	16.58	15.75	17.92	17.50	16.06	15.70	14.20
FeO*	10.93	9.40	11.11	9.27	9.60	9.69	11.26	10.47
MnO	0.181	0.152	0.172	0.157	0.155	0.163	0.176	0.173
MgO	12.57	5.15	7.88	4.56	4.76	7.33	8.11	9.74
CaO	10.29	9.77	8.79	9.05	8.90	9.10	8.86	10.09
Na2O	2.71	3.57	3.42	3.58	4.26	3.93	3.44	2.97
K2O	1.35	1.98	1.30	2.12	2.21	1.71	1.04	1.13
P2O5	0.502	0.712	0.441	0.694	0.778	0.555	0.357	0.392
Sum	99.21	97.33	99.38	98.71	99.54	99.48	99.94	100.24
SO3 >/=	0.00	0.17	0.06	0.00	0.00	0.01	0.00	0.00
Normalized Major Elements (Weight %):								
SiO2	46.92	49.32	49.04	50.03	49.53	49.43	49.44	49.23
TiO2	2.079	2.068	1.783	1.991	2.080	1.784	1.592	1.713
Al2O3	12.15	17.04	15.85	18.16	17.58	16.14	15.71	14.17
FeO*	11.02	9.66	11.18	9.39	9.64	9.74	11.27	10.44
MnO	0.183	0.156	0.173	0.159	0.155	0.164	0.176	0.173
MgO	12.67	5.29	7.93	4.62	4.79	7.37	8.11	9.72
CaO	10.38	10.04	8.85	9.17	8.94	9.14	8.86	10.07
Na2O	2.74	3.67	3.44	3.63	4.27	3.95	3.44	2.96
K2O	1.37	2.03	1.31	2.15	2.22	1.72	1.04	1.13
P2O5	0.506	0.732	0.444	0.703	0.781	0.558	0.357	0.392
Total	100.00	100.00	100.00	100.00	100.00	100.00	100.00	100.00
Unnormalized Trace Elements (ppm):								
Ni	358	46	150	14	27	95	142	160
Cr	736	80	250	11	23	276	304	597
Sc	28	23	23	22	22	25	26	29
V	245	202	202	211	206	211	207	238
Ba	705	1057	749	688	780	619	789	626
Rb	24	24	14	24	26	18	13	19
Sr	591	930	609	902	940	750	480	469
Zr	190	234	167	239	251	213	142	159
Y	23	25	22	26	26	22	22	24
Nb	49.2	42.0	29.9	46.3	45.6	45.0	22.8	32.3
Ga	17	22	21	21	22	21	21	18
Cu	91	41	67	38	41	67	60	77
Zn	94	93	109	90	97	95	105	90
Pb	5	6	5	8	7	8	4	5
La	40	45	26	48	49	39	23	32
Ce	74	90	53	80	98	78	51	59
Th	5	5	3	7	6	6	4	5
Nd	32	42	24	36	45	31	22	25
U	3	2	2	1	2	2	3	2
sum tr.	3308	3008	2527	2510	2712	2620	2441	2666
in %	0.33	0.30	0.25	0.25	0.27	0.26	0.24	0.27
sum m+tr	99.54	97.63	99.63	98.96	99.81	99.75	100.18	100.50
M+Toxides	99.64	97.69	99.69	99.02	99.87	99.81	100.24	100.58
***Major elements are normalized on a volatile-free basis, with total Fe expressed as FeO.**								

NiO	455.3	58.2	191.4	17.8	34.5	120.5	181.1	203.7
Cr2O3	1076.2	116.5	365.0	15.8	33.2	404.0	443.9	873.1
Sc2O3	42.9	34.7	35.1	34.4	33.7	37.7	39.7	44.5
V2O3	359.7	297.2	297.6	310.7	302.9	310.3	304.2	349.4
BaO	786.7	1180.0	836.3	767.7	870.4	690.6	880.6	698.9
Rb2O	26.2	25.7	15.1	26.4	28.0	19.2	14.4	20.8
SrO	698.4	1099.5	720.6	1066.6	1111.5	886.5	568.0	554.5
ZrO2	256.0	316.6	225.6	322.2	339.2	287.3	192.1	214.6
Y2O3	29.2	32.1	28.1	32.4	32.5	28.3	28.1	30.1
Nb2O5	70.4	60.1	42.8	66.2	65.2	64.4	32.6	46.2
Ga2O3	23.4	29.6	28.0	27.6	29.8	28.8	27.7	24.6
CuO	114.4	50.8	84.1	46.9	51.4	83.7	75.6	96.1
ZnO	117.4	117.0	136.9	112.1	121.7	118.7	131.9	113.1
PbO	5.1	6.4	5.6	8.2	7.3	8.1	4.5	5.2
La2O3	46.8	52.8	30.8	55.8	57.7	46.2	26.9	37.1
CeO2	91.3	110.3	64.5	98.5	120.7	96.3	62.7	72.9
ThO2	5.2	6.0	3.4	7.6	6.1	7.1	4.0	6.0
Nd2O3	36.7	49.1	27.8	42.5	51.9	36.2	25.8	28.8
U2O3	3.3	1.8	2.3	1.3	2.1	2.2	2.8	2.1
Cs2O	0.0	0.0	0.0	0.0	0.0	0.0	0.0	0.0
As2O5	0.0	0.0	0.0	0.0	0.0	0.0	0.0	0.0
W2O3	0.0	0.0	0.0	0.0	0.0	0.0	0.0	0.0
sum tr.	4245	3644	3141	3061	3300	3276	3046	3422
in %	0.42	0.36	0.31	0.31	0.33	0.33	0.30	0.34

APPENDIX B
VARIATION DIAGRAMS FOR MAFIC VOLCANIC ROCK SAMPLES FROM THE FOOTWALL AND HANGING WALL OF THE WASHINGTON FAULT ZONE, MOHAVE COUNTY, ARIZONA

(Diagrams prepared by R.F. Biek, UGS, using IgPet software by Terra Soft, Inc.)

See figure 1 for sample locations

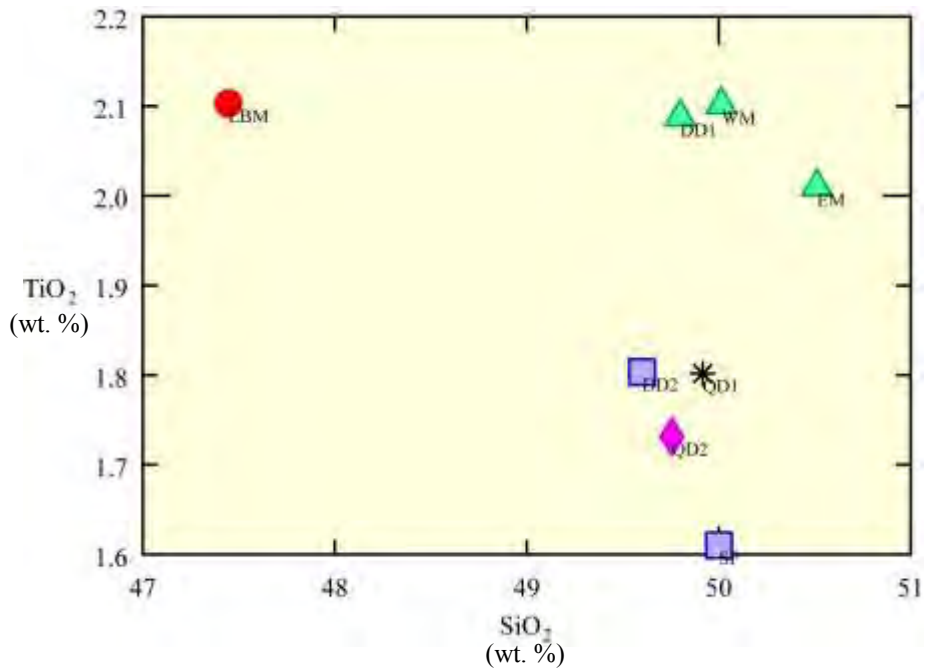
2.2
2.1
2.0
1.9
1.8
1.7
1.6
TiO2
(wt. %)
LBM
DD1
WM
EM
DD2
QD1
QD2
SI
47
48
49
50
51
SiO2
(wt. %)

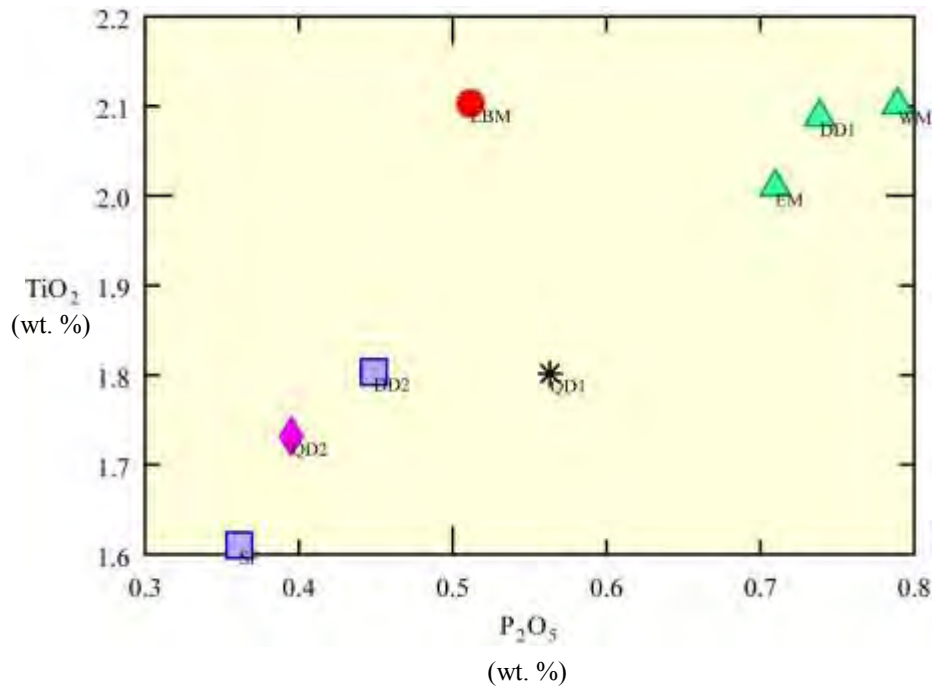
2.2
2.1
2.0
1.9
1.8
1.7
1.6
TiO2
(wt. %)
LBM
DD1
WM
EM
DD2
QD1
QD2
SI
0.3
0.4
0.5
0.6
0.7
0.8
P2O5
(wt. %)

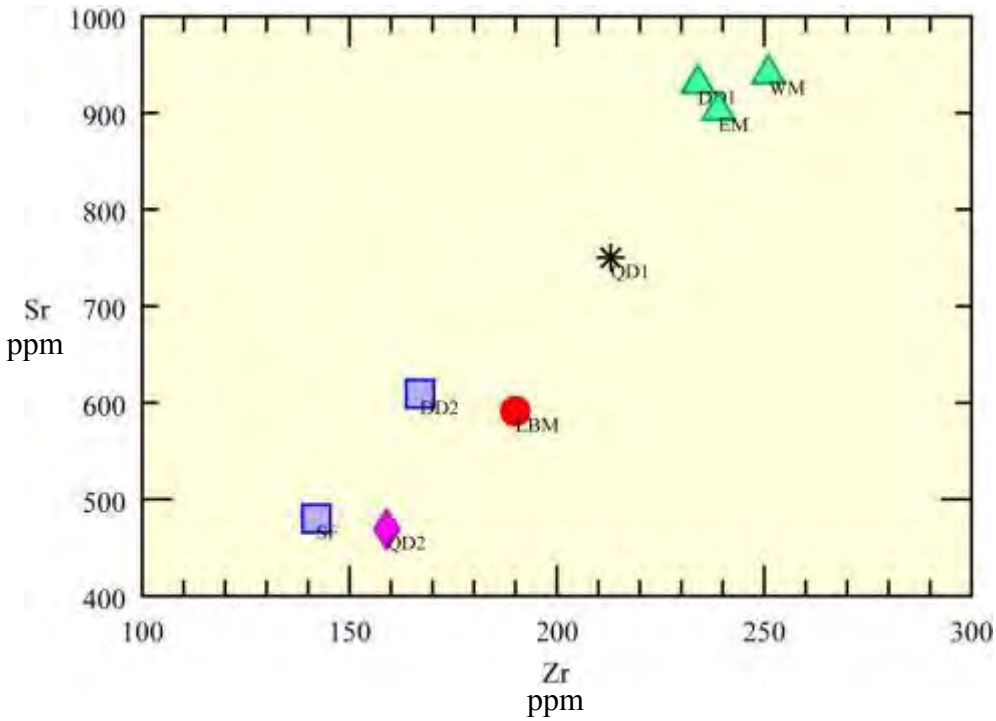
1000
900
800
700
600
500
400
Sr
ppm
100
150
200
250
300
Zr
ppm
WM
DD1
EM
QD1
DD2
LBM
SI
QD2

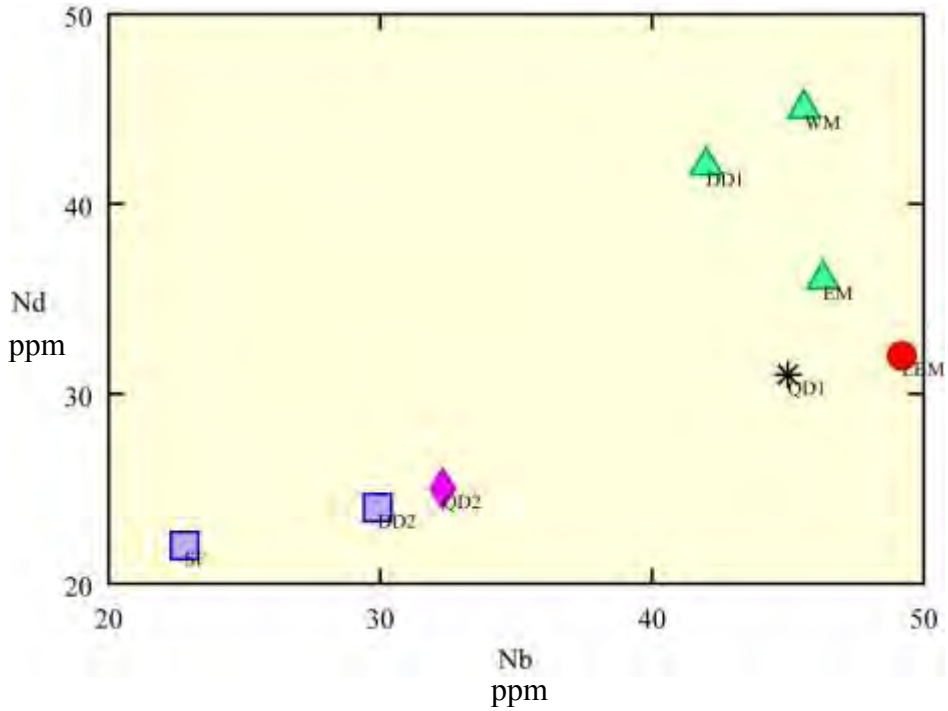
50
40
30
20
Nd
ppm
20
30
40
50
Nb
ppm
WM
DD1
EM
LBM
QD1
QD2
DD2
SI

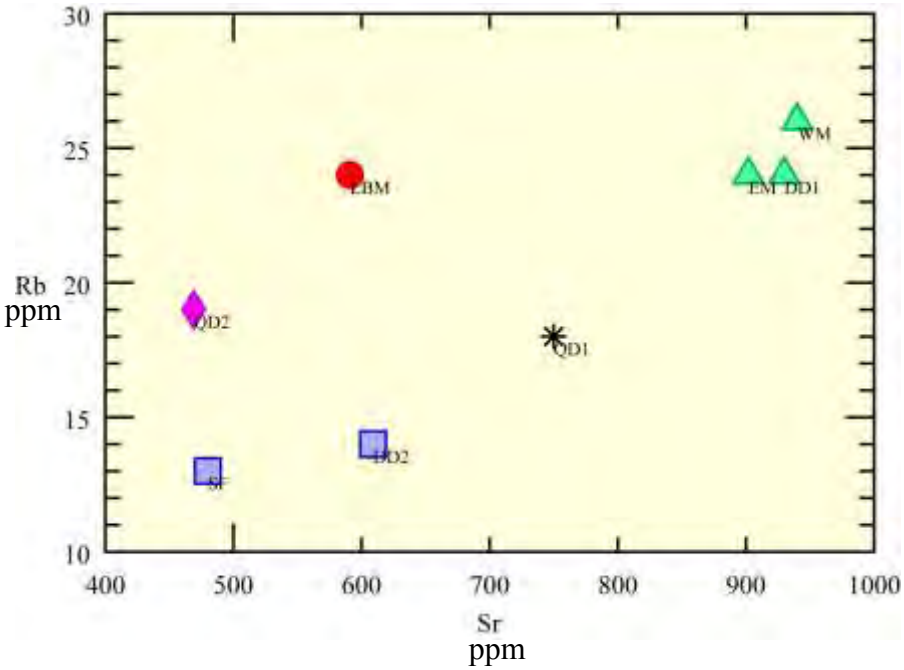
30
25
20
15
10
Rb
ppm
400
500
600
700
800
900
1000
Sr
ppm
WM
LBM
EM
DD1
QD2
QD1
HD2
SI

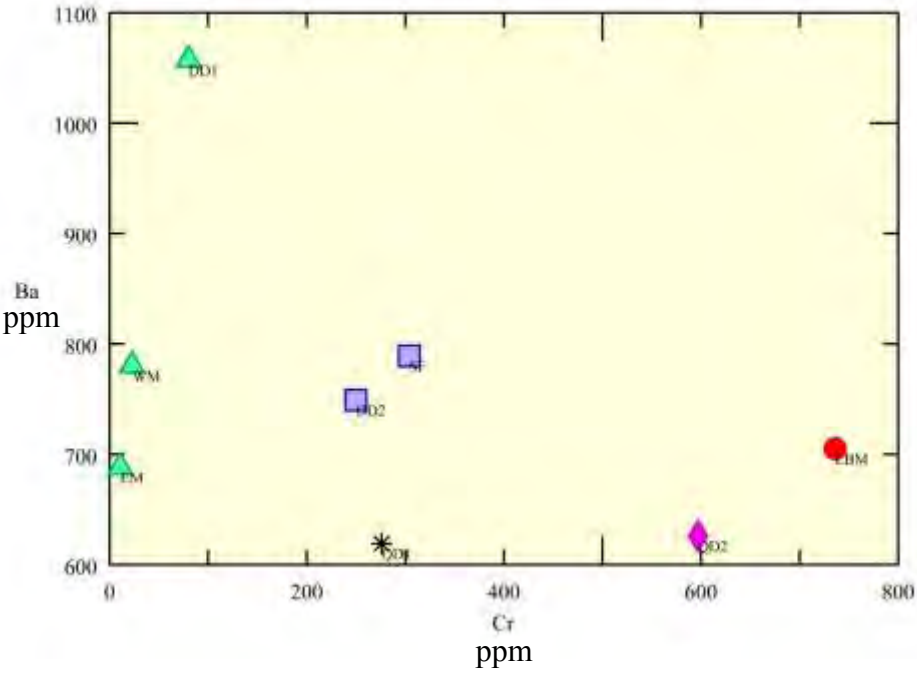
1100
1000
900
800
700
600
Ba
ppm
0
200
400
600
800
Cr
ppm
DD1
WM
SI
HD2
EM
LBM
QD1
QD2

APPENDIX C

$^{40}AR/^{39}AR$ RADIOMETRIC AGES FOR MAFIC VOLCANIC ROCK SAMPLES FROM THE FOOTWALL AND HANGING WALL OF THE WASHINGTON FAULT ZONE, MOHAVE COUNTY, ARIZONA

(Analyses performed by the New Mexico Geochronology Research Laboratory at the New Mexico Institute of Mining and Technology)

See figure 1 for sample locations

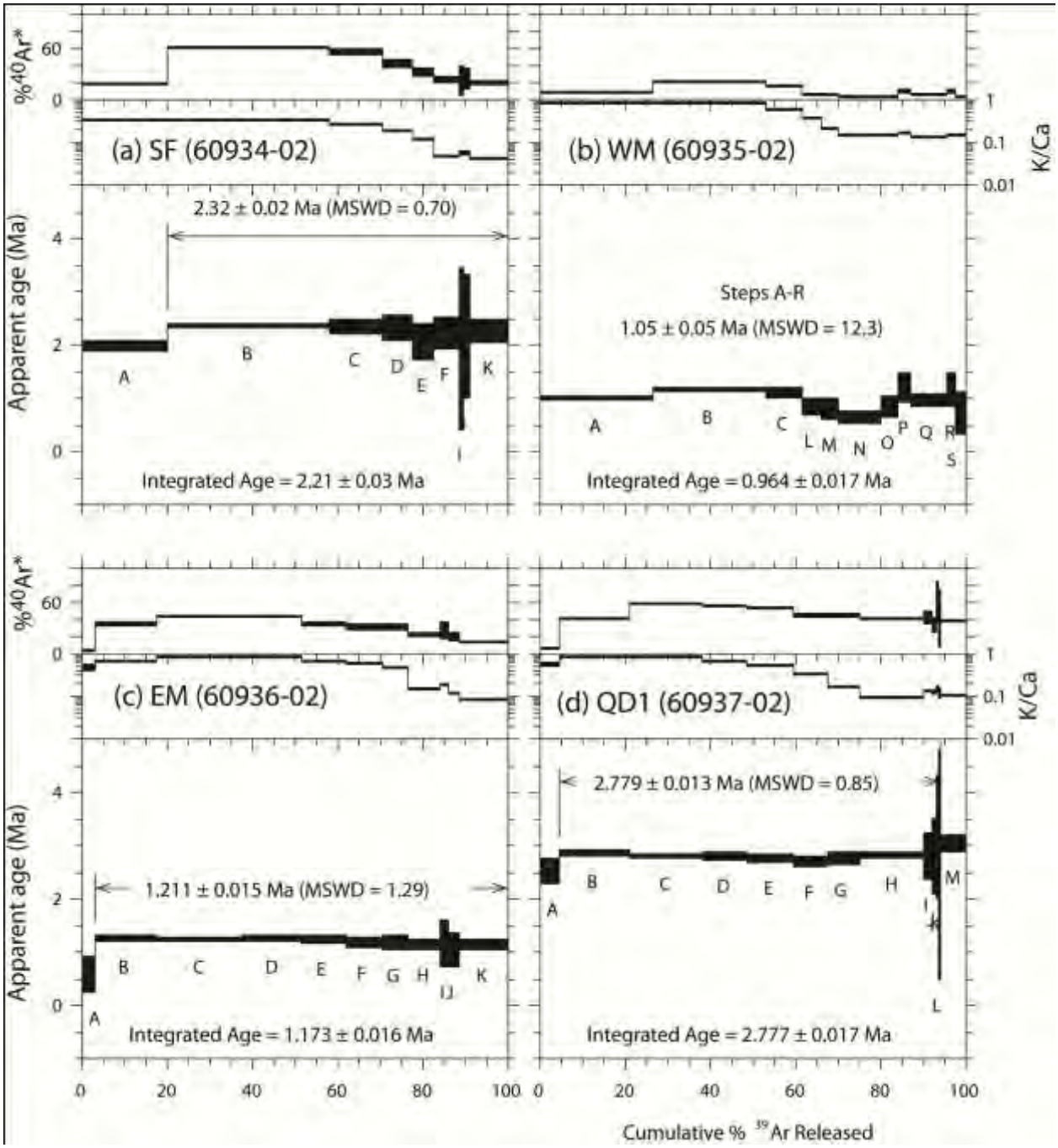
%40Ar*
K/Ca
(a) SF (60934-02)
(b) WM (60935-02)
2.32 ± 0.02 Ma (MSWD = 0.70)
Steps A-R
1.05 ± 0.05 Ma (MSWD = 12.3)
Apparent age (Ma)
Integrated Age = 2.21 ± 0.03 Ma
Integrated Age = 0.964 ± 0.017 Ma
(c) EM (60936-02)
(d) QD1 (60937-02)
2.779 ± 0.013 Ma (MSWD = 0.85)
1.211 ± 0.015 Ma (MSWD = 1.29)
Integrated Age = 1.173 ± 0.016 Ma
Integrated Age = 2.777 ± 0.017 Ma
Cumulative % 39Ar Released

SURFACE-FAULT-RUPTURE-HAZARD INVESTIGATION FOR A TRANSPORTATION CORRIDOR, FORT PEARCE SECTION, WASHINGTON FAULT ZONE, WASHINGTON COUNTY, UTAH

by

David B. Simon[1], John R. Hanson[2], Peter D. Rowley[3], and David K. Black[2]

[1]Simon Bymaster, Inc.
[2]Rosenberg Associates, Inc.
[3]Geologic Mapping, Inc.

CONTENTS

PROJECT DESCRIPTION 152
PURPOSE 152
SCOPE OF WORK 153
SETTING 155
EVIDENCE OF QUATERNARY SURFACE FAULTING 155
GENERAL SITE CONDITIONS 156
GEOLOGY 156
LINEAMENT ANALYSIS 156
  Lineaments L1 and L2 156
  Lineament L3 157
  Lineament L4 157
SUBSURFACE EXPLORATION 158
FAULTING 159
  Trench T-1 159
  Trench T-1 Radiocarbon Ages 159
  Trench T-1 OSL Ages 160
  Trench T-2 160
  Trench T-3 161
  Trench T-4 161
  Trench T-4 Radiocarbon Ages 162
  Trench T-5 162
  Trench T-5 Anthropologic Hearth 162
  Trench T-5 Ages 163
  Trench T-6 164
  Trench T-7 164
  Trench T-8 164
  Trenches T-9 and T-10 165
  Trench T-11 165
  Trench T-12 165
  Trench T-13 166
  Washington Fields Trench WFT-1 166
    WFT-1 General 166
    WFT-1 Ages 167
CONCLUSIONS 168
REFERENCES 169

TABLES

Table 1 Site geologic units 171
Table 2 Purpose of trenches 172
Table 3 Summary of trench data 173
Table 4 Table of displacements per surface-faulting earthquake 173
Table 5 Ages from Washington Fields trench WFT-1 174
Table 6 OSL age ranges for WFT-1 174

Table 7 Cumulative displacements within WFT-1 174

DRAWINGS

Drawing 1a-d Geologic maps
Drawings 2-22 Trench logs

APPENDICES

Appendix A Figures.....175
Figure 1 Location map 176
Figure 2 Surface fault rupture special study area map 177
Figure 3 Lineament map.....178
Appendix B Atomic mass spectrometer radiocarbon age data.....179
Appendix C OSL age analyses.....181
Appendix D Western GeoArch Research age analyses - trench T-5.....183

PROJECT DESCRIPTION

This report presents the findings of a surface-fault-rupture-hazard investigation performed for phase 3 of a Utah Department of Transportation (UDOT) multiphase transportation corridor project in the St. George metropolitan area, Washington County, Utah. The location of the proposed transportation corridor ("study area") is shown on figure 1 (figures are in appendix A).

The south end of the phase 3 corridor is about 4 miles (6.4 km) north of the Arizona/Utah border, and the north end is near the Washington Fields area of Washington City, Utah (figure 1). The 3.7 mile (6 km) long transportation corridor includes three elevated interchanges: one near the south end of the transportation corridor (Interchange 9); one near central part of the transportation corridor at Warner Valley Road (Interchange 10), and; a third near the northern part of the transportation corridor (Interchange 11). Between Interchanges 9 and 11 the transportation corridor essentially follows Washington Fields Road (4700 East Street).

The Washington fault zone has been documented within the study area (Hayden, 2005; Lund and others, 2008; Biek and others, 2009; Rosenberg Associates, 2009), and exhibits geomorphology suggestive of Holocene-age surface faulting. As shown on figure 2, the Washington fault zone crosses the central part of the proposed transportation corridor (Hayden, 2005; Lund and others, 2008; Rosenberg Associates, 2009), and Interchanges 10 and 11 are adjacent to the west side of the Fort Pearce section (Knudsen this volume) of the Washington fault zone.

The Utah Geological Survey (UGS) Quaternary *Fault and Fold Database and Map of Utah* (Black and others, 2003) indicates that surface deformation on the Washington fault zone in the study area is as young as latest Pleistocene. In a later study (Lund and others, 2008), the UGS classified the Washington fault zone as a “well-defined late Quaternary (movement within the past 130,000 years) fault,” and established a surface-fault-rupture hazard special study area for the fault zone (figure 2).

PURPOSE

The surface-fault-rupture-hazard investigation performed for the phase 3 transportation corridor had a twofold purpose:

1. To use the characteristics of past surface faulting within the study area as a scientific basis for providing recommendations to UDOT to reduce the potential for damage and injury from future, presumably similar, surface faulting.

2. To prevent structures designed for human occupancy[1] and critical facilities[2] from being constructed over a Holocene-age[3] fault by providing suitable building setbacks from Holocene-age faults.

This report focuses on the geologic and paleoseismic aspects of the investigation and does not present or discuss engineering geologic design recommendations for proposed construction of the transportation corridor. Engineering geologic design recommendations were provided to UDOT, which included structural setbacks from the Fort Pearce section and a recommendation to relocate two interchanges.

SCOPE OF WORK

This investigation consisted of five principal tasks:

Task 1: Geologic Mapping

Rosenberg Associates (2009) prepared a geologic strip map for the proposed transportation corridor; the purpose of the map was two-fold:

a. To generate a geologic base map for the study area (drawings 1a-d)

b. To utilize the geologic map to develop a program of subsurface investigation to evaluate the surface-faulting hazard to the proposed transportation corridor, and in particular the raised interchange structures.

Task 2: Literature Review

Available published geologic literature concerning rock units, faulting, and seismicity in the area was reviewed. In addition to published literature, unpublished technical reports addressing surface faulting were reviewed for the northern part of the study area in the Washington Fields area (Applied Geotechnical Engineering Consultants; AGEC, 2007) and for flood-retention structures near the north/north-central parts of

---

[1] Structure Designed for Human Occupancy are typically considered any structure used or intended for supporting or sheltering any use or occupancy, which is expected to have an occupancy rate of at least 2000 person-hours per year, but does not generally include an accessory building (structure not designed for human occupancy, which may include tool or storage sheds, gazebos, and swimming pools, etc).

[2] Critical facilities are here considered Category II and III structures as defined in the 2009 International Building Code (IBC, table 1604.5, p. 307; International Code Council, 2009). Critical facilities include essential facilities.

[3] Holocene age: less than 10,000 years.

the transportation corridor (Earth Science Associates; ESA, 1982; Bowman and others, 2011).

Task 3: Evaluation of Aerial Photographs

Several sets of aerial photographs of the study area were examined stereoscopically for the presence of photo lineaments which might indicate surface faulting.

Task 4: Field Reconnaissance

A field reconnaissance of the study area was performed, to document evidence of surface faulting and evaluate geologic units and pertinent surface features.

Task 5: Subsurface Exploration

Thirteen trenches were excavated to evaluate subsurface deposits for the presence of faulting. Trench locations are shown on drawings 1a-d. The trenches, totaling about 3610 feet (1100 m) in length, were excavated by a track backhoe with a 36-inch (91-cm) wide bucket to depths of about 15 feet (4.6 m) below existing ground surface. Following excavation, trenches were surveyed to an accuracy of about 0.1 foot (3 cm) by Utah licensed professional surveyors (Rosenberg Associates, St. George, Utah).

In 2007, AGEC (2007) performed a fault investigation in the Washington Fields area (figure 1), which consisted of excavating several trenches in an attempt to expose the main trace of the Washington fault zone. During the AGEC study, the UGS obtained samples for age analysis from AGEC Trench T-1. The UGS believed that the trenches were to be backfilled following logging; therefore, due to time constraints, the UGS only generated a reconnaissance-level trench log (William Lund, Utah Geological Survey, verbal communication, 2010).

In the absence of a detailed log and with ages from only one trench, the UGS considered the uncertainty too great to adequately characterize the timing of surface faulting on the Washington fault zone (William Lund, Utah Geological Survey, verbal communication, 2010).

Fortunately for this study, the AGEC (2007) trenches in the Washington Fields area were not backfilled. As part of this investigation, parts of the north and south walls of AGEC Trench T-1 (referred to hereafter in this report as WFT-1) were cleaned and logged so that the UGS ages could be further evaluated. A detailed log for about 103 feet (31 m) of trench WFT-1was completed.

Materials exposed in the all trenches are described on the trench logs drawings 2 through 22, and were classified, when applicable, in accordance with the Unified Soil

Classification System (ASTM Method D 2488). Color designations follow standard Munsell Soil Color notations. Trench excavations and field-logs were periodically reviewed by William Lund and Tyler Knudsen, geologists with the UGS.

SETTING

An overview of the Washington fault zone, including the physiographic and seismic setting, and characteristics of the fault zone, are provided in Lund (this volume).

EVIDENCE OF QUATERNARY SURFACE FAULTING

In trench WFT-1, a 13-foot (4 m)-wide fault zone consisting of at least three, west-dipping, splays was exposed. The UGS (Lund and others, 2008) conducted a reconnaissance-level investigation of the exposed fault and noted:

1. Colluvial-wedge deposits provided evidence for at least three surface-faulting earthquakes that displaced mixed alluvial-colluvial-eolian deposits from about 1 foot (0.3 m) to just less than 3.2 feet (1 m).

2. The most recent earthquake displaced a buried organic horizon (Bkb) and an overlying weakly indurated sand deposit.

3. Fault extended to within 10 inches (25 cm) of the existing ground surface, where it was buried by a modern eolian sand deposit.

From WFT-1 the UGS collected five samples of colluvial/eolian sand from within and below presumed colluvial wedges and submitted them for optically stimulated luminescence (OSL) dating to constrain the ages of the surface-faulting earthquakes. Based on the OSL data, the UGS concluded (Lund and others, 2008):

1. The Washington fault zone has experienced a minimum of three surface-faulting earthquakes in the past 75,600 ± years.

2. The most recent surface faulting earthquake (MRE) occurred shortly before 18,600 ± years.

3. The penultimate surface faulting earthquake (PE) occurred shortly before 30,700 ± years, and a third surface faulting earthquake occurring shortly before 67,800 ± years.

Further evidence of Quaternary surface faulting and previous paleoseismic studies of the Washington fault zone are discussed in Lund (this volume).

GENERAL SITE CONDITIONS

Most of the property within the study area is undeveloped. Three single-family residential structures are near Interchange 10. The structures are adjacent to the west side of Washington Fields Road immediately south of the intersection with Warner Valley Road (figure 1). Undeveloped residential subdivisions are present north of Interchange 11. Vegetation along the transportation corridor consists of a sparse ground cover of native grass, sage brush, and low mesquite. Numerous west-trending ephemeral drainages cross the study area.

GEOLOGY

The areal distribution of the geologic units documented along the transportation corridor is shown on drawings 1a-d. Most of the transportation corridor is underlain by Quaternary-age unconsolidated surficial deposits of alluvial-fan and pediment origin; these deposits cover bedrock units of Triassic and Permian age (Hayden, 2005; Biek and others, 2009; Rosenberg Associates, 2009; Hayden and Willis, 2011; Knudsen, this volume). Detailed descriptions of the geologic units observed in the exploratory trenches are presented on drawings 2 through 22 and are summarized in table 1.

LINEAMENT ANALYSIS

Topographic maps and stereoscopically-paired aerial photographs of the study area were examined for the presence of photo-lineaments which might be indicative of surface faulting. Lineaments suggestive of faulting primarily corresponded to previously mapped traces of the Washington fault zone (Hayden, 2005; Biek and others, 2009; Rosenberg Associates, 2009; Hayden and Willis, 2011), and consisted of north-northeast trending linear topography, alignment of vegetation, and linear color contrasts. However, four lineaments not associated with previously mapped faults were identified. The locations of the lineaments are shown on figure 3.

Lineaments L1 and L2

Lineaments L1 and L2 consists of a north-south oriented linear ridge and a north-south oriented linear saddle near the middle of a ridge (see figure 3 and drawing 1a and 1b); the paired-lineaments were strongly expressed on aerial photographs. The lineaments, which cross the transportation corridor at the proposed location of Interchange 9, were described by Rosenberg Associates (2009) as follows:

"During this investigation we mapped a new fault, defined by a linear scarp, not

recognized previously, that parallels and lies about a half mile west of the main strand of the Washington fault zone. ESA (1982) noted that the scarp was a "suspicious feature" that might be fault related. ESA (1982) excavated two trenches across the feature when they were studying the Stucki Dam, but did not document any faults and concluded that the feature was not a fault. It is possible that the ESA (1982) trenches were not deep enough.

The new fault is poorly exposed in the basin-fill sediments (QTs on drawings 1a-d) that are overlain by a caliche-capped pediment surface (Qe/Qafo on drawings 1a) in the southern part of the map. North of the linear scarp, the fault is concealed (dotted) but projected northward to truncate the northeast end of a bedrock hogback made up of the upper part of the Moenkopi Formation and the lower part of the Chinle Formation. It appears the subsidiary fault joins the main strand in the northern part of the map, but is buried beneath younger surficial deposits and its trace is conjectural.

The new fault crosses the transportation corridor and Interchange 9 near the south edge of the map area. Displacement along the fault is down to the east, antithetic to the main strand of the Washington fault zone. The two faults create a graben filled in with sediment (QTs on drawing 1a) derived from erosion of material on the upthrown sides. Antithetic faults and grabens on the downthrown sides of large normal faults are common. We interpret this fault to part of the Washington fault zone."

Lineament L3

Lineament L3 appears on aerial photographs as a weakly to moderately expressed tonal linear feature in an area of young alluvium (Qaf on drawings 1a and 1c). The lineament is about 250 feet (75 m) west of Interchange 10 (drawing 1c), and was described by Rosenberg Associates (2009):

"Although we were not able to corroborate photo lineaments in the area of the Gypsum Wash Dam, we did map a north-trending lineament about 0.2 miles (0.3 km) long, whose south end is 0.25 miles (0.4 km) north of Interchange 10 (drawing 1c). This feature has no surface topographic expression but appears on aerial photographs as a tonal linear feature in an area of young alluvial deposits (Qaf on drawing 1a) about 100 feet (30.5 m) west of the exposed main trace of the fault. We interpret the lineament to be associated, in some manner, with the main splay of the Washington fault zone."

Lineament L4

Lineament L4 consists of a linear slope strongly expressed on aerial photographs and topographic maps (Rosenberg Associates, 2009). The linear slope is immediately east of the Gypsum Wash Dike and about 1000 feet (300 m) east of the corridor at Interchange 11 (drawing 1c).

SUBSURFACE EXPLORATION

The purpose of the subsurface exploration was twofold:

1. Evaluate the origin of the lineaments identified in the Rosenberg Associates (2009) study, and;

2. Assess the part of the study area situated within the surface-fault-rupture special study area established for the Washington fault zone by the UGS (Lund and others, 2008; figure 2).

Initially, six trenches were excavated to:

1. Evaluate subsurface deposits for the presence of faulting.

2. Verify the presence or absence of mapped faults within the study area as indicated by others (Hayden, 2005; Biek and others, 2009; Rosenberg Associates, 2009; Hayden and Willis, 2011).

3. Intercept faults that project into the study area.

4. Intercept lineaments identified from aerial photographs and topographic maps.

5. Provide the minimum footage of trenching necessary, such that surface fault rupture within the study area could be adequately assessed.

Due to documentation of faults in the initial six trenches, seven supplemental trenches were excavated to:

1. Further refine fault locations (or the absence thereof);

2. Accurately define building restriction areas, and/or;

3. Provide additional exposures for evaluating the age of movement along particular faults.

The primary purpose of each trench is summarized in table 2. Materials exposed in the trenches are described on drawings 2 through 22. The length and orientation of each trench, and whether or not a fault was documented within the trench, are presented in table 3.

FAULTING

Faults were documented in nine of the 13 trenches excavated for this study (table 3) as well as in WFT-1 of the AGEC (2007) Washington Fields investigation. Displacement of bedrock and alluvial units ranged from a few inches (7 ± cm) to about 5 feet (1.5 m). The number of surface-faulting earthquakes and average displacement per surface-faulting earthquake are shown on table 4. Multiple surface-faulting earthquakes were identified in T-2 and T-6, and the depth of the trench at each fault location likely represents the cumulative displace along the particular fault.

To constrain the ages of surface-faulting earthquakes, selected samples were submitted to Paleo Research Institute for charcoal extraction and atomic mass spectrometer radiocarbon analysis (AMS) and/or to Utah State University for OSL age analysis. Results of the AMS and OSL analyses are presented in appendices B and C, respectively.

Trench T-1

The purpose of T-1 (drawings 1c and 2 and 3) was to locate the main trace of the Washington fault zone and to evaluate the area east of Interchange 10 for the presence of faults. A fault, trending N. 76° E. and dipping about 72° E., was documented at station 0+98 (f-1, drawings 2 and 3). The fault closely corresponds to the main trace of the Washington fault zone as mapped by others (Hayden, 2005; Biek and others, 2009; Rosenberg Associates, 2009). Displacement along the fault appears to be largely normal slip (west side down), juxtaposing Moenkopi Formation bedrock against Holocene-age alluvial deposits.

Two fault-scarp-derived colluvial wedges (units 6 and 7, drawings 2 and 3) were documented adjacent to the west side of the fault. Each colluvial wedge is representative of a surface-faulting earthquake. The colluvial wedges are overlain by 4.5 ± feet (1.4 ± m) of stratigraphically continuous alluvial sediments (unit 8, drawing 2). The amount of cumulative displacement or displacement per surface-faulting earthquake could not be determined; however, based on trench depth and the absence of bedrock on the west side of the fault, cumulative displacement is equal to the depth of the trench at the location of the fault (≥ 6.5 ± feet) (≥ 2 ± m) or a minimum of 3.2 ± feet (1 ± m) per surface-faulting earthquake.

Trench T-1 Radiocarbon Ages

A sample of each colluvial-wedge (units 6 and 7, drawing 2; samples S3 and S2, respectively), and a sample of an alluvial unit overlying the youngest colluvial wedge (unit 8, drawing 2; sample S1) were submitted for charcoal extraction and AMS analysis.

All three units sampled were expected to be Holocene age. However, the AMS ages obtained were stratigraphically inverted (younger ages are below older ages), and therefore, inconclusive. Sample T1-S1 (unit 8; drawing 2) contained sufficient particulate organics to yield

a radiocarbon age of 2140 ± 15 radiocarbon years before present (RCYBP) (table B-1, appendix B). This age calibrates to 2160-2060 calendar years before present (cal yr B.P.).

Sample T1-S2 (unit 7, drawing 2) contained a small quantity of *Pinus* charcoal, which was selected for analysis in preference to continuing the extraction process to recover particulate organics. Sample T1-S2 yielded a radiocarbon age of 205 ± 15 RCYBP, which calibrates to 20 years to present cal yr B.P. Sample T1-S3 (unit 6, drawing 2) yielded a radiocarbon age of 465 ± 15 RCYBP on particulate organics, which calibrates to 530-500 cal yr B.P.

The very recent ages reported for units 6 and 7 (drawing 2) indicate that there has been considerable mixing, bioturbation, intrusion of modern to very recent material, and likely contamination by carbon associated with 1950s nuclear bomb testing. Washington County is "downwind" of the 1950s nuclear testing at the Nevada Test Site.

Trench T-1 OSL Ages

A sample of each colluvial wedge (units 6 and 7, drawing 2; samples S3 and S2, respectively) was submitted for OSL age analysis. However, the ages obtained were also stratigraphically inverted and therefore inconclusive. A sample from unit 6 (stratigraphically below unit 7) yielded an OSL age of 10,000 ± 1000 years. An OSL age of 15,000 ± 10,000 years was reported for unit 7.

Trench T-2

The purpose of T-2 (drawing 1c and 4) was to locate the main trace of the Washington fault zone and to evaluate the area east of Interchange 10 for the presence of faults. A zone of faults was documented between stations 0+5 and 0+12 (drawing 4). The primary fault (f-1), at station 0+12, trends N. 08° W., dips about 30° E. and thrusts older Moenkopi Formation bedrock over younger, likely Holocene-age alluvial sediments.

Although the Washington fault zone is a normal fault (west side down), the thrust fault documented in T-2 is likely due to compression forces in an area where the main fault either bends or overlaps with another trace in an en echelon manner. Displacement along the fault could not be determined. Cumulative displacement may be equal to at least the depth of the trench (9 ft [2.7 m]).

A second fault (f-2), trending N. 02° W. and dipping 70° E., was observed at station 0+42.5. The fault displaces Moenkopi Formation bedrock about 1.2 feet (0.4 m) down to the west. The fault is overlain by 9.5 feet (2.9 m) of unbroken and stratigraphically continuous alluvial sediments. It appears that the fault is confined to bedrock, and is pre-Holocene age.

Two samples of alluvial-fan sediments on the west side of the thrust fault (unit 15; drawing 4) were submitted to Paleo Research Institute for charcoal extraction and atomic mass

spectrometer radiocarbon analysis (appendix B). The alluvial-fan sediments were expected to be late Pleistocene to Holocene age. Particulate organics could be extracted from sample T2-S1; however, sample T2-S2 yielded no particulate carbon, and could therefore not be analyzed.

Ages during the atomic bomb testing era to modern are reported as Fraction Modern. The particulate organics extracted from sample T2-S1 appeared very similar to those recovered from trench T-1, although the sample apparently contained very modern carbon, yielding a Fraction Modern of 1.058100 ± 0.00150. This age calibrates between December 1955 and July 1957, indicating that there has been considerable mixing, bioturbation, and intrusion of modern to very recent material, and contamination by carbon associated with 1950s nuclear bomb testing.

Trench T-3

The purpose of T-3 (drawings 1c and 5 and 6) was to locate the main trace of the Washington fault zone and to evaluate the area east of Interchange 10 for the presence of faults. Unbroken and stratigraphically continuous alluvial sediments were documented throughout the entire length (500 ± ft; 152 ± m) of trench T-3 (drawings 5 and 6). Trench depth was 15 ± feet (4.6 ± m). Geomorphic and stratigraphic relations suggest these sediments are likely Holocene-age.

Trench T-4

The purpose of T-4 (drawing 1c and 7) was to further refine the location of the fault documented in T-1 and to provide additional exposures for evaluating the age of movement along the fault. T-4 was located about 100 ± feet (30 ± m) north of T-1, and was one of the more important trenches with regard to determining the number of surface-faulting earthquakes and the amount of displacement per event. The trench crosses a moderately eroded, remnant fault scarp associated with the Washington fault zone. The scarp (drawing 1a) is about 50 ± feet (15 ± m) long. To the north, the fault scarp was likely removed during construction of Warner Valley Road, and to the south by erosion from adjacent ephemeral drainages.

Six faults were documented in T-4 (drawing 7). Cross-section projections suggest the faults likely coalesce at a relatively shallow depth (within 50 ± ft; 15 ± m). Displacement along the faults appears to be largely normal slip (west side down), juxtaposing:

1. Moenkopi Formation bedrock against Holocene-age alluvium, and;

2. Holocene-age alluvium against Holocene-age alluvium.

Two colluvial wedges were documented in T-4, both associated with fault f-4 (station 0+32.5). Each colluvial wedge is representative of a surface-faulting earthquake. Faults f-1 through f-5 (stations 0+21 to 0+32.5) comprise a zone of faulting with a net vertical displacement of about 6.5 feet (2 ± m), yielding an average displacement per surface-faulting

earthquake of about 3.3 feet (1 ± m). Based on stratigraphic relations (primarily whether or not unit 11 is displaced), faults f-4 and f-6 represent the most recent earthquake (MRE) and faults f-1, f-2, f-3, and f-5 represent the penultimate earthquake (PE).

Geologic units across f-6 are not correlative; therefore, it was not possible determine displacement associated with f-6. The fault propagates to within 1.3 ± feet (0.4 ± m) of the existing ground surface, where the fault is overlain by deposits associated with an active ephemeral drainage; this data strongly suggests f-6 represents the most recent surface-faulting earthquake. At the time of surface displacement, a fracture opened along the west side of f-6 (from 2 to 5 ft wide [0.6 to 1.5 m]), which was filled with adjacent sediments.

Fault f-5, at station 0+32.5, is an antithetic fault. Displacement of geologic units indicates that this fault was not active during the MRE. Unit 6 (drawing 7) is likely a faulting derived colluvial wedge representative of a third surface-faulting earthquake.

Trench T-4 Radiocarbon Ages

A sample from each colluvial wedge (units 8 and 9, drawing 7) and one sample of an alluvial unit underlying the older colluvial wedge (unit 10, drawing 7) were submitted to Paleo Research Institute for charcoal extraction and AMS analysis (appendix B).

The sediments sampled were expected to be Holocene age. However, the samples from T-4 yielded very recent ages (1951 to 1957) (table B-1, appendix B), which we attribute to the small amount of charcoal analyzed, modern organic contamination from bioturbation, and contamination by carbon associated with 1950s nuclear bomb testing.

Trench T-5

The purpose of T-5 (drawings 1c and 8 and 9) was to locate the main trace of the Washington fault zone and to evaluate the area east of Interchange 10 for the presence of faults. Unbroken and stratigraphically continuous alluvial sediments were documented throughout the entire length of T-5. The trench extended to an average depth of 10 ± feet (3 ± m). Near station 0+55, the trench was about 20 feet (6 ± m) deep.

Stratigraphically continuous Moenkopi Formation bedrock was documented in the eastern part of the trench from stations 0+00 to 0+60, at which point, the bedrock was overlain by stratigraphically continuous alluvial sediments.

Trench T-5 Anthropologic Hearth

Within unit 10, at about station 1+43, a buried anthropologic hearth was documented (see drawing 8). Several areas of anthropologic charcoal staining were also observed within unit 4 and unit 10 east of station 0+43. Unit 10 overlies unit 4 and is therefore a younger deposit.

The archaeological significance of the hearth and cultural charcoal staining were investigated by Bighorn Archaeological Consultants, LLC and Western GeoArch Research (WGR). WGR submitted eight samples from the anthropologic hearth and cultural charcoal staining to Beta Analytical for charcoal extraction and AMS analysis, and two samples of unit 4 and one sample of unit 10 to the University of Illinois at Chicago Luminescence Laboratory for OSL age analysis.

Trench T-5 Ages

A summary of the WGR ages is presented in appendix D. A radiocarbon age of 2030 ± 40 RCYBP (2065 cal yr B.P.) was reported for the hearth within unit 10. A significantly smaller accumulation of charcoal, about 1.1 feet (0.3 m) above the hearth, yielded an age of 1900 ± 40 RCYBP (1885 cal yr B.P.).

Radiocarbon ages of other cultural charcoal staining in unit 4 ranged from 5730 ± 40 to 4640 ± 40 RCYBP; corresponding calendar calibrated years are 6525 to 5382 cal yr B.P. Therefore, the cultural charcoal staining within unit 4 provides a minimum age for the deposit.

OSL age analyses yielded a luminescence age for unit 4 of 12,910 ± 1415 to 9940 ± 1030 yr B.P. and an OSL age for unit 10 of 4830 ± 430 yr B.P.

West of station 0+45, units 4 and 10 are below the bottom of the trench. Unit 13, an alluvial deposit, cuts into units 10, 11, and 14, and therefore is younger than units 10, 11, and 14. Unit 13 is overlain by unit 12; the sediments comprising unit 12 are associated with the active ephemeral drainage (at about station 1+55) and are likely modern to a few hundred years old. The age of unit 13 was not specifically determined; however, geomorphic and stratigraphic relations and OSL ages of unit 10 indicate unit 13 is clearly Holocene-age, and younger than unit 10 (4830 ± 430 cal yr B.P.).

East of station 1+55, AMS and OSL age analyses indicate that the unbroken and stratigraphically continuous alluvial sediments are older than the MRE documented along the Washington fault zone in the Dutchman Draw study (Lund and others this volume).

West of station 1+55 (the active ephemeral drainage), unit 14 was the oldest geologic unit documented. Based on geomorphic and stratigraphic relations, unit 14 is likely contemporaneous with, or slightly younger than unit 10, on the order of 4000 to 5000 years old.

The unbroken and stratigraphically continuous alluvium exposed in T-5 west of Station 1+55 constitutes reasonable geologic evidence for the absence of faulting within these sediments. Based on the data presented above, unit 13 and 14 are older than the MRE documented along the Washington fault zone in the Dutchman Draw study (Lund and others this volume).

Trench T-6

The purpose of T-6 (drawing 1c and 10 and 11) was to locate the main trace of the Washington fault zone and to evaluate the area east of Interchange 10 for the presence of faults. A fault was documented at station 0+27.5, trending N. 08° W. and dipping about 80° E. Displacement along the fault is largely normal slip (west side down), juxtaposing Moenkopi Formation bedrock against Holocene-age alluvial-fan deposits and alluvium against alluvium.

The easterly dip to the fault is likely a result of the fault splaying/diverging near the surface where overburden pressures are essentially negligible. Displacement along the fault could not be determined. Cumulative displacement is likely equal to at least the depth of the trench near the faulted units, e.g., about 8.5 feet (2.6 m).

Unit 12 (alluvium) is the oldest faulted geologic deposit in the trench. Stratigraphically, unit 2 (alluvium) is older than unit 3 (see station 0+70, drawing 10). Unit 7 (alluvium) is the youngest unfaulted geologic unit. Geomorphic and stratigraphic relations suggest units 2, 3, and 12 are Holocene age and older than the MRE reported from the Dutchman Draw, Arizona area (Lund and others this volume).

Trench T-7

The purpose of T-7 (drawings 1b and 12 and 13) was to intercept lineaments L1 and L2 (see figure 3). T-7 was about 420 feet (128 m) long, and extended from the youngest valley-fill sediments on the east (Qaf on drawing 1), to the top of the linear ridge on the west (QTs on drawing 1). Stratigraphically continuous (e.g., not displaced) Pleistocene-age (Rosenberg, 2009) basin-fill sediments (QTs on drawing 1) were documented within the entire length of the trench. The basin-fill sediments dip about 10° west.

We attribute the linear ridge to erosion by ephemeral drainages. The north-south oriented linear saddle near the middle of the ridge is a result of differential erosion of soft, erosion-prone sand (units 9-14 and unit 16 on drawings 12 and 13) and more resistant calcium carbonate cemented sediments (units 8, 15, and 17 on drawings 12 and 13).

Trench T-8

The purpose of T-8 (drawings 1c and 14) was to intercept lineament L3 (figure 3). The main trace of the Washington fault zone is about 40 feet (12 m) east of the east end of T-8, adjacent to the east side of Washington Fields Road (drawing 1c).

Bedrock units were exposed along the entire length of the trench. The Petrified Forrest Member of the Chinle Formation was documented from about stations 0+00 to 0+64. The Dinosaur Canyon Member of the Moenave Formation was documented west of station 0+64.

Bedding was oriented near vertical and many bedding planes exhibited shearing. The contact between the two bedrock units is defined by a 5 ± (1.5 m) foot-wide zone of fault breccia. Starting at about Station 0+15 the bedrock units are unconformably overlain by unbroken and stratigraphically continuous alluvial sediments.

Numerous fault traces were documented in T-8 between stations 0+00 and 1+47. The faults are confined to the near vertical and highly sheared bedrock units. The absence of displacement within the alluvial sediments and uniform slope of the ground surface and contact between the bedrock and alluvial units is evidence that there is not a subsurface feature associated with the lineament observed on the aerial photographs.

T-8 is within a center pivot irrigation system, which is visible on 1982 aerial photographs but not on 2000 aerial photographs. Based on trench observations and the former center pivot, we interpret lineament L3 to be associated with farm irrigation.

Trenches T-9 and T-10

The purpose of trenches T-9 and T-10 (drawings 1c and 15 and 16) was to further refine the locations of the faults documented in T-8, particularly the fault identified at station 1+47 (which was relatively subtle), and to provide additional exposures for evaluating the age of movement along the faults. The exposures in T-9 and T-10 were very similar to T-8. The various faults were confined to near vertical and highly sheared bedrock units. The fault documented at station 1+47 in T-8 was also observed at station 0+45 in T-9. The bedrock units were overlain by unbroken and stratigraphically continuous alluvial sediments.

Trench T-11

The purpose of T-11 (drawings 1c and 17 and 18) was to locate the main trace of the Washington fault zone to confirm the findings of the ESA (1982) report regarding faulting in this area, and to evaluate the area near the proposed location of Interchange 11 for the presence of faults.

Several faults were documented in T-11, the majority of which were confined to Moenkopi Formation bedrock and did not displace recent (Holocene-age) alluvium. However, the fault at about station 4+22 (fault f-5 on drawing 18), displaces Holocene-age alluvium, and juxtaposes alluvium against Moenkopi Formation bedrock. The location of fault f-5 corresponds reasonably well with the primary trace of the Washington fault zone as documented by others (ESA, 1982; Hayden, 2005; Rosenberg Associates, 2009).

Trench T-12

The purpose of T-12 was to intercept lineament L3 (drawings 1c and 19). Although several bedrock faults were documented in T-12 with displacements ranging from 0.5 to 5 feet

(0.15 to 1.5 m), none of the faults corresponded to the lineament documented in the Rosenberg Associates (2009) study. Based on the presence of extensive construction fill and proximity to Gypsum Wash Dike, we attribute the linear slope to grading activities associated with construction of the Gypsum Wash Dike, adjacent to the west end of T-12.

Trench T-13

The purpose of T-13 (drawings1c and 20) was to evaluate the area west of Interchange 10 for the presence of faults. Unbroken and stratigraphically continuous alluvial sediments were documented throughout the entire length (500 ± ft; 152 ± m) of T-3 (drawings 20 and 21).

The depth of T-13 was 15 ± feet (4.6 ± m). Ages for the Holocene sedimentary deposits are not known. However, based on ages obtained from similar sediments in T-5 and T-8 and geomorphic and stratigraphic relations, these deposits are likely on the order of 4000 years old (Holocene-age), and older than the most recent surface-faulting earthquake documented along the Washington fault zone in the Dutchman Draw, Arizona study (Lund and others this study).

Washington Fields Trench WFT-1

WFT-1 General

The Washington Fields site is near the north end of the study area (drawing 1d). Trenching by AGEC (2007) at the Washington Fields site exposed the main trace of the Washington fault zone.

The UGS conducted a reconnaissance-level investigation of the exposed faults in WFT-1, and collected five samples from what was interpreted to be fault-scarp-derived colluvial deposits. To constrain the ages of the surface-faulting earthquakes, the samples were submitted for OSL age analysis.

Based on the OSL data, the UGS concluded that the Washington fault zone has experienced a minimum of three surface-faulting earthquakes in the past 75,600 ± years, with the most recent surface faulting earthquake occurring shortly before 18,600 ± years, the penultimate surface faulting earthquake occurring shortly before 30,700 ± years, and a third surface faulting earthquake occurring shortly before 67,800 ± years (Lund and others, 2008). However, due to the absence of a detailed trench log and ages from only one location, the UGS considered the uncertainty in the ages to great to adequately characterize the timing of surface-faulting on the Washington fault zone (William Lund, Utah Geological Survey, verbal communication, 2010).

WFT-1 was, in fact,, not backfilled following the AGEC (2007) investigation, and trench exposures were evaluated for this study to provide a detailed log (drawings 21 and 22) so that the UGS OSL ages could be interpreted and reliably utilized for evaluating the age of movement along the Washington fault zone.

Six faults were documented in WFT-1 (drawing 22). Displacement along the faults appears to be largely normal slip (west side down), juxtaposing:

1. Moenkopi Formation bedrock against Holocene-age alluvium, and;

2. Alluvium against alluvium. The faults likely coalesce at a relatively shallow depth (within 100 ± ft; 30 ± m).

Units 10, 12 and 15 likely represent fault-scarp-derived colluvium associated with either/or faults f-3 and f-4 (station 0+32.5). Each colluvial unit is representative of a surface-faulting earthquake. The absence of a geomorphic scarp suggests that scarps associated with these events that formed in the loose, unconsolidated, largely eolian sediments that underlie the Washington Fields were likely rapidly eroded.

WFT-1 Ages

To constrain the timing of surface faulting for this investigation, one sample of alluvial sediments and two samples of fault-scarp-derived colluvium were submitted to Paleo Research Institute for charcoal extraction and AMS analysis (appendix B). Both the UGS OSL and AMS ages (RA) obtained for this investigation are summarized in table 5.

The three samples submitted for AMS analysis, yielded relatively recent ages (table 5; table B-1, appendix B) (530 ± 15 to 925 ± 15), which we attribute to the small amount of charcoal analyzed, modern organic contamination from bioturbation, and contamination by carbon associated with 1950s nuclear bomb testing. The ages are not considered reliable.

Unit 10 was analyzed by both OSL and radiocarbon methods (table 5), which resulted in an OSL age of 18,590 ± 1160 BP versus a radiocarbon age of 530 ± 15 RCYBP (560-510 cal yr B.P.). Based on discussions with the individual laboratories, although older than anticipated (based on depth of unit below ground surface; about 3.5 feet) (1.1 meters), we believe the OSL age is likely more representative of the age of Unit 10 and is stratigraphically consistent with the other UGS OSL ages.

Another inconsistency with the OSL ages is that the ages of units 1 and 2 and units 5 and 6 are stratigraphically inverted. However, as shown on table 6, the error associated with each age is relatively large. Within the error ranges, the OSL ages can be viewed as stratigraphically consistent.

Findings derived from WFT-1 follow:

1. The faults documented extend to the ground surface.

2. The UGS samples submitted for OSL age analyses were not from colluvial wedges, but were obtained from faulted alluvial sediments that could be documented along the entire north wall of the trench.

3. Three surface-faulting earthquakes were documented within the past ~ 31 kyr.

4. Displacements of the various geologic units are shown in table 7.

5. The average displacement per surface-faulting earthquake is 4.2 ± feet (1.3 m).

6. The south wall of WFT-1 (drawing 25) did not resemble the north wall and is similar to fault f-6 in T-4 (see drawing 7); displacements documented within the south wall were about 4 feet (1.2 m).

CONCLUSIONS

Based on the scope of work performed for this investigation we conclude:

1. The Washington fault zone crosses parts of the proposed transportation corridor.

2. The UGS has classified the Washington fault zone as a "well-defined late Quaternary (movement within the past 130,000 years) fault," and established a surface-fault-rupture hazard special study area for the fault. The purpose of this investigation was to assess the proposed transportation corridor, particularly the elevated interchange structures, from the standpoint of surface-fault-rupture hazards.

3. Several "well-defined late Quaternary" faults have been documented within the study area (Hayden, 2005; Lund and others, 2008; Biek and others, 2009; Rosenberg Associates, 2009), several of which exhibit geomorphology suggestive of Holocene-age movement.

4. Most of the transportation corridor is underlain by Quaternary-age unconsolidated surficial deposits of alluvial-fan and pediment origin; these deposits cover bedrock units of Triassic and Permian age (Hayden, 2005; Hayden and Willis 2011).

5. Groundwater was not observed in the thirteen exploratory trenches, excavated to maximum depths of about 15 to 20 feet (4.6 to 6.1 m) below existing ground surface.

6. Results of the subsurface exploration indicate the faults documented in the study area are late Pleistocene to Holocene-age; therefore, the faults are considered active for structures associated with the transportation corridor.

7. Multiple surface-faulting earthquakes were documented in this investigation (trenches T-1, T-2, T-4, T-5, T-6, T-11, WFT-1).

8. In this investigation, average displacement per surface-faulting earthquake ranges from about 3.3 to 5 feet (1.1 to 1.5 meters). Three surface faulting earthquakes were documented occurring over the past ~ 31 kyr.

REFERENCES

AGEC (Applied Geotechnical Engineering Consultants), 2007, Surface fault rupture hazard study, proposed Zibby LLC, 47-acre site, Washington Fields, Washington, Utah (AGEC Project No. 2070301): unpublished technical report by Applied Geotechnical Engineering Consultants, Inc., of Sandy, Utah, dated June 11, 2007, prepared for Zibby LLC c/o Rosenberg Associates., St. George, Utah, 14 p.

Biek, R.F., Rowley, P.D., Hayden, J.M., Hacker, D.B., Willis, G.C., Hintze, L.F., Anderson, R.E., and Brown, K.D., 2009, Geologic map of the St. George and east part of the Clover Mountains 30' X 60' quadrangles, Washington and Iron Counties, Utah: Utah Geological Survey Map M-242, scale 1:100,000, DVD.

Black, B.D., Hecker, Suzanne, Hylland, M.D., Christenson, G.E., and McDonald, G.N., 2003, Quaternary fault and fold database and map of Utah: Utah Geological Survey Map 193DM, CD.

ESA (Earth Science Associates), 1982, Seismic safety investigation of eight SCS dams in southwestern Utah: unpublished consultant's report for the U.S. Soil Conservation Service, Portland, Oregon, 2 volumes.

Hayden, J.M., 2005, Geologic map of the Washington Dome quadrangle, Washington County, Utah: Utah Geological Survey Map 209, scale 1:24,000.

Hayden, J.M., and Willis, G.C., 2011, Geologic map of the St. George 7.5' quadrangle, Washington County, Utah: Utah Geological Survey Map 251DM, 20 p., 2 plates, scale1:24,000.

International Code Council, 2009, International building code: Country Club Hills, Illinois, 678 p.

Lund, W.R., Knudsen, T.R., Vice, G.S., and Shaw, L.M., 2008, Geologic hazards and adverse construction conditions, St. George – Hurricane metropolitan area, Washington County, Utah: Utah Geological Survey Special Study 127, 105 p, 14 plates, DVD.

Rosenberg Associates, 2009, Surface-fault-rupture hazard evaluation, Task I, Interchange 10 and 11, Southern Parkway, (Rosenberg Associates project no. 5507-P3 09R036.G), dated September 3, 2009: prepared for Horrocks Engineering, Pleasant Grove, Utah.

WGR, 2011, Western GeoArch Research, LLC., Geoarchaeological assessment of 42ws5277 and a proposed detention basin in the Southern Parkway study area, Washington, Utah: prepared for Horrocks Engineers Inc. (Pleasant Grove, Utah) and Utah Department of Transportation, dated March 2011, 70 p.

AERIAL PHOTOGRAPH REFERENCES

SOURCE	DATE	PHOTOGRAPHS	SCALE
BLM	07-19-2000	1-14 nos. 4 through 10	1:24,000
ESA (1982)	10-23-1982	AM: 6-3 through 6-7	1:24,000
		PM: 6-1 through 6-12	1:24,000

Table 1. *Site geologic units.*

Geologic Unit	**Unit Designation on Trench Profiles, Drawings 2 -22**	**Geologic Age**	**Approximate age** (years before present)
Pedogenic A-horizon	1	Holocene	≤ 2500 ±
Fault-scarp-derived colluvium	2	Holocene	≤ 1500 ±
Fan alluvium	3	Holocene to Pleistocene	≤ 150,000 ±
Bedrock units	4	Triassic	240 ± million

Table 2. *Purpose of trenches.*

Trench No.	Purpose					
	Evaluate subsurface deposits for the presence of faulting.	Evaluate Surface-Fault-Rupture Special Study area for the presence of faulting.	Verify the presence or absence of mapped faults within the study area as indicated by others.*	Evaluate lineaments identified from aerial photographs and topographic maps.	Supplemental trench to provide additional exposures for evaluating age of movement.	Generate detailed log so ages obtained by the UGS could be utilized for evaluating age of movement.
T-1	■	■	■			
T-2	■	■	■			
T-3	■	■	■			
T-4	■				■	
T-5	■	■	■			
T-6	■	■	■			
T-7	■	■		■		
T-8	■			■		
T-9	■			■		
T-10	■			■		
T-11	■	■	■			
T-12	■			■		
T-13	■	■				
WFT-1 North Wall						■
WFT-1 South Wall						■

** Hayden, 2005; Rosenberg Associates, 2009; Biek and others, 2009; Hayden and Willis, 2011.

Table 3. *Summary of trench data.*

Trench	Length		Fault(s) Documented	Trench Orientation
	(ft)	(m)		
T-1	537.5	163.9	■	S. 85° W.
T-2	109.5	33.4	■	S. 85° W.
T-3	407.5	124.2		S. 87° W.
T-4	92.5	128.2	■	S. 87° W.
T-5	460.0	137.2		S. 80° W.
T-6	340.5	103.8	■	S. 86° W.
T-7	421.0	128.3		S. 77° W.
T-8	242.5	73.9	■	S. 81° W.
T-9	63.5	19.4	■	N. 89° W.
T-10	53.0	16.2	■	S. 79° W.
T-11	473.5	144.3	■	N. 80° W.
T-12	226.5	69.0	■	N. 89° E.
T-13	181.0	55.2		N. 90° W.
WFT-1 North Wall	75.0	22.9	■	N. 89° W.
WFT-1 South Wall	28.0	8.5	■	N. 89° W.

Table 4. *Table of displacements per surface-faulting earthquake.*

Trench	Number of Surface-Faulting Earthquakes	Average Displacement Per Surface-Faulting Earthquake
T-1	2	≥ 3.2 ft. (1 m)
T-2	unknown	Could not be determined
T-4	2	3.3 ft. (1 m)
T-6	unknown	Could not be determined
WFT-1	4	3.5 to 6.5 ft. (1 to 2 m)

Table 5. *Ages from Washington Fields Trench WFT-1.*

Geologic Unit (youngest to oldest)	UGS Sample No.	RA Sample No.	OSL (B.P.)	14C[1] RCYBP	cal yr B.P.[2]	Description
12		WF S-1		645 ± 15	600 - 550	colluvial wedge
10	WD-3	WF S-2	18,590 ± 1160	530 ± 15	560 - 510	alluvium
15		WF S-3		925 ± 15	920 - 790	colluvial wedge
1	WD-5		30,810 ± 2110			alluvium
2	WD-4		30,590 ± 2100			alluvium
5	WD-2		75,570 ± 5130			alluvium
6	WD-1		67,750 ± 4560			alluvium

1 radiocarbon age
2 at two-sigma level

Table 6. *OSL age ranges for WFT-1.*

Unit (youngest to oldest)	**Age (B.P.)**	**B.P. Error (±)**	**Error Age Range (B.P.)**
10	18,590	1160	19,750 to 17,430
1	30,810	2110	32,920 to 28,700
2	30,590	2100	32,960 to 28,490
5	75,570	5130	80,700 to 70,440
6	67,750	4560	72,310 to 63,190

Table 7. *Cumulative displacements within WFT-1.*

Unit (oldest to youngest)	**Cumulative Displacement**	**Displacement**
7	23 ft (7 m)	unknown
5	19 ft (5.8 m)	4 ft (1.2 m)
3	14 ft (4.3 m)	5 ft (1.5 m)
1	10.5 ft (3.2 m)	3.5 ft (1.1 m)
9	4 ft (1.2 m)	6.5 ft (2 m)

LEGEND

Strike and dip of inclined bedding showing angle of Dip

Direction and Angle of Dip of Fault Plane

Test Pits

Phase 3A Alignment

Approx. Location of AGEC Trenches (2007)

Approx. Location of ESA Trenches (1982)

Approx. Location of RA Trenches (2010)

Fault1982

Silt Area

Faults

Pkh	Harrisburg Member of the Kaibab Formation
Qf	Artificial Fills
Qal	Stream Deposits
Qao	Older Alluvium
Qat	Stream Terrace Deposits
Qaf	Alluvial-Fan Deposits
Qe	Eolian Sand Deposits
Qed	Eolian Dune Sand Deposits
Qeo	Older Eolian Sand and Caliche Deposits
Qe/ Qafm	Older Eolian Sand and Caliche Deposits
Qms	Landslide Deposits
Qmt	Talus Deposits
Qc	Colluvial Deposits
Qac	Mixed Alluvial and Colluvial Deposits
Qae	Mixed Alluvial and Eolian Deposits
Qea	Mixed Eolian and Alluvial Deposits
Qbr	Radio Tower Flow
Qbv Qbvc 1-3	Volcano Mountain Flows, Cinder Cone, and Associated Deposits
Qbcp Qbcpc	Cinder Pits Flow
Qbi Qbic Qec/Qbi Qagi	Ivans Knoll Flow, Cinder Cone, and Associated Deposits
Qb	Basalt Flows Undivided
Jn	Navajo Sandstone
Jk	Kayenta Formation
Jms	Springdale Sandstone Member of the Moenave Formation
Jmw	Whitmore Point Member of the Moenave Formation
Jmd	Dinosaur Canyon Member of the Moenave Formation
TRcp	Petrified Forest Member of the Chinle Formation
TRcs	Shinarump Conglomerate Member of the Chinle Formation
TRmu	Upper Red Member of the Moenkpi Formation
TRms	Shnabkaib Member of the Moenkopi Formation
TRmm	Middle Red Member of the Moenkopi Formation
TRmv	Virgin Limestone Member of the Moenkopi Formation
TRml	Lower Red Member of the Moenkopi Formation

Revised: 6/13/2011

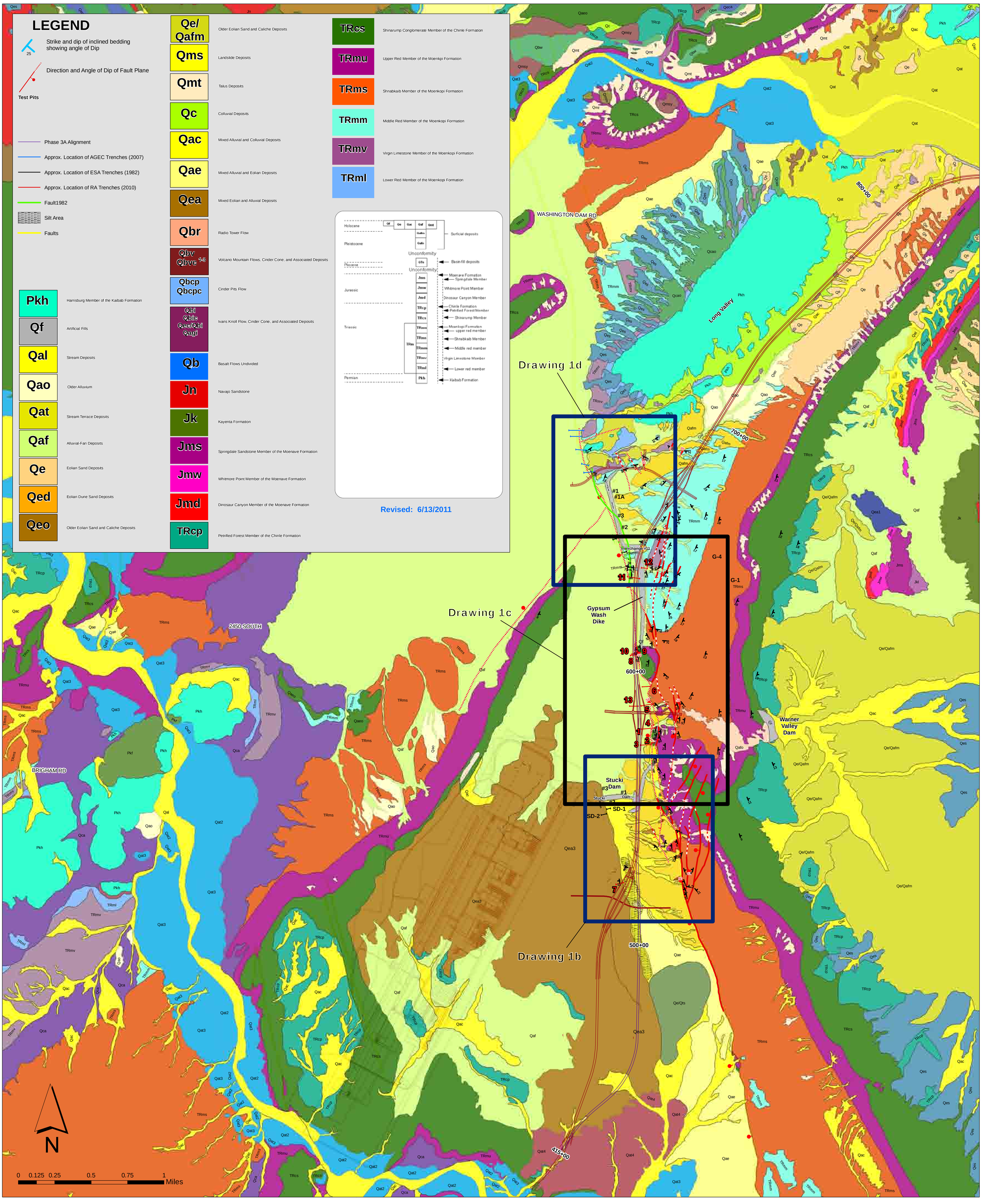

Drawing 1a. Geologic map

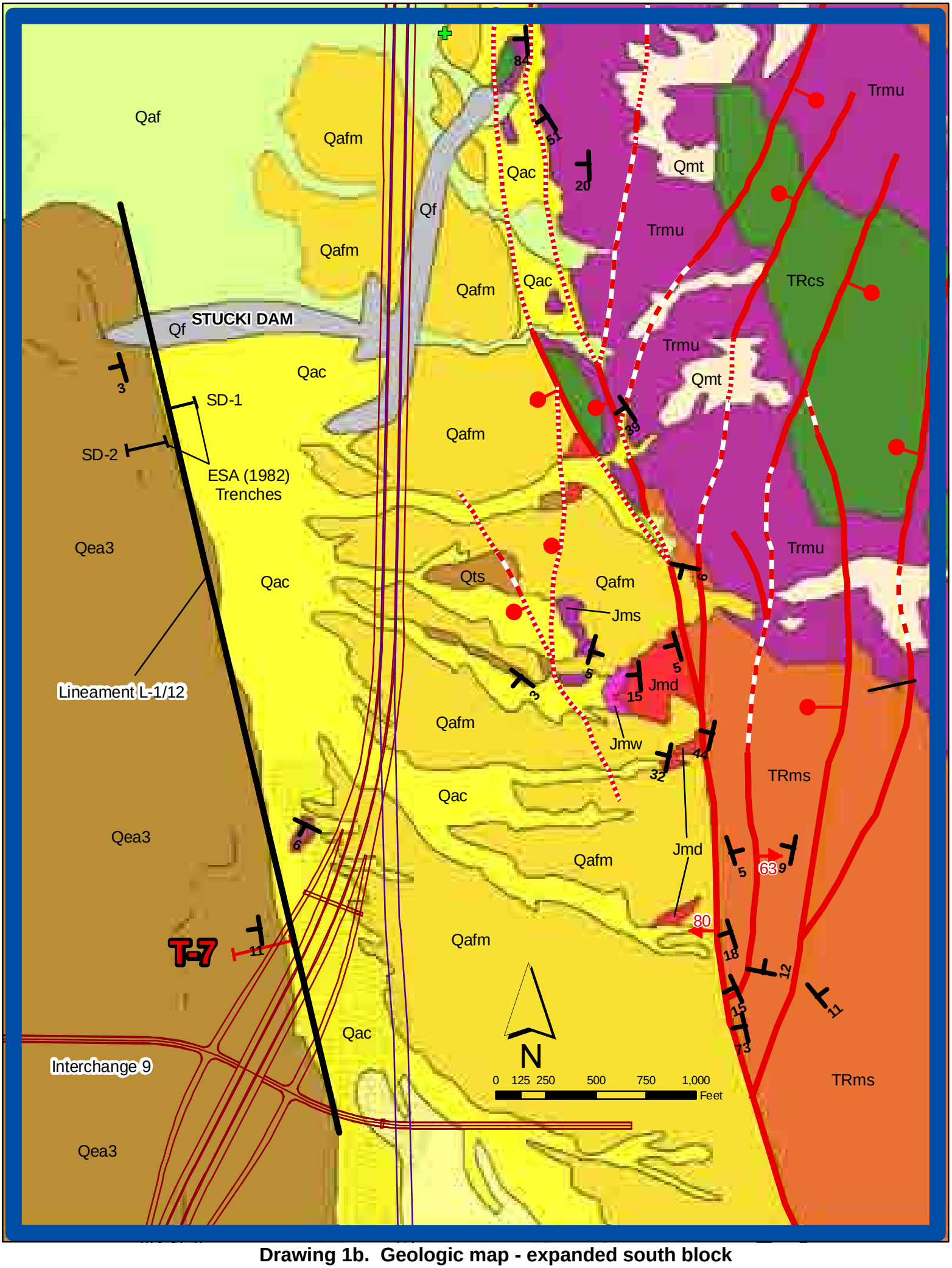

Drawing 1b. Geologic map - expanded south block

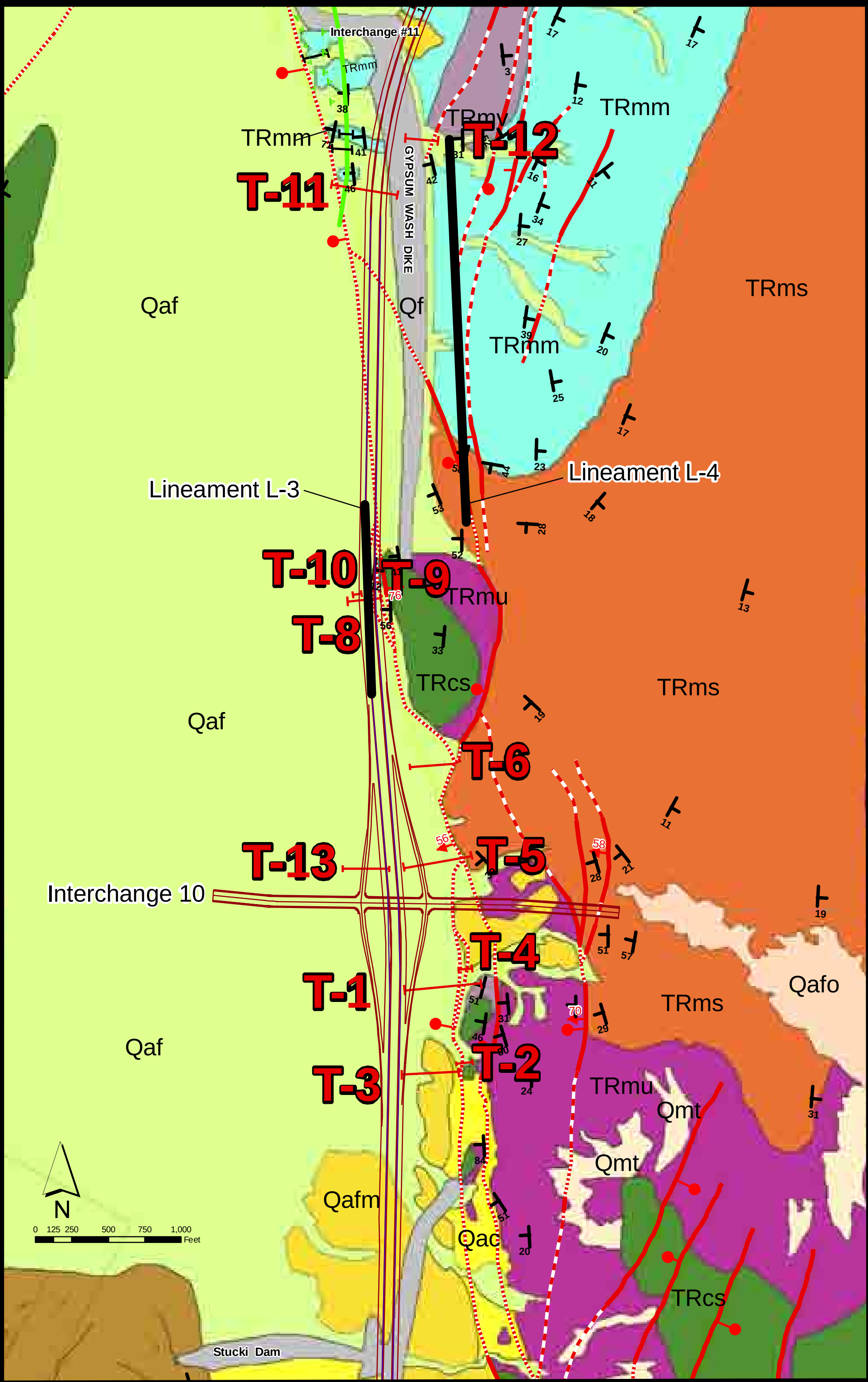

Drawing 1c. Geologic map - expanded middle block

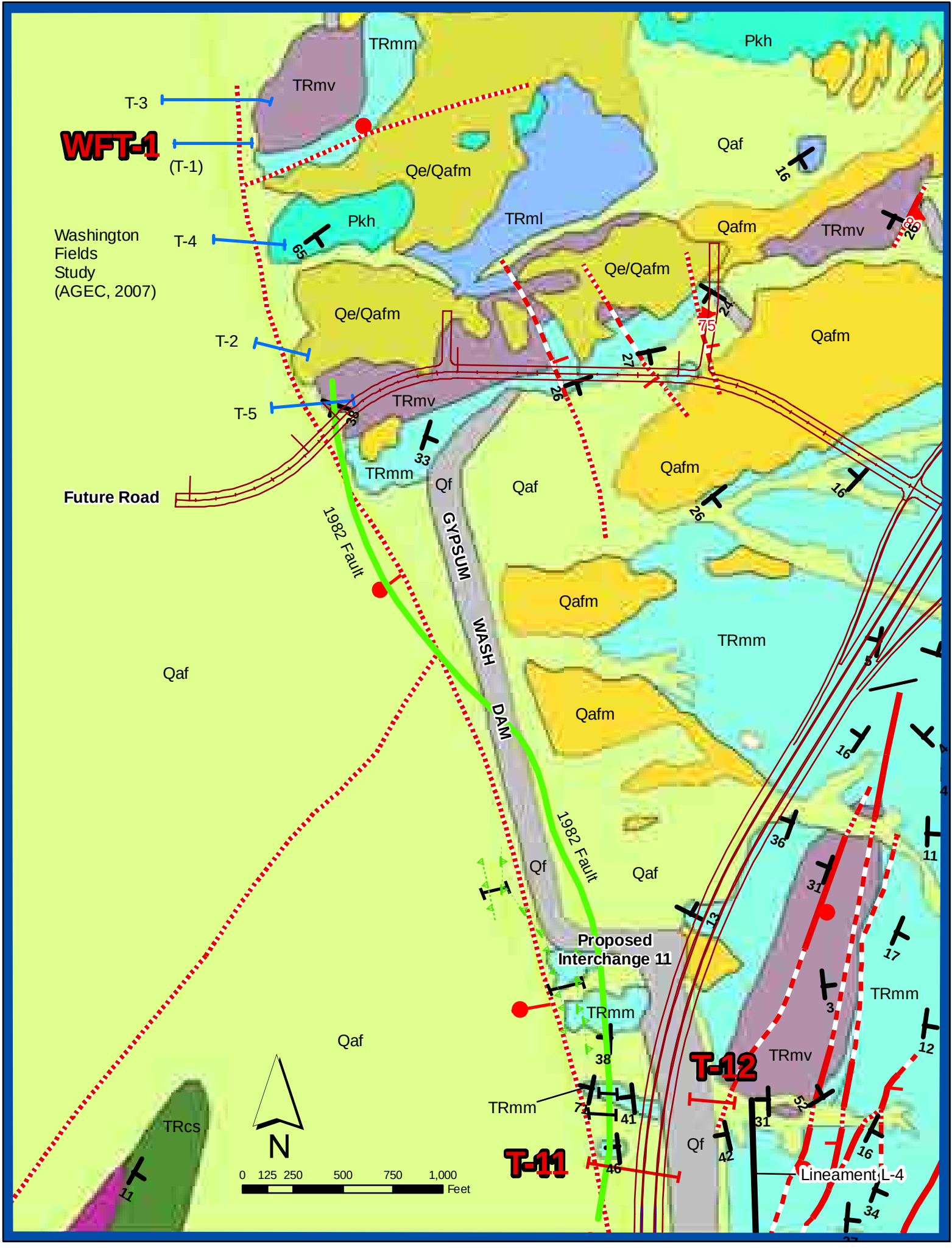

Drawing 1d. Geologic map - expanded north block

T-1

SOUTH WALL

N 85° E

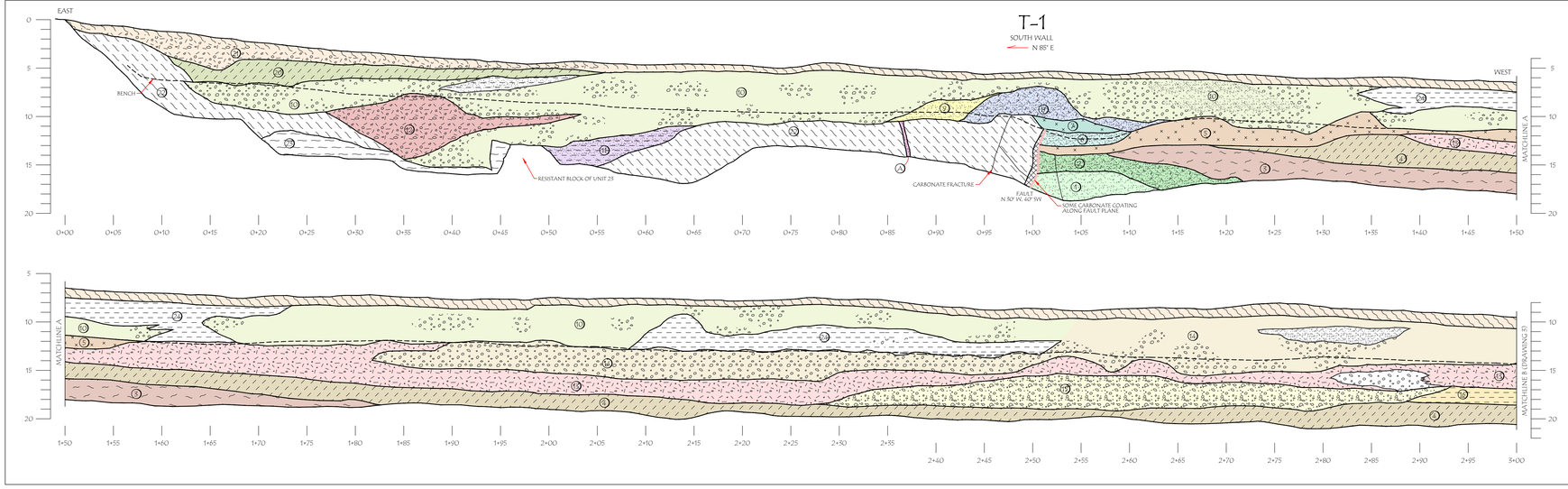

1. ALLUVIUM: SAND (SP) WITH SOME SILT, VERY FINE GRAINED; YELLOWISH RED (5YR 5/6).
2. ALLUVIUM: SILTY SAND (SM), VERY FINE GRAINED; REDISH YELLOW (5YR 7/6), MASSIVE.
3. ALLUVIUM: SILT (ML) WITH SOME VERY FINE GRAINED SAND WITH PINKISH WHITE (5YR 8/2) CARBONATE NODULES ≤ 0.5 INCHES LONG; RED (2.5YR 4/6), MASSIVE.
4. ALLUVIUM: SILT (ML) WITH VERY FINE GRAINED SAND; REDDISH BROWN (2.5YR 4/4) TO RED (2.5YR 4/6) WITH SOME CLAY, PIN-HOLE VOIDS, CARBONATE FILAMENTS, CARBONATE NODULES ≤ 0.2 INCHES LONG, MASSIVE.
5. ALLUVIUM (EOLIAN): SILT (ML), REDDISH YELLOW (5YR 6/8) WITH ≤5% CARBONATE FILAMENTS ≤ 0.1 INCH LONG.
6. FAULT DERIVED COLLUVIUM: SILT (ML) WITH SOME VERY FINE SAND; YELLOWISH RED (5YR 4/6).
7. FAULT DERIVED COLLUVIUM: SILT (EOLIAN?) LIGHT BROWN (7.5YR 6/4).
8. ALLUVIUM: SANDY SILT (ML) WITH ABOUT 25 ANGULAR TO SUBANGULAR CLASTS ≤ 1-INCH LONG, AVERAGE SIZE ≤ 0.2-INCHES, REDDISH YELLOWISH (7.5YR 6/6).
9. ALLUVIUM: SAND (SP) FINE TO COARSE GRAINED, WEAK HORIZONTAL BEDDING, WITH THIN (4 INCH THICK) DISCONTINUOUS LAYERS OF SILT AND 1±5 ANGULAR CLASTS ≤ 1-INCH LONG, AVERAGE SIZE ≤ 0.5 INCHES, STRONG BROWN (7.5YR 5/8).
10. GRAVELLY SAND (SP) MEDIUM TO COARSE GRAINED, WEAK HORIZONTAL BEDDING, 50-40% ANGULAR TO SUBANGULAR CLASTS ≤ 12 INCHES LONG, AVERAGE SIZE ≤ 5 INCHES, STRONG BROWN (7.5YR 5/8)
11. ALLUVIUM: SILT (ML), GYPSIFEROUS WITH CARBONATE FILAMENTS AND CARBONATE NODULES (~0.1-INCH), YELLOWISH RED (5YR 5/6).
12. ALLUVIUM: GRAVELLY SILT (ML) WITH SOME VERY FINE SAND AND 5-15% SUBANGULAR TO ANGULAR CLASTS ≤ 4-INCHES, AVERAGE SIZE ≤ 2 INCHES, WITH DISCONTINUOUS LAYERS OF VERY FINE SAND AND SANDY SILT, REDDISH YELLOW (5YR 6/6).
13. ALLUVIUM: SANDY SILT (ML) TO SILT (ML) WITH SOME SAND, DISCONTINUOUS PEBBLY SAND LENSES, CARBONATE FILAMENTS, AND 1-2% ANGULAR CLASTS ≤ 0.5 INCHES LONG, LIGHT BROWN (7.5YR 6/4).
14. ALLUVIUM: GRAVELLY SAND (SP) YELLOWISH RED (5YR 4/6), MEDIUM TO COARSE GRAINED, WITH ANGULAR CLASTS ≤ 6 INCHES, AVERAGE SIZE ≤ 4 INCHES, DISCONTINUOUS COARSE GRAINED SAND, PEBBLY SAND, AND SANDY GRAVEL LENSES, WEAK HORIZONTAL BEDDING.
15. ALLUVIUM: SAND (SP) MEDIUM TO COARSE GRAINED, WEAK HORIZONTAL, BEDDING WITH 5% ANGULAR CLASTS ≤ 2 INCHES LONG, AVERAGE SIZE ≤ 1-INCH, DISCONTINUOUS LENSES OF SANDY GRAVEL, PEBBLY SAND; YELLOWISH RED (5YR 4/6).
16. ALLUVIUM EOLIAN: SILT (ML) REDDISH YELLOW (5YR 6/6) WITH ≤ 1% ANGULAR CLASTS ≤ 0.5 INCHES LONG, AVERAGE SIZE ≤0.2 INCHES, CARBONATE FILAMENTS, THIN (≤ 1-INCH THICK) DISCONTINUOUS VERY FINE GRAINED SAND, AND CARBONATE LENSES.
20. ALLUVIUM: SANDY SILT (ML), MASSIVE, GYPSIFEROUS, WITH CARBONATE CLASTS (≤ 0.01 INCH), REDDISH YELLOW (5YR 6/6).
21. ALLUVIUM: SILTY SAND (SM), VERY FINE GRAINED, WITH 5% ANGULAR CLASTS ≤ 12 INCHES LONG, AVERAGE SIZE ≤ 4 INCHES, RED (2.5YR 4/6) WITH MODERN ORGANIC (A) HORIZON.
- A. FRACTURE FILLED WITH SANDY SILT YELLOWISH RED (5YR 4/6).
22. BEDROCK: MUDSTONE, THINLY BEDDED, FRACTURED, WEAK RED (10R 4/2), (PETRIFIED FOREST MEMBER OF THE CHINLE FORMATION).
23. BEDROCK: SANDSTONE, THINLY TO MODERATELY BEDDED, FRACTURED, WHITE (5YR 8/1).

SCALE: 1" = 5'

TRENCH PROFILE T-1

SOUTHERN CORRIDOR PHASE 3

WASHINGTON COUNTY, UTAH

ROSENBERG ASSOCIATES — CIVIL ENGINEERS · LAND SURVEYORS

PROJECT #	DRAWING #
5507-P3	2

T-1 (CONTINUED)

SOUTH WALL

N 85° E

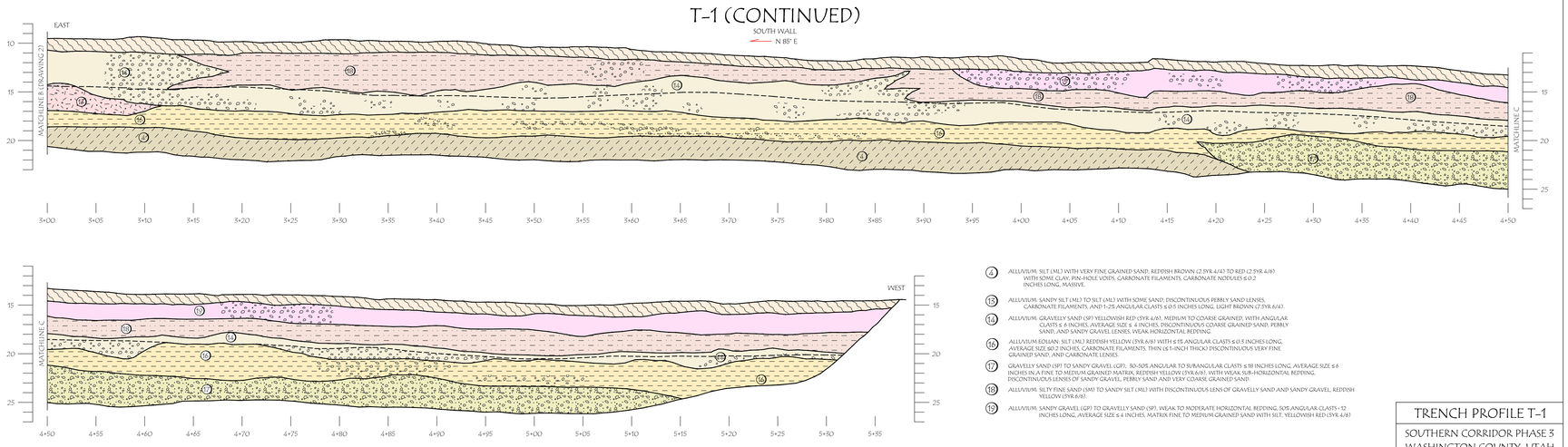

4. ALLUVIUM: SILT (ML) WITH VERY FINE GRAINED SAND; REDDISH BROWN (2.5YR 4/4) TO RED (2.5YR 4/6) WITH SOME CLAY, PIN-HOLE VOIDS, CARBONATE FILAMENTS, CARBONATE NODULES ≤ 0.2 INCHES LONG, MASSIVE.
13. ALLUVIUM: SANDY SILT (ML) TO SILT (ML) WITH SOME SAND, DISCONTINUOUS PEBBLY SAND LENSES, CARBONATE FILAMENTS, AND 1-2% ANGULAR CLASTS ≤ 0.5 INCHES LONG, LIGHT BROWN (7.5YR 6/4).
14. ALLUVIUM: GRAVELLY SAND (SP) YELLOWISH RED (5YR 4/6), MEDIUM TO COARSE GRAINED, WITH ANGULAR CLASTS ≤ 6 INCHES, AVERAGE SIZE ≤ 4 INCHES, DISCONTINUOUS COARSE GRAINED SAND, PEBBLY SAND, AND SANDY GRAVEL LENSES, WEAK HORIZONTAL BEDDING.
16. ALLUVIUM EOLIAN: SILT (ML) REDDISH YELLOW (5YR 6/6) WITH ≤ 1% ANGULAR CLASTS ≤ 0.5 INCHES LONG, AVERAGE SIZE ≤0.2 INCHES, CARBONATE FILAMENTS, THIN (≤ 1-INCH THICK) DISCONTINUOUS VERY FINE GRAINED SAND, AND CARBONATE LENSES.
17. GRAVELLY SAND (SP) TO SANDY GRAVEL (GP), 30-50% ANGULAR TO SUBANGULAR CLASTS ≤ 18 INCHES LONG, AVERAGE SIZE ≤ 6 INCHES IN A FINE TO MEDIUM GRAINED MATRIX, REDDISH YELLOW (5YR 6/6), WITH WEAK SUB-HORIZONTAL BEDDING, DISCONTINUOUS LENSES OF SANDY GRAVEL, PEBBLY SAND AND VERY COARSE GRAINED SAND.
18. ALLUVIUM: SILTY FINE SAND (SM) TO SANDY SILT (ML) WITH DISCONTINUOUS LENS OF GRAVELLY SAND AND SANDY GRAVEL, REDDISH YELLOW (5YR 6/6).
19. ALLUVIUM: SANDY GRAVEL (GP) TO GRAVELLY SAND (SP), WEAK TO MODERATE HORIZONTAL BEDDING, 50% ANGULAR CLASTS ≤ 12 INCHES LONG, AVERAGE SIZE ≤ 4 INCHES, MATRIX FINE TO MEDIUM GRAINED SAND WITH SILT, YELLOWISH RED (5YR 4/6)

SCALE: 1" = 5'

TRENCH PROFILE T-1

SOUTHERN CORRIDOR PHASE 3

WASHINGTON COUNTY, UTAH

ROSENBERG ASSOCIATES — CIVIL ENGINEERS · LAND SURVEYORS

PROJECT #	DRAWING #
5507-P3	3

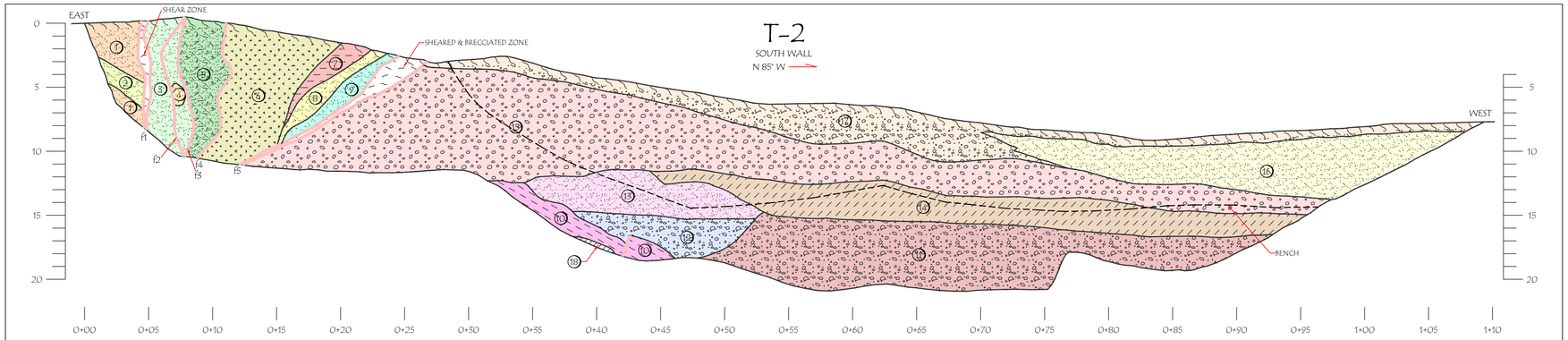

FAULT	ORIENTATION (STRIKE)	INCLINATION (DIP)	COMMENTS
f1	N 20° W	VERTICAL	0.2 TO 12-INCH WIDE CLAY GOUGE ZONE WITH GYPSUM YELLOW (5YR 6/6).
f2	N 05° W	VERTICAL	0.2-INCH WIDE CLAY GOUGE ZONE WITH GYPSUM, RED (2.5YR 4/6) AND LIGHT REDDISH GRAY (2.5YR 7/1).
f3	N 10° W	VERTICAL	0.2-INCH WIDE CLAY GOUGE ZONE WITH GYPSUM, LIGHT REDDISH GRAY (2.5YR 7/1).
f4	N 10° W	VERTICAL	0.15-INCH WIDE CLAYEY SAND GOUGE ZONE.
f5	N 08° W	65° E	0.2 TO 12-INCH WIDE SHEAR AND BRECCIATED CLAY GOUGE ZONE ALONG EAST SIDE OF FAULT, FISSURE, DARK GRAY (10YR 4/1).

1. BEDROCK (MOENKOPI FORMATION): SANDSTONE, WHITE (5YR 8/1), FINE TO MEDIUM GRAINED, WITH SOME IRON OXIDE STAINING AND IRON OXIDE NODULES.
2. SANDSTONE, LIGHT REDDISH BROWN (2.5YR 7/3), FRACTURED.
3. SILTY SANDSTONE, FINE GRAINED, MASSIVE, SOME IRON OXIDE STAINING, VERY PALE BROWN (10YR 8/4).
4. FRAGMENT OF MOENKOPI BEDROCK, SANDSTONE, RED (2.5YR 4/6), BRECCIATED.
5. BEDROCK: SILTY SANDSTONE, YELLOW (10YR 7/6), VERY FINE GRAINED, BRECCIATED.
6. BEDROCK: RED (2.5YR 5/6), CLAYSTONE, BRECCIATED WITH ≤ 6 TO 8-INCH LONG CLASTS OF REDDISH GRAY (2.5YR 1/6) TO PALE RED (2.5YR 6/2) SANDSTONE.
7. BEDROCK: GYPSIFEROUS CLAYSTONE, SHEARED / BRECCIATED, YELLOW (10YR 8/6).
8. BEDROCK: SANDSTONE, SHEARED / BRECCIATED, LIGHT GRAY (7.5YR 7/1).
9. BEDROCK: CLAYSTONE, SHEARED / BRECCIATED, WHITE (10YR 8/1) WITH IRON OXIDE STAINING
10. BEDROCK (MOENKOPI FORMATION): SANDSTONE, THIN BEDDED WITH INTERBEDS OF "PURPLE" SILTSTONE.
11. FAN ALLUVIUM: SANDY SILT (ML), YELLOWISH RED (5YR 5/6), MASSIVE DENSE, WITH 10% ANGULAR SANDSTONE CLASTS ≤ 18 INCHES LONG, AVERAGE SIZE ≤ 12 INCHES.
12. FAN ALLUVIUM: SILTY SAND (SM), VERY FINE GRAINED, REDDISH YELLOW (5YR 7/6) WITH 5% SANDSTONE CLASTS ≤ 10 INCHES LONG, AVERAGE SIZE ≤ 6 INCHES, MASSIVE.
13. FAN ALLUVIUM: SILTY SAND (SM), VERY FINE GRAINED, DENSE, MASSIVE, WITH 2% ANGULAR CLASTS ≤ 1 INCH LONG, PINK (7.5YR 7/4).
14. FAN ALLUVIUM: SANDY SILT (ML), YELLOWISH RED (5YR 4/6), GYPSIFEROUS.
15. FAN ALLUVIUM: SANDY SILT (ML), VERY FINE GRAINED, RED (2.5YR 5/6) WITH 3 TO 5% ANGULAR PALE RED (2.5YR 7/2) SANDSTONE CLASTS ≤ 12 INCHES LONG, AVERAGE SIZE ≤ 4 INCHES, SOME CARBONATE NODULES AND FILAMENTS.
16. SAND (SP) WITH SILT, VERY FINE GRAINED, PIN-HOLE VOIDS, WITH 2% CLASTS ≤ 1 INCH LONG, GYPSIFEROUS, YELLOWISH RED (5YR 4/6).
17. SILTY SAND (SM), VERY FINE GRAINED WITH 20% ANGULAR CLASTS ≤ 12 INCHES LONG, AVERAGE SIZE ≤ 6 INCHES, AND DISCONTINUOUS GRAVEL AND COARSE GRAINED SAND LENSES, REDDISH BROWN (5YR 5/4)
18. BEDROCK (MOENKOPI FORMATION): CLAYSTONE, PURPLE.

SCALE: 1" = 5'

TRENCH PROFILE T-2

SOUTHERN CORRIDOR PHASE 3
WASHINGTON COUNTY, UTAH

ROSENBERG & ASSOCIATES
CIVIL ENGINEERS • LAND SURVEYORS

PROJECT #	DRAWING #
5507-P3	4

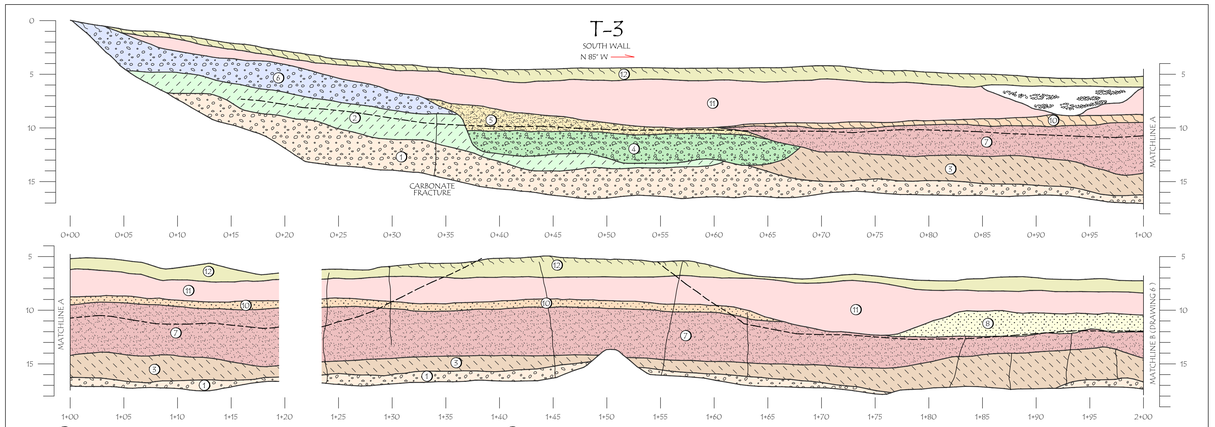

1. FAN ALLUVIUM: SANDY SILT (ML); YELLOWISH RED (5YR 5/6), MASSIVE, DENSE, WITH 10% ANGULAR SANDSTONE CLASTS ≤ 18 INCHES, AVERAGE SIZE ≤ 12 INCHES
2. FAN ALLUVIUM: SANDY SILT (ML); YELLOWISH RED (5YR 4/6), GYPSUM, WITH 5% SUBANGULAR CLASTS, AT EAST END WHERE TRENCH IS NEAR BEDROCK OUTCROP (STA 0+25)
3. SANDY SILT (ML); MASSIVE, DENSE, SOME GYPSUM, YELLOWISH RED (5YR 5/6) (STA 0+68)
4. GRAVELLY SAND (SP) FINE TO MEDIUM GRAINED WITH 20% SUBANGULAR CLASTS ≤ 18 INCHES, AVERAGE SIZE ≤ 0.5 INCHES, LIGHT BROWN (7.5YR 6/4), GYPSUM (STA 0+85)
5. SANDY SILT (ML) WITH 5% SUBANGULAR TO ANGULAR CLASTS ≤ 1 INCH AVERAGE SIZE ≤ 0.5 INCHES, YELLOWISH RED (5YR 5/6) (STA 0+88)
6. SANDY SILT (ML); YELLOWISH RED (5YR 4/6) WITH 15% ANGULAR CLASTS ≤ 24 INCHES, AVERAGE SIZE 12 INCHES, LARGER CLASTS CONCENTRATED ALONG TOP OF UNIT (STA 0+15)
7. SILTY SAND (SM) VERY FINE GRAINED, MASSIVE, SOME GYPSUM WITH 15 ANGULAR CLASTS ≤ 10 INCHES, AVERAGE SIZE ≤ 2 INCHES REDDISH YELLOW (5YR 6/8)
8. ALLUVIUM: SAND (SP), FINE TO MEDIUM GRAINED WITH SOME SILT AND 5% ANGULAR CLASTS ≤ 6 INCHES AVERAGE SIZE ≤ 5 INCHES, GYPSUM, RED (2.5YR 4/6)
9. ALLUVIUM: SAND (SP) FINE GRAINED, DENSE, MASSIVE WITH 20% ANGULAR CLASTS ≤ 5 INCHES, GYPSUM, LIGHT REDDISH BROWN (5YR 6/4)
10. ALLUVIUM: SAND (SP) FINE TO MEDIUM GRAINED; DARK RED (2.5YR 3/6) WITH MODERATE GYPSUM AND 5% ANGULAR CLASTS (PRIMARILY SANDSTONE) ≤ 4 INCHES
11. ALLUVIUM / COLLUVIUM: SANDY SILT (ML); MASSIVE, DENSE, YELLOWISH RED (5YR 5/6), WITH SOME GRAVEL LENSES AND PIN-HOLE VOIDS
12. ALLUVIUM / COLLUVIUM: SILTY SAND (SM) VERY FINE GRAINED, REDDISH BROWN (5YR 5/4) TO YELLOWISH RED (5YR 5/6) WITH GRAVEL LENSES, AND MODERN ORGANIC (A) HORIZON

SCALE: 1" = 5'

TRENCH PROFILE T-3		
SOUTHERN CORRIDOR PHASE 3 WASHINGTON COUNTY, UTAH		
ROSENBERG ENGINEERING CIVIL ENGINEERING • LAND SURVEYING	PROJECT # 5507-P5	DRAWING # 5

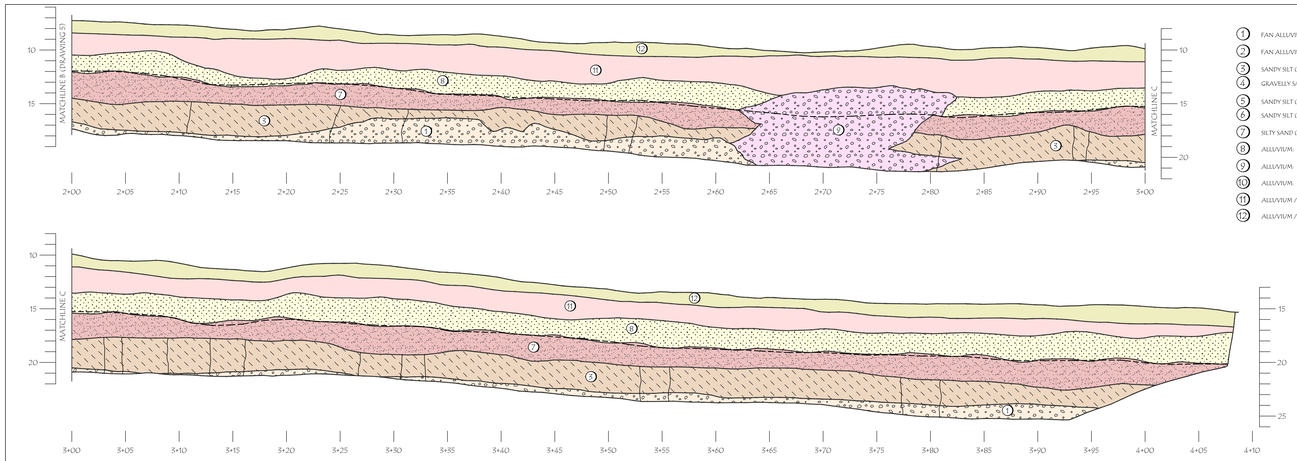

1. FAN ALLUVIUM: SANDY SILT (ML); YELLOWISH RED (5YR 5/6), MASSIVE, DENSE, WITH 10% ANGULAR SANDSTONE CLASTS ≤ 18 INCHES, AVERAGE SIZE ≤ 12 INCHES
2. FAN ALLUVIUM: SANDY SILT (ML); YELLOWISH RED (5YR 4/6), GYPSUM, WITH 5% SUBANGULAR CLASTS, AT EAST END WHERE TRENCH IS NEAR BEDROCK OUTCROP (STA 0+25)
3. SANDY SILT (ML); MASSIVE, DENSE, SOME GYPSUM, YELLOWISH RED (5YR 5/6) (STA 0+68)
4. GRAVELLY SAND (SP) FINE TO MEDIUM GRAINED WITH 20% SUBANGULAR CLASTS ≤ 18 INCHES, AVERAGE SIZE ≤ 0.5 INCHES, LIGHT BROWN (7.5YR 6/4), GYPSUM (STA 0+85)
5. SANDY SILT (ML) WITH 5% SUBANGULAR TO ANGULAR CLASTS ≤ 1 INCH AVERAGE SIZE ≤ 0.5 INCHES, YELLOWISH RED (5YR 5/6) (STA 0+88)
6. SANDY SILT (ML); YELLOWISH RED (5YR 4/6) WITH 15% ANGULAR CLASTS ≤ 24 INCHES, AVERAGE SIZE 12 INCHES, LARGER CLASTS CONCENTRATED ALONG TOP OF UNIT (STA 0+15)
7. SILTY SAND (SM) VERY FINE GRAINED, MASSIVE, SOME GYPSUM WITH 15 ANGULAR CLASTS ≤ 10 INCHES, AVERAGE SIZE ≤ 2 INCHES REDDISH YELLOW (5YR 6/8)
8. ALLUVIUM: SAND (SP), FINE TO MEDIUM GRAINED WITH SOME SILT AND 5% ANGULAR CLASTS ≤ 6 INCHES AVERAGE SIZE ≤ 5 INCHES, GYPSUM, RED (2.5YR 4/6)
9. ALLUVIUM: SAND (SP) FINE GRAINED, DENSE, MASSIVE WITH 20% ANGULAR CLASTS ≤ 5 INCHES, GYPSUM, LIGHT REDDISH BROWN (5YR 6/4)
10. ALLUVIUM: SAND (SP) FINE TO MEDIUM GRAINED; DARK RED (2.5YR 3/6) WITH MODERATE GYPSUM AND 5% ANGULAR CLASTS (PRIMARILY SANDSTONE) ≤ 4 INCHES
11. ALLUVIUM / COLLUVIUM: SANDY SILT (ML); MASSIVE, DENSE, YELLOWISH RED (5YR 5/6), WITH SOME GRAVEL LENSES AND PIN-HOLE VOIDS
12. ALLUVIUM / COLLUVIUM: SILTY SAND (SM) VERY FINE GRAINED, REDDISH BROWN (5YR 5/4) TO YELLOWISH RED (5YR 5/6) WITH GRAVEL LENSES, AND MODERN ORGANIC (A) HORIZON

SCALE: 1" = 5'

TRENCH PROFILE T-3		
SOUTHERN CORRIDOR PHASE 3 WASHINGTON COUNTY, UTAH		
ROSENBERG ENGINEERING CIVIL ENGINEERING • LAND SURVEYING	PROJECT # 5507-P5	DRAWING # 6

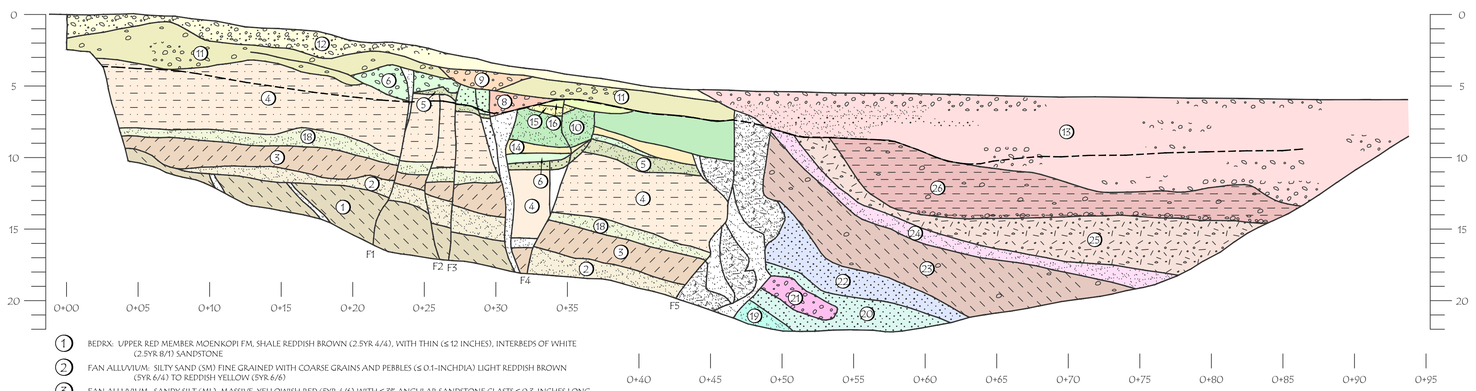

1. BEDRX: UPPER RED MEMBER MOENKOPI FM, SHALE REDDISH BROWN (2.5YR 4/4), WITH THIN (≤ 12 INCHES), INTERBEDS OF WHITE (2.5YR 8/1) SANDSTONE
2. FAN ALLUVIUM: SILTY SAND (SM) FINE GRAINED WITH COARSE GRAINS AND PEBBLES (≤ 0.1-INCH DIA) LIGHT REDDISH BROWN (5YR 6/4) TO REDDISH YELLOW (5YR 6/6)
3. FAN ALLUVIUM: SANDY SILT (ML), MASSIVE, YELLOWISH RED (5YR 4/6) WITH ≤ 3% ANGULAR SANDSTONE CLASTS ≤ 0.3-INCHES LONG, DENSE
4. FAN ALLUVIUM: SANDY SILT (ML), MASSIVE, VERY DENSE, YELLOWISH RED (5YR 4/6) WITH COARSE GRAINED SAND AND PEBBLE (≤ 0.1 INCH), ANGULAR SANDSTONE CLASTS ≤ 2 INCHES LONG, AND GYPSUM
5. WIND BLOWN SAND (SP) FINE GRAINED, HORIZONTAL, VERY THIN (≤ 0.2 INCH THICK) BEDDING, SOME WEAK CROSS-BEDDING, REDDISH YELLOW (5YR 6/8)
6. FAN ALLUVIUM: SILTY SAND (SP), FINE TO MEDIUM GRAINED WITH 20% SUBANGULAR CLASTS ≤ 2 INCHES, AVERAGE SIZE ≤ 0.5 INCHES, REDDISH YELOW (5YR 6/6) (STA 0+21)
7. FAULT DERIVED COLLUVIUM (?): SAND (SP) RDDISH YELLOW (5YR 6/6), PRIMARILY MASSIVE WITH SOME DISCONTINUOUS WEAK SUB-HORIZONTAL BEDDING, AND GRANULES OF GYPSUM
8. FAULT DERIVED COLLUVIUM (?): SANDY SILT (SM), REDDISH YELLOW (5YR 7/6 TO 5YR 6/6), WITH 3% ANGULAR S.S. AND SHALE CLASTS ≤ 2 INCHES, AVERAGE SIZE ≤ 0.2 INCHES
9. FAULT DERIVED COLLUVIUM (?): SANDY SILT (ML), YELLOWISH RED (5YR 5/6) WITH ANGULAR CLASTS OF S.S. AND SHALE ≤ 6 INCHES LONG, AVERAGE SIZE ≤ 1 INCH, WITH GYPSUM AND BURIED ORGANIC HORIZON (BWB) YELLOWISH RED (5YR 4/6) ALONG BASE OF WEST PART OF UNIT
10. FAN ALLUVIUM (STA 0+56) SILT SAND (SP) VERY FINE TO FINE GRAINED, VERY DENSE, GYPSUM, REDDISH YELLOW (5YR 6/6) TO YELLOWISH RED (5YR 5/6)
11. FAN ALLUVIUM: SANDY SILT (ML), MASSIVE, WITH 5% SUBANGULAR CLASTS ≤ 0.5 INCHES, YELLOWISH RED (5YR 5/6) (STA 0+08)
12. FAN ALLUVIUM: GRAVELLY SAND (SP), FINE GRAINED WITH 30% ANGULAR TO SUBANGULAR CLASTS ≤ 8 INCHES LONG, AVERAGE SIZE ≤ 4 INCHES, MASSIVE, YELLOWISH RED (5YR 5/6)
13. FLUVIAL: THIN TO MODERATELY BEDDED (≤ 0.3 INCHES TO 12 INCHES THICK) SAND GRAVEL, SANDY SILT, AND COARSE GRAINED SAND, BEDDING HORIZONTAL, SOME X-BEDDING, REDDISH BROWN (5YR 6/6)
14. ALLUVIUM: SILTY SAND (SM) VERY FINE GRAINED YELLOWISH RED (5YR 5/6)
15. ALLUVIUM: SANDY SILT (ML) REDDISH YELLOW (5YR 6/6)
16. ALLUVIUM: SILTY SAND (SM) VERY FINE GRAINED, GYPSUM, REDDISH YELLOW (5YR 6/6) TO YELLOWISH RED (5YR 5/6)
17. SILTY SAND (SM) VERY FINE GRAINED, PIN-HOLE VOIDS, RED (2.5YR 5/6 TO 2.5YR 4/6)
18. SILTY SAND (SM) FINE GRAINED
19. SANDY SILT (ML)
20. SILTY SAND (SM), FINE GRAINED, 1-2% ANGULAR CLASTS ≤ 0.5 INCH, ABUNDANT GYPSUM FRAGMENTS
21. SANDY GRAVEL LENS (GP) 50% ANGULAR CLASTS ≤ 8 INCHES, MATRIX FINE TO MEDIUM GRAINED SAND
22. SANDY SILT (ML), WITH CLAY, GYPSIFEROUS
23. SANDY SILT (ML), CLAYEY WITH 20% ANGULAR CLASTS ≤ 3 INCHES
24. SILTY SAND (SM) FINE GRAINED WITH 2% ANGULAR CLASTS ≤ 0.25 INCHES
25. SILTY SAND (ML) FINE GRAINED, SOME PIN-HOLE VOIDS
26. SANDY SILT (ML), GYPSIFEROUS WITH 10% ANGULAR CLASTS ≤ 3 INCHES, WELL DEVELOPED STONE-LINE ALONG BASE OF UNIT

SCALE: 1" = 5'

TRENCH PROFILE T-4

SOUTHERN CORRIDOR PHASE 3
WASHINGTON COUNTY, UTAH

ROSENBERG ASSOCIATES
CIVIL ENGINEERS • LAND SURVEYORS

PROJECT #	DRAWING #
5507-P3	7

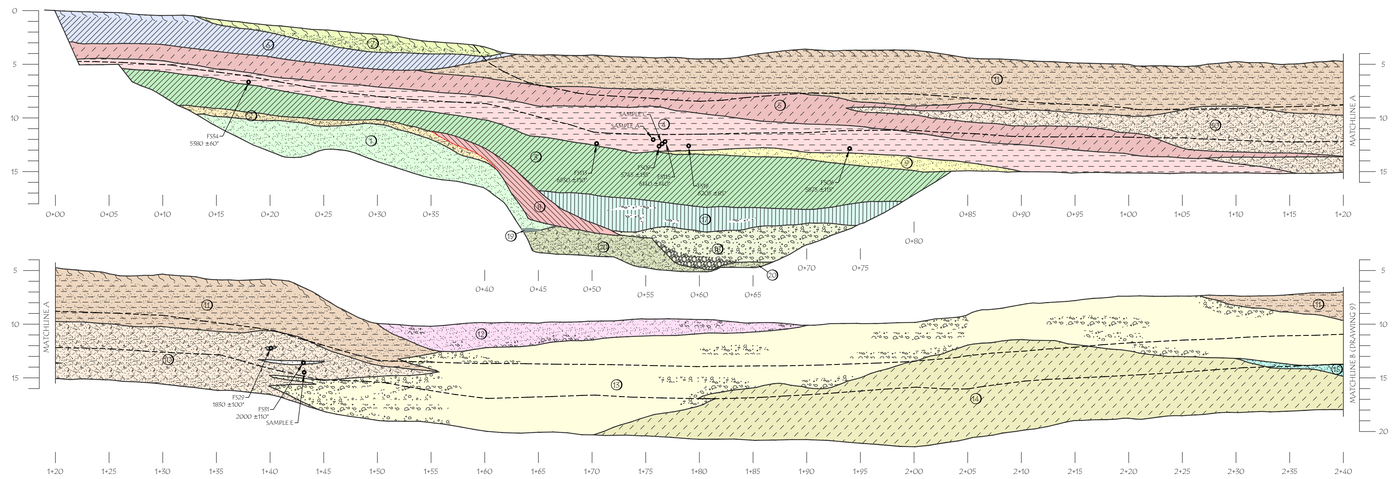

1. BEDRX: SANDSTONE WITH IN UPPER RED MEMBER, MOENKOPI FM, FINE GRAINED, SOME LITHIC FRAGMENTS, MODERATELY TO THINLY BEDDED, MODERATE TO INTENSELY SHEARED, BROWNISH YELLOW (10YR.6/6)
2. ALLUVIUM: SILT (ML) WITH SOME VERY FINE GRAINED SAND, YELLOW (10YR.7/6) (STA 0+85)
3. ALLUVIUM: SILT (ML) WITH VERY FINE GRAINED SAND, MASSIVE, REDDISH YELLOW (7.5YR.6/6) (STA 0+40)
4. ALLUVIUM: SILT (ML) WITH SOME VERY FINE GRAINED SAND, YELLOW (10YR.7/6) (STA 0+85)
5. ALLUVIUM: SANDY SILT (ML), MASSIVE, SOME PIN HOLE VOIDS, REDDISH YELLOW (7.5YR.6/6) (STA 0+80)
6. ALLUVIUM: SANDY SILT (ML), MASSIVE, SOME GYPSUM, REDDISH YELLOW (7.5YR.7/6) (STA 0+50)
7. ALLUVIUM: SANDY SILT (ML), MASSIVE, REDDISH YELLOW (7.5YR.7/6 TO 7.5YR.6/6)
8. FAULT DERIVED COLLUVIUM (?): SANDY SILT (ML), MASSIVE, SOME GYPSUM, YELLOW (10YR.7/6) TO BROWNISH YELLOW (10YR.6/6)
9. SILTY SAND (SM) VERY FINE GRAINED, YELLOWISH RED (5YR.5/6)
10. SILTY SAND (SM), VERY FINE GRAINED, SOME WEAKLY DEVELOPED HORIZONTAL BEDDING, YELLOWISH RED (5YR.5/6)
11. THINLY INTERBEDDED (≤ 12 INCHES THICK) SILTY SAND (SM), VERY FINE GRAINED AND SANDY SILT (ML), RED (2.5YR.5/8), SOME X-BEDDING
12. CHANNEL: SAND (SP), FINE GRAINED, THIN BEDDED (≤ 0.2 FEET THICK), SOME X-BEDDING AND SANDY GRAVEL LENSES, REDDISH YELLOW (5YR.5/6)
13. CHANNEL: SANDY GRAVEL (GP) WITH VERY THIN (≤ 0.5 INCHES THICK) DISCONTINUOUS SILTY SAND LAYERS, GRAVELS ANGULAR, ≤ 5 INCHES LONG, AVERAGE SIZE ≤ 0.5 INCHES, MATRIX SILTY SAND, FINE GRAINED LIGHT RED (2.5YR.6/8)
14. SANDY SILT (ML), MASSIVE, REDDISH YELLOW (5YR.7/6) WITH SOME DISCONTINUOUS SANDY GRAVEL LENSES
15. SANDY SILT (ML) MASSIVE, YELLOWISH RED (5YR.5/6)
16. SANDY GRAVEL (GP), SOME CLAST SUPPORTED, 75% ANGULAR CLASTS ≤ 12 INCHES, AVERAGE SIZE ≤ 0.5 INCH, YELLOWISH RED (5YR.5/6 TO 5/8)
17. SAND (SP) WITH SILT, FINE GRAINED, RED (2.5YR.4/8)
18. GRAVELLY SAND (SP) FINE TO MEDIUM GRAINED WITH 20% +/- ANGULAR CLASTS ≤ 1-INCH, RED (2.5YR.4/8)
19. BEDROCK: SANDY SILT WITH CLAY, BROWNISH YELLOW (10YR.6/6)
20. BEDROCK: SILT (ML) WITH VERY FINE SAND AND SOME CLAY, YELLOW (10YR.7/6)

* DATES ARE REPORTED AS RCYBP (RADIOCARBON YEARS BEFORE PRESENT, "PRESENT" AD 1950). TO CALCULATE RCYBP FOR AD 2010, ADD 60 YEARS.

TRENCH PROFILE T-5

SOUTHERN CORRIDOR PHASE 3
WASHINGTON COUNTY, UTAH

SCALE: 1" = 5'

ROSENBERG ASSOCIATES CIVIL ENGINEERS • LAND SURVEYORS

PROJECT #	DRAWING #
5507-P3	8

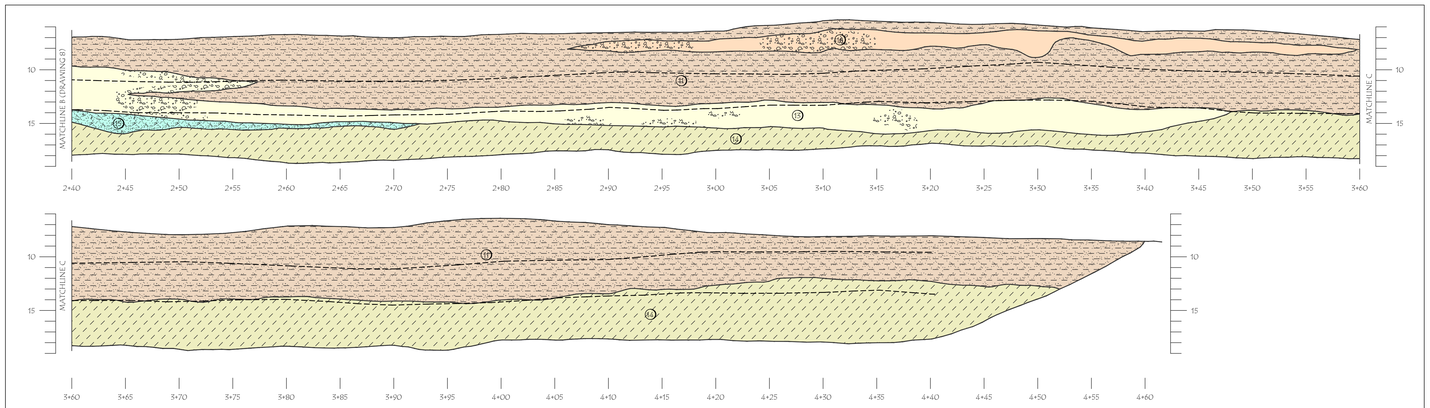

11. THINLY INTERBEDDED (≤ 12 INCHES THICK) SILTY SAND (SM), VERY FINE GRAINED AND SANDY SILT (ML), RED (2.5YR.5/8), SOME X-BEDDING
12. CHANNEL: SAND (SP), FINE GRAINED, THIN BEDDED (≤ 0.2 FEET THICK), SOME X-BEDDING AND SANDY GRAVEL LENSES, REDDISH YELLOW (5YR.5/6)
13. CHANNEL: SANDY GRAVEL (GP) WITH VERY THIN (≤ 0.5 INCHES THICK) DISCONTINUOUS SILTY SAND LAYERS, GRAVELS ANGULAR, ≤ 5 INCHES LONG, AVERAGE SIZE ≤ 0.5 INCHES, MATRIX SILTY SAND, FINE GRAINED LIGHT RED (2.5YR.6/8)
14. SANDY SILT (ML), MASSIVE, REDDISH YELLOW (5YR.7/6) WITH SOME DISCONTINUOUS SANDY GRAVEL LENSES
15. SANDY SILT (ML) MASSIVE, YELLOWISH RED (5YR.5/6)
16. SANDY GRAVEL (GP), SOME CLAST SUPPORTED, 75% ANGULAR CLASTS ≤ 12 INCHES, AVERAGE SIZE ≤ 0.5 INCH, YELLOWISH RED (5YR.5/6 TO 5/8)

TRENCH PROFILE T-5

SOUTHERN CORRIDOR PHASE 3
WASHINGTON COUNTY, UTAH

SCALE: 1" = 5'

ROSENBERG ASSOCIATES CIVIL ENGINEERS • LAND SURVEYORS

PROJECT #	DRAWING #
5507-P3	9

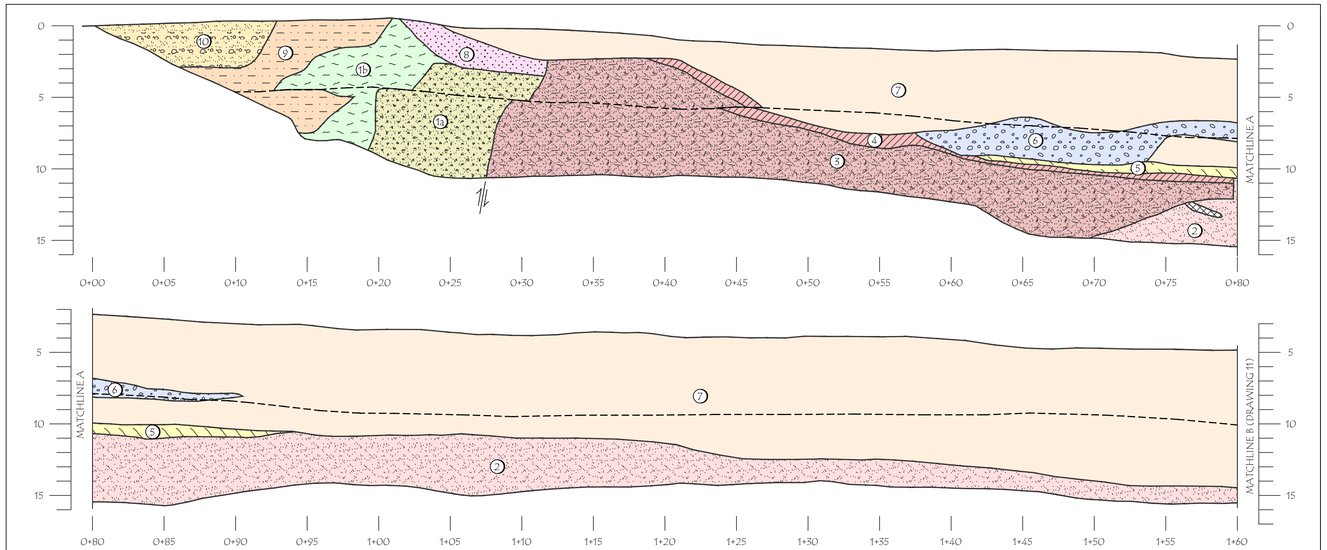

1a BEDROCK: SHALE, VERY THINLY BEDDED (≤ 0.2 INCH THICK), REDDISH BROWN (5YR 5/3) WITH VERY THIN (≤ 0.2 INCHES), WHITE (10YR 8/1) SHALE LAYERS

1b BEDROCK: SHALE, VERY THIN TO THINLY BEDDED (0.2 TO 6 INCHES THICK), MODERATELY FRACTURED, LIGHT GRAY (5YR 7/1), GYPSIFEROUS, WITH HONEYCOMB STRUCTURE

2 ALLUVIUM: SILTY SAND (SM), FINE GRAINED, REDDISH YELLOW (7.5YR 6/6), WITH 3% ANGULAR CLASTS ≤ 0.5 FEET, "HONEY-COMB" STRUCTURE, GYPSIFEROUS (STA 1+18)

3 ALLUVIUM: SANDY SILT (ML), MASSIVE, SOME PIN-HOLE VOIDS, PINK (7.5YR 8/3) (STA 0+66)

4 ALLUVIUM: SILT (ML) PERVASIVE CARBONATE STAINING, WHITE (2.5YR 8/1) TO PALE YELLOW (2.5YR 8/2) (STA 0+66)

5 ALLUVIUM: SANDY SILT (ML), MASSIVE, REDDISH YELLOW (5YR 6/6) (STA 0+76)

6 ALLUVIUM (CHANNEL): GRAVELLY SAND (SP), FINE TO MEDIUM GRAINED WITH 20% ANGULAR CLASTS ≤ 6 INCHES, AVERAGE SIZE ≤ 2 INCHES, SOME WEAKLY DEVELOPED HORIZONTAL BEDDING, PINKISH GRAY (7.5YR 7/2) (STA 0+65)

7 ALLUVIUM: SAND (SP) FINE TO MEDIUM GRAINED, PINK (7.5YR 8/3), WITH 10% ANGULAR CLASTS ≤ 6 INCHES, AVERAGE SIZE ≤ 3 INCHES WITH DISCONTINUOUS PINKISH WHITE (7.5YR 8/2) SILTY FINE GRAINED SAND LAYERS (STA 1+44)

8 ALLUVIUM: SAND (SP) MEDIUM GRAINED, MASSIVE, GYPSIFEROUS, VERY PALE BROWN (10YR 8/3), SOME "HONEY COMB BLOCKS (STA 0+21)

9 ALLUVIUM: SANDY SILT (ML) MASSIVE, MOTTLED PINK (7.5YR 7/4) TO PINK (7.5YR 8/3) (STA - 0+16)

10 ALLUVIUM (CHANNEL): SAND (SP) FINE TO COARSE GRAINED WITH THIN (≤ 6 INCHES) HORIZONTAL LAYERS OF GRAVELLY SAND , PINKISH WHITE (7.5YR 8/2)

SCALE: 1" = 5'

TRENCH PROFILE T-6

SOUTHERN CORRIDOR PHASE 3
WASHINGTON COUNTY, UTAH

ROSENBERG & ASSOCIATES
CIVIL ENGINEERS • LAND SURVEYORS

PROJECT #	DRAWING #
5507-P3	10

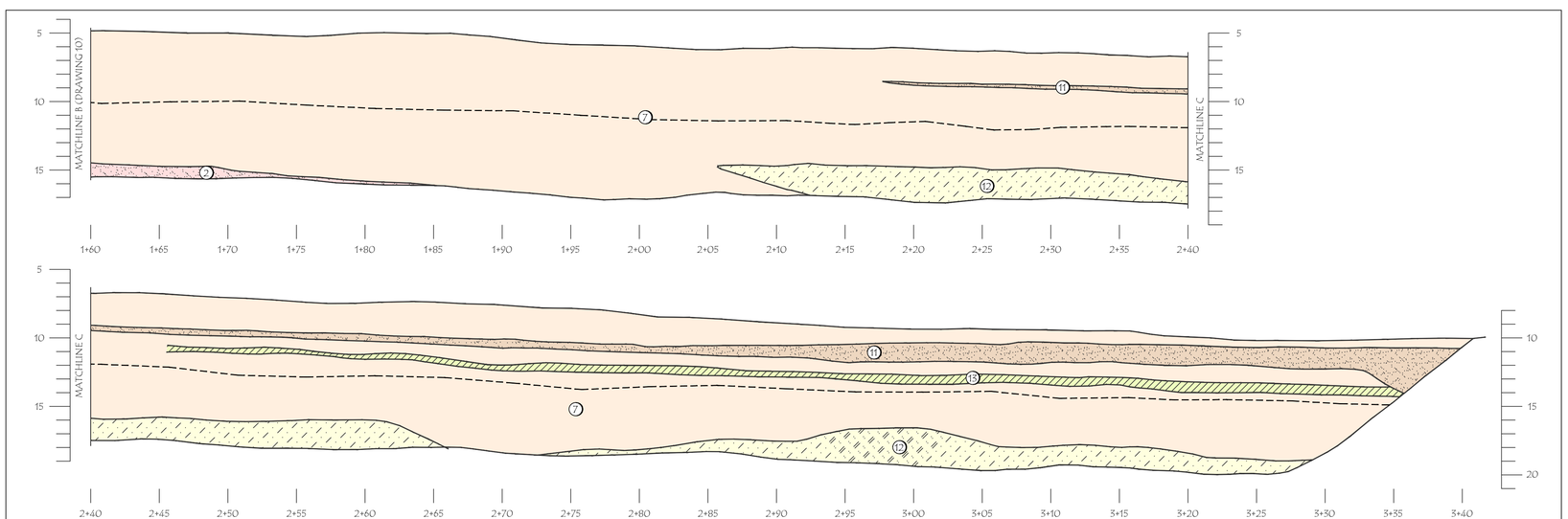

2 ALLUVIUM: SILTY SAND (SM), FINE GRAINED, REDDISH YELLOW (7.5YR 6/6), WITH 3% ANGULAR CLASTS ≤ 0.5 FEET, "HONEY-COMB" STRUCTURE, GYPSIFEROUS (STA 1+18)

7 ALLUVIUM: SAND (SP) FINE TO MEDIUM GRAINED, PINK (7.5YR 8/3), WITH 10% ANGULAR CLASTS ≤ 6 INCHES, AVERAGE SIZE ≤ 3 INCHES WITH DISCONTINUOUS PINKISH WHITE (7.5YR 8/2) SILTY FINE GRAINED SAND LAYERS (STA 1+44)

11 ALLUVIUM (STA 3+26): THINLY INTERBEDDED (0.2 TO 0.5 INCHES THICK) SILTY SAND (SM), COARSE GRAINED SAND (SP), AND PEBBLY SAND (SP), RED (2.5YR 5/6)

12 ALLUVIUM (STA 3+16): SANDY SILT (ML) SOME COARSE GRAINED SAND, CONTACT WITH OVERLYING UNIT NOT WELL DEFINED PINK (5YR 7/4), MASSIVE

13 ALLUVIUM (STA 3+26): SILT (ML), MASSIVE REDDISH YELLOW (5YR 6/6)

SCALE: 1" = 5'

TRENCH PROFILE T-6

SOUTHERN CORRIDOR PHASE 3
WASHINGTON COUNTY, UTAH

ROSENBERG & ASSOCIATES
CIVIL ENGINEERS • LAND SURVEYORS

PROJECT #	DRAWING #
5507-P3	11

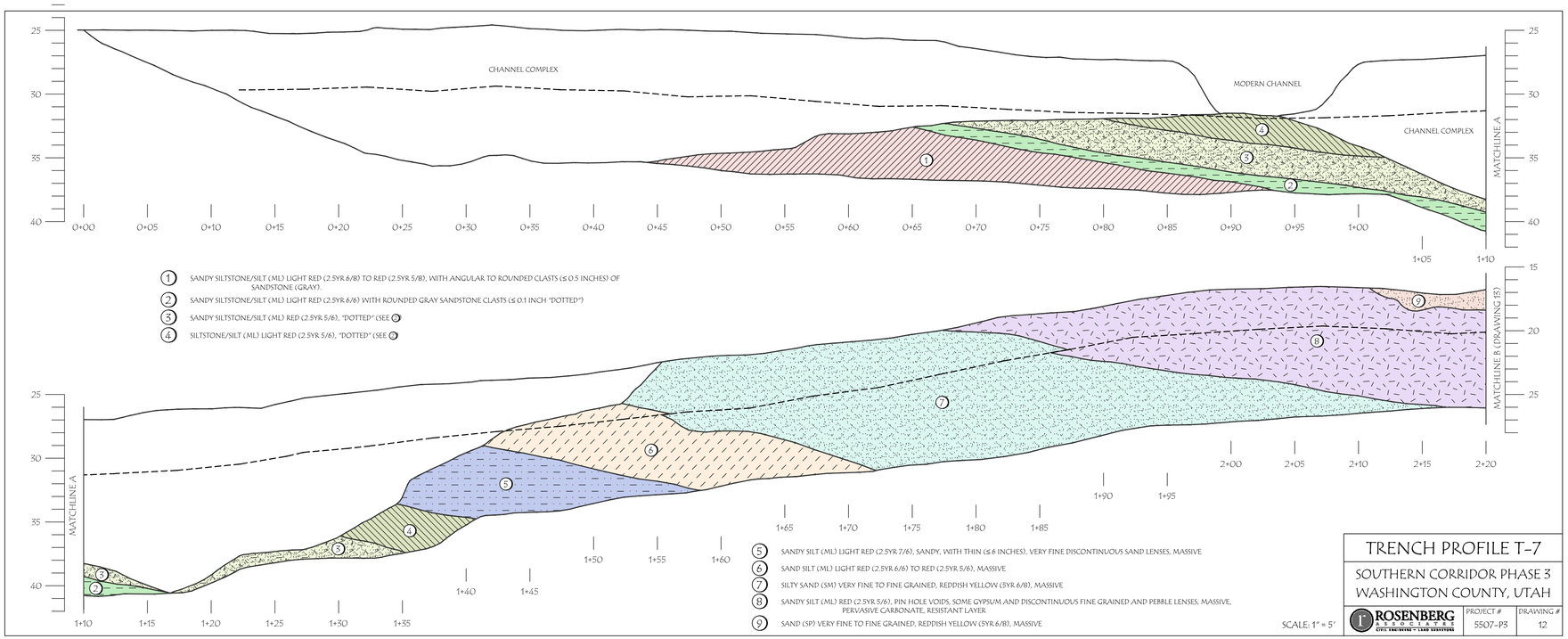

1. SANDY SILTSTONE/SILT (ML) LIGHT RED (2.5YR 6/8) TO RED (2.5YR 5/8), WITH ANGULAR TO ROUNDED CLASTS (≤ 0.5 INCHES) OF SANDSTONE (GRAY).
2. SANDY SILTSTONE/SILT (ML) LIGHT RED (2.5YR 6/6) WITH ROUNDED GRAY SANDSTONE CLASTS (≤ 0.1 INCH "DOTTED")
3. SANDY SILTSTONE/SILT (ML) RED (2.5YR 5/6), "DOTTED" (SEE 2)
4. SILTSTONE/SILT (ML) LIGHT RED (2.5YR 5/6), "DOTTED" (SEE 2)
5. SANDY SILT (ML) LIGHT RED (2.5YR 7/6), SANDY, WITH THIN (≤ 6 INCHES), VERY FINE DISCONTINUOUS SAND LENSES, MASSIVE
6. SAND SILT (ML) LIGHT RED (2.5YR 6/6) TO RED (2.5YR 5/6), MASSIVE
7. SILTY SAND (SM) VERY FINE TO FINE GRAINED, REDDISH YELLOW (5YR 6/8), MASSIVE
8. SANDY SILT (ML) RED (2.5YR 5/6), PIN HOLE VOIDS, SOME GYPSUM AND DISCONTINUOUS FINE GRAINED AND PEBBLE LENSES, MASSIVE, PERVASIVE CARBONATE, RESISTANT LAYER
9. SAND (SP) VERY FINE TO FINE GRAINED, REDDISH YELLOW (5YR 6/8), MASSIVE

SCALE: 1" = 5'

TRENCH PROFILE T-7

SOUTHERN CORRIDOR PHASE 3
WASHINGTON COUNTY, UTAH

ROSENBERG & ASSOCIATES CIVIL ENGINEERS • LAND SURVEYORS

PROJECT #	DRAWING #
5507-P3	12

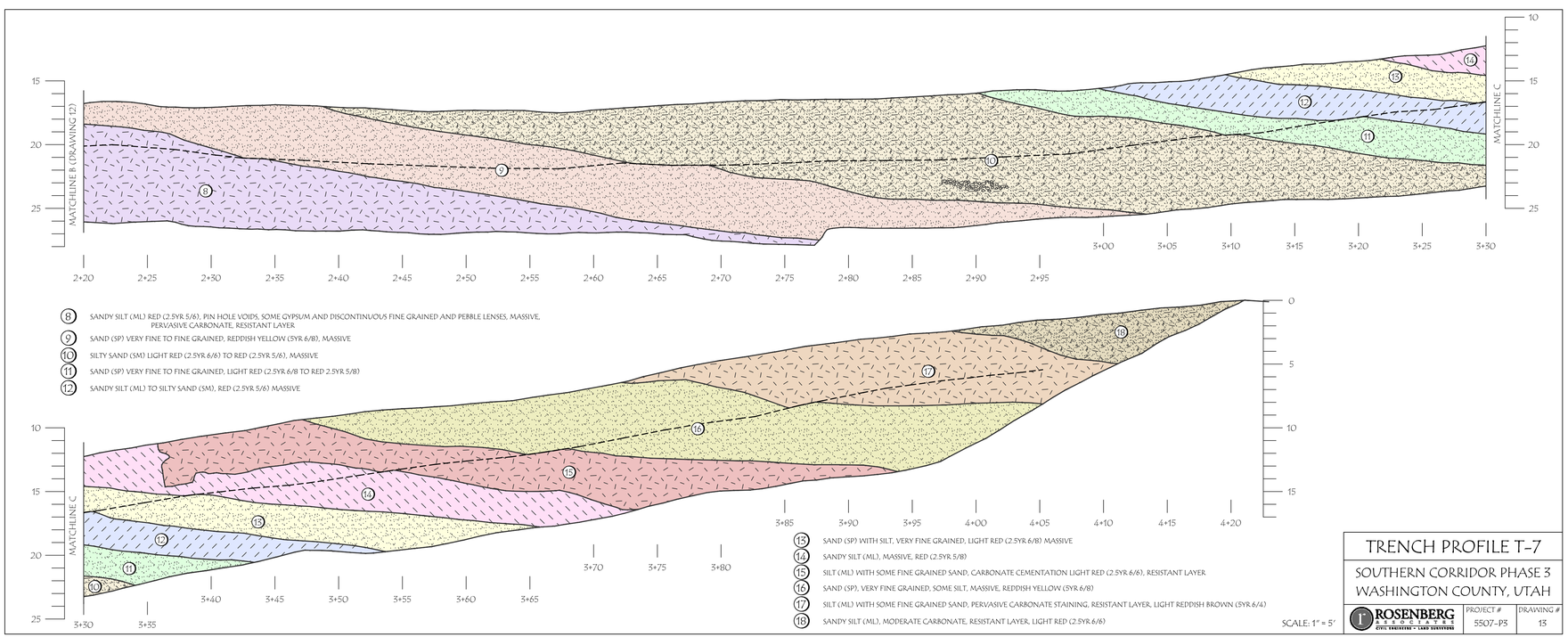

8. SANDY SILT (ML) RED (2.5YR 5/6), PIN HOLE VOIDS, SOME GYPSUM AND DISCONTINUOUS FINE GRAINED AND PEBBLE LENSES, MASSIVE, PERVASIVE CARBONATE, RESISTANT LAYER
9. SAND (SP) VERY FINE TO FINE GRAINED, REDDISH YELLOW (5YR 6/8), MASSIVE
10. SILTY SAND (SM) LIGHT RED (2.5YR 6/6) TO RED (2.5YR 5/6), MASSIVE
11. SAND (SP) VERY FINE TO FINE GRAINED, LIGHT RED (2.5YR 6/8 TO RED 2.5YR 5/8)
12. SANDY SILT (ML) TO SILTY SAND (SM), RED (2.5YR 5/6) MASSIVE
13. SAND (SP) WITH SILT, VERY FINE GRAINED, LIGHT RED (2.5YR 6/8) MASSIVE
14. SANDY SILT (ML), MASSIVE, RED (2.5YR 5/8)
15. SILT (ML) WITH SOME FINE GRAINED SAND, CARBONATE CEMENTATION LIGHT RED (2.5YR 6/6), RESISTANT LAYER
16. SAND (SP), VERY FINE GRAINED, SOME SILT, MASSIVE, REDDISH YELLOW (5YR 6/8)
17. SILT (ML) WITH SOME FINE GRAINED SAND, PERVASIVE CARBONATE STAINING, RESISTANT LAYER, LIGHT REDDISH BROWN (5YR 6/4)
18. SANDY SILT (ML), MODERATE CARBONATE, RESISTANT LAYER, LIGHT RED (2.5YR 6/6)

SCALE: 1" = 5'

TRENCH PROFILE T-7

SOUTHERN CORRIDOR PHASE 3
WASHINGTON COUNTY, UTAH

ROSENBERG & ASSOCIATES CIVIL ENGINEERS • LAND SURVEYORS

PROJECT #	DRAWING #
5507-P3	13

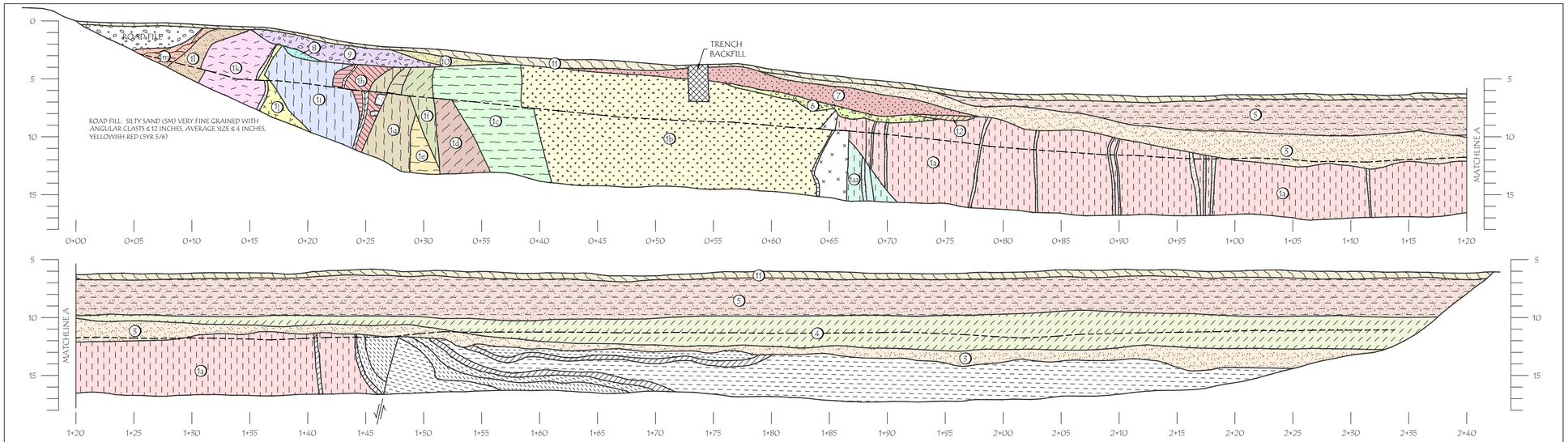

- (1a) SILTY CLAYSTONE, RED (2.5YR 4/6), FINE-MEDIUM GRAINED, GYPSIFEROUS, WITH THIN (≤ 12 INCH THICK) WHITE (10YR 8/1) SILTY CLAYSTONE INTERBEDS, MODERATELY WEATHERED
- (1b) CLAYSTONE, MASSIVE, GYPSIFEROUS, MODERATELY WEATHERED, WEAK RED (10R 4/2), SHEARED
- (1c) CLAYSTONE, GYPSIFEROUS, WEAK RED (10YR 5/3) WITH FRAGMENTS AND DISCONTINUOUS INTERBEDS OF WHITE (2.5Y 8/1) CLAYSTONE GIVING UNIT A MOTTLED APPEARANCE, SHEARED
- (1d) CLAYSTONE, WEAK RED (10R 5/3 TO 4/3, "PURPLE"), SHEARED
- (1e) CLAYSTONE, GYPSIFEROUS, WEAK RED (10R 4/2), SHEARED
- (1f) CLAYSTONE, SILTY, SHEARED, WEAK RED (10R 4/4)
- (1g) CLAYSTONE, REDDISH RED (2.5YR 4/4)
- (1h) FAULT ZONE (?) SHEARED, WITH ALTERNATING NEAR VERTICAL LAYERS OF LIGHT GRAY (7.5YR 7/1), DARK REDDISH BROWN (2.5YR 3/4), DARK REDDISH GRAY (2.5YR N4/1), AND REDDISH BROWN (2.5YR 5/3) CLAYSTONE WITH FRAGMENTS OF PALE RED (2.5YR 6/2) SILTY SANDSTONE (12 INCHES LONG)
- (1i) CLAYSTONE, REDDISH BROWN (2.5YR 4/4), WITH FRAGMENTS AND DISCONTINUOUS INTERBEDS OF WHITE (2.5Y 8/1) CLAYSTONE
- (1j) CLAYSTONE, DARK REDDISH BROWN (2.5YR 3/3)
- (1l) THINLY INTERBEDDED LIGHT GRAY (10YR 7/1) CLAYEY SANDSTONE AND DARK REDDISH BROWN (5YR 3/3) CLAYSTONE
- (1m) SANDSTONE, DEEPLY WEATHERED WITH PERVASIVE CARBONATE FILLED FRACTRUES AND VEINS, PINKISH WHITE (5YR 8/2)
- (1aa) CLAYSTONE, RED (2.5YR 5/6) WITH PINKISH GRAY (7.5YR 7/2) CLAYSTONE INTERBED (≤ 12 INCHES THICK)

TRENCH PROFILE T-8

SOUTHERN CORRIDOR PHASE 3
WASHINGTON COUNTY, UTAH

SCALE: 1" = 5'

ROSENBERG ASSOCIATES
CIVIL ENGINEERS • LAND SURVEYORS

PROJECT #	DRAWING #
5507-P3	14

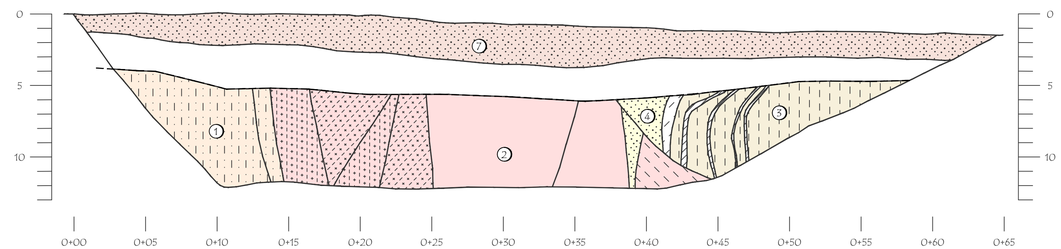

1. CLAYSTONE (BLUE CLAY), GYPSIFEROUS, NEAR VERTICAL BEDDING, INTENSELY SHEARED, WEAK RED (10R 4/3)
2. PETRIFIED FOREST MEMBER OF CHINLE FORMATION: CLAYSTONE, GYPSIFEROUS, NEAR VERTICAL BEDDING, INTENSELY SHEARED, WEAK RED (10R 4/2)
3. DINOSAUR CNY MEMBER OF MOENAVI FORMATION: UNIT 3 IN T-8, SILTY CLAYSTONE, RED (2.5YR 4/6) GYPSIFEROUS, WITH THIN (≤ 12 INCHES THICK) WHITE (10YR 8/1) SILTY CLAYSTONE INTERBEDS, MODERATELY WEATHERED
4. BRECCIA ZONE: HIGHLY/INTENSELY SHEARED, PRIMARILY UNITS 1 AND 3
7. ALLUVIUM: SANDY SILT (ML), REDDISH YELLOW (5YR 6/6) WITH 3±% ANGULAR CLASTS ≤ 3 INCHES LONG, WEAK STONE LINE

TRENCH PROFILE T-9

SOUTHERN CORRIDOR PHASE 3
WASHINGTON COUNTY, UTAH

SCALE: 1" = 5'

ROSENBERG ASSOCIATES
CIVIL ENGINEERS • LAND SURVEYORS

PROJECT #	DRAWING #
5507-P3	15

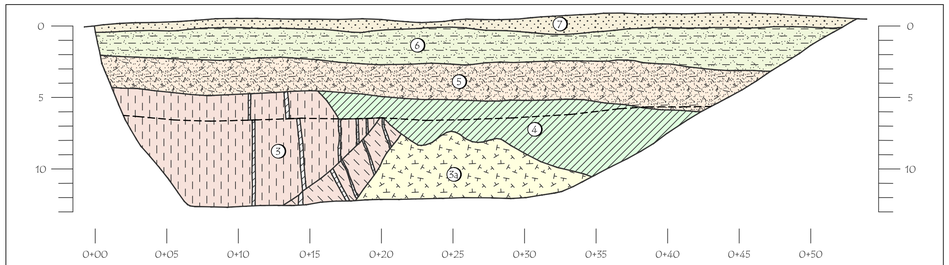

3 DINOSAUR CNY MEMBER OF MOENAVI FORMATION: UNIT 10 IN T-8, SILTY CLAYSTONE, RED (2.5YR 4/6) GYPSIFEROUS, WITH THIN (≤ 12 INCHES THICK) WHITE (10YR 8/1) SILTY CLAYSTONE INTERBEDS, MODERATELY WEATHERED

3a DINOSAUR CNY MEMBER: SANDY SILT (ML), GYPSIFEROUS, MASSIVE RED (2.5YR 5/6)

4 ALLUVIUM: SILT (ML), LIGHT RED (2.5YR 6/8), GYSIFEROUS, WITH 5% ANGULAR CLASTS ≤ Ø.2 INCHES LONG

5 ALLUVIUM: SILT (ML) WITH SOME FINE GRAINED SAND, PINK (5YR 7/4) (UNIT 9 IN T-8)

6 ALLUVIUM: UNIT 9 IN T-8: SILTY SAND (SM) VERY FINE GRAINED, RED (2.5YR 5/6 TO 4/6) WITH THIN (≤ 6 INCHES THICK) REDDISH YELLOW (5YR 6/6) SILTY SAND (SM) INTERBEDS ("STRIPPED" APPEARANCE)

7 ALLUVIUM: SANDY SILT (ML), REDDISH YELLOW (5YR 6/6) WITH 3±% ANGULAR CLASTS ≤ 3 INCHES LONG, WEAK STONE LINE

TRENCH PROFILE T-10

SOUTHERN CORRIDOR PHASE 3
WASHINGTON COUNTY, UTAH

SCALE: 1" = 5'

ROSENBERG ASSOCIATES
CIVIL ENGINEERS • LAND SURVEYORS

PROJECT #	DRAWING #
5507-P3	16

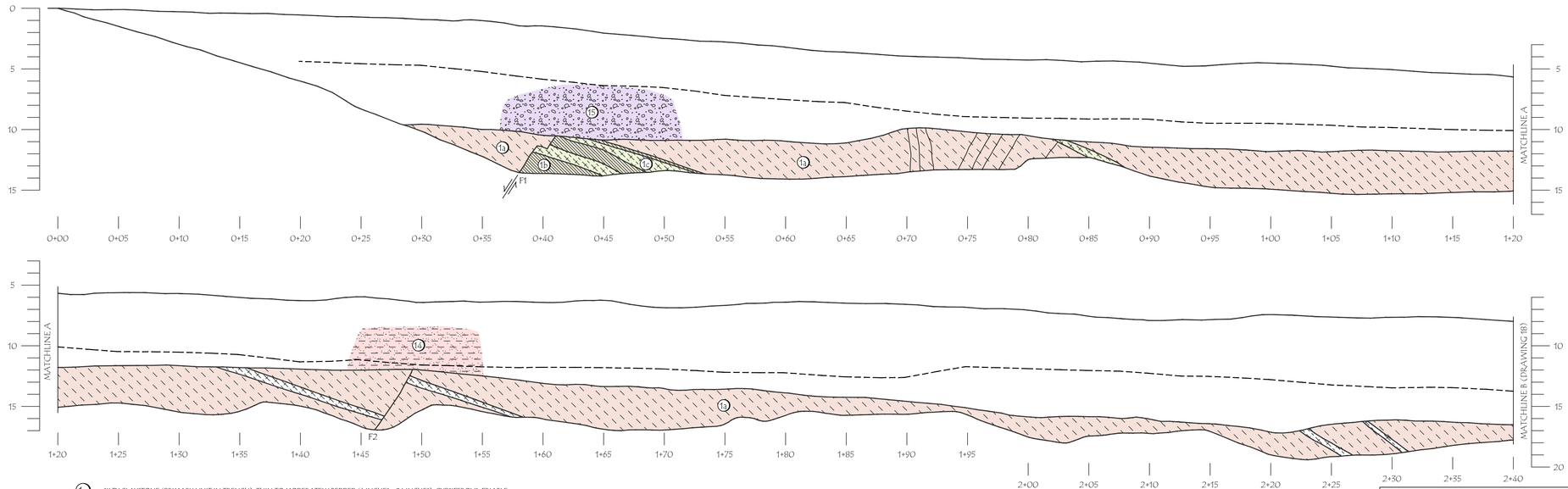

1a SILTY CLAYSTONE (PRIMARY UNIT IN TRENCH), THIN TO MODERATELY BEDDED (6 INCHES - 24 INCHES), GYPSIFEROUS, FRIABLE, INTENSELY FRACTURED AND "BROKEN", REDDISH BROWN (2.5YR 4/3), WITH NUMEROUS, EAST DIPPING TO VERTICAL GYPSUM VEINS (GYPSUM FILLED FRACTURES), GENERALLY ≥ 0.2 INCHES WIDE ("CHOCOLATE"), WEST DIPPING

1b CLAYEY SILTSTONE INTERBED, WELL INDURATED, VERY HARD, GYPSIFEROUS REDDISH YELLOW (5YR 6/6)

1c CLAYSTONE INTERBED ("GREEN"), LIGHT GREENISH GRAY (5GY 7/1 - GLEY)

1d ALLUVIUM: SAND (SP), FINE TO MEDIUM GRAINED, DARK REDDISH BROWN (5YR 3/4) WITH THIN (≤ 0.5 INCHES THICK) INTERBEDS (HORIZONTAL) OF REDDISH YELLOW (5YR 6/6) SILT (ML)

1e ALLUVIUM: SAND (SP) FINE TO MEDIUM GRAINED, REDDISH YELLOW (5YR 6/6) WITH DISCONTINUOUS PEBBLY SAND AND COARSE GRAINED SAND LENSES

SCALE: 1" = 5'

TRENCH PROFILE T-11

SOUTHERN CORRIDOR PHASE 3
WASHINGTON COUNTY, UTAH

ROSENBERG ASSOCIATES
CIVIL ENGINEERS • LAND SURVEYORS

PROJECT #	DRAWING #
5507-P3	17

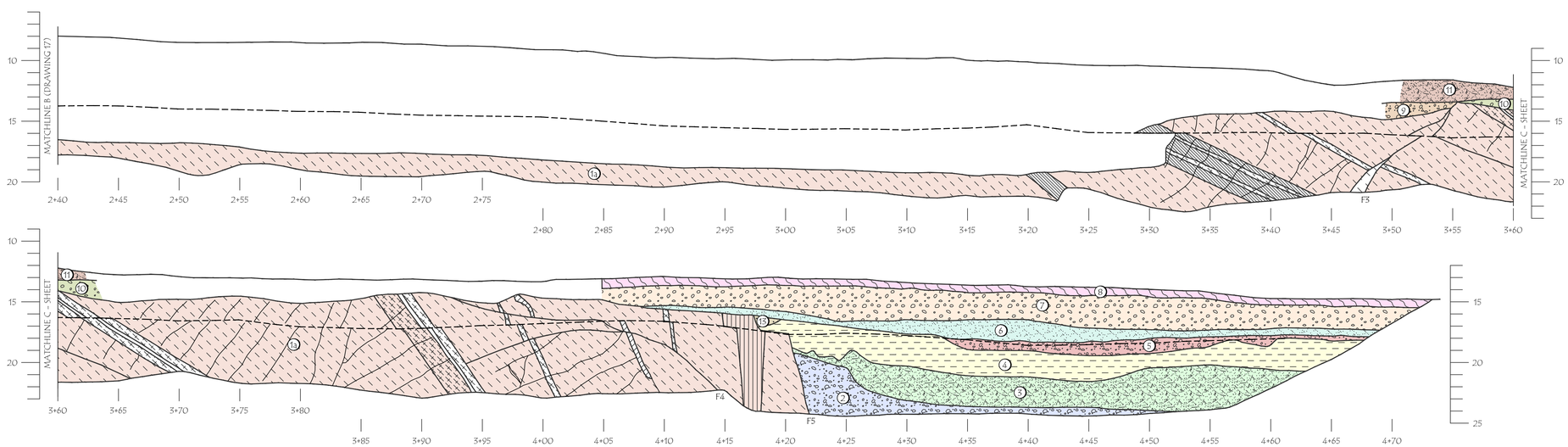

1a SILTY CLAYSTONE (PRIMARY UNIT IN TRENCH), THIN TO MODERATELY BEDDED (6 INCHES - 24 INCHES), GYPSIFEROUS, FRIABLE, INTENSELY FRACTURED AND "BROKEN", REDDISH BROWN (2.5YR 4/3), WITH NUMEROUS, EAST DIPPING TO VERTICAL GYPSUM VEINS (GYPSUM FILLED FRACTURES), GENERALLY ≥ 0.2 INCHES WIDE ("CHOCOLATE"), WEST DIPPING

2 ALLUVIUM: SILTY SAND (SM), FINE GRAINED, WITH 15% ANGULAR CLASTS ≤ 6 INCHES, AVERAGE SIZE ≤ 2 INCHES, REDDISH YELLOW (5YR 6/6) TO YELLOWISH RED (5YR 5/6, FLAT LIGHT 11/12/09)

5 ALLUVIUM: SANDY SILT (ML) REDDISH YELLOW (7.5YR 7/6), MASSIVE

4 ALLUVIUM: SILT (ML) SOME VERY FINE GRAINED SAND, REDDISH YELLOW (5YR 6/6)

5 ALLUVIUM: SAND (SP) FINE TO MEDIUM GRAINED WITH 20±% ANGULAR CLASTS ≤ 4 INCHES, AVERAGE SIZE ≤ 2 INCHES, REDDISH BROWN (5YR 5/4)

6 ALLUVIUM: SILT (ML) WITH SOME FINE GRAINED SAND , MASSIVE, REDDISH YELLOW (5YR 7/6 TO 6/6)

7 ALLUVIUM: GRAVELY SAND (SP) FINE TO MEDIUM GRAINED, LIGHT REDDISH BROWN (5YR 6/4), WEAK HORIZONTAL BEDDING WITH 25% ANGULAR CLASTS ≤ 8 INCHES, AVERAGE SIZE ≤ 4 INCHES

8 ALLUVIUM: CLAYEY SILT (ML) WITH SOME VERY FINE GRAINED SAND, REDDISH BROWN (5YR 5/4) AND WEAKLY DEVELOPED MODERN ORGANIC (A) HORIZON

9 ALLUVIUM: SAND (SP) FINE TO MEDIUM GRAINED WITH 5% ANGULAR CLASTS ≤ 0.3 INCHES LONG, REDDISH BROWN (5YR 5/4 NO SUN)

10 ALLUVIUM: SAND (SP) MEDIUM GRAINED WITH 15% ANGULAR CLASTS ≤ 0.6 INCHES, REDDISH YELLOW (5YR 6/6)

11 ALLUVIUM: SILTY SAND (SM), FINE GRAINED, YELLOWISH RED (5YR 5/6) WITH WEAKLY DEVELOPED MODERN ORGANIC (A) HORIZON

13 WEDGE (?) SAND (SP) FINE TO MEDIUM GRAINED, SOME SILT AND ANGULAR CLASTS OF ADJACENT MOENKOPI (≤ 0.5 INCHES LONG), YELLOWISH RED (5YR 5/6)

SCALE: 1" = 5'

TRENCH PROFILE T-11

SOUTHERN CORRIDOR PHASE 3
WASHINGTON COUNTY, UTAH

ROSENBERG ASSOCIATES
CIVIL ENGINEERS • LAND SURVEYORS

PROJECT #	DRAWING #
5507-P3	18

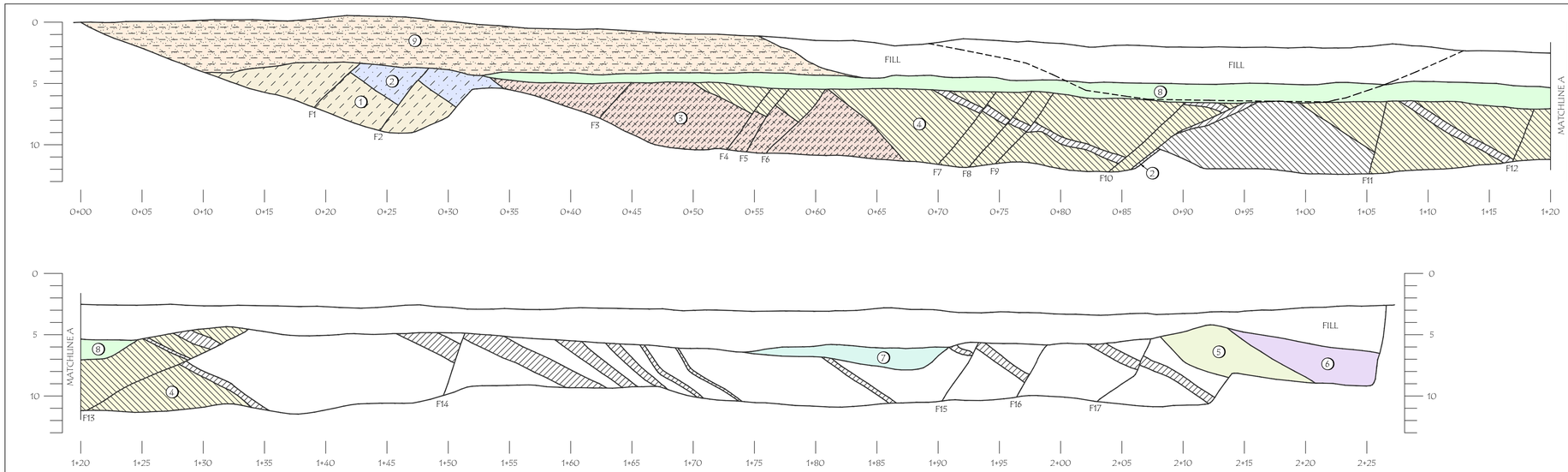

1. THINLY BEDDED (≤ 2 INCHES THICK) SILTSTONE, LIGHT GREENISH GRAY (GLEY 5GY 7/1) (MIDDLE RED MEMBER OF MOENKOPI ?)
2. MODERATELY BEDDED (≤ 12 INCHES THICK) SANDSTONE, FINE GRAINED, WELL CEMENTED (BACKHOE REFUSAL), SOME LITHIC CLASTS (≤ 0.1 INCH DIA) AND VUGS WITH SECONDARY GYPSUM, PALE YELLOW (2.5Y 8/4)
3. THINLY BEDDED (≤ 2 INCHES THICK) SILTSTONE, GRAY (7.5YR 6/1)
4. THINLY BEDDED (≤ 1 INCH THICK) CLAYEY SILTSTONE (PUNKY), BROWN (7.5YR 4/3)
   SILTY CLAYSTONE, LIGHT GREENISH GRAY (GLEY 5GY 7/1) INTERBED WITHIN UNIT 4)
5. SANDSTONE, LIGHT GRAY (10YR 7/1), WELL CEMENTED WITH GYPSUM, FINE GRAINED, VERY HARD, QUARTZITE-LIKE
6. SILTSTONE, RIPPLED WITH GYPSUM SEAMS, LIGHT GRAY (10YR 7/1)
7. SANDY SILT (ML), MASSIVE, PINK (5YR 7/3)
8. SAND (SP) FINE TO MEDIUM GRAINED, GYPSIFEROUS, DARK REDDISH BROWN (2.5YR 3/3) MASSIVE
9. SAND (SP) FINE TO COARSE GRAINED, THINLY BEDDED (≤ 1 INCH THICK), REDDISH BROWN (5YR 4/4), WITH WEAKLY DEVELOPED MODERN ORGANIC (A) HORIZON

SCALE: 1" = 5'

TRENCH PROFILE T-12

SOUTHERN CORRIDOR PHASE 3
WASHINGTON COUNTY, UTAH

ROSENBERG ASSOCIATES
CIVIL ENGINEERS • LAND SURVEYORS

PROJECT #	DRAWING #
5507-P3	19

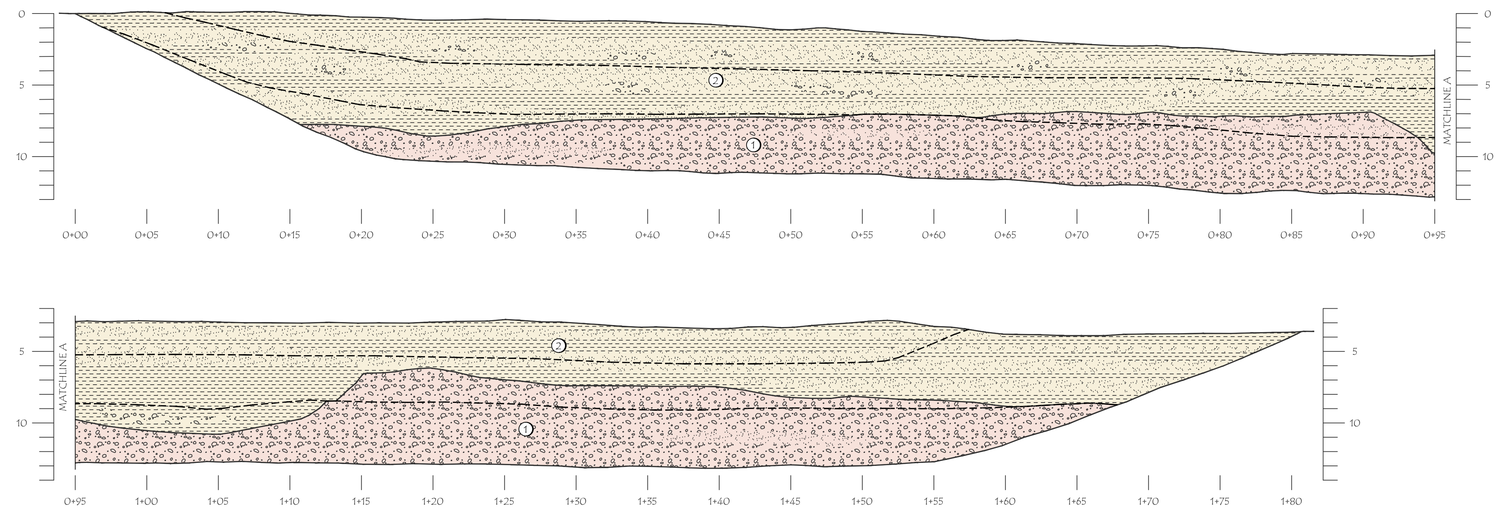

1 ALLUVIUM: GRAVELLY SAND (SP) TO SANDY GRAVEL (GP), FINE TO COARSE GRAINED CLASTS ≤ 12 INCHES, AVERAGE SIZE ≤ 3 INCHES, YELLOWISH RED (5YR 5/8), WITH DISCONTINUOUS FINE TO MEDIUM GRAINED SAND LENSES

2 ALLUVIUM: SILTY SAND (SM), FINE TO MEDIUM GRAINED, LIGHT RED (2.5YR 6/8) WITH THIN TO MODERATE (6 TO 12 INCHES THICK) SANDY SILT (ML) LIGHT REDDISH BROWN (5YR 6/4) GIVING UNIT "BACON" STRIPED APPEARANCE (SAME AS T-8 AND T-10). BOTH UNITS CONTAIN THIN (≤ 6-INCH THICK), DISCONTINUOUS LENSES OF PEBBLY COURSE GRAINED SAND.

TRENCH PROFILE T-13

SOUTHERN CORRIDOR PHASE 3
WASHINGTON COUNTY, UTAH

SCALE: 1" = 5'

ROSENBERG ASSOCIATES
CIVIL ENGINEERS • LAND SURVEYORS

PROJECT #	DRAWING #
5507-P3	20

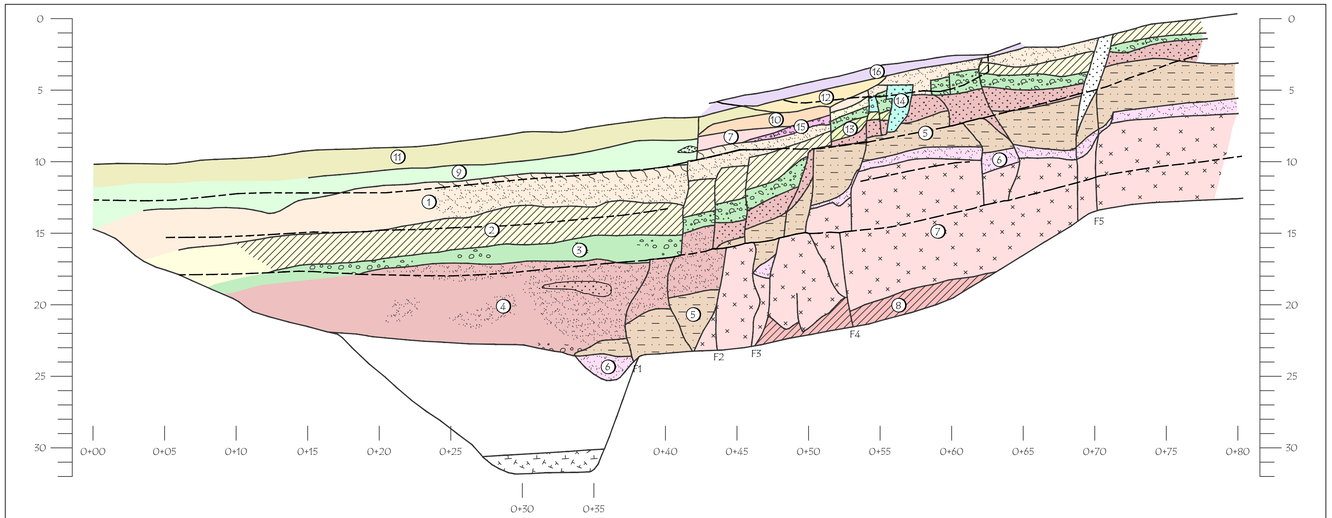

1. ALLUVIUM: SILTY SAND (SM), VERY FINE GRAINED, MASSIVE, REDDISH YELLOW (5YR 6/8), CAPPED BY ORGANICH HORIZON (BKh) WEAKLY DEVELOPED
2. ALLUVIUM (STA 0+85): SANDY SILT (ML), VERY FINE GRAINED, MASSIVE, REDDISH YELLOW (5YR 7/6) (STA 0+40)
3. ALLUVIUM: SANDY GRAVEL (GP), 60% ANGULAR CLASTS ≤ 2 INCHES, AVERAGE SIZE ≤ 1 INCH, MATRIX SILTY FINE GRAINED SAND, REDDISH YELLOW (5YR 7/6) SOME CARBONATE STAINING (STA 0+40)
4. ALLUVIUM: SILTY SAND (SM) VERY FINE GRAINED, MASSIVE (STA 0+47), YELLOWISH RED (5YR 5/6)
5. ALLUVIUM: SANDY SILT (ML), MASSIVE, WITH 10% ANGULAR GYPSUM CLASTS ≤ 0.5 INCHES, REDDISH YELLOW (5YR 6/6) TO YELLOWISH RED (5YR 5/6) (STA 0+75)
6. SAND (SP) WITH SOME SILT, FINE GRAINED, MASSIVE, YELLOWISH RED (5YR 5/6) WOME CARBONATE/GYPSUM STAINING (STA 0+75)
7. SANDY SILT (ML), MASSIVE, WITH 5% ANGULAR CLASTS ≤ 0.25 INCHES, PIN HOLE VOIDS, LIGHT BROWN (7.5YR 6/4), SOME GYPSUM (STA 0+35)
8. SAND (SP), WITH SILT, VERY FINE GRAINED, MASSIVE, YELLOW (10YR 7/6) (STA 0+55/SLOT)
9. SAND (SP), WITH SOME SILT (MASSIVE), VERY FINE TO FINE GRAINED, YELLOWISH RED (5YR 5/8) (STA 0+39 / UPPER)
10. FAULT DERIVED COLLUVIUM: SILTY SAND (SM) VERY FINE GRAINED, YELLOWISH RED (5YR 5/6) (STA 0+43)
11. SILTY SAND (SM), MASSIVE, REDDISH YELLOW (5YR 6/6)
12. FAULT DERIVED COLLUVIUM: SANDY SILT (ML) WITH 3% ANGULAR CLASTS ≤ 2 INCHES, AVERAGE SIZE ≤ 1 INCH, YELLOWISH RED (5YR 5/6)
13. SANDY SILT (ML), PIN-HOLE VOIDS, PERVASIVE CARBONATE COATING, REDDISH YELLOW (7.5YR 8/6), LIKELY WEDGE
14. INFILLING AT STA 0+56.5 & 0+55: SILTY SAND (SM), VERY FINE TO FINE GRAINED WITH 5% ANGULAR CARBONATE COATED CLASTS ≤ 0.25 INCHES, REDDISH YELLOW (5YR 6/6)
15. WEDGE: SILTY SAND (SM) VERY FINE TO FINE GRAINED WITH 50% ANGULAR CLASTS ≤ 3 INCHES, SOME CARBONATE CEMENTATION, YELLOWISH RED (5YR 5/6)
16. SILTY SAND (SM) FINE GRAINED WITH 10% SUBANGULAR CLASTS ≤ 1 INCH, YELLOWISH RED (5YR 5/6)

SCALE: 1" = 5'

TRENCH PROFILE WFT-1 (NORTH WALL)

SOUTHERN CORRIDOR PHASE 3
WASHINGTON COUNTY, UTAH

ROSENBERG & ASSOCIATES
CIVIL ENGINEERS • LAND SURVEYORS

PROJECT #	DRAWING #
5507-P3	21

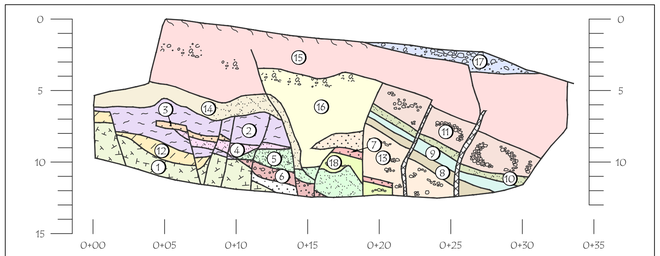

1. ?????
2. SILTY SAND (SM), FINE GRAINED, YELLOWISH RED (5YR 4/6)
3. GRAVEL LENS IN UNIT 2: GRAVELLY SAND (SP) FINE GRAINED WITH 40% GRAVELS / CLASTS TT ≤ 4 INCH, YELLOWISH RED (5YR 5/6)
4. SAND (SP) WITH SILT, FINE GRAINED, REDDISH YELLOW (5YR 6/6)
5. SAND (SP) SLIGHTLY LITHIC, FINE TO MEDIUM GRAINED REDDISH YELLOW (5YR 6/6), MOD. INDURATED
6. GRAVEL LENS (GP) 50% ANGULAR CLASTS ≤ 6 INCHES WITH A FINE GRAINED SAND MATRIX REDDISH YELLOW (5YR 6/6) TO YELLOWISH RED (5YR 5/6)
7. SAND (SP) LENS FINE GRAINED WITH SOME SILT AND CLAY AND 25% SUBANGULAR TO ANGULAR CLASTS ≤ 1 INCH, DK REDDISH BROWN (5YR 3/3) WITH SOME CARBON COATED CLASTS, WHITISH GRAY
8. SAND (SP) FINE GRAINED, REDDISH YELLOW (5YR 6/6) TO YELLOWISH RED (5YR 5/6), SOME CARBON/GYPSUM STAINING
9. SILTY SAND (SM) FINE GRAINED, YELLOWISH RED (5YR 5/6)
10. SILTY SAND (SM) WITH SOME CLAY AND GYPSIFEROUS FRAGMENTS YIELDING A MOITLED APPEARANCE, YELLOWISH RED (5YR 4/6)
11. GRAVELLY SAND (SP), FINE GRAINED WITH 22% ANGULAR CLASTS ≤ 5 INCHES, REDDISH YELLOW (5YR 7/6 TO 6/6) PERVASIVE GYSUM/CARBON STAINING CLASTS COATED WITH GYPSUM/CARBON
12. SILTY SAND (SM), FINE GRAINED YELLOWISH RED (5YR 5/6 TO 4/6) PIN-HOLE VOIDS
13. SILTY SAND (SM) FINE GRAINED YELLOWISH RED (5YR 5/8) WITH DISCONTINUOUS LENSES OF SILTY SAND (SM) YELLOWISH RED (5YR 4/6) WITH ANGULAR CLASTS 5% ≤ 2 INCHES
14. SAND (SP) WITH SOME SILT AND LITHIC FRAGMENTS ≤ 0.25 INCHES, FINE GRAINED YELLOWISH RED (5YR 5/8)
15. SAND (SP) SOME SILT, FINE GRAINED, YELLOWISH RED (5YR 4/6)
16. ZONE OF INFILLING PRIMARILY UNITS 14 AND 15
17. SAND (SP) VERY FINE GRAINED YELLOWISH RED (5YR 4/6) WITH 15% LITHIC CLASTS ≤ 0.25 INCHES , FEW CLASTS ≤ 6 INCHES
18. SAND (SP) VERY FINE TO FINE GRAINED YELLOWISH RED (5YR 5/6)

SCALE: 1" = 5'

TRENCH PROFILE WFT-1 (SOUTH WALL)

SOUTHERN CORRIDOR PHASE 3
WASHINGTON COUNTY, UTAH

ROSENBERG & ASSOCIATES
CIVIL ENGINEERS • LAND SURVEYORS

PROJECT #	DRAWING #
5507-P3	22

APPENDIX A

FIGURES

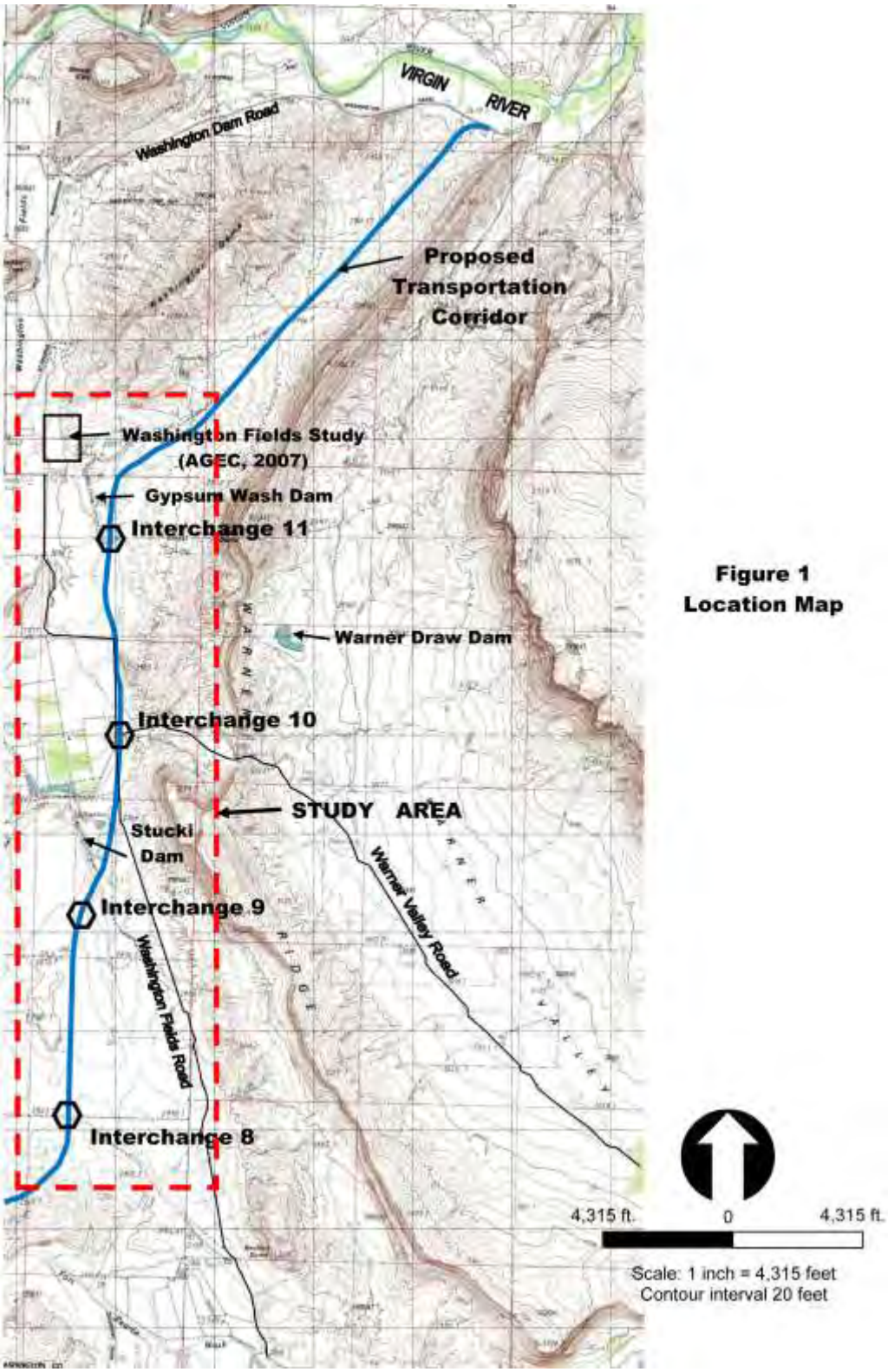

Figure 1
Location Map

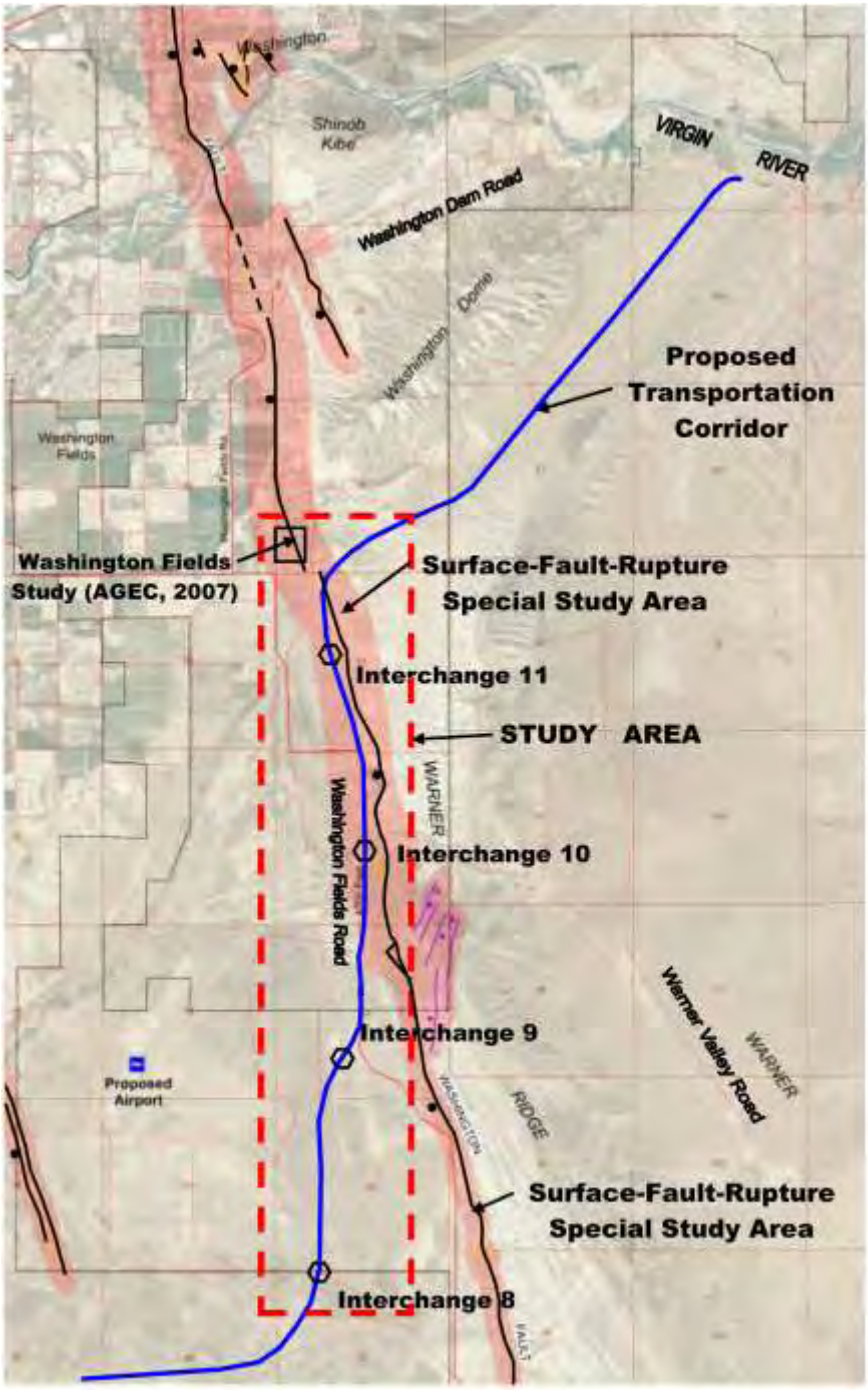

(Lund and Others, 2008)

Figure 2

Surface-Fault-Rupture Special Study Area Map

4,670 ft. 0 4,670 ft.

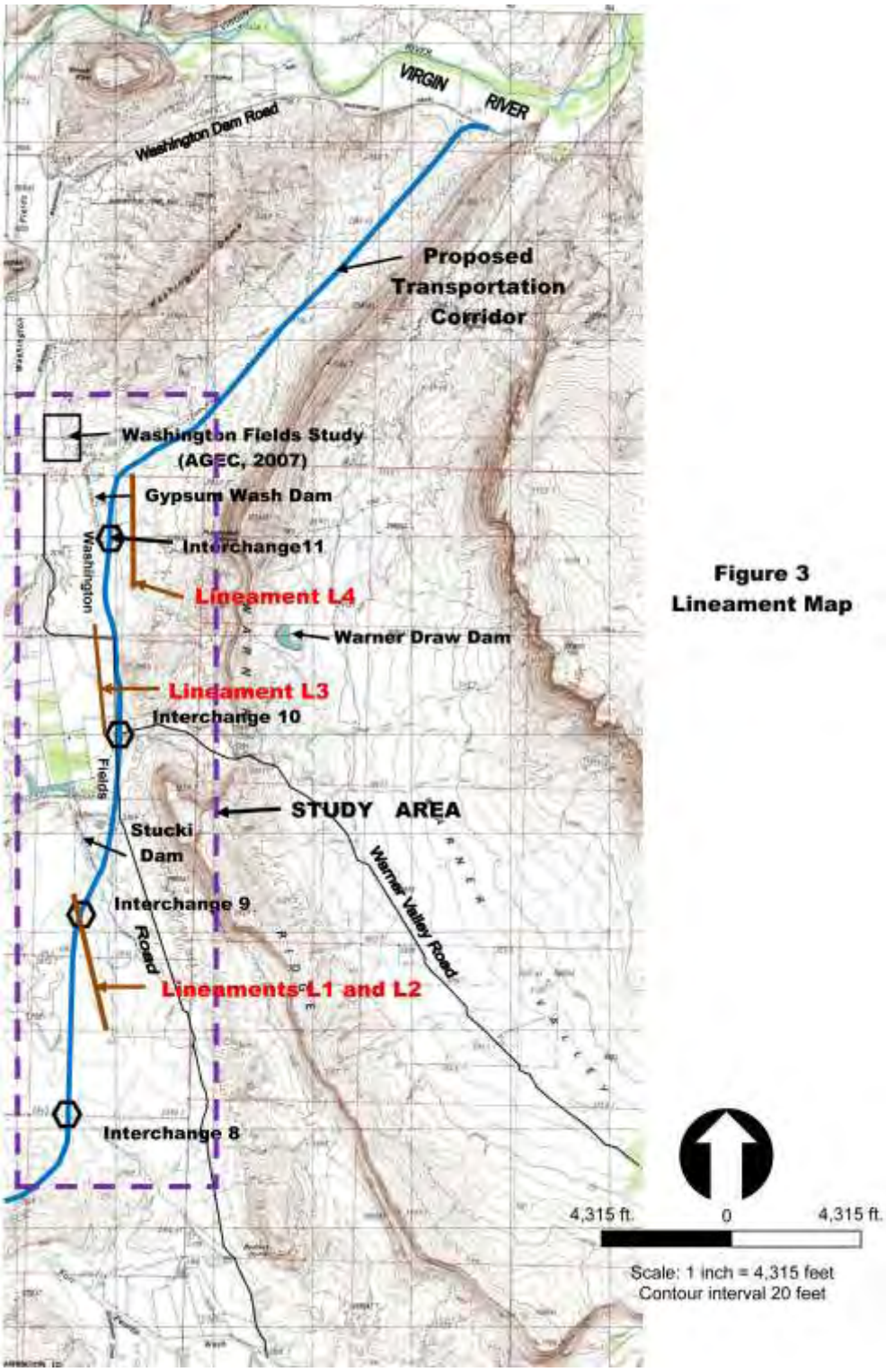

Figure 3
Lineament Map

APPENDIX B

ATOMIC MASS SPECTROMETER RADIOCARBON AGE DATA

Table B-1
Radiocarbon Ages

Trench	Sample No.	Geologic Unit	Location	Age	
				RCYBP	cal yr B.P.[1]
T-1	S-1	8 (alluvium)	see drawing 2	2140 ± 15	2160 - 2060
	S-2	7 (alluvium)	see drawing 2	205 ± 15	20
	S-3	6 (alluvium)	see drawing 2	465 ± 15	530 - 500
T-2	S-1	15 (alluvium)	see drawing 4	1.058 ± 0.0015	December 1955 to July 1957
	S-2	15 (alluvium)	see drawing 4	No particulate carbon	
T-4	S-3	8 (colluvial wedge)	see drawing 8	1.051 ± 0.0017	October 1955 to May 1957
	S-4	9 (colluvial wedge)	see drawing 8	00.9982 ± 0.0013	November 1951 to July 1955
	S-5	10 (fan alluvium)	see drawing 8	1.0045 ± 0.0017	May 1952 to October 1955
WFT-1 (north wall)	S-1	12 (colluvial wedge)	see drawing 22	645 ± 15	600 - 550
	S-2	10 (colluvial wedge)	see drawing 22	530 ± 15	560 - 510
	S-3	15 (colluvial wedge)	see drawing 22	925 ± 15	920 - 790

[1] at two sigma level

APPENDIX C

OSL AGE ANALYSES

USU LUMINESCENCE LABORATORY
1770 north research park way, suite 123, north logan, ut, 84341

PRELIMINARY OSL AGE REPORT

Project: Washington Fault, Utah Geological Survey **Project #:** 068
Scientists: William Lund **Report Date:** June 11, 2012
Report by: Tammy Rittenour

Preliminary OSL Age Information[1]

USU num.	Sample num.	Num. of aliquots[2]	Equivalent Dose[3], De (Gy)	Dose Rate (Gy/ka)	OSL Age (ka)
USU-1119[4]	WV T1 OSL-2	4 (4)	35 ± 25	2.49 ±0.11	**15 ± 10**
USU-1120[4]	WV T1 OSL-3	2 (3)	20 ± 1	2.46 ± 0.11	**10 ± 1**
USU-1121	WV T4 OSL-10	3 (4)	75 ± 30	2.48 ± 0.11	**30 ± 10**
USU-1122	WV T4 OSL-11	4 (4)	45 ± 15	2.37 ± 0.11	**20 ± 8**
USU-1123	WV WF-4	3 (4)	30 ± 15	2.01 ± 0.09	**15 ± 10**
USU-1124	WV WF-5	3 (4)	10 ± 5	1.77 ± 0.08	**5 ± 2**

[1]Preliminary age analysis using the single-aliquot regenerative-dose procedure of Murray and Wintle (2000) on 2-mm small-aliquots of quartz sand.

[2]Number of aliquots used for preliminary age calculation, number of preliminary aliquots measured in parentheses.

[3]Preliminary De calculated using the mean and standard deviation.

[4]Sample contaminated with feldspar, requires second treatment of hydrofluoric acid.

Dose Rate Information[1]

USU num.	Sample num.	Depth (m)	Grain size (µm)	H_2O[2] (%)	U (ppm)	Th (ppm)	%K	Rb (ppm)	Cosmic[3] (Gy/ka)
USU-1119	WV T1 OSL-2	1.7	90-150	0.36%	2.2±0.2	5.9±0.5	1.41±0.04	54.3±2.2	0.19±0.02
USU-1120	WV T1 OSL-3	2.0	90-150	0.41%	2.0±0.1	5.6±0.5	1.46±0.04	55.9±2.2	0.19±0.02
USU-1121	WV T4 OSL-10	0.52	90-150	0.55%	2.1±0.2	6.3±0.6	1.36±0.03	51.4±2.1	0.23±0.02
USU-1122	WV T4 OSL-11	1.04	90-150	0.51%	2.1±0.2	6.0±0.5	1.29±0.03	47.2±1.9	0.21±0.02
USU-1123	WV WF-4	0.5	90-125	0.14%	1.0±0.1	3.4±0.3	1.34±0.03	47.1±1.9	0.23±0.02
USU-1124	WV WF-5	0.43	90-150	0.24%	0.8±0.1	3.2±0.3	1.16±0.03	41.7±1.7	0.23±0.02

[1]Radioelemental concentrations determined by ICP-MS and ICP-AES techniques from ALS Chemex; dose rate is derived from concentrations by conversion factors from Guerin et al. (2011).

[2]Assume 3±3%wt H_2O is representative of burial history.

[3]Contribution of cosmic radiation to the dose rate was calculated by using sample depth, elevation, and longitude/latitude following Prescott and Hutton (1994).

APPENDIX D

WESTERN GEOARCH RESEARCH AGE ANALYSES - TRENCH T-5

Appendix D
Western GeoArch Research Ages - Trench T-5

Big Horn Designation	Beta/USU Report No.	Geologic Unit	Feature	T-5 Station Number	AGE		
					Conventional ^{14}C age (RCYBP) [1] or OSL Age	Two-sigma calibrated conventional ^{14}C age[2]	Calendar calibrated years before present (cal yr B.P.)[3]
FS06	278065	0.5 ft. above base of UNIT 4	charcoal staining in the middle excavation block on the south side of the trench	0+74	5150 ± 40	5895	5855
FS09	278066	0.5 ft. above base of UNIT 4	charcoal staining in the middle excavation block on the south side of the trench	0+56.5	4980 ± 40	5707	5767
FS19	278067	0.5 ft. above base of UNIT 4	general charcoal staining in the middle excavation block on the south side of the trench	0+58	5400 ± 40	6211	6273
FS29	278068	UNIT 10	hearth in Bighorn western-most excavation block in the north trench profile	1+40	1900 ± 40	1825	1885
FS31	278069	UNIT 10	hearth in Bighorn western-most excavation block in the north trench profile	1+43	2030 ± 40	2005	2065
FS34	278070	base of UNIT 4	hearth on the east end of the trench in the north profile	0+17	4640 ± 40	5382	5442
FS113	278638	base of UNIT 4	hearth on the south edge of Bighorn larger middle excavation block (feature 11).	0+50.5	5730 ± 40	6525	6585
FS115	278639	1.2 ft. above base of UNIT 4	hearth in the southeast corner of Bighorn larger middle excavation block (feature 10).	0+57.5	5360 ± 40	6140	6200
Optical Stimulation Luminescence Ages (OSL)							
OSL A*	UIC 2769	UNIT 4**	Qaf sediments	0+56	9940 ± 1030	na	9940
OSL C*	UIC 2770	UNIT 4**	Qaf sediments	0+57	12,910 ± 1415	na	12,910
OSL E	UIC 2768	UNIT 10	Qaf sediments	1+43	4830 ± 430	na	4830

*location of OSL A is 3.75 ± ft. above location of OSL C **Unit 4 is stratigraphically below Unit 10

1 The Conventional Radiocarbon Age (^{14}C) represents the Measured Radiocarbon Age corrected for isotopic fractionation, calculated using the delta ^{13}C. The Conventional Radiocarbon Age is not calendar calibrated.
2 Weighted average of multiple intercepts calculated using OxCal (http://c14.arch.ox.ac.uk). Two-Sigma Calibrated ^{14}C RCYBP.
3 For ^{14}C ages, "present" = AD 1950 plus 62 years.